



**HAL**  
open science

# Molecular mechanisms of vascular smooth muscle cell trans-differentiation and calcification in atherosclerosis

Monika Roszkowska

► **To cite this version:**

Monika Roszkowska. Molecular mechanisms of vascular smooth muscle cell trans-differentiation and calcification in atherosclerosis. Biochemistry, Molecular Biology. Université de Lyon; Instytut biologii doświadczalnej im. M. Nenckiego (Pologne), 2018. English. NNT : 2018LYSE1059 . tel-01880436

**HAL Id: tel-01880436**

**<https://theses.hal.science/tel-01880436>**

Submitted on 24 Sep 2018

**HAL** is a multi-disciplinary open access archive for the deposit and dissemination of scientific research documents, whether they are published or not. The documents may come from teaching and research institutions in France or abroad, or from public or private research centers.

L'archive ouverte pluridisciplinaire **HAL**, est destinée au dépôt et à la diffusion de documents scientifiques de niveau recherche, publiés ou non, émanant des établissements d'enseignement et de recherche français ou étrangers, des laboratoires publics ou privés.



N°d'ordre NNT : 2018LYSE1059

## **THESE de DOCTORAT EN COTUTELLE**

opérée au sein de

**l'Université Claude Bernard Lyon 1**

et

**l'Institut Nencki de Biologie Expérimentale à Varsovie**

**Ecole Doctorale N°205**

**Interdisciplinaire Sciences-Santé**

**Spécialité de doctorat : Biochimie**

Soutenue publiquement le 30/03/2018, par :

**ROSZKOWSKA Monika**

---

# **Mécanismes moléculaires de la trans-différenciation des cellules musculaires lisses et calcification dans l'athérosclérose**

---

Devant le jury composé de :

Pr. Catherine CHAUSSAIN	Univ Paris Descartes	Rapporteur
Dr. Romuald MENTAVERRI	Univ de Picardie Jules Verne, Amiens	Rapporteur
Pr. Zbigniew GACIONG	Univ de Médecine, Varsovie	Rapporteur
Pr. David MAGNE	MEM <sup>2</sup> , Univ Lyon 1, France	Directeur de thèse
Pr. Slawomir PIKULA	Institut Nencki, Varsovie	Directeur de thèse
Dr. Agnieszka STRZELECKA-KILISZEK	Institut Nencki, Varsovie	Examineur

# UNIVERSITE CLAUDE BERNARD - LYON 1

## **Président de l'Université**

Président du Conseil Académique

Vice-président du Conseil d'Administration

Vice-président du Conseil Formation et Vie Universitaire

Vice-président de la Commission Recherche

Directrice Générale des Services

**M. le Professeur Frédéric FLEURY**

M. le Professeur Hamda BEN HADID

M. le Professeur Didier REVEL

M. le Professeur Philippe CHEVALIER

M. Fabrice VALLÉE

Mme Dominique MARCHAND

## ***COMPOSANTES SANTE***

Faculté de Médecine Lyon Est – Claude Bernard

Faculté de Médecine et de Maïeutique Lyon Sud – Charles Mérieux

Faculté d'Odontologie

Institut des Sciences Pharmaceutiques et Biologiques

Institut des Sciences et Techniques de la Réadaptation

Département de formation et Centre de Recherche en Biologie Humaine

Directeur : M. le Professeur G.RODE

Directeur : Mme la Professeure C. BURILLON

Directeur : M. le Professeur D. BOURGEOIS

Directeur : Mme la Professeure C. VINCIGUERRA

Directeur : M. X. PERROT

Directeur : Mme la Professeure A-M. SCHOTT

## ***COMPOSANTES ET DEPARTEMENTS DE SCIENCES ET TECHNOLOGIE***

Faculté des Sciences et Technologies

Département Biologie

Département Chimie Biochimie

Département GEP

Département Informatique

Département Mathématiques

Département Mécanique

Département Physique

UFR Sciences et Techniques des Activités Physiques et Sportives

Observatoire des Sciences de l'Univers de Lyon

Polytech Lyon

Ecole Supérieure de Chimie Physique Electronique

Institut Universitaire de Technologie de Lyon 1

Ecole Supérieure du Professorat et de l'Education

Institut de Science Financière et d'Assurances

Directeur : M. F. DE MARCHI

Directeur : M. le Professeur F. THEVENARD

Directeur : Mme C. FELIX

Directeur : M. Hassan HAMMOURI

Directeur : M. le Professeur S. AKKOUCHE

Directeur : M. le Professeur G. TOMANOV

Directeur : M. le Professeur H. BEN HADID

Directeur : M. le Professeur J-C PLENET

Directeur : M. Y.VANPOULLE

Directeur : M. B. GUIDERDONI

Directeur : M. le Professeur E.PERRIN

Directeur : M. G. PIGNAULT

Directeur : M. le Professeur C. VITON

Directeur : M. le Professeur A. MOUGNIOTTE

Directeur : M. N. LEBOISNE

## Acknowledgements

*My PhD thesis was prepared at the University Lyon 1 in Villeurbanne, France and at the Nencki Institute of Experimental Biology in Warsaw, Poland, under the co-supervision of Professor David Magne and Professor Slawomir Pikula. I greatly appreciate their excellent guidance in scientific work, inspiring discussions, encouragement and support.*

*I wish to thank Dr. Laurence Bessueille from the University of Lyon and Dr. Agnieszka Strzelecka-Kiliszek from the Nencki Institute for teaching and helping me during laboratory work, but also for precious remarks, suggestions and discussions.*

*I would like to thank the following people for interesting discussions, technical help, and accompanying my work in last few years:*

University Lyon 1:

*Professor René Buchet  
Dr. Anne Briolay  
Dr. Maya Fakhry  
Dr. Carole Bougault  
Dr. Najwa Skafi  
Alaeddine El Jamal  
Jihen Zouaoui*

Nencki Institute of Experimental Biology:

*Magdalena Mikulska  
Lukasz Bozycki  
Dr. Marcin Wos  
Dr. Anna Cmoch  
Barbara Sobiak  
Szymon Suski  
Henryk Bilski*

*I would like to acknowledge the French Embassy in Warsaw for the scholarship “Doctorat en Cotutelle 2014–2017” and Polish and French Governments for the Hubert Curien Partnership Polonium 2015/2016 no. 33540RG.*

*Last but not least, I am grateful for my family for their love, constant support and giving me the opportunity of broad education.*



## List of Publications

### *Original articles*

- Fakhry M\*, Roszkowska M\*, Briolay A, Bougault C, Guignandon A, Diaz-Hernandez JI, Diaz-Hernandez M, Pikula S, Buchet R, Hamade E, Badran B, Bessueille L, Magne D. TNAP stimulates vascular smooth muscle cell trans-differentiation into chondrocytes through calcium deposition and BMP-2 activation: Possible implication in atherosclerotic plaque stability. *Biochim Biophys Acta*. 1863(3) (2017) 643-653. \* contributed equally.
- Roszkowska M, Strzelecka-Kiliszek A, Bessueille L, Buchet R, Magne D, Pikula S. Collagen promotes matrix vesicle-mediated mineralization by vascular smooth muscle cells. *J Inorg Biochem*. 186 (2018) 1-9.

### *Review articles*

- Strzelecka-Kiliszek A, Mebarek S, Roszkowska M, Buchet R, Magne D, Pikula S. Functions of Rho family of small GTPases and Rho-associated coiled-coil kinases in bone cells during differentiation and mineralization. *Biochim Biophys Acta*. 1861(5 Pt A) (2017) 1009-1023.
- Roszkowska M, Strzelecka-Kiliszek A, Magne D, Pikula S, Bessueille L (2016) Membranes and pathophysiological mineralization. *Postepy Biochemii* 62 (2016) 511-517.

### *Oral communications*

- “Tissue-nonspecific alkaline phosphatase stimulates vascular smooth muscle cell trans-differentiation into chondrocyte-like cells: a possible role for apatite crystals” - 18<sup>th</sup> edition of the JFBTM Conference, Nancy, France, 1-3.06.2016
- “Tissue-nonspecific alkaline phosphatase and vascular calcification: localization of the enzyme in lipid rafts and its function” - 2<sup>nd</sup> PhD Student Conference at the Nencki Institute of Experimental Biology, Warsaw, 29.10.2015

### *Poster communications*

- “TNAP stimulates vascular smooth muscle cell trans-differentiation into chondrocyte-like cells via crystal formation and BMP-2 activation” - 19<sup>th</sup> edition of “Journées Francaises de Biologie des Tissus Minéralisés” (JFBTM Conference), Lyon, France, 18-20.05.2017
- “The matrix vesicle-mediated mineralization depends on a balance between annexins and fetuin-A” - EMBO Young Scientist Forum, Warsaw, 2-3.06.2015
- “The role of tissue-nonspecific alkaline phosphatase and phospholipase D in mineralization” - BIO Congress, Warsaw, 9-12.09.2014

## **Abstract**

### **Molecular mechanisms of vascular smooth muscle cell trans-differentiation and calcification in atherosclerosis**

Vascular calcification (VC) is a hallmark of atherosclerosis plaques. Calcification (formation of apatite) of advanced lesions share common features with endochondral ossification of long bones and appears to stabilize plaques. This process is associated with trans-differentiation of vascular smooth muscle cells (VSMCs) into chondrocyte-like cells. On the other hand, microcalcification of early plaques, which is poorly understood, is thought to be harmful. The two proteins necessary for physiological mineralization are tissue-nonspecific alkaline phosphatase (TNAP) and collagen. Under pathological conditions, TNAP is activated by inflammatory cytokines in VSMCs, whereas collagen is produced constantly. The activation of TNAP appears to induce calcification of these cells.

Therefore, the objective of this PhD thesis was to study the role of TNAP and generated apatite crystals in the VSMC trans-differentiation and determine underlying molecular mechanisms. Based on the obtained results, we propose that activation of BMP-2, a strong inducer of ectopic calcification, and formation of apatite crystals generated by TNAP represents a likely mechanism responsible for stimulation of VSMC trans-differentiation.

Moreover, we were interested in localization and function of mineralization markers such as TNAP and annexins in mineralization process mediated by trans-differentiated VSMCs and VSMC-derived matrix vesicles (MVs). We observed that, similarly as in the case of typical mineralizing cells, increased TNAP activity in VSMC-derived MVs and association with collagen were important for their ability to mineralize.

**Keywords:** vascular smooth muscle cell, tissue-nonspecific alkaline phosphatase, vascular calcification, chondrocyte.

## Substantial French Summary

### **Mécanismes moléculaires de la trans-différenciation des cellules musculaires lisses et calcification dans l'athérosclérose**

En conditions physiologiques, la formation de cristaux de phosphate de calcium est restreinte au squelette. D'autre part, plusieurs conditions pathologiques, en particulier associées au vieillissement, sont associées à des calcifications ectopiques, qui peuvent affecter les tissus vasculaires. Les calcifications vasculaires ont un fort impact sur la structure et les propriétés des artères affectées. Chez les patients atteints d'athérosclérose, les calcifications vasculaires sont une caractéristique des plaques d'athérome. La calcification de la plaque d'athérosclérose varie de microcalcifications diffuses à des macrocalcifications formées par un processus ressemblant à une ossification endochondrale, qui fait intervenir un tissu intermédiaire cartilagineux. Très probablement, ces macrocalcifications résultent de la trans-différenciation des cellules musculaires lisses (CMLs) en cellules de type ostéoblastique et/ou chondrocytaire. Alors que les macrocalcifications semblent stabiliser la plaque, les microcalcifications sont très probablement nuisibles. Le fait que les microcalcifications précoces ont été rapportées comme étant des structures particulièrement dangereuses pour la stabilité de la plaque, la résolution des mécanismes responsables de leur formation nécessite une attention particulière.

En outre, il n'existe pas aujourd'hui de thérapie permettant de freiner significativement le développement des calcifications vasculaires. Nous nous intéressons particulièrement au rôle de la phosphatase alcaline non spécifique du tissu (TNAP) dans la calcification vasculaire, puisqu'il s'agit de la seule enzyme connue à ce jour pour être absolument nécessaire à la minéralisation physiologique. L'absence d'origine génétique d'activité TNAP cause l'hypophosphatasie, qui dans les cas sévères, se manifeste en effet par la mort *in utero* de fœtus complètement dépourvus de cristaux osseux. Il a été montré que la TNAP induit la minéralisation tissulaire en hydrolysant un inhibiteur constitutif de la minéralisation, le pyrophosphate inorganique (PP<sub>i</sub>). Il est probable que la phosphatase alcaline doive être ancrée à la membrane plasmique par son ancre glycosylphosphatidylinositol (GPI) pour être pleinement active.

Des découvertes récentes suggèrent que la TNAP peut être activée dans les CMLs par les cytokines pro-inflammatoires, le facteur de nécrose tumorale (TNF- $\alpha$ ) et l'interleukine 1 bêta (IL-1 $\beta$ ). Des travaux précédents de l'équipe ont montré que l'ajout

de phosphatase alcaline ou la surexpression de TNAP dans les CMLs suffit à stimuler l'accumulation de calcium de façon significative. A la lumière de ces résultats, nous avons émis l'hypothèse que la TNAP induite dans les CMLs en conditions inflammatoires, suffit à induire la minéralisation et la trans-différenciation des CMLs. Nos objectifs étaient donc de déterminer l'effet de la TNAP dans la trans-différenciation des CMLs, et d'étudier les mécanismes impliqués dans son induction.

Nous avons observé par PCR quantitative que l'ajout de phosphatase alcaline purifiée dans les CMLs de souris MOVAS, en l'absence de donneurs de phosphate, augmente les niveaux de transcrits de marqueurs chondrocytaires et ostéoblastiques, tels que l'agrécan et l'ostéocalcine, mais aussi de la protéine morphogénétique osseuse BMP-2. L'agrécan est le protéoglycane le plus abondant dans le cartilage et un marqueur précoce de la différenciation des chondrocytes. L'ostéocalcine est une protéine carboxylée abondante associée aux cristaux osseux, et est un marqueur de la différenciation des ostéoblastes et des chondrocytes hypertrophiques. Puisque l'ostéocalcine peut être exprimée par les ostéoblastes et les chondrocytes, nous avons mesuré l'expression du facteur de transcription plus spécifique des ostéoblastes, osterix, qui n'augmentait pas mais diminuait en présence de phosphatase alcaline exogène, suggérant que les CMLs ont trans-différencié en chondrocytes et non en ostéoblastes.

Cependant, notre résultat le plus intéressant est probablement que le traitement des CMLs par des cristaux seuls ou associés à une matrice collagénique a reproduit les effets de la TNAP. La culture de cellules MOVAS en présence de cristaux de phosphate de calcium, ou sur une matrice de collagène de type I, a en effet permis de mesurer une augmentation significative de l'expression de l'aggrécan et de BMP-2, qui est un facteur de croissance ostéogénique puissant.

Nous suspectons que la TNAP agit en hydrolysant le pyrophosphate inorganique (PP<sub>i</sub>) et en générant des cristaux d'apatite. Ces cristaux ensuite induisent l'expression du facteur ostéogénique BMP-2 qui stimule la trans-différenciation des CMLs. Nous avons en effet observé que et l'inhibition des effets de la BMP-2 par ajout de Noggin annule les effets de la TNAP. Ces résultats suggèrent que l'induction de la TNAP en conditions inflammatoires pourrait suffire à induire des microcalcifications.

L'inflammation et l'IL-1 $\beta$  en particulier jouent des rôles importants dans le développement de l'athérosclérose. L'IL-1 $\beta$  est sécrétée par les cellules par un mécanisme qui nécessite l'activation de l'inflammasome NLRP3. Plusieurs structures cristallines sont connues pour activer l'inflammasome. Il est donc possible que les cristaux d'apatite puissent

produire leurs effets par activation de l'inflammasome NLRP-3 et sécrétion de l'IL-1 $\beta$ . Ce mécanisme est au centre des derniers travaux du laboratoire.

De plus, nous étions intéressés par les mécanismes gouvernant la localisation et la fonction de la TNAP avec un intérêt particulier pour les annexines. Nous avons tout d'abord localisé la TNAP à la membrane des CMLs cultivées dans les conditions de minéralisation. Nous avons ensuite observé que l'activité TNAP des CMLs induit la minéralisation sans doute en grande partie quand la TNAP est associée aux vésicules matricielles et aux fibres de collagène. Donc, de la même manière que dans le cas des cellules minéralisantes classiques, l'association avec le collagène semble importante pour l'activité de TNAP dans les vésicules matricielles des CMLs et la minéralisation.

Dans les plaques d'athérosclérose, la localisation précise des microcalcifications et leur association possible avec le collagène sont des questions qui sont encore discutées. Cependant, il semble que la quantité de collagène est un facteur critique pour la stabilité de la plaque. Les lésions athérosclérotiques vulnérables contiennent généralement un bouchon fibreux mince et pauvre en collagène. Certains résultats suggèrent que les microcalcifications sont particulièrement dangereuses lorsqu'elles sont situées dans un tel bouchon fibreux.

Sur la base de nos observations, nous proposons un mécanisme de stimulation par la TNAP de la calcification des plaques d'athérosclérose. Nos résultats sont cohérents avec le modèle récemment proposé par Chatrou et ses collaborateurs (Chatrou *et al.*, Plos One, 2015). Ils ont observé que des microcalcifications étaient présentes avant les "ostéochondrocytes" dans les plaques athérosclérotiques humaines et ont émis l'hypothèse qu'ils sont la cause et non la conséquence de la trans-différenciation des CMLs. En outre, nous proposons que l'activation de la TNAP par des cytokines inflammatoires telles que le TNF- $\alpha$  et l'IL-1 $\beta$  dans les CMLs, l'hydrolyse subséquente de PP<sub>i</sub> et la génération de cristaux d'apatite est un mécanisme central lors de la formation de microcalcifications. Nos résultats suggèrent que les cristaux stimulent la BMP-2 qui peut initier la trans-différenciation des CMLs.

En résumé, nos expériences déjà effectuées, et celles en cours, permettront de mieux comprendre les mécanismes moléculaires qui gouvernent l'expression et la fonction de la TNAP dans les artères affectées. D'un point de vue thérapeutique, ces études font de la TNAP une cible prometteuse pour inhiber la formation de microcalcifications.

**Mots-clé:** cellule musculaire lisse, phosphatase alcaline, calcification vasculaire, chondrocyte.

## Substantial Polish Summary

### **Molekularne mechanizmy procesów transdyferencji komórek mięśni gładkich oraz zwapnienia ścian naczyń krwionośnych towarzyszących miażdżycy**

W organizmie człowieka w warunkach fizjologicznych minerał jest wytwarzany w tkance kostnej, jednak starzenie organizmu wiąże się z występowaniem patologicznego zwapnienia ścian naczyń krwionośnych. Zwapnienie (tworzenie apatyty) naczyń towarzyszy procesowi odkładania się blaszki miażdżycowej już we wstępnych etapach rozwoju arteriosklerozy. Liczne zwapnienia znacząco wpływają na strukturę i właściwości tętnic wieńcowych oraz głównych arterii organizmu. W tętnicach pacjentów z zaawansowaną arteriosklerozą występują tzw. „makrozwapnienia”, będące konsekwencją zachodzenia w naczyniach krwionośnych procesu analogicznego do kostnienia śródchrzęstnego. Za molekularne podłoże zwapnienia naczyń uważa się obecnie tzw. proces „transdyferencji” komórek mięśni gładkich naczyń (ang. vascular smooth muscle cells, VSMC) w komórki o fenotypie chondrocytów. Najnowsze doniesienia literaturowe wskazują również na obecność w naczyniach krwionośnych tzw. „mikrozwapnień”, które zagrażają stabilności złogów miażdżycowych, jednakże przyczyna ich powstawania nie została dotychczas poznana. Z uwagi na fakt, iż mikrozwapnienia uważa się za struktury szczególnie zagrażające stabilności blaszki miażdżycowej, zbadanie mechanizmów odpowiedzialnych za ich występowanie wymaga szczególnej uwagi.

Tkankowo niespecyficzna alkaliczna fosfataza (ang. tissue-nonspecific alkaline phosphatase, TNAP) oraz kolagen to dwa białka konieczne do zajścia procesu fizjologicznej mineralizacji. W komórkach VSMC, które wydzielają kolagen, aktywność TNAP może być indukowana przez cytokiny prozapalne, prowadząc do zapoczątkowania procesu patologicznej mineralizacji. Do tej pory nie została opracowana skuteczna terapia zapobiegająca rozwojowi zwapnienia naczyń. W naszych badaniach skupiliśmy się nad rolą białka TNAP w tym procesie. Mutacje genów kodujących TNAP mogą skutkować występowaniem rzadkiej choroby zwanej hipofosfatazją. Perinatalna odmiana tej choroby dotyczy płodów, które są całkowicie pozbawione szkieletu kostnego. TNAP zapoczątkowuje proces mineralizacji poprzez hydrolizę głównego konstytutywnego inhibitora mineralizacji, nieorganicznego pirofosforanu ( $PP_i$ ). Najprawdopodobniej, dla pełnej aktywności, białko TNAP występuje w komórce głównie

w formie zakotwiczonej w błonie plazmatycznej za pomocą glikozylofosfatydiloinozytolu (GPI).

Jak już wspomniano, białko TNAP może być aktywowane w komórkach VSMC przez cytokiny prozapalne, takie jak czynnik martwicy nowotworów (ang. tumor necrosis factor alpha, TNF- $\alpha$ ) oraz interleukina 1 $\beta$  (ang. interleukin 1 $\beta$ , IL-1 $\beta$ ). Zaobserwowano również, że nadekspresja genu kodującego TNAP w szczurzych komórkach VSMC, A7R5, spowodowała znaczącą stymulację mineralizacji. Wysunęliśmy więc hipotezę, że białko TNAP odgrywa także ważną rolę w procesie transdiferencjacji komórek VSMC. W związku z tym celem niniejszej pracy doktorskiej było zbadanie wpływu TNAP oraz wytworzonych kryształów apatytu na proces transdiferencjacji komórek VSMC w komórki zdolne do mineralizacji.

Dodanie egzogennej alkalicznej fosfatazy do hodowli mysich komórek VSMC, MOVAS, podwyższyło ekspresję genów kodujących znaczniki mineralizacji, takich jak agrekan oraz osteokalcyna, jak również białka morfogenetycznego kości BMP-2 (ang. bone morphogenetic protein 2). Agrekan jest jednym z głównych składników tkanki chrzęstnej, zaś gen kodujący to białko jest znacznikiem różnicowania się komórek w kierunku chondrocytów. Osteokalcyna to białko mogące wiązać się z kryształami apatytu, będące znacznikiem różnicowania komórek w kierunku osteoblastów i chondrocytów. Ponieważ osteokalcyna może być syntetyzowana zarówno przez osteoblasty, jak i chondrocyty, zbadaliśmy ekspresję znacznika specyficznego wyłącznie dla osteoblastów - genu kodującego czynnik transkrypcyjny osterix, którego ekspresja w odpowiedzi na obecność egzogennej alkalicznej fosfatazy w hodowli komórek MOVAS nie wzrosła, lecz uległa obniżeniu, świadcząc o różnicowaniu komórek MOVAS w komórki przypominające chondrocyty.

Co ciekawe, hodowla komórek MOVAS w obecności kryształów apatytu zawieszonych w pożywce hodowlanej lub związanych z powierzchnią pokrytą kolagenem typu I wpłynęła znacząco na wzrost poziomu mRNA genów kodujących agrekan oraz BMP-2. BMP-2 jest czynnikiem zdolnym do indukcji procesu ektopowej mineralizacji. W niniejszej pracy doktorskiej dowiedziono zatem, że kryształy apatytu wpływają na ekspresję znaczników mineralizacji w komórkach VSMC w sposób analogiczny do działania TNAP.

Ponadto opisano lokalizacje oraz funkcje białek będących znacznikami mineralizacji, takich jak TNAP oraz aneksyny w komórkach VSMC stymulowanych do mineralizacji oraz w wydzielonych przez nie pęcherzykach macierzy pozakomórkowej (ang. matrix vesicles, MVs). Zaobserwowano podwyższoną aktywność TNAP w pęcherzykach związanych z kolagenem, co sugeruje ważną rolę tego białka w procesie mineralizacji komórek VSMC.



Prawdopodobny mechanizm odpowiedzialny za stymulację procesu transdiferencjacji komórek VSMC przez białko TNAP zachodzi poprzez hydrolizę  $PP_i$  oraz wytworzenie kryształów apatytu odpowiedzialnych za indukcję ekspresji czynnika BMP-2. Co więcej, indukcja TNAP w komórkach VSMC może stanowić mechanizm odpowiedzialny za tworzenie mikrozwapnień. Otrzymane wyniki są zgodne z modelem zaproponowanym przez Chatrou i współpracowników, którzy ostatnio zaobserwowali, że mikrozwapnienia były obecne przed "osteochondrocytami" w blaszkach miażdżycowych człowieka i postawili hipotezę, że są one przyczyną, a nie konsekwencją procesu transdiferencjacji.

Podsumowując, otrzymane wyniki przyczyniają się do częściowego wyjaśnienia mechanizmów molekularnych procesu transdiferencjacji komórek VSMC w komórki zdolne do mineralizacji. Na podstawie uzyskanych wyników można stwierdzić, że białko TNAP jest obiecującym celem terapeutycznym dla terapii zmierzających do zahamowania procesu tworzenia mikrozwapnień.

**Słowa kluczowe:** komórka mięśni gładkich naczyń krwionośnych, tkankowo niespecyficzna alkaliczna fosfataza, zwapnienie ścian naczyń krwionośnych, chondrocyt.



## Table of Contents

Chapter 1. Introduction .....	18
1.1. Atherosclerosis .....	18
1.1.1. Atherosclerosis – the main cause of cardiovascular system diseases .....	18
1.1.2. Atherosclerotic plaque progression .....	21
1.1.3. The role of lipids, lipoproteins and fatty acids in atherosclerosis .....	23
1.1.4. The role of cholesterol crystals in atherosclerosis .....	24
1.2. Vascular calcification in atherosclerosis .....	25
1.2.1. Macrocalcification in atherosclerosis .....	26
1.2.2. Microcalcification in atherosclerosis .....	27
1.2.3. Therapeutic strategies against atherosclerosis and vascular calcification .....	28
1.3. Molecular mechanisms of physiological mineralization .....	30
1.3.1. Osteoblast differentiation and membranous ossification .....	33
1.3.2. Chondrocyte differentiation and endochondral ossification .....	34
1.3.3. Matrix vesicles (MVs) as sites of mineral nucleation .....	39
1.3.4. Key proteins involved in mineralization process .....	41
1.4. Molecular mechanisms of pathological calcification .....	44
1.4.1. Formation of artery macrocalcification – possible mechanisms .....	46
1.4.2. Formation of artery microcalcification – possible mechanisms .....	47
Chapter 2. Aims .....	52
Chapter 3. Materials and methods .....	54
3.1. Cell culture and treatment .....	54
3.1.1. Murine VSMC cell culture .....	54
3.1.2. Murine primary chondrocyte cell culture .....	54
3.1.3. Cell treatments .....	55
3.2. Biochemical and analytical methods .....	55
3.2.1. Alizarin Red staining .....	55
3.2.2. Measurement of protein concentration .....	55
3.2.3. Measurement of TNAP activity .....	55
3.2.4. NBT-BCIP .....	56
3.2.5. MTT assay .....	57
3.2.6. LDH assay .....	57
3.3. Apatite crystals preparation .....	57
3.3.1. Apatite collagen complexes (ACCs) preparation .....	57
3.3.2. Apatite crystals (ACs) synthesis .....	58
3.4. Gene expression analysis .....	58
3.4.1. RNA extraction and Reverse Transcription .....	58
3.4.2. Quantitative Polymerase Chain Reaction (RT-qPCR) .....	59

3.5. Cellular fractionation.....	60
3.5.1. Isolation of total membranes.....	60
3.5.2. Isolation of collagen-free MVs.....	61
3.5.3. Isolation of collagen-attached MVs.....	61
3.6. Lipid analysis.....	62
3.6.1. Measurement of cholesterol content.....	62
3.7. Protein analysis.....	63
3.7.1. SDS-PAGE and Western Blot.....	63
3.7.2. Protein staining.....	64
3.7.3. Immunofluorescence.....	64
3.8. Transmission electron microscopy (TEM) and energy dispersive X-ray microanalysis (TEM-EDX).....	66
3.8.1. Sample preparation.....	66
3.8.2. TEM.....	66
3.8.3. TEM-EDX and mapping.....	66
3.9. Statistical analysis.....	67
Chapter 4. Results.....	69
4.1. Mineralization abilities of cellular models.....	69
4.1.1. Characterization of MOVAS.....	69
4.1.2. Characterization of murine primary chondrocytes.....	72
4.2. The role of TNAP in MOVAS trans-differentiation and mineralization.....	72
4.2.1. MOVAS trans-differentiation into chondrocyte-like cells.....	72
4.2.2. The effect of ACs generated by TNAP on <i>Acan</i> gene expression.....	73
4.2.3. The effect of ACs generated by TNAP on <i>Bmp-2</i> gene expression.....	75
4.2.4. Study of ACs cytotoxicity.....	77
4.3. TNAP and annexins localization and function in MV-mediated mineralization of MOVAS.....	80
4.3.1. TNAP localization in MOVAS.....	80
4.3.2. Morphology of MOVAS and released MVs.....	81
4.3.3. The role of TNAP in MV-mediated mineralization.....	84
4.3.4. Study of the role of cholesterol in mineralization.....	86
4.3.5. Localization of lipid rafts in MOVAS.....	87
4.3.6. Localization and function of annexins.....	89
4.3.7. MV chemical composition.....	91
Chapter 5. Discussion.....	96
References.....	104
Annex.....	123

## List of Abbreviations

<b>AA</b>	Ascorbic acid
<b>ACs</b>	Apatite crystals
<b>ACCs</b>	Apatite collagen complexes
<b>Anx</b>	Annexin
<b>Apo</b>	Apolipoprotein
<b>ATF4</b>	Activating transcription factor 4
<b>ATP</b>	Adenosine triphosphate
<b>BCA</b>	Bi-cinchoninic acid
<b>BMP</b>	Bone morphogenic protein
<b>β-GP</b>	β-glycerophosphate
<b>Ca</b>	Calcium
<b>CAC</b>	Coronary artery calcium
<b>cDNA</b>	Complementary deoxyribonucleic acid
<b>Chol</b>	Cholesterol
<b>CPC</b>	Cetylpyridinium chloride
<b>CT</b>	Computed tomography
<b>DHA</b>	Docosahexaenoic acid
<b>DMEM</b>	Dulbecco's modified Eagle's medium
<b>ECL</b>	Enhanced chemiluminescence
<b>ECM</b>	Extracellular matrix
<b>EPA</b>	Eicosapentaenoic acid
<b>ER</b>	Endoplasmic reticulum
<b>FBS</b>	Fetal bovine serum
<b>FGF</b>	Fibroblast growth factor
<b>FTIR</b>	Fourier transform infrared spectroscopy
<b>GAG</b>	Glycosaminoglycan
<b>GAPDH</b>	Glyceraldehyde-3-phosphate dehydrogenase
<b>GFP</b>	Green fluorescent protein
<b>GM 1</b>	Ganglioside 1
<b>GPI</b>	Glycosyl-phosphatidylinositol

<b>HCl</b>	Hydrochloric acid
<b>HDL</b>	High density lipoprotein
<b>HEPES</b>	4-(2-hydroxyethyl)-1-piperazineethanesulfonic acid
<b>HIF</b>	Hypoxia inducible factor
<b>HMG-CoA</b>	3-hydroxy-3-methylglutaryl-coenzyme A
<b>HRP</b>	Horseradish peroxidase
<b>IAP</b>	Intestinal alkaline phosphatase
<b>IHD</b>	Ischemic heart disease
<b>IL</b>	Interleukin
<b>LDH</b>	Lactate dehydrogenase
<b>LDL</b>	Low density lipoprotein
<b>M-CSF</b>	Macrophage-colony stimulating factor
<b>MGP</b>	Matrix Gla protein
<b>MMP</b>	Matrix metalloproteinase
<b>mRNA</b>	Messenger ribonucleic acid
<b>MSC</b>	Mesenchymal stem cell
<b>MV</b>	Matrix vesicle
<b>NAD<sup>+</sup></b>	Nicotinamide adenine dinucleotide
<b>NADH</b>	Nicotinamide adenine dinucleotide hydrogen
<b>NADPH</b>	Nicotinamide adenine dinucleotide phosphate hydrogen
<b>NLRP3</b>	NOD-like receptor family, pyrin domain containing 3
<b>NPP1</b>	Nucleotide pyrophosphatase phosphodiesterase
<b>OCN</b>	Osteocalcin
<b>OPN</b>	Osteopontin
<b>P</b>	Phosphorus
<b>PBS</b>	Phosphate buffered saline
<b>PC</b>	Phosphatidylcholine
<b>PCR</b>	Polimerase chain reaction
<b>PEA</b>	Phosphatidyletanolamine
<b>PET</b>	Positron emission tomography
<b>Phospho-1</b>	Phosphatase orphan 1
<b>P<sub>i</sub></b>	Inorganic phosphate

<b>PIC</b>	Protease inhibitor cocktail
<b>P<sub>i</sub>T</b>	Inorganic phosphate transporter
<b>pNP</b>	Paranitrophenol
<b>pNPP</b>	Paranitrophenyl phosphate
<b>PP<sub>i</sub></b>	Inorganic pyrophosphate
<b>PS</b>	Phosphatidylserine
<b>PTH</b>	Parathyroid hormone
<b>Runx-2</b>	Runt-related transcription factor 2
<b>RT</b>	Room temperature
<b>SCL</b>	“Synthetic cartilage lymph” solution
<b>SDS-PAGE</b>	Sodium dodecyl sulfate-polyacrylamide gel electrophoresis
<b>SEM</b>	Standard error of the mean
<b>Sox-9</b>	SRY (Sex determining region Y)-Box 9
<b>TBS</b>	Tris buffered saline
<b>TBST</b>	Tris buffered saline supplemented with Tween-20
<b>TEM-EDX</b>	Transmission electron microscopy-Energy dispersive X-ray microanalysis
<b>TGF-β</b>	Transforming growth factor-β
<b>TNAP</b>	Tissue-nonspecific alkaline phosphatase
<b>TNF-α</b>	Tumor necrosis factor alpha
<b>VC</b>	Vascular calcification
<b>VCAM-1</b>	Vascular cell adhesion molecule
<b>VEGF</b>	Vascular endothelial growth factor
<b>VSMC</b>	Vascular smooth muscle cell
<b>WCL</b>	Whole cell lysate
<b>WT</b>	Wild type

# **Chapter I**

## **Introduction**

## **Chapter 1. Introduction**

### **1.1. Atherosclerosis**

Nowadays, cardiovascular system diseases are classified among the most important clinical issues worldwide. Vascular calcification (VC) is a complication that occurs in human arteries and accompanies age-related diseases, such as atherosclerosis. In the 19<sup>th</sup> century, the pathologist Rudolph Virchow was the first who described VC associated with atherosclerosis as a passive, degenerative process. Later, medial calcific sclerosis was characterized by Johann Georg Mönckeberg. In 1990's, VC was no longer concerned as a passive process of mineral precipitation. Currently, VC is recognized as a pathobiological process sharing many features with normal bone formation (Demer and Tintut, 2008). In this work, we particularly focused on VC associated to atherosclerosis.

#### **1.1.1. Atherosclerosis - a main cause of cardiovascular system diseases**

Atherosclerosis underlies the majority of pathologies affecting circulatory system. It is a progressive chronic inflammatory disease initiated by the accumulation of lipids and fibrous elements in subendothelial (intimal) layers of artery walls. Atherosclerosis progression may lead to stenosis, characterized by limited blood flow, and resulting in the insufficient oxygen and nutrition supply to the tissues and organs (Hahn and Schwartz, 2009). However, the most severe clinical events are due to atherosclerotic vulnerable plaque rupture, resulting in the exposure of the plaque content to the artery lumen, where thrombotic occlusions are formed. In the heart, atherosclerosis may lead to heart failure (referred as myocardial infarction), whereas in brain, it may cause cerebral infarction (ischemic stroke). Atherosclerosis may concern also peripheral tissues, leading to hypertension, aneurysms and limb ischemia.

Although clinical complications of atherosclerosis usually occur in the population of middle aged to elderly patients, it was demonstrated that initiation of atherosclerotic lesion development begins much earlier, during childhood (Doherty *et al.*, 2004). Thus, it is possible that atherosclerosis remains asymptomatic for many years. Epidemiological studies revealed numerous environmental risk factors of this pathology, such as age, hyperlipidemia, hypertension, diabetes mellitus, obesity, smoking, stress, physical inactivity and infections (Criqui *et al.*, 2014). As far as the aging population is concerned, calcification of the aortic arch was reported to occur in more than 25% of population at the age of 60 and above. However,

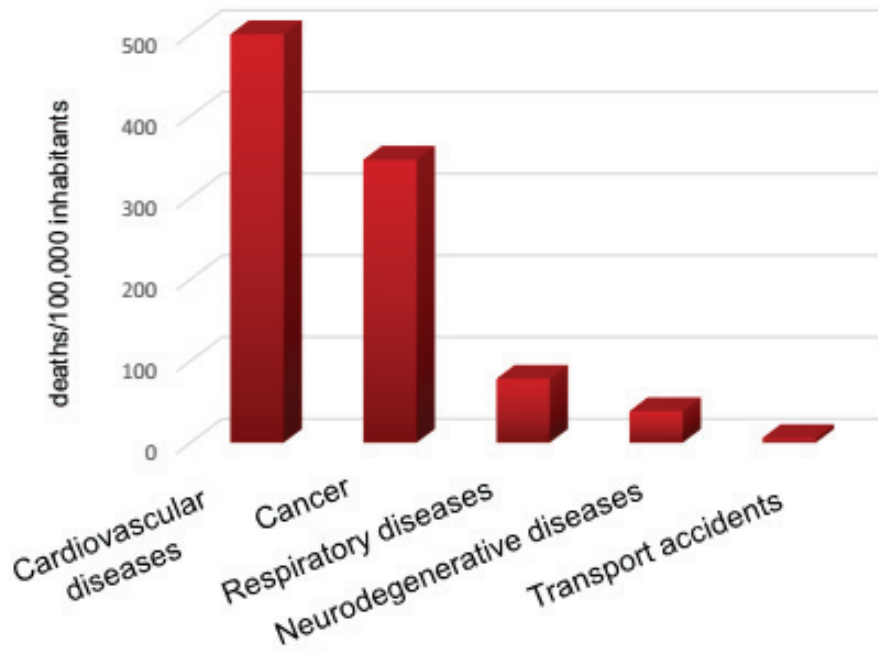
an interesting study of ancient Egyptian mummies performed by Clarke and collaborators revealed that atherosclerosis concerned humans long before modern civilization and current risk factors have appeared (Clarke *et al.*, 2014). Moreover, according to Murphy and collaborators, it was estimated that arterial calcification accompanies human population for at least 5 millenia, as demonstrated by computed tomographic imaging of “ice mummy” discovered in the Tyrolean Alps (Murphy *et al.*, 2003).

Cardiovascular diseases are the major cause of death in Europe, claiming around 2 million European Union inhabitants per year. Ischemic heart disease (IHD) and cerebral infarction (ischemic stroke) are the most common causes of death among wide spectrum of cardiovascular diseases. According to Global Burden of Disease Study carried out for the year of 2013, IHD and stroke were the world’s first and third causes of death, representing nearly 30% of all-cause mortality. Nevertheless, over twenty three years, between 1990 and 2013, cardiovascular mortality dropped globally by 20% (GBD 2013 Mortality and Causes of Death Collaborators, 2015). However, although this mortality rate decreased on a global scale, the prevalence of severe atherosclerosis is still increasing, in part due to aging of population, as well as due to changing lifestyle and diet (Barquera *et al.*, 2015). Unfortunately, it is likely that in the coming decades it will reach epidemic proportions.

Interestingly, there are significant differences in mortality rates between nationalities. Circulatory system disorders and cancer are currently two leading causes of death in the European Union (EU) (**Fig. 1A**) and United States of America (USA) (**Fig. 1B**). For instance, ischemic heart disease and lung cancer were on the top of the list of most common causes of death in countries such as the USA, France and Poland, however, in the case of Poland it is a cerebral infarction (ischemic stroke), which occupies a high second position, between IHD and lung cancer. Also, there are differences in mortality rates over developed and developing countries. The major cause of death among citizens of developed countries is IHD, whereas in developing countries on the leading causes of death are lower respiratory infections (GBD 2013 Mortality and Causes of Death Collaborators, 2015).



A



B

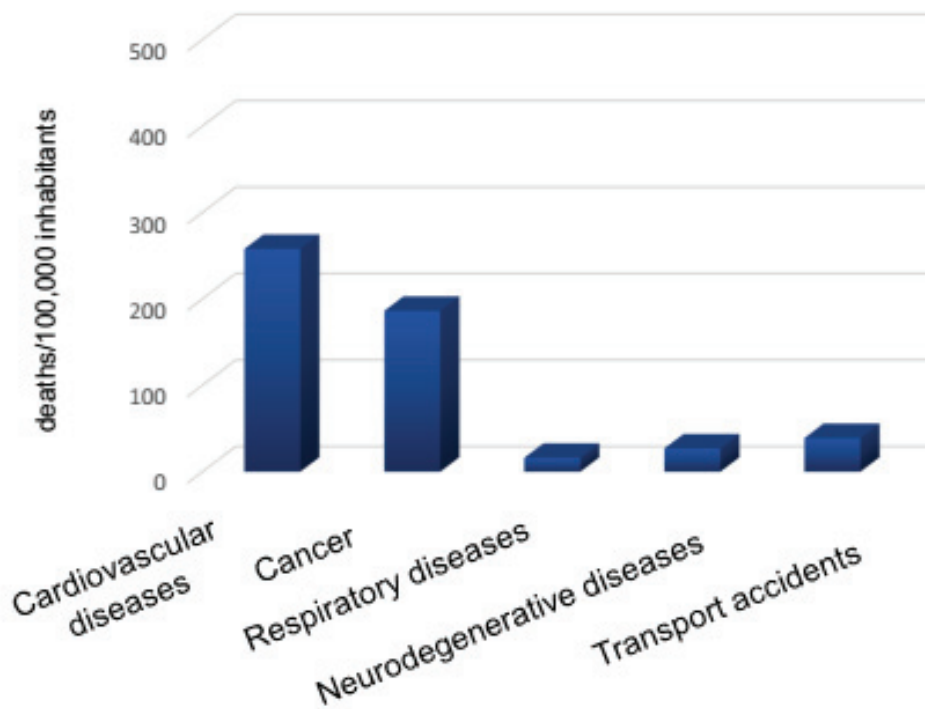


**Figure 1. Cardiovascular diseases and cancer are two major causes of death.** Mortality rates in the EU (A) (according to Eurostat data, 2014) and in the USA (B) (according to US National Institutes of Health, 2010) were presented.

### 1.1.2. Atherosclerotic plaque progression

Lipid accumulation provokes various consequences leading to activation of adaptive processes in the organism preventing the cytotoxic effect of the excessive material. Lipoprotein uptake by macrophages and vascular smooth muscle cells represents a kind of physiological response to this unfavorable process. Nevertheless, the cellular response mechanism finally converts into a pathology that contributes to atherosclerotic plaque formation. According to the response-to-retention model proposed by Williams and Tabas, the key event that initiates atherogenesis is subendothelial retention of lipoproteins within the artery wall (Williams and Tabas, 1995).

Atherosclerotic plaque formation begins with the formation of fatty streak lesions in the arterial intima, a thin layer of endothelial cells (Okura *et al.*, 2000; Uchida *et al.*, 2013). This process is initiated by accumulation of apolipoprotein B (apoB)-containing lipoproteins, which bind to proteoglycans of the extracellular matrix (ECM) through ionic interactions and activate endothelium (Skålen *et al.*, 2002). Activated endothelial cells secrete pro-inflammatory agents such as chemokines and adhesion molecules, particularly vascular cell adhesion molecule (VCAM-1), to attract monocytes from the circulation and promote their entry to the subendothelial space. Recruited monocytes differentiate into macrophages driven by a macrophage-colony stimulating factor (M-CSF) (Lusis, 2000). Next, monocyte-derived macrophages phagocytose retained lipoproteins, forming foam cells enriched in cytoplasmic lipid droplets. Interestingly, native LDLs are not taken up by macrophages, rather oxidatively modified particles (oxLDLs) are highly atherogenic (Linton *et al.*, 2000). Foam cells contribute to the development of fatty streak lesions by initiating and amplifying the inflammatory response. In addition, some reports indicate that, similarly to macrophages, smooth muscle cells may also accumulate cholesterol and become foam cells (Glass and Witztum, 2001).

There are two major factors that contribute to atherosclerotic plaque progression – first one is the domination of cell death mechanisms within the plaque, most probably due to prolonged endoplasmic reticulum (ER) stress induced by various stimuli (Tabas, 2010). The second reason is the deficiency of functional macrophages. In consequence, apoptotic cells cannot be efficiently cleared, and instead, they undergo secondary necrosis (Moore and Tabas, 2011). Therefore, there is a formation of lipid-rich necrotic core, being a hallmark of advanced lesions, referred as atheroma. Also, in response to cytokines and growth factors secreted by macrophages and T cells, smooth muscle cells migrate from the medial to the intimal layer of a blood vessel wall. Vascular smooth muscle cells (VSMCs) are responsible for fibrous cap

formation, which is a layer of collagen rich ECM that covers both fatty streak and necrotic core (Lusis, 2000). At this stage of atherosclerosis, referred as fibroatheroma, the early symptoms of VC may occur.

In consequence of fibrous cap disruption within vulnerable plaque, the plaque content is exposed to the bloodstream allowing platelet aggregation as well as subsequent thrombus formation at the site of the rupture (Fig. 2). Complicated lesions contribute to occlusion of narrowed arteries which may lead to acute coronary syndromes such as myocardial and cerebral infarction, due to insufficient oxygen supply to the heart and the brain (Virmani *et al.*, 2002).

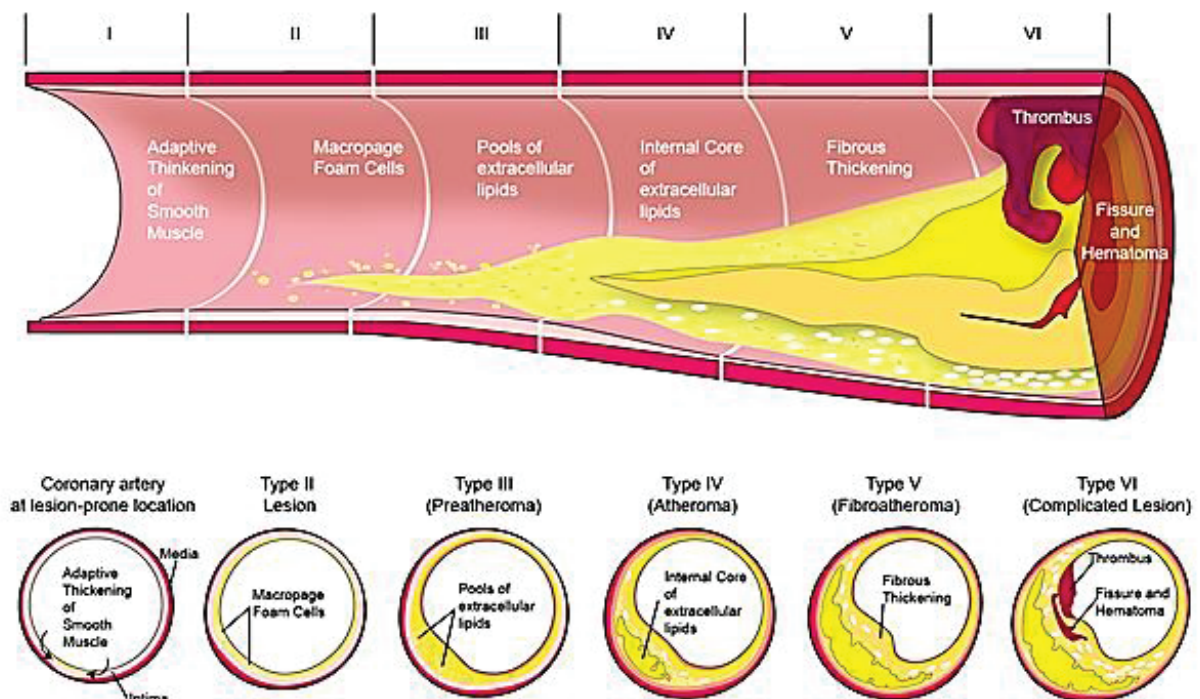


**Figure 2. Stages of atherosclerosis progression** (adapted from *Stary et al., 1995*).

Regarding early events of atherosclerosis, they may occur before the age of ten of citizens living in industrialized societies. Even in the first decade of life, proteoglycan-rich susceptible areas were detected within the blood vessel walls (Doherty *et al.*, 2004). Also, the early lipoprotein retention is possible to take place during this period. In the teens, responses to lipoprotein retention are likely to begin, as well as monocyte entry into the endothelium. The age of twenty and above, is characterized by the appearance of advanced responses, including maladaptive inflammation and cell death (Tabas *et al.*, 2007).

Under normal conditions, the arterial intima maintains vessel wall homeostasis by production of anti-inflammatory and cytostatic agents, thus, it protects the arteries from

the unfavourable processes of leukocyte, platelet and VSMC adhesion and proliferation. Atherosclerosis begins as a result of increased permeability of endothelium to biologically active lipoproteins, leading monocyte recruitment and foam cell formation. Moreover, another pathological process which may proceed simultaneously is endothelial dysfunction, being the consequence of an increase in reactive oxygen species and a decreased level of a free radical, nitric oxide.

### **1.1.3. The role of lipids, lipoproteins and fatty acids in atherosclerosis**

Cholesterol metabolism is precisely controlled, however, disruption of its homeostasis by different factors may result in various disorders. It is known for almost a century that accumulation of lipids in the intimal layer of a vessel wall, especially excess cholesterol, is a hallmark of atherosclerosis (Steinberg, 2005). Cholesterol is a principal sterol synthesized by all animals. It is a major structural component of cell membranes, is essential to keep their integrity and fluidity, and is derived either from nutrition or endogenous synthesis (McNamara, 2000). A key function of this lipid is the assembly and maintenance of lipid raft microdomains (Simons and Ikonen, 2000). Moreover, it serves as a precursor for biosynthesis of steroid hormones, bile acid and vitamin D.

Because of its hydrophobic nature, free cholesterol is practically insoluble in aqueous environments, that is why lipoproteins are particles which are the most appropriate for cholesterol transport via bloodstream. Lipoproteins are assemblies consisting of hydrophobic core of cholesteryl esters and triglycerides surrounded by hydrophilic monolayer of phospholipids, free cholesterol and apolipoproteins. Apolipoproteins can be recognized and bound by specific receptors on cell membranes in order to carry their lipid cargo specifically towards its destination. Thus, apolipoproteins are kind of molecular addresses which are necessary for the distribution and delivery of fats around the body (Getz and Reardon, 2009). There are different classes of circulating lipoproteins such as chylomicrons, very low-density lipoproteins (VLDL), low-density lipoproteins (LDL) and high-density lipoproteins (HDL).

LDL is a major atherogenic lipoprotein and together with apolipoprotein B100 (ApoB100), the main structural protein of LDL, is directly associated with the initiation of early atherogenesis. In consequence of subendothelial retention, aggregated LDLs are prone to oxidative modifications. The precise mechanisms responsible for lipoprotein modification are not completely understood, however, two secretory enzymes, phospholipase A2 and sphingomyelinase, were shown to be responsible for lipoprotein oxidation and hydrolysis (Moore and Tabas, 2011). Also, several other enzymes, such as lipoxygenase and nicotinamide

adenine dinucleotide phosphate hydrogen (NADPH) oxidase for instance, produce strong oxidants able to easily oxidize lipoproteins (Przybylska *et al.*, 2016). In contrary, dietary antioxidants appear to protect from LDL oxidation.

Four main fatty acids: palmitic acid, stearic acid, oleic acid and arachidonic acid constitute the majority of the total fatty acid pool in atherosclerotic plaques of *apoE<sup>-/-</sup>* mice (Freigang *et al.*, 2013). According to observations of Pilz and collaborators, increased level of free saturated fatty acids in the circulation exert a negative effect on cardiovascular system and is associated with a risk of atherosclerosis (Pilz *et al.*, 2006). Studies conducted in healthy subjects provided the evidence that free saturated fatty acids may directly induce oxidative stress and activate the immune response (Tripathy *et al.*, 2003). Palmitate was shown to activate the nucleotide-binding domain, leucine-rich repeat and pyrin domain 3 (NLRP3) inflammasome, resulting in increased interleukin (IL)-1 $\beta$  secretion (Wen *et al.*, 2011). Several fatty acids, especially oleic acid, have been recently identified as potent inducers of vascular inflammation by selective stimulation of the release of IL-1 $\alpha$ , providing a link between metabolic stress and innate inflammatory response in atherosclerosis (Freigang *et al.*, 2013). On the other hand, increased intake of unsaturated fatty acids, such as eicosapentaenoic acid (EPA) and docosahexaenoic acid (DHA), was shown to act beneficially on cardiovascular system by reducing the outcomes related to coronary heart disease (Wang *et al.*, 2006). This is the reason why the consumption of an appropriate amount of dietary unsaturated fatty acids is important for the prevention of cardiovascular complications.

#### **1.1.4. The role of cholesterol crystals in atherosclerosis**

Around thirty years ago, Small and collaborators characterized physical properties of cholesterol accumulated in the arteries. Interestingly, they detected extracellular cholesterol in a crystal form in advanced atherosclerotic lesions (Small, 1988). Later, Abela and colleagues demonstrated that crystal formation is responsible for increased volume of lipid-rich necrotic cores *in vivo* (Abela and Aziz, 2005). Also, they observed that cholesterol crystallization *in vitro* results in the formation of large sharp-edged crystals with a potential to damage biological membranes.

Although these crystals were firstly detected in advanced plaques, further observations in human and mice revealed their presence in early lesions as well, where they may contribute to plaque vulnerability and rupture (Grebe and Latz, 2013). Indeed, scanning electron microscopy analysis of human coronary arteries confirmed this hypothesis, providing



the evidence that cholesterol crystals perforated the fibrous cap only in patients who died from acute coronary syndrome (Abela *et al.*, 2009).

At the cellular level, it seems that the presence of crystalline cholesterol inside the cells may result either from accumulation and saturation of free cholesterol (Tangirala *et al.*, 1994) or phagocytosis of crystals by macrophages (Dewell *et al.*, 2010; Rajamäki *et al.*, 2010). Moreover, saturation of free cholesterol in macrophages was shown to have a cytotoxic effect (Kellner-Weibel *et al.*, 1999).

Interestingly, crystalline cholesterol has been shown to exert an immunostimulatory effect during the development of atherosclerosis. Cholesterol crystals were observed to colocalize with inflammatory cells in a vessel wall, where they activate the immune response resulting in secretion of cytokines from the IL-1 family, mainly IL-1 $\beta$  (Dewell *et al.*, 2010). Furthermore, a recent study suggest that HDL particles may reduce cholesterol crystal-induced inflammation by inhibiting inflammasome activation (Thacker *et al.*, 2016).

## 1.2. Vascular calcification in atherosclerosis

The aorta is the main and the largest artery in the human body, originating from the left ventricle of the heart and extending down to the abdomen, where it splits into two smaller arteries. The aorta distributes oxygenated blood to all parts of the body through the systemic circulation. Arterial wall is composed of three distinct layers: the tunica intima (endothelium), tunica media (the layer of VSMCs along with elastic fibers) and adventitia (myofibroblasts and blood vessels) (**Fig. 3**). Moreover, coronary arteries are the arteries of the coronary circulation that transport blood into and out of the cardiac muscle. They are mainly composed of the left and right coronary branched arteries. Atherosclerosis may affect both large and coronary arteries, however, coronary arteries or their branches often become seriously blocked.

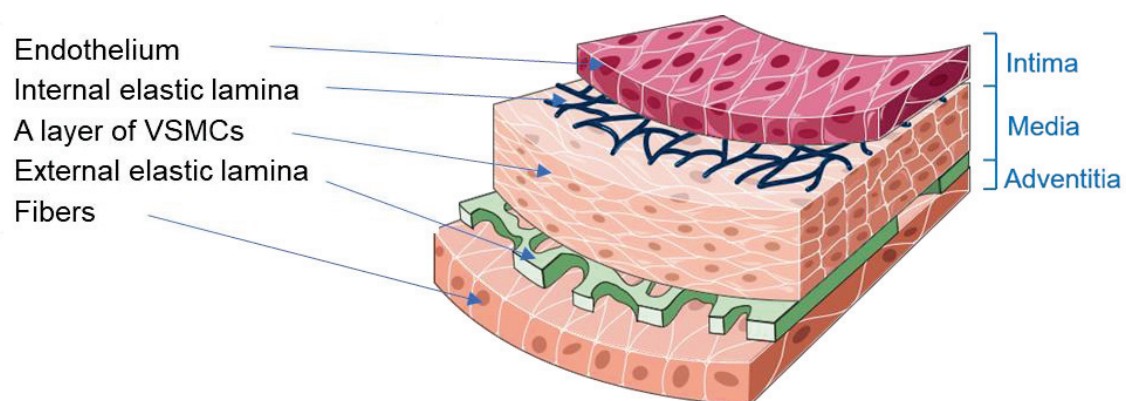


**Figure 3. Artery physiology** (*Servier Medical Art* database, modified).

### 1.2.1. Macrocalcification in atherosclerosis

It is known for decades that advanced human atherosclerotic plaques frequently become calcified. In the case of atherosclerosis, calcification occurs exclusively in the intimal (endothelial) layer of an artery wall (Stary, 2000). It was shown that the composition of calcified atherosclerotic plaque is like that of bone, consisted of carbonated apatite and the predominance of glycosaminoglycans (GAGs) (Duer *et al.*, 2008). It has been estimated that over 70% of atherosclerotic plaques observed in the aging population are calcified (Mintz *et al.*, 1995). From the histological point of view, calcifications with the size of 5 mm and above were defined as macrocalcifications (Pugliese *et al.*, 2015). In advanced lesions of *apoE*<sup>-/-</sup> mice, cells resembling chondrocytes as well as collagen type II were detected together with apatite crystal deposits (Rosenfeld *et al.*, 2000; Rattazzi *et al.*, 2005) (Fig. 4). Therefore, macrocalcifications may be formed as a result of a process analogical to physiological endochondral ossification (Fitzpatrick *et al.*, 1994).

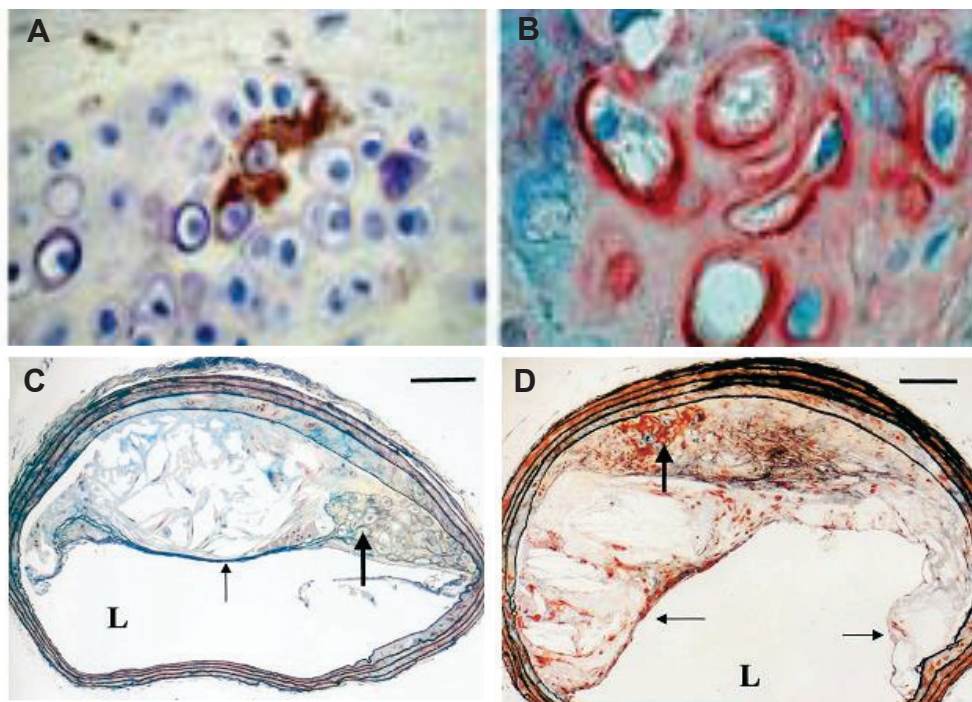


**Figure 4. Chondrocyte-like cells found in advanced atherosclerotic lesions of *apoE*<sup>-/-</sup> mice.** Chondrocyte-like cells within small areas of calcification in the innominate arteries from *apoE*<sup>-/-</sup> mouse between 45 and 75 weeks of age; von Kossa stain for apatite (A); Immunostain with anti-type II collagen antibody (B) (Rattazzi, *et al.*, 2005). Chondrocyte-like cells detected in the artery of a 42-week old *apoE*<sup>-/-</sup> mouse (C, **thick black arrow**) and in the artery of a 60-week old *apoE*<sup>-/-</sup> mouse (D, **thick black arrow**) (Rosenfeld *et al.*, 2000).

Increased biomechanical stresses in the fibrous cap of atherosclerotic plaques contribute to plaque rupture and, consequently, to thrombosis and myocardial infarction. Although coronary calcification is thought to be a predictor of cardiovascular events, the relationship between atheroma calcification and biomechanical stress is not well established. Interestingly, according to studies of Huang and collaborators, macrocalcifications do not increase fibrous cap stress in typical ruptured or stable human coronary atherosclerotic lesions. Thus, macrocalcifications do not seem to decrease the mechanical stability of the atherosclerotic plaques of coronary arteries (Huang *et al.*, 2001). Conversely, it was proposed that macrocalcifications prevent the immune response by serving as a barrier against further accumulation of inflammatory cells (Pugliese *et al.*, 2015).

### **1.2.2. Microcalcification in atherosclerosis**

Recent findings suggest that not all calcifications are equivalent with determination of plaque stability. Intravascular ultrasound analysis revealed that it is the size and the extent of calcium deposits which influence plaque stability (Ehara, 2004). High-resolution micro-computed tomography ( $\mu$ CT) analysis revealed distinct morphology of atherosclerotic plaque calcifications (**Fig. 5**). Minor calcifications were discovered at the early stages of atherosclerosis, which were not detectable before by techniques characterized by a lower resolution. Those calcifications with a diameter less than 10  $\mu$ m were classified as microcalcifications (Pugliese *et al.*, 2015). Spotty microcalcifications have been observed in early atherosclerotic lesions, before chondrocytes or osteoblasts can be detected in the plaques (Rojiers *et al.*, 2011). It is likely that microcalcifications are characterized by a sheet-like morphology, whereas macrocalcifications correspond to osteoid metaplasia (Herisson *et al.*, 2011).

Based on an interesting *in silico* analysis, it was proposed that microcalcifications are particularly dangerous when located in a fibrous cap (Vengrenyuk *et al.*, 2010). Indeed, a histology and  $\mu$ CT analysis of 22 non-ruptured human atherosclerotic plaques revealed that almost all fibrous caps contained microcalcifications with a size between 0.5 and 5  $\mu$ m, and, those growing above 5  $\mu$ m were identified as particularly harmful (Kelly-Arnold *et al.*, 2013). The presence of microcalcifications ( $> 5 \mu$ m) within the cap of human fibroatheroma has been shown to produce a 200-700% increase in local biomechanical stress, being the cause of transformation of a stable plaque into a vulnerable one (Maldonado *et al.*, 2015).



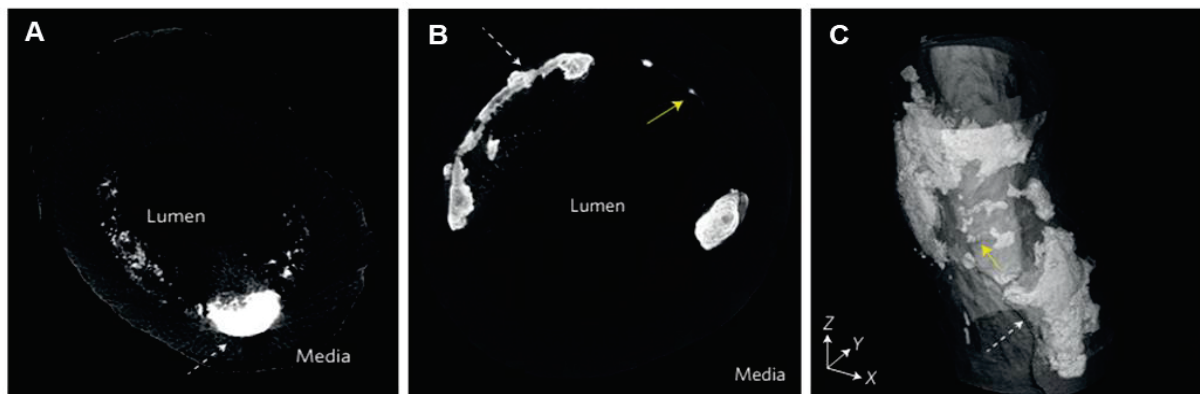


**Figure 5. Distinct morphology of atherosclerotic calcifications.** Apical views from a  $\mu$ CT scan of: a coronary artery with large calcification (**A, dashed arrow**); a carotid artery with large calcification (**B, dashed arrow**) and microcalcifications (**B, yellow arrow**). 3D reconstruction of  $\mu$ CT sections of a carotid artery with large (**C, dashed arrow**) and small (**C, yellow arrow**) calcifications (Hutcheson *et al.*, 2016).

These observations suggest that microcalcifications are much more dangerous for human health than macrocalcifications of advanced plaques (Hutcheson *et al.*, 2014). Thus, the presence of microcalcifications within early atherosclerotic lesions may serve as a predictor of vulnerable plaque rupture. The identification microcalcifications by new imaging methods may allow early identification and prevention of acute cardiovascular events. Therefore, it is crucial to understand how microcalcifications are formed, for future efficient prediction of acute coronary complications.

### 1.2.3. Therapeutic strategies against atherosclerosis and vascular calcification

#### Prevention

As already mentioned, cardiovascular diseases are the leading cause of death worldwide. What is worrying is that at least 25% of patients experiencing nonfatal acute myocardial infarction or sudden death had no previous symptoms (Greenland *et al.*, 2001). The identification of such asymptomatic individuals is crucial for the introduction of preventive strategies. The coronary artery calcium score (CAC) plays an important role in cardiovascular risk assessment, showing a significant association with the medium- or long-term occurrence of major cardiovascular events (Neves *et al.*, 2017). CAC volume is positively and independently associated with the risk of incident cardiovascular disease and incident heart disease (Criqui *et al.*, 2014). It seems that CAC is a better method to predict coronary

complication than measurement of cholesterol level in the blood. The characterization of coronary-artery calcification by  $\mu$ CT reflects the total coronary atherosclerosis load and the risk of future cardiovascular events.

Positron emission tomography and X-ray computed tomography (PET/CT) imaging of atherosclerosis using  $^{18}\text{F}$ -sodium fluoride ( $^{18}\text{F}$ -NaF) has the potential to identify pathologically high-risk microcalcification (Irkle *et al.*, 2015).  $^{18}\text{F}$ -NaF PET/CT imaging can distinguish between areas of macro- and microcalcification. This is the first and only currently available clinical imaging platform that can non-invasively detect culprit and non-culprit coronary plaques in patients with atherosclerosis (Joshi *et al.*, 2014; Dweck *et al.*, 2016).

### Therapeutic strategies

Several therapies exist to treat one of the diseases underlying VC, which is atherosclerosis. The most common strategy is the use of statins, which are inhibitors of 3-hydroxy-3-methylglutaryl-coenzyme A (HMG-CoA) reductase. In order to understand the therapeutic effect of these lipid-lowering agents, it is necessary to know the principles of cholesterol metabolism in a human body. The cellular level of cholesterol is regulated by distinct mechanisms, such as, LDL receptor-mediated endocytosis, HDL-mediated reverse transport and regulation of HMG-CoA activity. Cholesterol synthesis, similarly to other sterols, begins from the conversion of acetyl-CoA units, that are subsequently converted into HMG-CoA, which in turn is transformed into mevalonate by HMG-CoA reductase, a rate-controlling enzyme of mevalonate pathway.

Recent data suggest that statins, in addition to their lipid-lowering ability, can also reduce the production of reactive oxygen species and increase the resistance of LDL to oxidation (Rosenson, 2004). While the introduction of statins was a milestone in prevention of cardiovascular complications, they are not able to eliminate atherosclerotic cardiovascular disease (Ladeiras-Lopes *et al.*, 2015). Also, they may cause some side effects, such as muscle pain and increased risk of diabetes mellitus.

Apart from lowering LDL cholesterol, it is very important to apply some immunomodulatory strategies targeting chronic inflammation during atherosclerosis. Therefore, several anti-inflammatory pharmacotherapies have been elaborated, for example targeting IL-1 $\beta$  (Khan *et al.*, 2015; Yamashita *et al.*, 2015). Besides, the inhibitors of ECM enzymes, such as MMPs and cathepsins were shown as possible targets for the prevention of plaque rupture (Rader and Daugherty, 2008).

However, no efficient therapy is currently available to reverse or prevent VC in atherosclerosis. Efficient therapeutic strategies are necessary to elaborate based on the correct understanding of the underlying mechanisms driving the process of VC. One of the obstacles is the similarity of pathological arterial calcification and physiological bone mineralization.

PP<sub>i</sub> is a molecule which was shown to decrease not only physiological mineralization, but also VC (Towler, 2005). Indeed, O'Neill and collaborators have shown a negative correlation between plasma PP<sub>i</sub> and VC in end-stage renal disease (O'Neill *et al.*, 2010). PP<sub>i</sub> administration in uremic rodents strongly decreased VC (O'Neill *et al.*, 2011; Riser *et al.*, 2011). However, PP<sub>i</sub> usage is not suitable for long-term treatment for humans, because it cannot be administered orally and its half-life in circulation is very short, around 30 min (Persy and McKee, 2011).

Bisphosphonates are analogues of PP<sub>i</sub>. It was shown that administering bisphosphonates prevented atherosclerotic plaque formation in rabbits and monkeys by inhibition of calcification (Kramsch *et al.*, 1981). Many of bone disease treatments, such as bisphosphonates, calcitriol and estradiol may interfere with VC.

Another emerging strategy against VC is the inhibition of tissue-nonspecific alkaline phosphatase (TNAP) activity. TNAP is considered as a druggable target for the treatment and/or prevention of VC associated with chronic kidney disease. Until recently, levamisole was the most potent TNAP inhibitor available commercially, however, it cannot be used *in vivo*, since 1 mM levamisole is necessary to block calcification in cultures of aortas from uremic rats, a level which cannot be achieved *in vivo* (Debray *et al.*, 2013). Indeed, levamisole is not entirely specific for TNAP isozyme, has low affinity and is not particularly effective in inhibiting the pyrophosphatase activity of TNAP (Sergienko *et al.*, 2009). In this context, two laboratories have developed novel TNAP inhibitors. Jose Luis Millan's group in USA has developed TNAP inhibitors with higher potency and selectivity than levamisole (Narisawa *et al.*, 2007; Sergienko *et al.*, 2009; Sidique *et al.*, 2009). Also, in the MEM<sup>2</sup> laboratory (ICBMS, Lyon University) a family of inhibitors more potent than levamisole has been patented (Debray *et al.*, 2013).

### **1.3. Molecular mechanisms of physiological mineralization**

Physiological mineralization is a process necessary for the formation of mineralized skeleton during fetal development. However, it concerns also remodeling processes which are constantly continued during ontogenesis, in order to adapt to changing biomechanical environment by the removal of older, microdamaged bone and replacement with new,

mechanically stronger bone, preserving bone strength. At a first glance, bone seems to be a static tissue, but in fact, it is a dynamic system that plays multiple functions within the body.

Mineralized skeleton permits the movement and locomotion of the body by serving as an attachment for muscles, it provides also a scaffold that protects internal organs as well as comprises the environment for hematopoiesis. Moreover, it serves as a repository of calcium and phosphate ions. Bone morphogenetic proteins (BMPs), Wnts, fibroblast growth factors (FGFs), hedgehog proteins, insulin-like growth factors and retinoids are molecules being essential for normal bone formation. These locally produced factors undergo regulation by systemic factors such as growth hormone, parathyroid hormone (PTH), estrogen, androgen, vitamin D and glucocorticoids that control bone growth (Kronenberg, 2003).

Interestingly, it has been shown that bone may function as an endocrine organ being in charge of producing hormones, such as osteocalcin (OCN) and fibroblast growth factor-23 (FGF-23) (Lee *et al.*, 2007; Fukumoto and Martin, 2009). Osteoblasts secrete OCN which stimulates insulin production by pancreatic  $\beta$ -cells, but also activates peripheral tissues to increased glucose uptake (Lee *et al.*, 2007). FGF-23 is produced by osteocytes and acts on kidney as an inhibitor of vitamin D hydroxylation as well as a promoter of phosphorus excretion. Vitamin D has a well-known beneficial effect on bone homeostasis, being required for normal bone formation. Interestingly, recent findings suggest that this vitamin plays a dual role in mineralization. On the one hand, in case of sufficient calcium supply, vitamin D and its metabolites improve the calcium balance and facilitate mineral deposition in bone matrix. On the other hand, in case of calcium deficiency, biologically active form of vitamin D enhances bone resorption, thus, it has an inhibitory effect on mineralization (Eisman and Bouillon, 2014).

There are two subtypes of bone tissue: cortical (compact) bone and cancellous (trabecular or spongy) bone. Cortical (compact) bone is harder, stronger and stiffer than trabecular bone. Interestingly, cortical bone takes up 80% of the total weight of a human skeleton. Cancellous (trabecular) bone is softer and weaker than compact bone. It is highly vascularized and frequently contains red bone marrow. Trabecular bone occupies the inner part of long bone, whereas the outer region is built by a thick layer of cortical bone that contains Haversian canals that allows contact of bone tissue with nerves as well as blood and lymphatic vessels (**Fig. 6A**).

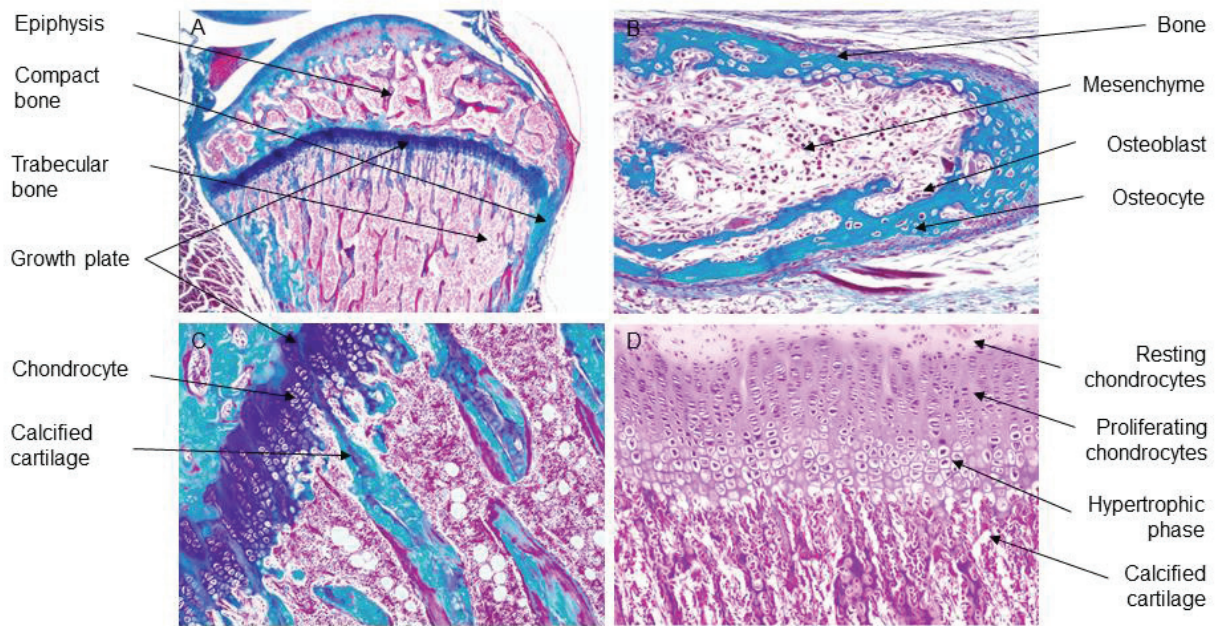


**Figure 6. Bone and cartilage histology.** The specimens were stained with Masson's Trichrome which stains cartilage in violet and mineralized bone in blue. Images of long bone morphology (A), intramembranous ossification (B), endochondral ossification (C), chondrocyte growth sequence (D) were presented ([http://medcell.med.yale.edu/histology/bone\\_lab](http://medcell.med.yale.edu/histology/bone_lab)).

Regarding the initiation of human ossification, long bone formation begins during the third month of fetal development. During the fourth month, most primary ossification centers appears in the bone diaphysis. Secondary ossification mostly occurs after birth. While the period between birth to the age of five, secondary ossification centers appear in the epiphysis. Over time, ossification is spreading rapidly from the ossification centers and various bones are becoming ossified. Between the age of twenty-three and twenty-five, the sternum, clavicles, and vertebrae become completely ossified. By the age of twenty-five, nearly all bones are completely ossified, and the growth plate disappears.

Bone is a metabolically active tissue composed of cells such as osteocytes, osteoblasts and osteoclasts. Osteoblasts mediate the process of bone formation by increased TNAP activity and the ability to release matrix vesicles (MVs). Besides, osteocyte is the most abundant cell type in bone. Osteocytes are kind of mechanotransducers that respond to mechanical forces in order to regulate bone homeostasis (Bonewald, 2011). These cells are in charge of keeping a balance between the processes of bone formation and bone resorption. Mineralized ECM is not convenient for diffusive transport of metabolites, that is why nutrients are transmitted by osteocyte cytoplasmic flagella, by which osteocytes are in direct contact with blood vessels.



Bone resorption is mediated by osteoclasts. Osteoclast formation, activation, and resorption is regulated by the ratio between receptor activator of nuclear factor kappa-light-chain-enhancer of activated B cells (NF- $\kappa$ B) ligand (RANKL) and osteoprotegerin (OPG) (Clarke, 2008; Walsh and Choi, 2014). Activated osteoclasts secrete hydrogen ions causing local acidification. In consequence, inorganic ECM components undergo dissolution. In parallel, organic phase of ECM is degraded by lysosomal enzymes, followed by phagocytosis and intracellular digestion of fragmented organic structures.

### **1.3.1. Osteoblast differentiation and intramembranous ossification**

Bone develops by two distinct processes, either through direct conversion of connective tissue into bone, known as intramembranous ossification, or indirectly through the replacement of an initially formed cartilage by bone tissue during the process called endochondral ossification. In general, flat bones form by membranous bone formation, whereas long bones are formed by a combination of endochondral and membranous ossification.

Intramembranous ossification is a process of direct conversion of embryological mesenchymal tissue into bone, without the intermediate stage of cartilage formation. The process begins when mesenchymal cells differentiate into osteoblasts, having the ability to secrete osteoid (**Fig. 6B**), principally composed of fibrillar collagen type I, being a scaffold for subsequent mineral deposition. At the end of membranous ossification, approximately 50 to 70% of osteoblasts undergo apoptosis, while the other cells become inactive bone-lining cells or osteocytes (Clarke, 2008). For instance, craniofacial bones and clavicles are formed by this process.

Osteoblasts originate from local mesenchymal stem cells (MSCs) called osteoprogenitor cells, whereas osteoclasts derive from macrophages, differentiating from bone marrow hematopoietic stem cells. Runt-related transcription factor 2 (Runx2) is the major transcription factor of MSC to osteoblast differentiation, however, there are several other transcription factors (ex.  $\beta$ -catenin, osterix, ATF4) and growth factors, such as members of Wnt and bone morphogenic protein families, contributing to this process (Fakhry, 2013). MSCs expressing Runx2 differentiate into immature osteoblasts, which are characterized by the expression of proteins such as collagen type I, TNAP and osteopontin (OPN). Subsequently, these cells further mature, mineralize their ECM and begin to express OCN.

### 1.3.2. Chondrocyte differentiation and endochondral ossification

Long bones are generally formed through endochondral ossification, a process being essential also during long bone elongation and the natural healing of bone fractures. Bone is synthesized over a hyaline cartilage template within a growth plate located just below the epiphysis of long bone and comprises a region in which cartilage proliferates and undergoes mineralization (**Fig. 6C**). In other words, during endochondral ossification, hyaline cartilage is formed as a precursor of bone formation.

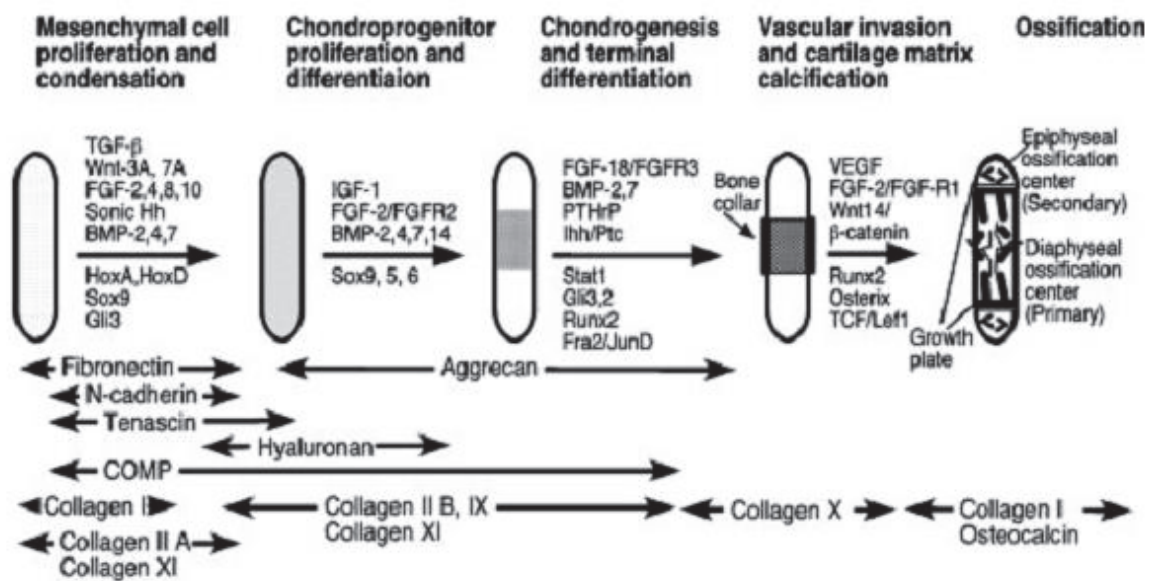


**Figure 7. Control of chondrogenesis during the development of long bones (Goldring *et al.*, 2006).**

Endochondral ossification begins when MSCs form condensations (**Fig. 7**). Cells of condensations become chondrocytes, which are called pre-hypertrophic chondrocytes. These cells produce a matrix rich in collagen type II in the primary ossification center, where they begin to undergo hypertrophy. Hypertrophic chondrocytes secrete collagen type X being a protein necessary for the process of hematopoiesis (Sweeney *et al.*, 2010). Hypertrophic chondrocytes perform multiple tasks during ossification. They direct the mineralization of the surrounding matrix and attract blood vessels from the perichondrium through the production of vascular endothelial growth factor (VEGF). Hypertrophic chondrocytes direct neighboring perichondrial cells to become osteoblasts, which in turn secrete a characteristic matrix, forming a bone collar. Finally, hypertrophic chondrocytes undergo apoptosis. Osteoblasts of primary spongiosa are precursors of eventual trabecular bone, whereas

osteoblasts of bone collar become cortical bone. At the bone ends, the secondary ossification center forms through cycles of chondrocyte hypertrophy, vascular invasion and osteoblast activity. The growth plate below the secondary center of ossification forms the columns of proliferating chondrocytes, being in charge of lengthening the bone. Finally, hematopoietic marrow expands in marrow space along with stromal cells (Kronenberg, 2003).

During chondrogenesis, the environment becomes hypoxic, and hypoxia inducible factor (HIF-1 $\alpha$ ) is necessary for chondrocyte survival during hypoxia (Magne *et al.*, 2005, Duval *et al.*, 2009). HIF-1 $\alpha$  induces VEGF expression, which in turn activates angiogenesis required for the replacement of cartilage by bone. It is controversial whether programmed cell death of hypertrophic chondrocytes plays an active or passive role in cartilage mineralization (Cheung *et al.*, 2003). What is known is that chondrocyte terminal differentiation, apoptosis, and type X collagen expression are downregulated by PTH (Harrington *et al.*, 2004). The ECM becomes mineralized in part by hypertrophic chondrocytes (**Fig. 6D**), and later, definitive bone matrix is formed through the coordinated action of mineralizing osteoblasts and bone resorbing osteoclasts which erode cartilage and build bone.

Chondrogenesis is subjected to complex regulation by an interaction of various signals (**Fig. 7**). It is initiated by MSC condensations under the control of TGF- $\beta$  which induces the expression of Sox9 transcription factor that belongs to the SOX protein family, known for being responsible for regulation of the development of various organs. MSCs in the presence of Sox9 become pre-hypertrophic chondrocytes. Then, TGF- $\beta$  and BMP-2 activate Wnt/ $\beta$ -catenin signaling pathway that mediates chondrocyte hypertrophic differentiation through the activation of Runx2 transcription factor (Dong *et al.*, 2006). Runx2 controls the hypertrophic phase of chondrocyte differentiation (Yoshida *et al.*, 2004). In hypertrophic chondrocytes, forced expression of Runx2 was shown to induce the expression of collagen type X and matrix metalloprotease-13 (MMP-13) as well as TNAP activity (Goldring *et al.*, 2006). MMP13 is responsible for the degradation of cartilaginous collagens (especially collagen type II) and proteoglycans (mainly aggrecan), contributing to the process of cartilage replacement by bone (Little *et al.*, 2002). Therefore, Runx2, MMP-13, collagen type X and TNAP are specific markers of chondrocyte hypertrophy.

BMP signaling is important for the formation of mesenchymal condensations (Li and Cao, 2006) and subsequent differentiation towards chondrocytes (Pizette and Niswander, 2000). BMP-2, -3, -4, -5 and -7 are expressed in perichondrium, BMP-2 and -6 are expressed in hypertrophic chondrocytes, while BMP-7 is expressed in proliferating chondrocytes (Kronenberg, 2003). Interestingly, BMP-2 and BMP-7 display opposite actions on chondrocyte



differentiation. Differentiation of MSCs towards chondrocytes may be stimulated by BMP-2, whereas it may be suppressed by BMP-7 (Caron *et al.*, 2013).

Terminal endochondral ossification is controlled by growth factors, mainly BMPs and FGFs, but also PTH, estrogen, androgen, vitamin D and canonical Wnt signaling pathway. Bone morphogenetic proteins (BMPs) are members of transforming growth factor- $\beta$  (TGF- $\beta$ ) superfamily, characterized by a strong ability to induce bone formation. More than 30 BMP-related proteins have been identified. They play a crucial role at different stages of embryogenesis, such as suppression of epithelial growth and stimulation of neural differentiation, being a necessary step during embryonal development. When injected subcutaneously in mice, these growth factors are able to induce endochondral bone formation (Urist and Strates, 1971). Also, they may induce the process of marrow stromal cell differentiation towards osteoblasts, chondrocytes or adipocytes. BMPs stimulate osteoblast differentiation by enhancing the expression of osteogenesis-driving transcription factors such as Runx2 and osterix, as well as osteoblast-related genes encoding TNAP, OCN, collagen type I and OPN. In consequence, differentiated bone cells begin to produce BMPs, which mediate skeletogenesis as well as the maintenance of bone mass within mature skeleton.

BMPs act through cell surface serine/threonine kinase BMP type-I and type-II receptors, which in turn activate intracellular signaling pathways. Smad is the major pathway activated by BMPs, which requires formation of phosphorylated Smad1/5/8 heterocomplexes with Smad 4 to induce translocation into the nucleus. Then, nuclear Smad complexes regulate transcription of BMP target genes through binding to sequence motifs in the promoter regions of BMP-responsive genes, and via interaction with transcription factors. Moreover, Wnt/ $\beta$ -catenin signaling has been shown to be involved in bone biology. It was demonstrated that Wnt autocrine loop mediates the induction of alkaline phosphatase expression and mineralization by BMP-2 in pre-osteoblastic cells (Rawadi, 2003).

BMP activity may be modulated by different antagonists, which are small peptides characterized by a high affinity to BMPs and the ability to prevent their interaction with specific receptors. Noggin is one of BMP antagonists, expressed in Spemann's organizer, being the structure that mediates gastrulation process in the vertebrate embryo. Thus, at the certain stage of development, the embryo secretes noggin to promote neural differentiation and suppress epithelial growth. Regarding the distribution of noggin, it is expressed, as many BMPs, in condensing cartilage and immature chondrocytes as demonstrated in a murine model (Brunet *et al.*, 1998). An important role for BMP signaling during chondrocyte differentiation was supported by the observation of oversized growth plate in *noggin*<sup>-/-</sup> mice (Brunet *et al.*,

1998). Furthermore, addition of BMP-2 delayed terminal differentiation of hypertrophic chondrocytes, whereas noggin accelerated terminal hypertrophic differentiation (Minina *et al.*, 2002). In the case of osteoblasts, noggin expression is limited, however, its transcript levels undergo upregulation by BMP-2, 4 and 6, as a mechanism protective against excessive exposure of skeletal cells to BMPs (Gazzerro *et al.*, 1998).

Cartilage is more elastic than bone. It is because cartilage is mainly consisted of collagen type II that forms fibrous network with collagens type XI and type IX and by abundant proteoglycans that ensure elastic properties of the tissue. It contains chondrocytes, being a unique cell type present within the tissue. Depending on mechanical and structural properties, there are three subtypes of cartilage distinguished: hyaline, fibrocartilage and elastic cartilage (Naumann *et al.*, 2002). They are diversified according to different cellular content as well as distinct ECM composition.

Among all cartilage types, hyaline cartilage is the most abundant in the body. Hyaline cartilage formation governs the generation of long bones, ribs and vertebrae during embryogenesis and development. During ontogenesis, its main function is the reduction of friction within joints, long bone elongation and support. In this type of cartilage, chondrocytes often form clusters. In vertebrate skeleton, hyaline cartilage is present mainly in articular cartilage at the ends of bone where it occurs as a part of a joint. Hyaline cartilage is characterized by a high content of proteoglycans which represent approximately 15% of the wet mass of the tissue. Interestingly, articular cartilage is avascular and devoid of nerves and lymphatic vessels. Chondrocytes are nourished by synovial fluid diffusion through the matrix by mechanical forces.

Fibrous cartilage (fibrocartilage) is also associated with the skeletal system. It is present mainly in knee and spine intervertebral discs. It has been reported that this cartilage subtype occurs temporarily at fracture sites upon healing. Fibrocartilage is a tough form of cartilage that consists of chondrocytes settled among bundles of collagen fibers within the matrix. The principal function of this tissue is dealing with the mechanical stress that occurs between neighboring vertebrae of the spine. Elastic cartilage is present in small organs such as the external ear pinna and eustachian tube, where it ensures flexibility. In this cartilage type, chondrocytes are located within a network of elastic fibers located in the cartilage matrix.

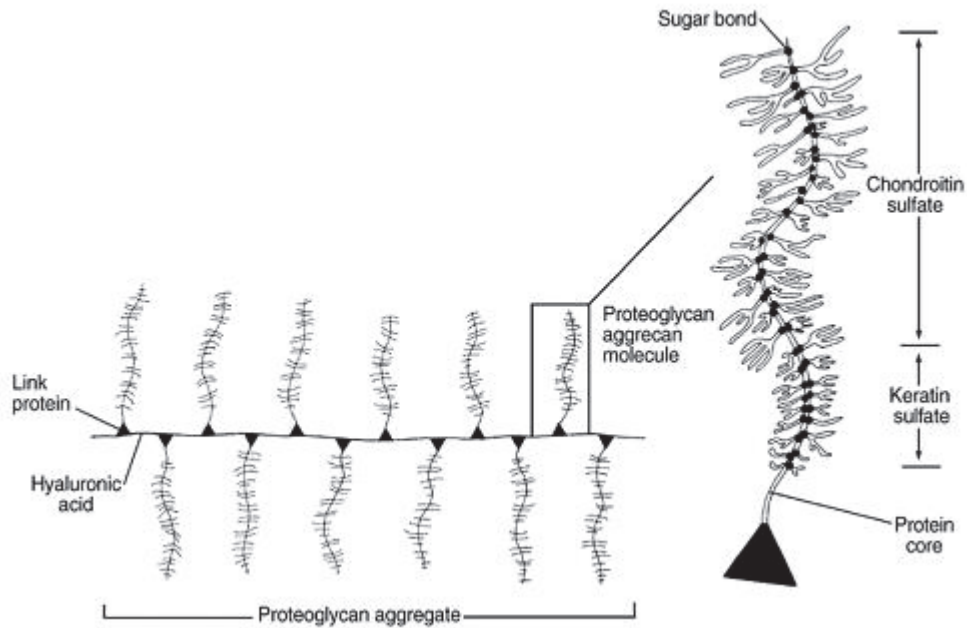


**Figure 8. Aggrecan structure** (Pearle *et al.*, 2005).

Cartilage, especially hyaline cartilage, is enriched in ECM proteoglycans. Approximately 20% of cartilage weight consists of ECM containing mainly proteoglycans and collagens and, in less quantity, noncollagenous proteins, glycoproteins, lipids and phospholipids. Proteoglycans are large molecules comprising a protein core, serine residues and several GAGs, which in case of aggrecans are chondroitin sulfate and keratin sulfate. GAGs are linked by covalent bonds to the protein core. The sulfate groups ensure a negative charge of macromolecule that attract cations, resulting in swelling and elasticity. Proteoglycans create a network by interactions with hyaluronic acid and collagens. The elastic properties of cartilage are provided by hydrophilic proteoglycans, macromolecules containing side chains of GAGs. Also, compact nature of proteoglycans of articular cartilage reduces pressure and liquid phase movements during compression within a joint (Carter and Wong, 2003).

Aggrecan is the most abundant proteoglycan in cartilage. It contains three globular domains and it forms proteoglycan aggregates composed of a central filament of hyaluronic acid with up to one hundred molecules of aggrecan which interacts with a protein part (Kiani *et al.*, 2002) (**Fig. 8**). Other less abundant and smaller proteoglycans like perlecan, versican, lumican, biglycan and decorin are also present in cartilage (Knudson and Knudson, 2001).

### 1.3.3. Matrix vesicles (MVs) as sites of mineral nucleation

Matrix vesicles are extracellular organelles discovered by Anderson in 1970's (Anderson, 1967). A broad range of MVs originating from mineralizing cells have been identified, with a diameter ranging from 100 nm to 300 nm (Anderson *et al.*, 2010). These nanostructures are thought to be involved in the initiation of ECM mineralization by accumulation of  $\text{Ca}^{2+}$  and  $\text{P}_i$  and subsequent apatite formation. Membranous ion channels and transporters are suspected of being in charge of the supply of  $\text{Ca}^{2+}$  and  $\text{P}_i$  ions inside the vesicles.  $\text{P}_i$  transport into MVs may be mediated by  $\text{P}_i$  transporters ( $\text{P}_i\text{T}$ ), whereas annexins (Anx) are putative transporters of  $\text{Ca}^{2+}$  ions.

In consequence of mineral nucleation, it is hypothesized that growing crystals cause the disruption of MV membrane, leading to the release of apatite crystals into the ECM, where mineralization process is continued. During ECM mineralization, crystal expansion is regulated by different molecules and those interactions are necessary to regulate apatite crystal growth. On the other hand, inorganic pyrophosphate ( $\text{PP}_i$ ) is a strong mineralization inhibitor with the crystal binding properties (Addison *et al.*, 2007). One of the ECM protein is OPN, glycoprotein known as an inhibitor of mineralization with strong mineral binding properties (Addison *et al.*, 2007; Yuan *et al.*, 2014). Collagens and proteoglycans interact with the surface of MVs and they rather stimulate mineralization (Kim and Kirsch, 2008). Annexins associated with the surface of MV may interact with those ECM molecules. It was demonstrated that AnxA2 and AnxA6 bind chondroitin sulfate of proteoglycans in a  $\text{Ca}^{2+}$ -dependent manner (Takagi *et al.*, 2002).

Annexins are calcium and lipid binding proteins that are ubiquitous in all eukaryotic organisms (excluding yeasts), from *Arabidopsis thaliana* to *Homo sapiens* (Bandorowicz-Pikula, 2007). Annexins are involved maintenance of  $\text{Ca}^{2+}$  homeostasis in bone cells and in extracellular MVs, where they are putative ion transporters mediating  $\text{Ca}^{2+}$  influx (Balcerzak *et al.*, 2003). Kirsch and collaborators demonstrated that MVs isolated from non-mineralizing hypertrophic chondrocytes showed no significant  $\text{Ca}^{2+}$  uptake, however, the addition of exogenous AnxA2, AnxA5 and AnxA6 restored their ability to take up  $\text{Ca}^{2+}$  (Kirsch *et al.*, 2000). However, annexin structure does not resemble the structure of typical ion channels and probably it rather facilitates calcium binding than transports  $\text{Ca}^{2+}$  itself (Gerke and Moss, 2002).

Annexins may be associated either with outer or inner leaflet of MV membrane (**Fig. 9**). Annexins associated with the inner leaflet of MV may be a part of a structure known

as nucleation core, consisting of three key components: amorphous calcium phosphate (ACP), phosphatidylserine-calcium-phosphate complex (PS-CPLX) and AnxA5 (Wu *et al.*, 1993). *In vitro* studies of synthetic nucleation cores revealed that ACP mediates only 20% of mineral formation. The internal layer of MVs is enriched in phosphatidylserine (PS), a lipid that has a high affinity to  $\text{Ca}^{2+}$  ions and is able to bind both calcium and phosphate (Kirsch *et al.*, 1994). Incorporation of PS was shown to significantly retard the induction time of mineral formation. Interestingly, AnxA5 is able to catalyze the mineral nucleation of CPLX by 10-20 fold by transforming the weakly nucleating binary PS-CPLX into a ternary complex (PS-CPLX-AnxA5) with a powerful nucleation activity (Genge *et al.*, 2007).

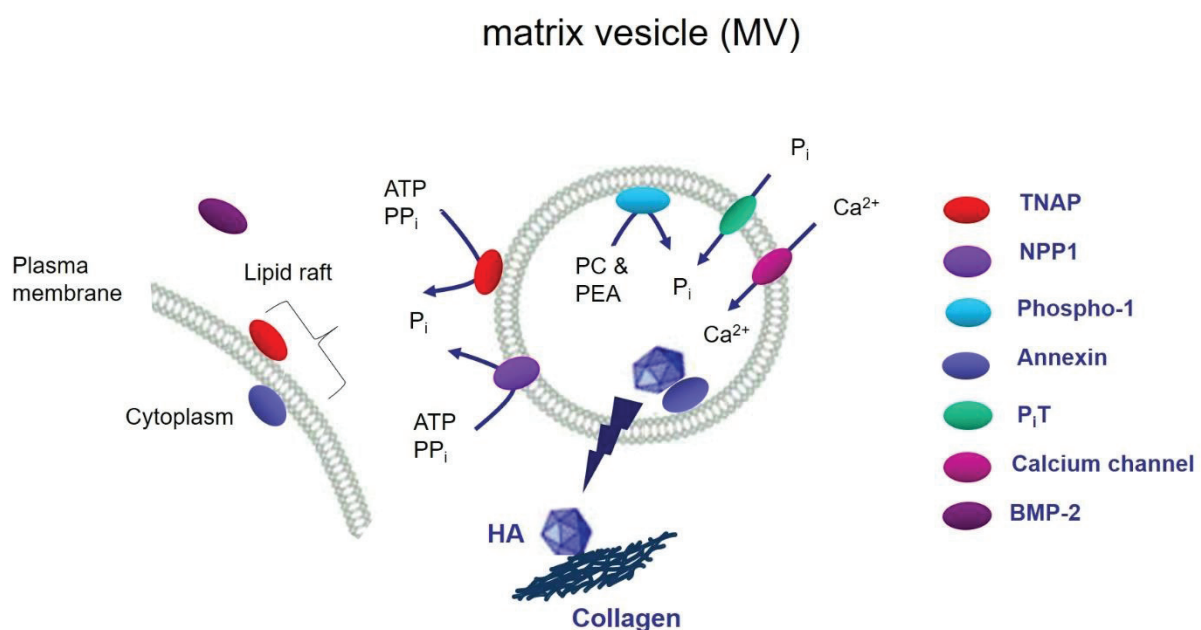


**Figure 9. Schematic diagram of proteins involved in MV-mediated mineralization** (according to Millán, 2013).

Beside AnxA5, it was demonstrated, by Gillette and collaborators, that AnxA2 is a protein involved in osteoblastic mineralization. AnxA2 overexpression resulted in an increase of TNAP activity associated with lipid microdomains in a cholesterol-dependent manner (Gillette, 2003). Conversely, AnxA2 and AnxA5-deficient osteoblasts exhibited decreased TNAP activity (Genetos *et al.*, 2014).

Nevertheless, the fact that mice deficient in annexins develop normal skeleton raises the question about a direct effect of annexins on mineralization process (Brachvogel *et al.*, 2003; Belluoccio *et al.*, 2010; Grskovic *et al.*, 2012). It was demonstrated that mineralizing MVs are enriched in multiple annexins: AnxA1, AnxA2, AnxA4-A7 and AnxA11 (Cmoch

*et al.*, 2011). Therefore, a substitution of AnxA5 and AnxA6 function in MVs by other annexins, AnxA2 for instance, is a possible explanation of the effects observed in knockout animals (Sekrecka *et al.*, 2007).

Various hypotheses were proposed to explain the mechanisms of MV biogenesis, such as budding from cellular membranes, extrusion of preformed structures, cellular degeneration and subunit secretion followed by extracellular assembly (Rabinovitch and Anderson, 1976). Accumulating data and the previous results of our laboratory supports the hypothesis stating that MVs originate from microvilli of cellular plasma membrane (Hale and Wuthier, 1987; Thouverey *et al.*, 2009).

Numerous proteomic analysis of MVs secreted by different mineralizing cells revealed a variety of MV proteins (Balcerzak *et al.*, 2008; Xiao *et al.*, 2009; Thouverey *et al.*, 2011). Among many protein types, TNAP, ectonucleotide pyrophosphatase phosphodiesterase 1 (NPP1) as well as phosphatase orphan 1 (Phospho-1) were identified (**Fig. 9**). NPP1 and TNAP have antagonistic effects on mineral formation due to their opposing functions, either production of PP<sub>i</sub>, the constitutive mineralization inhibitor, by NPP1 or its hydrolysis by TNAP (Hessle *et al.*, 2002). Interestingly, double ablation of *Phospho1* (encoding Phospho-1) and *Alpl* (encoding TNAP), completely abolishes mineralization of osteoblast-derived MVs, leading to the complete absence of skeletal mineralization (Yadav *et al.*, 2011). This strongly suggests that the P<sub>i</sub> needed for initiation of MV-mediated mineralization is produced inside the vesicles by Phospho-1 which cleaves membrane phospholipids, such as phosphatidylcholine (PC) and phosphatidylethanolamine (PEA) (Millán, 2013).

#### **1.3.4. Key proteins involved in mineralization process**

Tissue-nonspecific alkaline phosphatase (TNAP)

Alkaline phosphatases are ubiquitous among organisms, from bacteria to human. Three human isoforms are tissue specific, present in intestine, placenta and germ cells, which are 90–98% homologous. TNAP, encoded by *Alpl* gene, occurs in bone, liver and kidney and is 50% identical to other three isozymes. Moreover, it may be expressed in the central nervous system, fibroblasts and endothelial cells (Millán and Whyte, 2016). During synthesis of the enzyme, monomeric precursors dimerize and each monomer binds one magnesium, two zinc, and one calcium ion as cofactors (Millán, 2006).

The difference between bone, liver and kidney isoforms of TNAP consists of their posttranslational glycosylation which influence and determine their catalytic activities.



For instance, TNAP is O-glycosylated in bone, but not in the liver (Halling Linder *et al.*, 2009). Interestingly, a structure referred as crown domain is present exclusively in mammalian alkaline phosphatases (Fig. 10). In the case of TNAP, this domain stabilizes the binding of uncompetitive TNAP inhibitors as well as determines isozyme-specific properties, such as heat stability and association to collagen (Le Du and Millan, 2002).

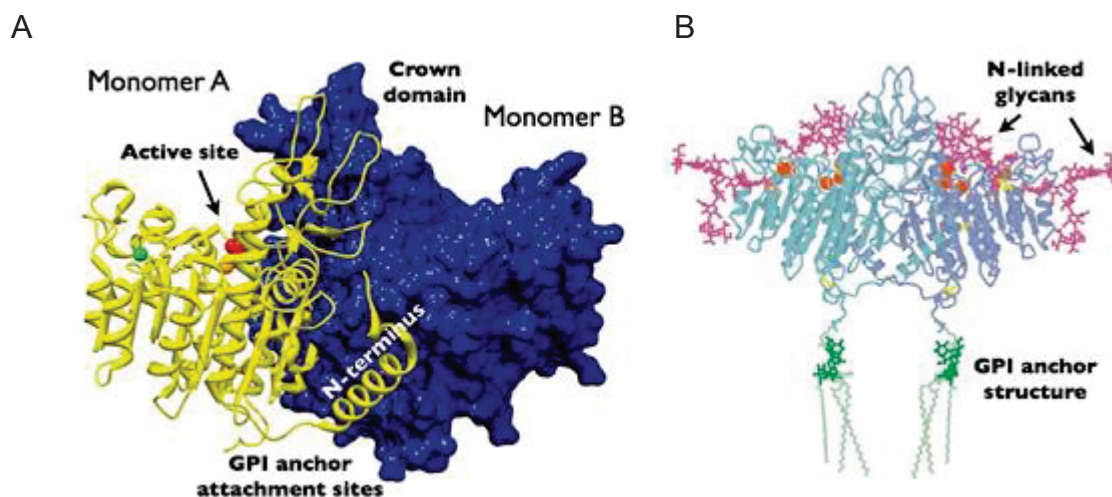


**Figure 10. Three-dimensional structure of alkaline phosphatase (A).** Modeled structure of the GPI anchor attached to the 3D structure of PLAP (B) (Buchet *et al.*, 2013a).

Regarding catalytic properties, alkaline phosphatases catalyze hydrolysis of phosphoric acid monoesters with release of inorganic phosphate ( $P_i$ ). For instance, TNAP has the ability to hydrolyze nucleotides such as adenosine triphosphate (ATP) and its metabolites. However, the known physiological substrates of TNAP include  $PP_i$ , and pyridoxal-5'-phosphate, being a predominant form of vitamin B6 (Buchet *et al.*, 2013a).

Mammalian alkaline phosphatases, unlike these of bacteria, are cell surface-bound proteins that attach to the membrane via a glycosylphosphatidylinositol (GPI) anchor. Bone TNAP is a GPI-anchored protein localized on the plasma membrane of osteoblasts and hypertrophic chondrocytes. Whether TNAP anchorage is necessary for mineralization is debatable. Nevertheless, GPI anchor may be cleaved by the enzymatic action of phospholipases found in plasma membranes, and may be released into the circulation and other biological fluids.

Mutations in *Alpl*, the human gene encoding TNAP cause hypophosphatasia, a rare metabolic bone disease, characterized by skeletal hypomineralization due to TNAP deficiency and extracellular accumulation of  $PP_i$  (Millán and Whyte, 2016) A mild form of this disease

is characterized by poorly mineralized bones, rickets and teeth loss in children as well as osteomalacia and dental problems in adults. A severe form of hypophosphatasia results in death of fetuses due to profound skeletal hypomineralization or death of infants as a consequence of rib fractures and respiratory dysfunction.

Similarly, deletion of the gene encoding TNAP, *Akp2*, in mice, caused symptoms similar to those of hypophosphatasia (Fedde *et al.*, 1999) and abnormal craniofacial bone development (Liu *et al.*, 2014). Conversely, *in vivo* overexpression of murine TNAP increased skeletal mineralization (Narisawa *et al.*, 2013). This effect may be explained by the fact that TNAP may function not only as a major pyrophosphatase during mineralization, but also as an enzyme that modifies phosphorylation status of OPN. It is known that OPN requires post-translational phosphorylation in order to act as mineralization inhibitor (Gericke *et al.*, 2005; Yuan *et al.*, 2014).

As already mentioned, TNAP and Phospho-1 are two phosphatases regulating the process of mineral nucleation. It is hypothesized that Phospho-1 is responsible for initiating crystal formation by  $P_i$  generation in the MV interior, supported by  $P_i$  influx mediated by  $P_i$ Ts. Interestingly, at the level of MVs, NPP1 acts more as an ATPase and pyrophosphatase than as an enzyme generating  $PP_i$  (Ciancaglini *et al.*, 2009). Thus, TNAP and NPP1 are in charge of  $PP_i$  hydrolysis in the perivesicular space and the extravesicular progression of mineralization (Millán, 2013) (**Fig. 9**).

## Collagens

Collagens are the most abundant proteins in mammals, comprising up to 30% of all proteins present in the body. They belong to the protein family consisted of 28 members, ordered from I to XXVIII. Biosynthesized collagens are deposited in the ECM where most of them form supramolecular assemblies, such as fibrils, formed by collagens type I-III, hexagonal networks or transmembrane collagenous domains (Shoulders and Raines, 2009). The fibrillar collagen structure comprises a region consisting of three polypeptide chains ( $\alpha$ -chains) which form a triple helix stabilizing the matrix. The polypeptide chains are constituted mainly with glycine and proline residues. The hydroxyprolines ensure the stability via hydrogen bonds along the length of the molecule (Ricard-Blum, 2011).

Fibrillar collagens are major collagens in vertebrates where they play a structural role by contributing to the molecular architecture, shape, and mechanical properties of tissues and organs, such as skin and ligaments. Moreover, they interact with cells via several receptor families and regulate their proliferation, migration, and differentiation.



Certain collagen types with a restricted tissue distribution have specific biological functions. Collagens are the ECM components which contribute to elastic properties of bone and cartilage. In bone, the main protein from collagen family is collagen type I. For instance, collagen type I may attach to osteoblast cell membranes through the arginine-glycine-aspartate (RGD) motif and stimulate osteoblast proliferation (Harada *et al.*, 1991).

Osteoblasts deficient in ATF4, a transcription factor required during cell differentiation towards osteoblasts, had impaired collagen type I synthesis and exhibited reduced mineralization compared to wild type cells (Murshed, 2005). Furthermore, collagen type XXIV was described as another marker of osteoblast differentiation and bone formation (Matsuo *et al.*, 2008).

In cartilage, the most abundant is collagen type II, which represents approximately 90% of all collagens present in the tissue (Shoulders and Raines, 2009). Apart from collagen type II, there are other cartilage collagens, which are less expressed, however, they may also play a role in mineralization process. As already mentioned, collagen type X is major hypertrophic cartilage matrix protein and is necessary for the process of hematopoiesis (Sweeney *et al.*, 2010). The four collagens, types III, VI, IX and XI, also play a roles during cartilage mineralization, stabilizing the fibril network mainly composed of collagen type II. Another transmembrane protein is collagen type XIII which affects bone and cartilage formation by mediating the adjustment of bone mass to mechanical stress (Ylönen *et al.*, 2005), while collagen type XXVII is involved in the transition of cartilage to bone during skeletogenesis (Hjorten *et al.*, 2007).

The physical interaction of MVs with collagen may facilitate the deposition of mineral between the fibrils. Specific binding of MVs allows insertion of crystal among fibrillar structures (Golub, 2009). It was shown *in vitro* that the interaction of collagen type II and collagen type X with AnxA5 stimulates the uptake of  $Ca^{2+}$  ions by MVs and subsequent mineralization (Kirsch *et al.*, 2000). Moreover, selective removal of collagens from MV surface significantly reduced their ability to take up  $Ca^{2+}$ . Therefore, collagens type I and type II serve as a scaffold for the subsequent deposition of apatite crystals generated by MVs in bone and cartilage, respectively (Genge *et al.*, 2008).

#### **1.4. Molecular mechanisms of pathological calcification**

In the past, VC was concerned as a passive, degenerative, inevitable process of aging (Demer and Tintut, 2006). However, the development of murine models contributed

to significant progress in the field of studies concerning the origin of VC in atherosclerosis. Regarding the fact that normal mice do not develop atherosclerotic plaques, elaboration of a useful model required modulation of genes encoding important proteins involved in cholesterol metabolism. Apolipoprotein E (ApoE) is one of the major ligands of the LDL receptor (LDLR) which is responsible for the cellular LDL uptake. Thus, the absence of LDLR ligand, ApoE, prevents the purification of chylomicron, VLDL and LDL remnants, resulting in increased level of cholesterol in the blood (Ma *et al.*, 2012).

The ApoE-deficient (*apoE*<sup>-/-</sup>) mouse has become a major model of atherosclerosis thanks to its disposition to quickly develop atherosclerotic lesions, being fed with a high fat diet (Nakashima *et al.*, 1994). In comparison, LDLR knockout (*ldlr*<sup>-/-</sup>) mice require a cholesterol-rich diet for the induction of hypercholesterolemia. It is possible to observe fatty streaks in the proximal aorta of a 3-month-old *apoE*<sup>-/-</sup> mouse and at 10 weeks, foam cell lesions may be seen by light microscopy. Intermediate lesions containing foam cells and VSMCs may be seen at 15 weeks, and fibrous plaques appear at 20 weeks of age (Tamminen *et al.*, 1999; Meir, 2004). Advanced atherosclerotic lesions become highly calcified with 100% frequency by 75 weeks of age (Rattazzi, 2005).

Atherosclerosis is a relatively slow chronic inflammatory disorder that develops during decades, that is why *apoE*<sup>-/-</sup> mice are widely used models of this disease, since they allow the analysis of atherosclerotic lesions after several months. Although not all aspects of murine atherosclerosis are identical to humans, a recent study revealed a significant overlap of mouse and human genes associated with coronary artery disease (von Scheidt *et al.*, 2017). Therefore, observations from mouse models may provide useful information which are relevant for understanding the processes underlying human atherosclerosis.

Interestingly, it was demonstrated that the mere increase in Ca and P *in vivo* was not sufficient to induce any calcification in mice (Murshed *et al.*, 2005). The current hypothesis of the origin of artery calcification indicates that it is formed, at least in part, as a result of trans-differentiation of VSMCs into cells similar to growth plate chondrocytes (Sun *et al.*, 2012). Under physiological conditions, the endothelial layer is very thin. During atherosclerosis progression, VSMCs migrate from the media towards the intima where they proliferate and produce a fibrous tissue to stabilize the plaques by covering both fatty streak and necrotic core (Ross, 1993; Lusis, 2000). Possibly, trans-differentiated VSMCs may also contribute to formation of artery calcification.

*In vitro* studies of human VSMCs revealed that those cells cultured in media containing normal physiological levels of inorganic phosphate (1.4 mmol/L) did not mineralize.

Interestingly, it was observed that those cells cultured in media containing phosphate levels comparable to those seen in hyperphosphatemic individuals (>1.4 mmol/L) showed dose-dependent increase in mineral deposition. Moreover, elevated phosphate treatment also enhanced the expression of the osteoblastic differentiation markers, *Ocn* and *Runx2*.

In the light of those findings, better understanding of the processes leading to formation of artery calcification appears crucial. In the next chapters, different hypothesis concerning the origin of micro- and macrocalcifications will be presented and discussed.

### **1.4.1. Formation of artery microcalcification – possible mechanisms**

#### Extracellular vesicles

As already mentioned, early stages of physiological mineralization are mediated by nanostructures called matrix vesicles that are released by mineralizing cells and serve as nucleation sites for apatite synthesis. Furthermore, there are plenty of reports showing that VSMC-derived MVs are necessary for the progression of smooth muscle cell calcification (Bobryshev *et al.*, 2008; Chen *et al.*, 2008; Kapustin *et al.*, 2011). There is also a single evidence suggesting that macrophages may release exosomes similar to MVs with a capacity of apatite nucleation (New *et al.*, 2013).

Sortilin is a protein that has been recently characterized as a key regulator of vascular cell calcification due to its capacity to load TNAP to MVs. Interestingly, mice deficient in a gene encoding this protein, *Sort1*, had decreased arterial calcification, while normal bone formation was not affected (Goettsch *et al.*, 2016).

#### Cell apoptosis/necrosis

Atherosclerotic lesions are composed of lipids and connective tissue elements, but contain also multiple types of cells, including endothelial cells, VSMCs and immune cells. Those cells, especially VSMCs and macrophages, may undergo cell death within the plaque (Geng and Libby, 1995; Clarke and Bennett, 2006). It was shown that apoptosis may precede VSMC calcification and that VSMC-derived apoptotic bodies may act as nucleating structures for calcium crystal formation (Proudfoot *et al.*, 2000). In addition, macrophages may undergo apoptosis in response to cholesterol-induced cytotoxicity and endoplasmic reticulum (ER) stress (Feng *et al.*, 2003). Interestingly, necrotic death of macrophages was shown to contribute to atherosclerosis development (Lin *et al.*, 2013).

Generally, calcium exerts a toxic effect on cells, that is why its cellular content is very low, between 10 and 100 nM. Mitochondria contain small amounts of calcium, however, the majority of cellular Ca is stored in the ER, while phosphate ions are mainly located in the cytoplasm. In certain pathological conditions, like atherosclerosis, as a result of cell apoptosis or necrosis, a passive precipitation of calcium phosphate crystals may occur. It is possible when the product  $P_i \times Ca$  concentration exceeds 6 mM, which does not occur under physiological conditions.

#### Loss of MGP

Matrix Gla protein (MGP) is a secretory protein expressed in cartilage, bone matrix, arterial vessel wall, and other tissues. MGP was shown to be secreted by chondrocytes, VSMCs, endothelial cells and fibroblasts. It is a potent inhibitor of VC (Khavandgar *et al.*, 2014). MGP-deficient (*Mgp*<sup>-/-</sup>) mice exhibited progressive deposition of apatite minerals in the arterial walls and died within two months of age due to plaque rupture (Luo *et al.*, 1997). However, the principle of the inhibitory effect of MGP on VC is not fully understood. What is known is that MGP activity depends on carboxylation of glutamate residues, a process that requires vitamin K as a cofactor, and may be inhibited by warfarin (Price *et al.*, 1998; Schurgers *et al.*, 2013).

At least two mechanisms have been proposed to explain MGP inhibitory effect on VC. The first one is a direct inhibition of crystal growth by MGP binding to apatite crystals (Chatrou *et al.*, 2015). Therefore, it is possible that loss of inhibitors such as MGP is correlated with initiation of atherosclerosis (Chatrou *et al.*, 2015). The second mechanism relies on the MGP capacity to inhibit BMP signal transduction (Malhotra *et al.*, 2015).

### **1.4.2. Formation of artery macrocalcification – possible mechanisms**

#### Inflammatory cytokines: TNF- $\alpha$ and IL-1 $\beta$

Atherosclerosis accompanies age-related diseases that are associated with a low grade pro-inflammatory state, which may be defined as “inflammaging”. This chronic inflammatory process is characterized by increased levels of C-reactive protein (CRP) and cytokines, such as tumor necrosis factor (TNF)- $\alpha$  and interleukin (IL)-6 in the circulation (Bessueille and Magne, 2015).

TNF- $\alpha$  is one of the most potent pro-inflammatory cytokines and is produced by macrophages present in atherosclerotic plaque. Activated T cells release TNF- $\alpha$  as well as

Th1 cytokines, that in turn activate other immune cells to secrete IL-6. IL-6 subsequently stimulates production of the proteins of acute-phase, including CRP (Hansson, 2005). *ApoE*<sup>-/-</sup> mice deficient in TNF- $\alpha$  exhibited a significant reduction in lesion volume, suggesting a crucial role of TNF- $\alpha$  during development of atherosclerosis (Br n n *et al.*, 2004). Interestingly, TNF- $\alpha$  may directly stimulate TNAP (Fig. 11A, B). Several studies indicated that TNF- $\alpha$  may activate VSMCs to form calcium deposits (Tintut *et al.*, 2000; Shioi, 2002; Lee *et al.*, 2010; Lencel *et al.*, 2011). Interestingly, TNF- $\alpha$  may exert its effects by stimulating the release of BMP-2, a potent bone anabolic factor (Ikeda *et al.*, 2012).

Another important pro-inflammatory cytokine involved in atherosclerosis progression is IL-1 $\beta$ . In mice lacking IL-1 $\beta$ , a decrease in atherosclerotic plaque formation was observed (Kirii *et al.*, 2003). Also, the anti-atherogenic effect of IL-1 $\beta$  blockade was observed in several mouse models (Devlin *et al.*, 2002; Isoda *et al.*, 2004; Chamberlain *et al.*, 2009). Similarly to TNF- $\alpha$ , IL-1 $\beta$  may stimulate TNAP activity and calcification in VSMCs (Lencel *et al.*, 2011).

IL-1 $\beta$  is secreted by immune cells by the mechanism that requires inflammasome activation. The NLRP3 inflammasome protein complex was shown to be involved both in response to pathogenic infections as well as in chronic inflammation. This oligomer is consisted of multiple proteins: nucleotide-binding domain, leucine-rich repeat and pyrin domain (NLRP3), as well as ASC adaptor protein together with pro-caspase 1.

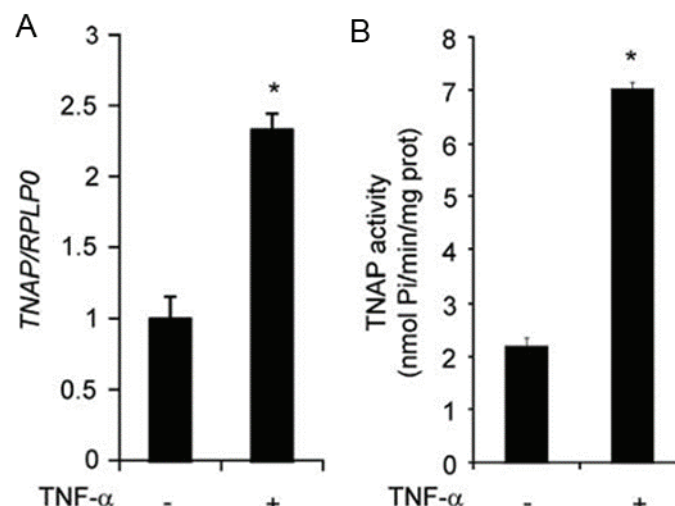


**Figure 11. TNF- $\alpha$  stimulates TNAP in human VSMCs.** In human VSMCs, TNF- $\alpha$  at 1 ng/ml increased the levels of TNAP at 48 h, as measured by quantitative PCR (A) and TNAP activity after 7 days (B) (Lencel *et al.*, 2011).

NLRP3 inflammasome activation has been shown recently to be required for vascular cell calcification (Wen *et al.*, 2013). Its activation requires two signals (Fig. 12) - the first

pathway includes activation of NF- $\kappa$ B transcription factor which after translocation to the nucleus triggers *nlrp3* and *il1b* gene transcription, leading to production of NLRP3 and pro-IL-1 $\beta$  proteins (Church *et al.*, 2008). In the non-infectious context, this process may be stimulated by TNF- $\alpha$  by its interaction with TNFR I or TNFR II receptors. Then, NLRP3 protein together with ASC and pro-caspase 1 assemble to form the NLRP3 inflammasome complex. The second signal may be activated by crystalline structures inducing caspase 1 maturation, which subsequently cleaves pro-IL-1 $\beta$ , resulting in IL-1 $\beta$  secretion.

Various crystalline structures were linked to inflammasome activation that underlie the progression of several diseases. For instance, monosodium urate crystals were shown to activate NLRP3 in gout disease (Martinon *et al.*, 2006), calcium pyrophosphate dihydrate crystals in pseudogout, silica crystals in silicosis (Hornung *et al.*, 2008) as well as cholesterol crystals during atherosclerosis (see section 1.1.4).

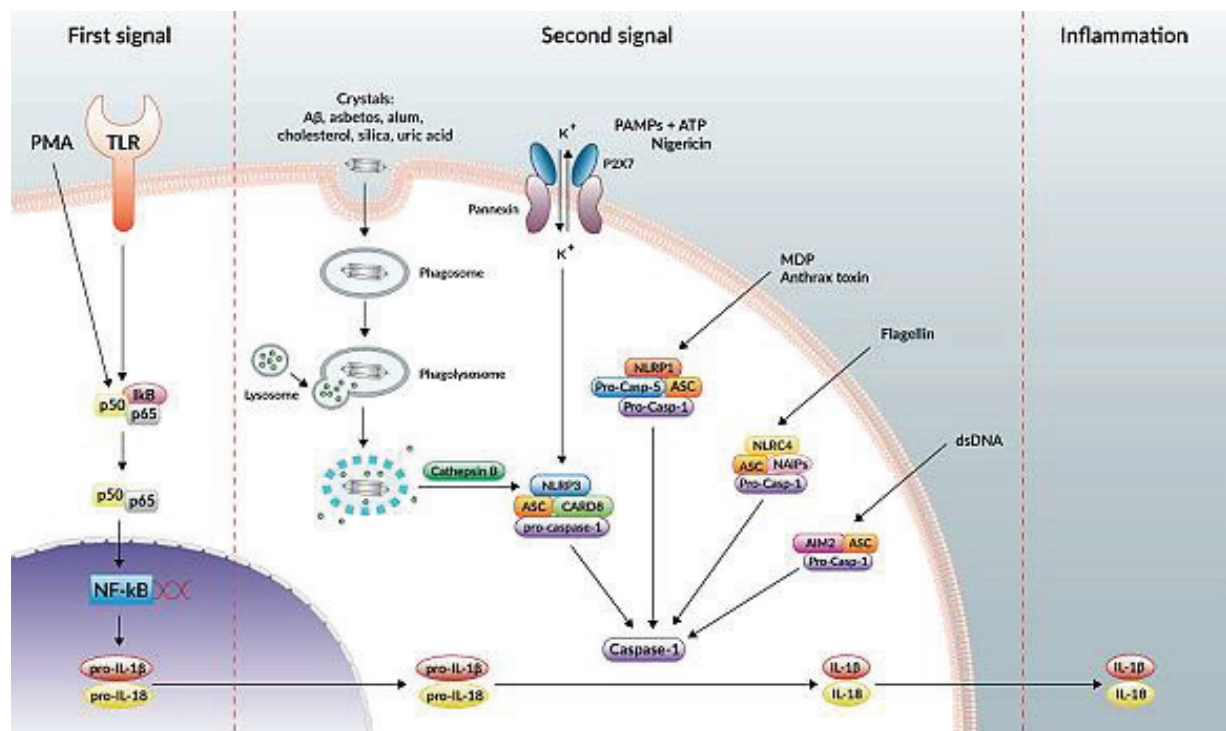


**Figure 12. The mechanisms of inflammasome activation.**

(<http://www.invivogen.com/review-inflammasome>).

#### Endochondral or intramembranous ossification

As described in section 1.1.2, in advanced lesions of *apoE*<sup>-/-</sup> mice, cells resembling chondrocytes as well as collagen type II were detected in a vicinity of apatite crystals (Rosenfeld



*et al.*, 2000; Rattazzi, 2005). Therefore, it is likely that macrocalcifications are formed by a process similar to endochondral ossification. However, in the case of human atherosclerosis, it is not yet clear whether VC results from endochondral or intramembranous ossification. Bone marrow, osteoblast-like cells, chondrocyte-like cells, osteoclast-like cells, and even osteocytes may be found in human atherosclerotic plaques (Doherty *et al.*, 2004; Pugliese *et al.*, 2015). Besides, synthesis of collagen type I appears to be upregulated in atherosclerotic lesions (Rekhter *et al.*, 1993). The expression of some chondrocyte-specific markers, but not all, was detected in both calcified and non-calcified human lesions, that is why the exact mechanism by which human macrocalcifications are formed remains controversial (Aigner *et al.*, 2008).

Therefore, in our laboratories we are currently interested in mechanisms leading to trans-differentiation of VSMCs into mineralization-competent cells. In particular, Maya Fakhry, a PhD student in MEM<sup>2</sup> laboratory, investigated the role of TNAP in VSMC trans-differentiation. In her PhD thesis, she demonstrated that overexpression of TNAP in A7R5 rat VSMCs, which in our hands failed to mineralize, resulted in a dramatic increase (by over 15-fold) in the expression of *Acan*, being an early marker of chondrocyte differentiation (Fig. 13A). Moreover, upon TNAP overexpression, she observed a significant stimulation of calcium accumulation in the matrix (Fig. 13B).

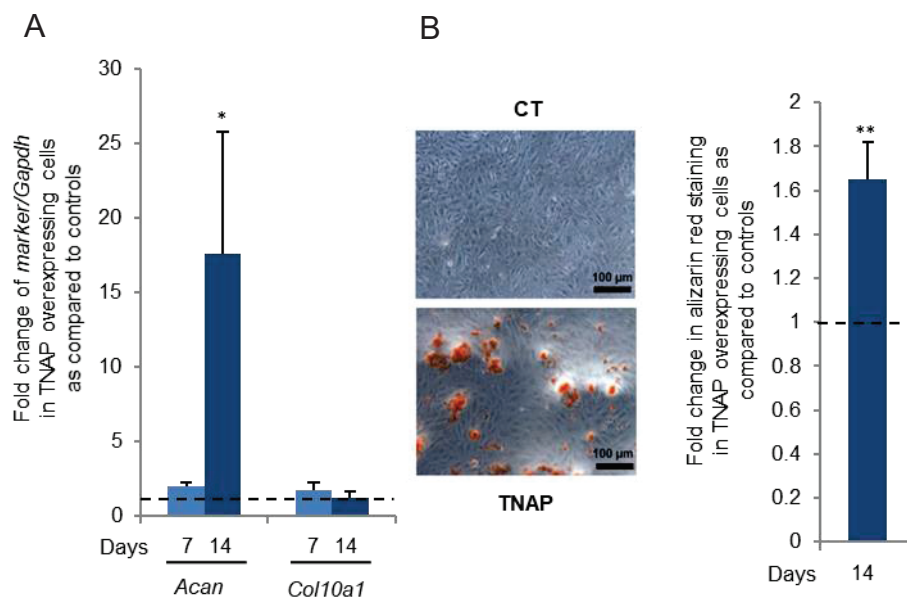


**Figure 13. Alkaline phosphatase activity stimulated MOVAS mineralization (Fakhry *et al.*, 2017).**

# **Chapter II**

## **Aims**



## Chapter 2. Aims

Recent findings suggest that TNAP may be activated in VSMCs by TNF- $\alpha$  and IL-1 $\beta$ , two inflammatory cytokines stimulating the progression of atherosclerosis (**Fig. 12A, B**). In parallel, it was demonstrated that TNAP overexpression, specifically in VSMCs, was sufficient to induce artery calcification in mice (Sheen *et al.*, 2015). Moreover, our recent results revealed that TNAP overexpression in VSMCs was sufficient to induce mineralization (**Fig. 13B**).

Therefore, our hypothesis is that TNAP is involved in trans-differentiation of VSMCs into mineralization-competent cells and subsequent calcification. The objective of our work was to understand TNAP effect on VSMC trans-differentiation and investigate underlying molecular mechanisms.

In our work, we applied two complementary approaches:

- to investigate a possible role of apatite crystals generated by TNAP in the stimulation of VSMC trans-differentiation. MOVAS cells were cultured on either mineralized or non-mineralized collagen followed by gene expression analysis of osteochondrocyte differentiation markers. Identical analysis were performed after culturing MOVAS with different doses of apatite crystals present in a culture medium.
- to study localization and function of mineralization markers such as TNAP and annexins in mineralization process mediated by trans-differentiated VSMCs and VSMC-derived MVs. TNAP and annexin distribution and TNAP activity was analyzed in MOVAS cells as well as in two fractions of extracellular vesicles produced by VSMCs: collagen-free and collagen-attached MVs.

# **Chapter III**

## **Materials and methods**

## **Chapter 3. Materials and methods**

### **3.1. Cell culture and treatment**

#### **3.1.1. Murine VSMC cell culture**

Murine VSMC MOVAS cell line was purchased from ATCC (Molsheim, France). The cells were routinely cultured in Dulbecco's Modified Eagle's Medium (DMEM) containing 4.5 g/l glucose and supplemented with 10% fetal bovine serum (FBS), 100 U/ml penicillin, 100 µg/ml streptomycin, 20 mmol/l HEPES and 2 mmol/l L-glutamine. The cells were cultured in the presence of 50 µg/ml ascorbic acid (AA, Sigma) in order to allow collagen secretion. Only where indicated, trans-differentiation was stimulated by the addition of 10 mM β-glycerophosphate (β-GP, Sigma) (Chung *et al.*, 1992).

#### **3.1.2. Murine primary chondrocyte cell culture**

Murine primary chondrocytes were extracted from articular cartilage (knee-joints and femoral head capsules) from 4- to 6-day old newborn litters of SWISS mice (Janvier labs) after decapitation and dissection, as already published (Gosset *et al.*, 2008). Animal procedures were performed according to guidelines from the Directive 2010/63/EU of the European Parliament concerning the use of animals for scientific purposes (approval numbers A 69266 0501 and BH2012-63).

Extracted tissues were collected in phosphate-buffered saline (137 mM NaCl, 2.7 mM KCl, 8 mM Na<sub>2</sub>HPO<sub>4</sub>, 1.5 mM KH<sub>2</sub>PO<sub>4</sub>, pH 7.4, PBS) supplemented with antibiotics, 100 U/ml penicillin and 100 µg/ml streptomycin. Extraction of chondrocytes was performed after several steps of enzymatic digestion by Liberase (Roche), a mixture of enzymes including collagenase I, collagenase II and trypsin, necessary to degrade components of the ECM. Extracted cells were seeded in DMEM containing 1 g/l glucose and supplemented with 10% FBS, 100 U/ml penicillin, 100 µg/ml streptomycin, 20 mmol/l HEPES and 2 mmol/l L-glutamine until confluence and not subcultured, to avoid the process of chondrocyte dedifferentiation into fibroblasts. Primary chondrocytes were then cultured in DMEM containing 4.5 g/l glucose and supplemented with 10% FBS, 100 U/ml penicillin, 100 µg/ml streptomycin, 20 mmol/l HEPES and 2 mmol/l L-glutamine. Mineralization was stimulated by the addition of 50 µg/ml AA and 10 mM β-GP.

### **3.1.3. Cell treatments**

To determine the effect of alkaline phosphatase on MOVAS trans-differentiation, the cells were treated with 8 U/ml of intestinal alkaline phosphatase (IAP, Sigma), after 17 days of culture in mineralizing conditions in the presence of 50 µg/ml AA and 10 mM β-GP. Day 17 is a period preceding the onset of TNAP activity on day 21 (Bessueille *et al.*, 2015). Treatment with exogenous alkaline phosphatase was followed by gene expression analysis of different chondrocyte markers by quantitative PCR (qPCR). TNAP inhibitor, levamisole (Sigma), was applied at the concentration of 100 µM to inhibit TNAP activity and check its effect on gene expression in primary chondrocytes. 100 ng/ml of noggin (Immunotools), an antagonist of proteins from BMP-2 family, was used in MOVAS to study the involvement of BMP-2 in the stimulation of trans-differentiation. For the investigation of the role of inflammasome in trans-differentiation, MOVAS cells were treated with 10 ng/ml TNF-α (R&D Systems) and 0.1 ng/ml IL-1β (R&D Systems).

## **3.2. Biochemical and analytical methods**

### **3.2.1. Alizarin Red staining**

The cells were rinsed with PBS and stained with 2% solution of Alizarin Red S (Sigma), pH 4.2, for 10 minutes. After several washings with H<sub>2</sub>O, extraction of the stain was performed by incubation of the cells with 100 mM cetylpyridinium chloride (CPC, Sigma) for 2 h at room temperature (RT). Calcium deposition was determined by measurement of the absorbance at 570 nm. The results were expressed as µmol AR-S per culture condition.

### **3.2.2. Measurement of protein concentration**

For the determination of protein concentration in the samples, Bi-Cinchoninic Acid (BCA) Protein Assay (Thermo Scientific) was applied, according to manufacturer's instructions. Absorbance was measured at 562 nm and protein concentration was calculated relative to the standard curve of bovine serum albumin (BSA).

### **3.2.3. Measurement of TNAP activity**

To determine TNAP activity based on the amount of p-nitrophenol (pNP) released after dephosphorylation of p-nitrophenyl phosphate (pNPP, Sigma), the cells were collected in 0.2% Nonidet P-40 and disrupted by sonication. Then, cell lysates were centrifuged (800g, 5

min, 4°C) and each supernatant was moved to separate well of 96-well plate. pNPP reagent (10 mM pNPP, 0.56 M 2-amino-2-methyl-1-propanol (AMP), 1 mM MgCl<sub>2</sub>, pH 10.3) was added to each well. The absorbance was measured at 405 nm in a plate reader at 37°C. TNAP specific activity was expressed as nmol of p-nitrophenol (pNP) formed per min per mg of protein.

### 3.2.4. NBT-BCIP

5-bromo-4-chloro-3-indolyl phosphate (BCIP) is hydrolyzed by alkaline phosphatase to form an intermediate that undergoes dimerization to produce an indigo dye. The nitroblue tetrazolium (NBT) is reduced to the NBT-formazan by the two reducing equivalents generated by the dimerization (Fig. 14). This reaction proceeds at a steady rate, allowing accurate control of the relative sensitivity and control of the development of the reaction.

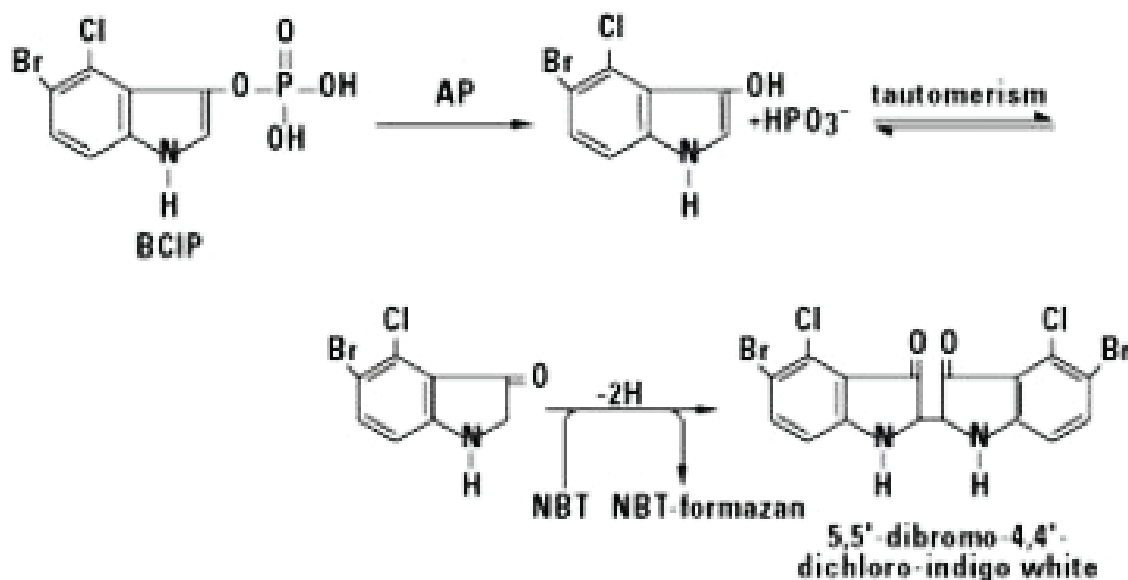


**Figure 14. Chemical reaction of NBT and BCIP substrates with alkaline phosphatase.**

The samples were prepared in mild denaturing conditions, in a buffer containing 60 mM Tris-HCl pH 6.8 and 2% SDS. Samples containing 10  $\mu\text{g}$  protein were loaded onto 7.5% polyacrylamide gels with 0.1% SDS. After electrophoresis, the gels were incubated in a buffer composed of 100 mM Tris-HCl pH 9.0, 150 mM NaCl, 1 mM MgCl<sub>2</sub>, 33  $\mu\text{g}/\text{ml}$  (NBT, Promega) and 16.5  $\mu\text{g}/\text{ml}$  (BCIP, Promega) at 37°C until the bands became clearly visible. The gels were photographed using InGenius LHR Gel Imaging System (Syngene).

### **3.2.5. MTT assay**

Cell viability assay after treatment of MOVAS with different concentrations of apatite crystals (ACs) was performed. MTT test was performed in 400  $\mu$ l of cell culture medium. 10  $\mu$ l of the 5 mg/ml MTT stock solution was added to each well to reach final MTT concentration of 0.125 mg/ml. Afterwards, the plates were incubated for 4 h at 37°C. Then, the medium was discarded followed by the addition of 400  $\mu$ l of DMSO to each well and absorbance was measured at 570 nm.

### **3.2.6. LDH assay**

Pierce LDH Cytotoxicity Assay Kit (Thermo Scientific) was applied according to the manufacturer's instructions. Lactate dehydrogenase (LDH) is a cytosolic enzyme which upon disruption of a plasma membrane is released into cell culture medium. The amount of the LDH released can be quantified by the reaction in which LDH catalyzes the conversion of lactate to pyruvate via nicotinamide adenine dinucleotide (NAD<sup>+</sup>) reduction to nicotinamide adenine dinucleotide hydrogen (NADH). Diaphorase then uses NADH to reduce a tetrazolium salt (INT) to a red formazan product that can be measured at 490 nm. The level of formazan formation directly reflects the amount of LDH released into the medium, providing an information about the cytotoxicity.

Cytotoxicity of apatite crystals (ACs) was determined after treatment of MOVAS with 30 and 300  $\mu$ g/ml ACs. 50  $\mu$ l of supernatants were collected at each time point and moved into a 96-well plate for the LDH assay.

## **3.3. Apatite crystal preparation**

### **3.3.1. Apatite collagen complexes (ACCs) preparation**

Each step of ACC preparation was performed under sterile conditions, as described earlier (Perrier *et al.*, 2010). Briefly, 35 mm dishes were coated with 0.1 mg/ml calf skin type I collagen (Sigma) solution in 0.1 M acetic acid and dried overnight. The next day, the dishes were rinsed with PBS and left once again to dry overnight. The day after, the dishes were either incubated with 0.4 mg/ml IAP and 0.4 mg/ml phosvitin (Sigma) for 3 h in 37°C, or left unmineralized. Next, the dishes were rinsed with H<sub>2</sub>O, followed by overnight incubation in the presence of 6 mM solution of calcium  $\beta$ -GP (Sigma) at 37°C. The dishes were subsequently washed with H<sub>2</sub>O, sterilized under the UV light for 30 min and left to dry overnight. Dry dishes were stored at 4°C until use. Calcium deposition on mineralized matrices was verified

by AR-S (Fig. 20). The presence of apatite on mineralized matrices was analyzed with Fourier transform infrared spectroscopy (FTIR), using a Nicolet iS10 spectrometer (64 scans at  $4\text{ cm}^{-1}$  resolution Fig. 20).

### 3.3.2. Apatite crystals (ACs) synthesis

Each step of ACs preparation was performed under sterile conditions. ACs were prepared by addition of sodium phosphate (0.4 M, pH = 7.2), to DMEM 4.5 g/l glucose supplemented with 0.5% FBS, to reach a final concentration of 10 mM inorganic phosphate. The solution was incubated for 24 h at  $37^{\circ}\text{C}$ . Precipitated crystals were collected after series of centrifugations at 5000 g for 5 min and washing steps with fresh medium. Next, crystals were resuspended in 10 ml of medium, disrupted in an ultrasonic bath for 10 minutes, centrifuged at 5000 g and dried overnight.














### 3.4. Gene expression analysis

#### 3.4.1. RNA extraction and reverse transcription

Total RNA was extracted using the NucleoSpin RNA II kit (Macherey-Nagel) following the manufacturer's protocol (Fig. 15).

1  $\mu\text{g}$  of RNA was retro-transcribed into cDNA with 0.5  $\mu\text{l}$  of Superscript II reverse transcriptase (Life Technologies). Each RNA sample was incubated for  $75^{\circ}\text{C}$  for 5 min (for denaturation of the double strand), followed by the addition of the PCR mix consisted of 0.5 mM dNTP, 5  $\mu\text{M}$  random hexamers, 5 mM DTT and reverse transcriptase in 5xRT buffer, to reach the final reaction volume of 20  $\mu\text{l}$ .

**Figure 15. Schematic diagram of RNA isolation** (Macherey-Nagel).

<b>Lyse cells</b>		350 $\mu\text{L}$ RA1 3.5 $\mu\text{L}$ $\beta$ -mercaptoethanol Mix
<b>Filtrate lysate</b>	 	11,000 x g, 1 min
<b>Adjust RNA binding conditions</b>		350 $\mu\text{L}$ 70% ethanol Mix
<b>Bind RNA</b>	 	Load sample 11,000 x g, 30 s
<b>Desalt silica membrane</b>	 	350 $\mu\text{L}$ MDB 11,000 x g, 1 min
<b>Digest DNA</b>		95 $\mu\text{L}$ DNase reaction mixture RT, 15 min
<b>Wash and dry silica membrane</b>	  	1 <sup>st</sup> wash 200 $\mu\text{L}$ RAW2 2 <sup>nd</sup> wash 600 $\mu\text{L}$ RA3 3 <sup>rd</sup> wash 250 $\mu\text{L}$ RA3 11,000 x g, 30 s 11,000 x g, 2 min
<b>Elute highly pure RNA</b>	 	60 $\mu\text{L}$ RNase-free $\text{H}_2\text{O}$ 11,000 x g, 1 min



Reverse transcription PCR program:

- 42°C, 30 min
- 99°C, 5 min

As a last step, each cDNA product was diluted 5x with H<sub>2</sub>O.

### 3.4.2. Quantitative polymerase chain reaction (real time PCR)

Real time PCR was performed in CFX96-2 Light Cycler (Bio-Rad) and relative quantification of gene expression was determined by CFX Manager Software using the  $2^{-\Delta\Delta Cq}$  method. Cq represents the number of cycles needed to exceed the base line signal during amplification. *Gapdh* (glyceraldehyde-3-phosphate dehydrogenase) gene was used as reference gene.

5 µl of iTaq Universal SYBR green supermix (Bio-Rad), 1 µl of 3 µM forward primer, 1 µl of 3 µM reverse primer and 0.5 µl of PCR-grade H<sub>2</sub>O was added to 2.5 µl of cDNA to reach the final reaction volume of 10 µl. Each sample was amplified in duplicate. Primers for real time PCR were summarized in **Tab. 1**.

Real time PCR program:

- 95°C, 30 s
  - 95°C, 6 s
  - 60°C, 15 s
  - 72°C, 25 s
  - 65°C → 95°C (melt curve with an increment of 0.5°C/5 s)
- } 45 cycles

**Table 1. Summary of primers used.** m – mouse, For – forward primer, Rev – reverse primer, Acan – aggrecan, Bmp-2 – bone morphogenic protein-2, Id1 – inhibitor of DNA binding 1, Gapdh – glyceraldehyde 3-phosphate dehydrogenase, Runx2 - Runt-related transcription factor 2, Col2a1 – collagen type II, Col10a1 – collagen type X, Ocn – osteocalcin, Osx – osterix.

Gene	GenBank accession number	Sequences 5'-3'
<i>mRunx2</i>	NM_009820.5	For: GCCGGGAATGATGAGAACTA' Rev: GGACCGTCCACTGTCACTTT
<i>mCol2a1</i>	NM_031163.3	For: GGCAACAGCAGGTTACAT Rev: ATGGGTGCGATGTCAATAA
<i>mCol10a1</i>	NM_009925.4	For: CAAACGGCCTCTACTCCTCTGA Rev: CGATGGAATTGGGTGGAAAG
<i>mOcn</i>	NM_001037939.2	For: AAGCAGGAGGGCAATAAGGT Rev: CGTTTGTAGGCGGTCTTCA
<i>mOsx</i>	NM_130458.3	For: AGGCACAAAGAAGCCATACG Rev: GCCCAGGAAATGAGTGAGG
<i>mAcan</i>	NM_007424.2	For: GTGCGGTACCAGTGCACTGA Rev: GGGTCTGTGCAGGTGATTCG
<i>mBmp2</i>	NM_007553	For: TGGAAGTGGCCCATTTAGAG Rev: TGACGCTTTTCTCGTTTGTG
<i>mId1</i>	NM_010495.3	For: GCGAGATCAGTGCCTTGG Rev: GAGTCCATCTGGTCCCTCAG
<i>mGapdh</i>	NM_001289726.1	For: GGCATTGCTCTCAATGACAA Rev: TGTGAGGGAGATGCTCAGTG

### 3.5. Cellular fractionation

#### 3.5.1. Isolation of total membranes

The fractions of total membranes were isolated according to Briolay and collaborators (Briolay *et al.*, 2013). Briefly, MOVAS cells ( $25 \times 10^6$  cells) were disrupted in a Potter homogenizer (40 strokes) on ice in a TNE buffer consisted of 25 mM Tris-HCl, 150 mM NaCl 5 mM ethylenediaminetetraacetic acid (EDTA) (pH 7.5) and supplemented with 10  $\mu$ g/ml protease inhibitor cocktail (PIC, Sigma). The homogenate was then centrifuged at 900 g for 10 min at 4°C. The supernatant was collected and then ultracentrifuged at 100,000 g for 45 min at 4°C in an Optima LE-80K ultracentrifuge (Beckman Coulter). Afterwards, the pellet of total

membranes (plasma membrane and cytoplasmic vesicular structures) was resuspended in 200  $\mu$ l of TNE buffer.

### **3.5.2. Isolation of collagen-free MVs**

Isolation of MVs was performed according to the procedures described earlier (Wuthier *et al.*, 1985; Chen *et al.*, 2008).  $1 \times 10^8$  of MOVAS cells were seeded on 100 mm culture dishes. At confluence, the cells were cultured for 21 days in the presence or absence of 50  $\mu$ g/ml AA and 10 mM  $\beta$ -GP. Afterwards, the culture medium was collected, centrifuged (1,000 x g, 30 min, 4°C, to remove apoptotic bodies) in a MPW 350R centrifuge (MPW Medical Instruments) and subjected to ultracentrifugation (100,000 x g, 30 min, 4°C) in an Optima L-100 XP ultracentrifuge (Beckman Coulter), as indicated in **Fig. 16**. The pellet of collagen-free MVs was resuspended in 100  $\mu$ l of “synthetic cartilage lymph” solution (SCL), composed of 100 mM NaCl, 12.7 mM KCl, 1.42 mM NaH<sub>2</sub>PO<sub>4</sub>, 1.83 mM NaHCO<sub>3</sub>, 0.57 mM MgCl<sub>2</sub>, 0.57 mM Na<sub>2</sub>SO<sub>4</sub>, 5.55 mM D-glucose, 63.5 mM sucrose, and 16.5 mM HEPES (pH 7.4) and stored in -20°C (Buchet *et al.*, 2013b).

### **3.5.3. Isolation of collagen-attached MVs**

To obtain the fraction of collagen-attached MVs, the cells were rinsed with PBS and incubated in digestion buffer containing 200 U/ml collagenase from *Clostridium histolyticum* (Sigma), 120 mM NaCl, 10 mM KCl, 250 mM sucrose and 20 mM Tris-HCl pH 7.4 for 3 h at 37°C. The cells were scraped, centrifuged (800 x g, 30 min, 4°C, to remove cell debris) and subjected to ultracentrifugation (30,000 x g, 30 min, 4°C, to separate basolateral membranes and microsomes). The supernatant was ultracentrifuged in an Optima L-100 XP ultracentrifuge (250,000 x g, 30 min, 4°C) to collect the vesicles (**Fig. 16**). The pellet of collagen-attached MVs was resuspended in SCL and stored at -20°C.

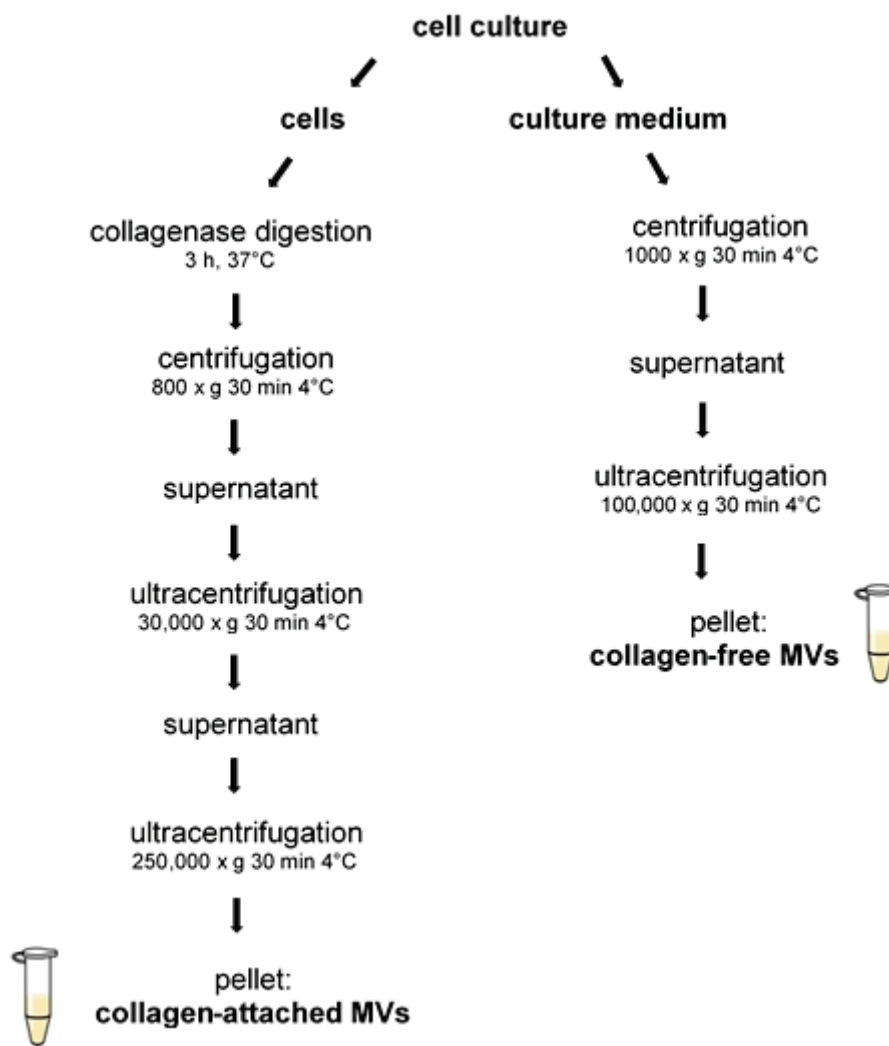


**Figure 16. Schematic diagram of MV isolation** (according to Wuthier *et al.*, 1985; Chen *et al.*, 2008).

### 3.6. Lipid analysis

#### 3.6.1. Measurement of cholesterol content

Cholesterol (Chol) content in cellular fractions was determined by the Amplex Red Cholesterol Assay Kit (Invitrogen) according to the manufacturer’s instructions. By this method, both free and esterified Chol were detected, since cholesteryl esters are hydrolyzed into Chol by cholesterol esterase present in working solution. The principle of the assay is Chol oxidation by cholesterol oxidase, giving a side product of the reaction, H<sub>2</sub>O<sub>2</sub>. Amplex Red reagent is a probe highly sensitive for the detection of H<sub>2</sub>O<sub>2</sub>. In the presence of horseradish peroxidase (HRP), Amplex Red reagent reacts with H<sub>2</sub>O<sub>2</sub>, producing highly fluorescent resorufin.

Analyzed samples as well as Chol standards (0–8 µg/ml), were incubated for 30 min at 37°C in the presence of working solution 0.5 M K<sub>3</sub>PO<sub>4</sub>, 0.25 M NaCl, 25 mM cholic acid, 0.5% Triton X-100, 300 µM Amplex Red, 2 U/ml HRP, 2 U/ml cholesterol oxidase and 0.2 U/ml cholesterol esterase (pH 7.4). The reaction was stopped after 30 min and afterwards fluorescence was measured in a plate reader with the excitation at 550 nm and emission at 585 nm. Chol content in the samples was calculated relative to the standard curve of cholesterol and normalized by the amount of protein.

### **3.7. Protein analysis**

#### **3.7.1. SDS-PAGE and Western Blot**

Whole cell lysates (WCLs) were prepared by scratching and harvesting of the cells in a buffer containing 0.1% Triton X-100, 50 mM Tris-HCl, 80 mM NaCl and 10 µg/ml PIC (pH 7.4) and disrupted by sonication on ice (2 x 10 sec, 20% power) using a S-250D digital sonifier (Branson Ultrasonic). Cell lysates and fractions of vesicles (25 µg) were prepared for SDS-PAGE analysis by addition of the Laemmli 5x sample buffer and boiling at 95°C for 5 min. Proteins were separated by SDS-PAGE on 10% acrylamide gels (1.5 h, 190 V) and then transferred onto nitrocellulose membranes (BioRad) for 1 h at 500 mA. Immunoblots were washed with Tris-buffered saline (10 mM Tris-HCl, 140 mM NaCl, pH 7.4, TBS) and then incubated in blocking solution (5% skimmed milk solution in TBS) for 1 h. Afterwards, the membranes were incubated overnight at 4°C with one of primary antibodies (summarized in **Tab. 2**) prepared in 2.5% skimmed milk in TBS supplemented with 0.05% Tween 20 (TBST). After several washings with TBST, the membranes were incubated for 1.5 h at RT with anti-rabbit or anti-mouse IgG–HRP-linked antibody (Cell Signaling) prepared in 5% skimmed milk in TBST. β-actin immunostained with monoclonal β-actin-HRP Conjugate antibody (Sigma) was presented as a control. After washing, the protein bands were visualized using Enhanced chemiluminescence (ECL) reagent (Millipore). Band optical density was measured by use of InGenius laser densitometer (Syngene BioImaging Co.).

**Table 2. List of antibodies used for Western Blot analysis.**

Antigen	Detected band molecular weight (kDa)	Host	Supplier	I° antibody dilution	II° antibody dilution
anti-TNAP	60	Rabbit	Abcam	1:500	1:1000
anti-AnxA2	36	Mouse	BD Transduction Laboratories	1:2500	1:5000
anti-AnxA6	70	Mouse	BD Transduction Laboratories	1:2500	1:5000
anti- $\beta$ -actin	42	Mouse	Sigma	1:25000	-

### 3.7.2. Protein staining

WCLs were prepared by scratching and harvesting of the cells in a buffer containing 0.1% Triton X-100, 10 mM Tris-HCl, 140 mM NaCl and 10  $\mu$ g/ml PIC (pH 7.4) and disrupted by sonication. Cell lysates and fractions of vesicles (25  $\mu$ g) were prepared by addition of the Laemmli 5x sample buffer and boiling at 95°C for 5 min. Afterwards, proteins were separated on 10% acrylamide gels. To visualize protein profiles of different fractions of MOVAS, the gels were washed with demineralized water (3 x, 5 min). Then, the gels were incubated with AMRESCO Blue Bandit Protein Stain (VWR) for 1h. After incubation, they were washed several times with demineralized water and photographed.

### 3.7.3. Immunofluorescence

To analyze TNAP, AnxA2 and AnxA6 location in MOVAS, the cells were seeded at low density (1000 cells/cm<sup>2</sup>) on coverslips coated with 30  $\mu$ g/ml Collagen Type I from rat tail (Sigma) and cultured in the presence of 50  $\mu$ g/ml AA and 10 mM  $\beta$ -GP for 1-4 days. The cells were washed with PBS and fixed with 3% paraformaldehyde for 20 min at RT. After washing with PBS, the cells were incubated with 50 mM NH<sub>4</sub>Cl in PBS for 10 min at RT. In case of AnxA2 and AnxA6, permeabilization step was included using 0.1% TX-100 in PBS for 5 min on ice. Afterwards, the cells were washed with TBS and subjected to blocking (5% FBS in TBS) for 1 h. The samples were incubated for 1.5 h at RT with anti-TNAP, anti-AnxA2 or anti-AnxA6 antibody prepared in 0.5% FBS in TBST (**Tab. 3.**). Then, the cells were washed several times with TBST and incubated for 1 h at RT with anti-Rabbit or anti-Mouse Alexa

Fluor 488 or Alexa Fluor 594 secondary antibody prepared in 0.5% FBS in TBST. After extensive washing several times with TBS and once with H<sub>2</sub>O, coverslips were mounted with Mowiol 4-88 (Calbiochem), supplemented with 1,4-diazabicyclo[2.2.2]octane (DABCO, Sigma) on microscope slides. Images were taken by Zeiss AxioObserver Z.1 fluorescence microscope at the 630 x magnification with DIC contrast and appropriate fluorescent filters.

To observe AnxA6 distribution in living cells, MOVAS cells were transfected with AnxA6-EGFP-N3 plasmid (BD Biosciences Clontech) using Effectene Transfection Reagent (QIAGEN) according to manufacturer's instructions. Effectene Reagent was used in conjunction with the Enhancer and the DNA-condensation buffer (Buffer EC). In the first step of Effectene–DNA complex formation, the DNA was condensed by interaction with the Enhancer in a defined buffer system. Effectene Reagent was then added to the condensed DNA to produce condensed Effectene–DNA complexes.

More precisely, DNA dissolved in TE buffer (10 mM Tris-HCl, 1 mM EDTA, pH 7.4) was diluted to a final concentration of 0.3 µg/µl with an EC buffer. Then, enhancer was added, the samples were vortexed for 1 s and incubated for 5 min at RT. Then, Effectene reagent was added, the samples were vortexed and incubated for 10 min at RT. The Effectene–DNA complexes were mixed with the culture medium and added drop by drop to the cells. After overnight incubation at 37°C, the cells were washed with fresh culture medium and incubated in the presence or absence of 50 µg/ml AA and 10 mM β-GP for 4 days. Images were taken by Zeiss AxioObserver Z.1 fluorescence microscope at the 630 x magnification using appropriate fluorescent filter.

**Table 3. List of antibodies used for immunofluorescence analysis.**

Antigen	Host	Supplier	I° antibody dilution	II° antibody	II° antibody dilution
anti-TNAP	Rabbit	Abcam	1:50	Alexa Fluor 594	1:100
anti-AnxA2	Mouse	BD Transduction Laboratories	1:200	Alexa Fluor 488	1:400
anti-AnxA6	Mouse	BD Transduction Laboratories	1:200	Alexa Fluor 488	1:400



## **3.8. Transmission electron microscopy (TEM) and energy dispersive X-ray microanalysis (TEM-EDX)**

### **3.8.1. Sample preparation**

Cell cultures were washed with PBS and fixed with 5 ml of 3% paraformaldehyde/1% glutaraldehyde mixture in 100 mM sodium phosphate buffer pH 7.2 for 1 h at RT. After washing, samples were postfixed with 2 ml of 1% osmium tetroxide in 100 mM sodium phosphate buffer pH 7.2 for 20 min at RT in the dark. Then, probes were dehydrated in a graded ethanol solution series at RT (25% for 5 min, 50% for 10 min, 75% for 15 min, 90% for 20 min, twice 100% for 30 min and 12 h). The cells were mechanically scraped and centrifuged at 132 x g for 1 min ((MPW-350R centrifuge, MPW Medical Instrument). Pellets were suspended and incubated in mixtures of the LR White resin (Polysciences Inc.)/100% ethanol at volume ratios of 1:2 and 1:1 (30 min each at RT). Finally, samples were infiltrated twice with 100% LR White resin for 1 h at RT, moved to Snap Fit gelatin capsules (Agar Scientific Ltd.) and polymerized at 56°C for 48 h. Sections (700Å) were cut using ultra 45° diamond knife (Diatome) on a NOVA ultramicrotome (LKB) and placed on formvar-covered and carbon-labelled 300 Mesh Ni grids (Agar Scientific Ltd.).

10 µl of MV suspension was dropped on Formvar/Carbon 300 Mesh Ni grids (Agar Scientific Ltd.) placed in a porcelain multi-well plate. Then, the sample-covered grids were dried for 30 min at RT. Afterwards, they were counterstained with 2.5% uranyl acetate solution in ethanol for 20 min at RT, protected from light. Finally, the grids were rinsed with 50% ethanol, deionized water and dried for 24 h.

### **3.8.2. TEM**

Cell slices and MVs were observed by JEM-1400 transmission electron microscope (TEM, JEOL Co.) equipped with energy-dispersive full range X-ray microanalysis system (EDS INCA Energy TEM, Oxford Instruments), tomographic holder and 11 Megapixel TEM Camera MORADA G2 (EMSIS GmbH). Images were taken at magnifications between 50 000 and 150 000 x.

### **3.8.3. TEM-EDX and mapping**

Point measurements of MV chemical composition by X-ray microanalysis were also performed. The content of analyzed elements: C, O Ca and P was expressed as atomic %

of summarized atomic weights of all known elements of a Periodic Table present in the sample. After performing spectral and compositional analysis, Ca/P ratio was calculated per each point measurement. Mapping of Ca and P distribution in MVs was performed by use of EDX INCA Software (Oxford Instruments).

### **3.9. Statistical analysis**

All experiments were repeated independently, at least three times. Results were expressed as mean  $\pm$  standard error of the mean (SEM). Statistical analysis were performed according to two tailed un-paired student t-test. Results were considered significant with \* at  $p < 0.05$ , \*\* at  $p < 0.01$  and \*\*\* at  $p < 0.001$ .

# **Chapter IV**

## **Results**

## Chapter 4. Results

### 4.1. Mineralization abilities of a cellular model

#### 4.1.1. Characterization of MOVAS

As a research model of vascular cell calcification we selected a cell line of murine VSMCs, MOVAS, whereas murine primary chondrocytes served as a model of physiological mineralization. Regarding the morphology of MOVAS VSMCs, they are rhomboid and rather similar in size (**Fig. 17B**), in contrast to cuboid chondrocytes which exhibit different sizes (**Fig.17A**). Both cell types had the ability to quickly reach confluence. At day 7 of culture, the first symptoms of calcium deposition were observed in both cell types (**Fig. 17C, 17D**). Primary chondrocytes, characterized by TNAP activity exceeding by 100-fold the activity of TNAP in MOVAS, needed 10 days of culture in mineralizing conditions to efficiently mineralize (**Fig. 17E**), whereas MOVAS VSMCs, with lower mineralization abilities, deposited mineral after 21 days (**Fig. 17F**). Based on previous studies, it is known that MOVAS cell line is characterized by the ability to mineralize *in vitro* as well as by increased expression of genes encoding proteins typical for bone tissue, such as TNAP, OCN and P<sub>i</sub>T-1 upon treatment with typical stimulators of mineralization, AA and  $\beta$ -GP (Mackenzie, 2011). Another study by Idelevich and collaborators revealed that MOVAS cell line may serve as a model of pathological mineralization (Idelevich *et al.*, 2011). Moreover, this cell line has been recently used for interesting studies on the effect of saturated fatty acid lipotoxicity on VC (Masuda *et al.*, 2015).

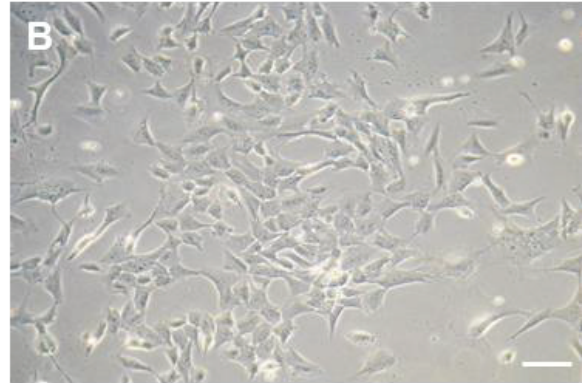
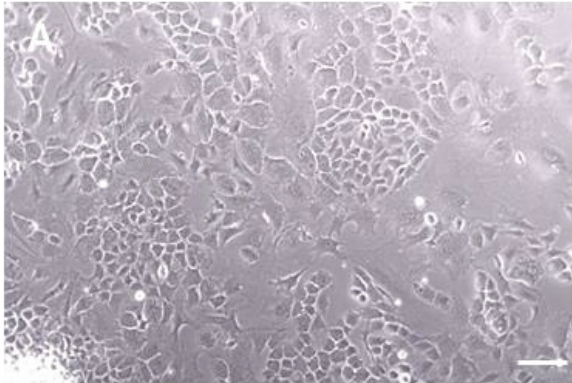
Firstly, we checked if, in our hands, MOVAS cells have the ability to mineralize. According to Mackenzie and collaborators, MOVAS cells exhibited increased TNAP activity and prominent mineralization at day 21 of osteogenic stimulation. Indeed, after 21 days of trans-differentiation in the presence of AA and  $\beta$ -GP, we observed calcium deposition in trans-differentiated cells stained with Alizarin Red (**Fig. 18A right panel, 18B right panel**). Quantitative analysis revealed an increase in calcium deposition by approximately 2-fold in trans-differentiated MOVAS compared to resting cells (**Fig. 18C**) and a significant increase in TNAP activity (**Fig. 18D**). Thus, we confirmed that MOVAS cells are able to mineralize in a typical osteogenic medium.

Murine primary chondrocytes

MOVAS VSMCs

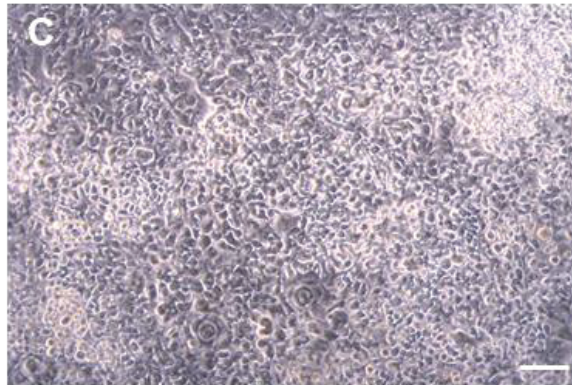
D 0

D 0



D 7

D 7



D 10

D 21

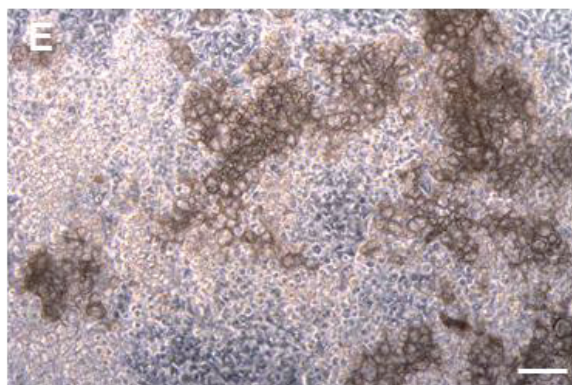
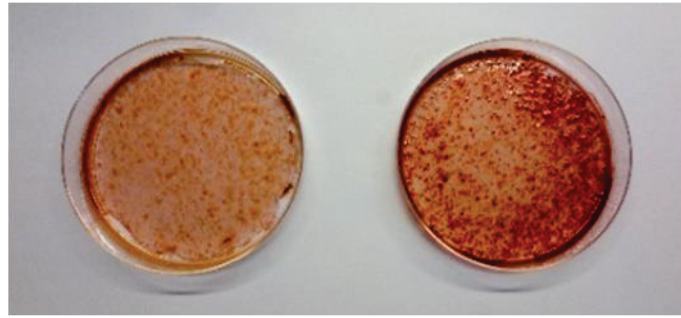


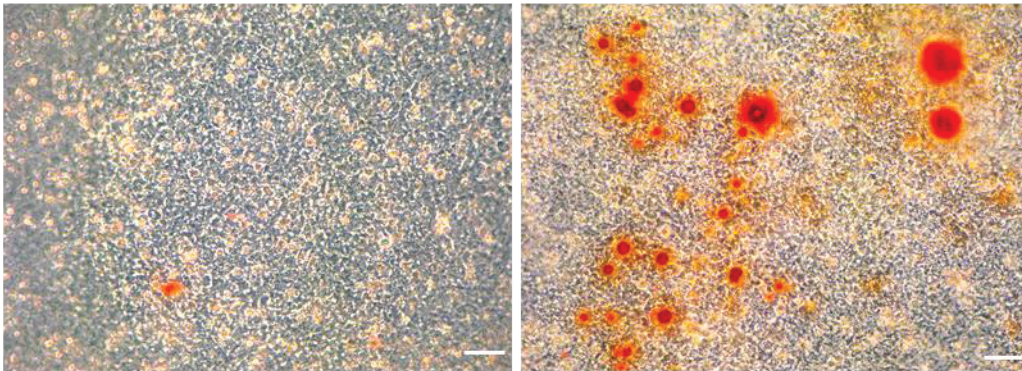
**Figure 17. Morphology of murine primary chondrocytes and MOVAS.** Microscopic view of murine primary chondrocytes (A, C, E) and MOVAS VSMCs (B, D, F) at different time points of osteogenic stimulation in the presence of AA and  $\beta$ -GP. Photos taken by Zeiss Axiovert light microscope. Representative photos were shown. Magnification 100 x, scale bar - 100  $\mu$ m.



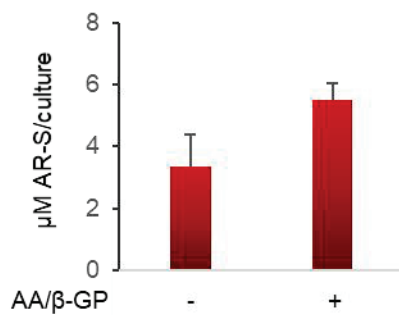
A



B



C



D

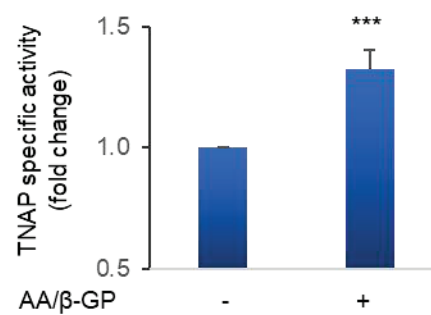


**Figure 18. Mineralization by MOVAS.** (A) Calcium deposits stained with Alizarin Red after 21 days of treatment in the presence (+) or absence (-) of 50 µg/ml AA and 10 mM β-GP. (B) Calcium deposits visualized by the Zeiss Axiovert light microscope. Representative photos were shown. Magnification 100 x, scale bar – 100 µm. (C) Quantitative analysis of Alizarin Red staining after extraction of the stain with 100 mM CPC. (D) TNAP specific activity of MOVAS WCLs after 21 days of treatment in the presence (+) or absence (-) of 50 µg/ml AA and 10 mM β-GP.

### 4.1.2. Characterization of murine primary chondrocytes

In our studies, murine primary chondrocytes served as a model of physiological mineralization. Their mineralization abilities *in vitro* have been characterized. These chondrocytes had increased TNAP activity after 10 days when cultured with 50  $\mu\text{g/ml}$  AA, independently of the addition of  $\beta\text{-GP}$  (**Fig. 19A**), but the presence of 10 mM  $\beta\text{-GP}$  significantly increased mineralization (**Fig. 19B**). Conversely, the addition of levamisole, a well-known inhibitor of TNAP activity, significantly decreased mineralization by those cells (**Fig. 19C**).

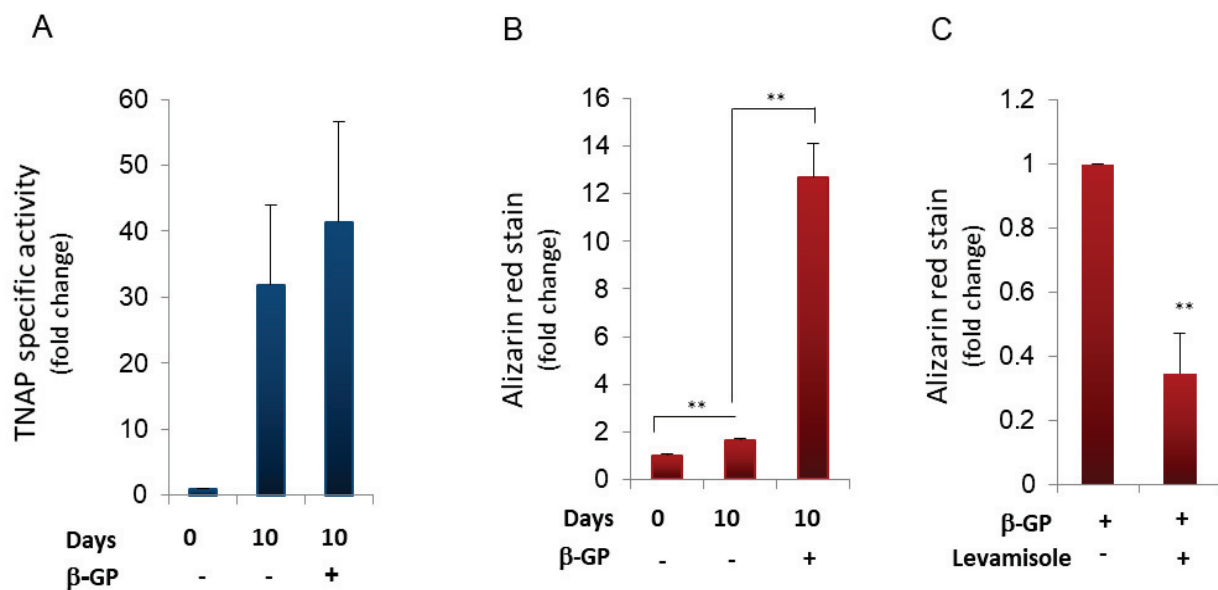


**Figure 19. Characterization of murine primary chondrocytes.** (A) TNAP activity measured in WCLs of primary chondrocytes in the presence (+) or absence (-) of  $\beta\text{-GP}$ . (B) Calcium deposition by primary chondrocytes cultured in the presence (+) or absence (-) of  $\beta\text{-GP}$  or 100  $\mu\text{M}$  levamisole (C) determined by Alizarin Red staining.

## 4.2. The role of TNAP in MOVAS trans-differentiation and mineralization

### 4.2.1. MOVAS trans-differentiation into chondrocyte-like cells

At day 17 of culture in mineralizing conditions, MOVAS were treated with exogenous alkaline phosphatase for 7 days in the absence of  $\beta\text{-GP}$  to avoid a non-physiological rise of  $\text{P}_i$  levels due to  $\beta\text{-GP}$  hydrolysis. When cells were cultured under these conditions, we observed an up-regulation of the mRNA encoding the early chondrocyte marker, *Acan*, and one of the late ones - *Ocn*.

Since *Ocn* is also expressed by osteoblasts, we sought to investigate whether VSMCs also trans-differentiate in osteoblasts after treatment with exogenous alkaline phosphatase.



mRNA levels of the osteoblast-specific transcription factor osterix were measured, which did not increase but instead they decreased in the presence of exogenous alkaline phosphatase, suggesting that VSMCs trans-differentiated into chondrocytes and not osteoblasts (**Fig. 20**).

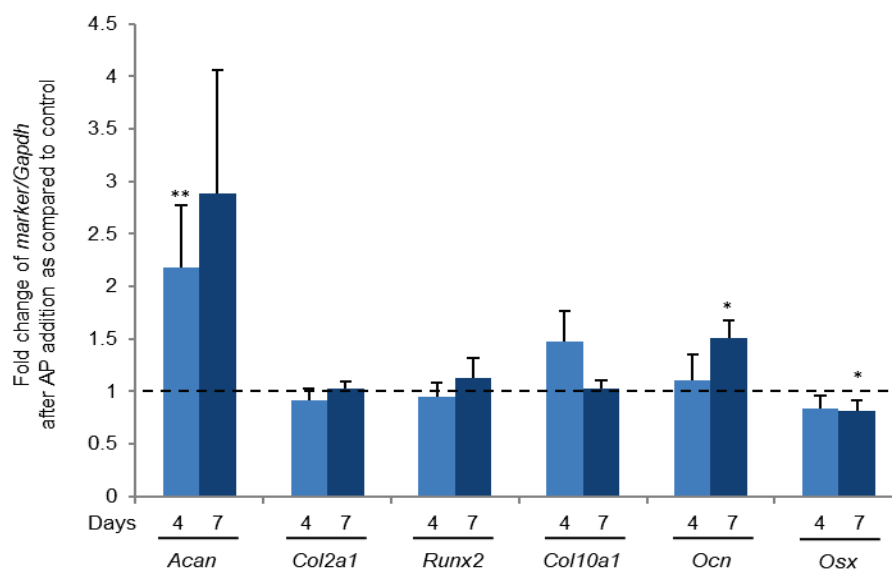


**Figure 20. Alkaline phosphatase activity stimulated MOVAS trans-differentiation towards chondrocytes.** MOVAS cells were cultured from confluence to day 17 with AA and  $\beta$ -GP. On day 17,  $\beta$ -GP was removed and 8 U/ml of alkaline phosphatase were added. mRNA levels were quantified by RT-qPCR after 4 and 7 days of treatment, and normalized with Gapdh mRNA levels.

#### 4.2.2. The effect of ACs generated by TNAP on *Acan* gene expression

Moving further, the major question that we asked was whether TNAP stimulates this process through  $PP_i$  hydrolysis and the generation of ACs. Firstly, we prepared dishes coated with collagen, either left unmineralized or mineralized by addition of alkaline phosphatase and phosphite as a source of phosphate (**Fig. 21A**). FTIR analysis revealed that the crystals obtained on mineralized collagen consisted of a carbonated apatite (**Fig. 21B**), similar in organization and composition to carbonated apatite that forms in the cartilage growth plate and atherosclerotic plaques (Duer *et al.*, 2008).

Then, we cultured VSMCs on these unmineralized or mineralized synthetic collagen matrices. Interestingly, we observed a significant increase of *Acan* levels when VSMCs were cultured on mineralized collagen as compared to unmineralized collagen (**Fig. 22A**). Moreover, MOVAS cells were treated with different concentrations (3-300  $\mu$ g/ml) of ACs suspended in a culture medium after 17 days of culture in mineralizing conditions in the presence of 50  $\mu$ g/ml AA and 10 mM  $\beta$ -GP, being a period preceding the onset of TNAP activity on day 21

(Bessueille *et al.*, 2015). Similarly, VSMCs treated with ACs in suspension, in the absence of collagen, also showed the same 2-fold increase in *Acan* levels (**Fig. 22B**).

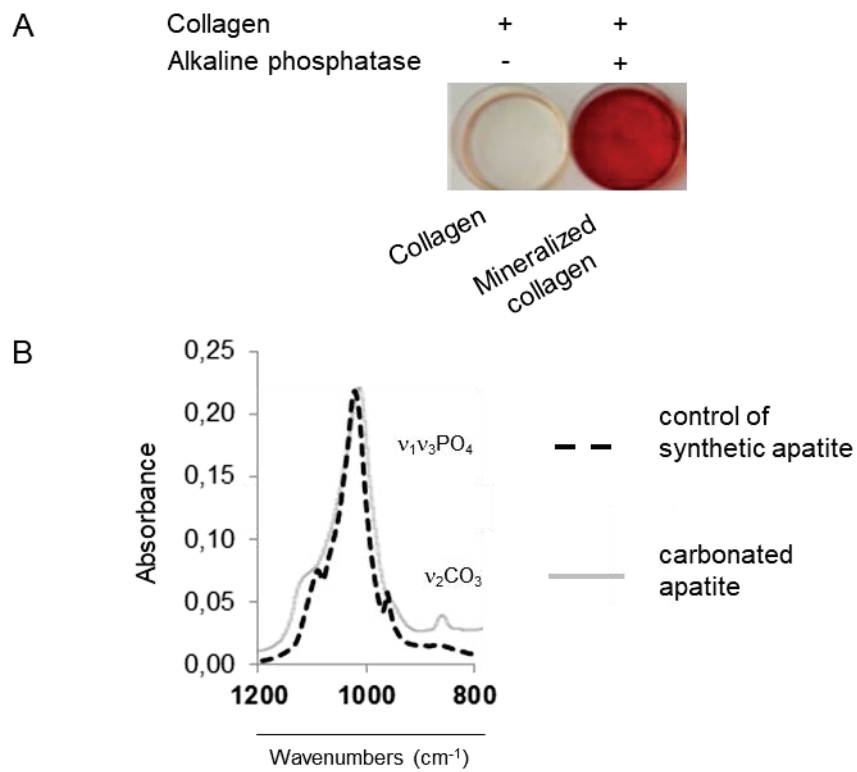


**Figure 21. Detection of calcium deposited on apatite collagen complexes (ACCs) after induction of mineralization.** Detection of calcium on mineralized collagen matrices by AR-S (**A**); FTIR analysis of obtained mineral (**B**).

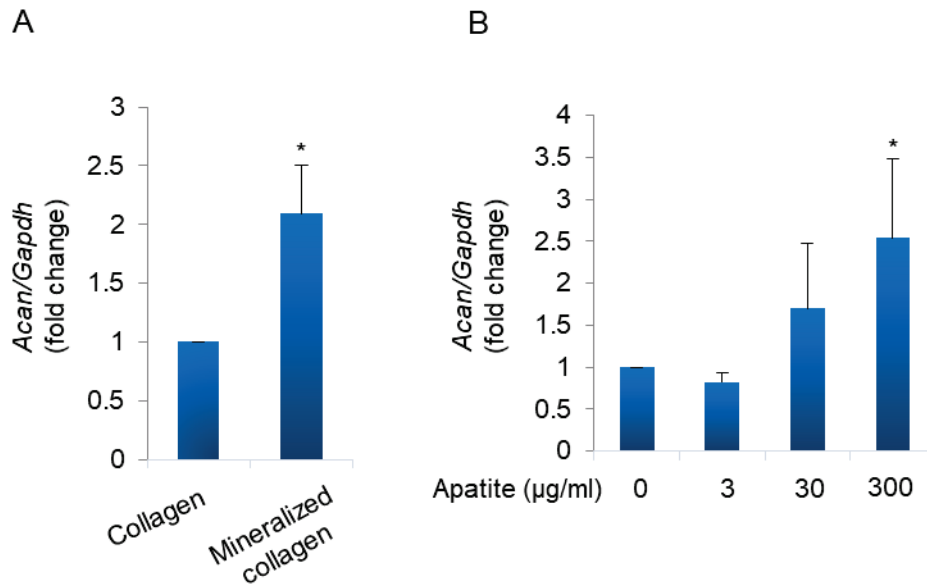


**Figure 22.** The effect of apatite collagen complexes (ACCs) and apatite crystals in suspension (ACs) on *Acan* gene expression in MOVAS determined by quantitative PCR (qPCR). MOVAS cells were cultured on either mineralized ACCs (Mineralized collagen) or non-mineralized ACCs (Collagen) for 7 days (A), MOVAS cultured in the presence of different concentrations of ACs in suspension for 7 days at day 17 of stimulation (B).

#### 4.2.3. The effect of ACs generated by TNAP on *Bmp-2* gene expression

In order to begin identifying factors involved in the effects of TNAP and crystals on chondrocyte gene expression, we focused on bone morphogenetic protein-2 (BMP-2), one of the most potent anabolic growth factors (Biver *et al.*, 2013). BMP-2 was shown to be expressed in human atherosclerotic plaques after calcification has been initiated (Chatrou *et al.*, 2015). In cultured VSMCs, its expression was induced by apatite crystals (Sage *et al.*, 2011).

Experiments were performed at day 17 of osteogenic treatment in the presence of 50 µg/ml AA and 10 mM β-GP, just before the period of maximum TNAP activity on day 21. We observed that *Bmp-2* expression was increased by approximately 2-fold when VSMCs were cultured on mineralized collagen as compared with unmineralized collagen, and that ACs alone were also able to significantly stimulate *Bmp-2* expression by 4-fold (Fig. 23A, B). In addition, we observed an increase in *Bmp-2* levels in response to addition of exogenous alkaline phosphatase by 3-fold (Fig. 23C). Furthermore, hypertrophic chondrocytes treated with levamisole had decreased levels of *Bmp-2* as well as its transcriptional target *Id1* by approximately 2-fold, suggesting a loss of BMP-2 activity upon inhibition of TNAP (Fig. 24A).

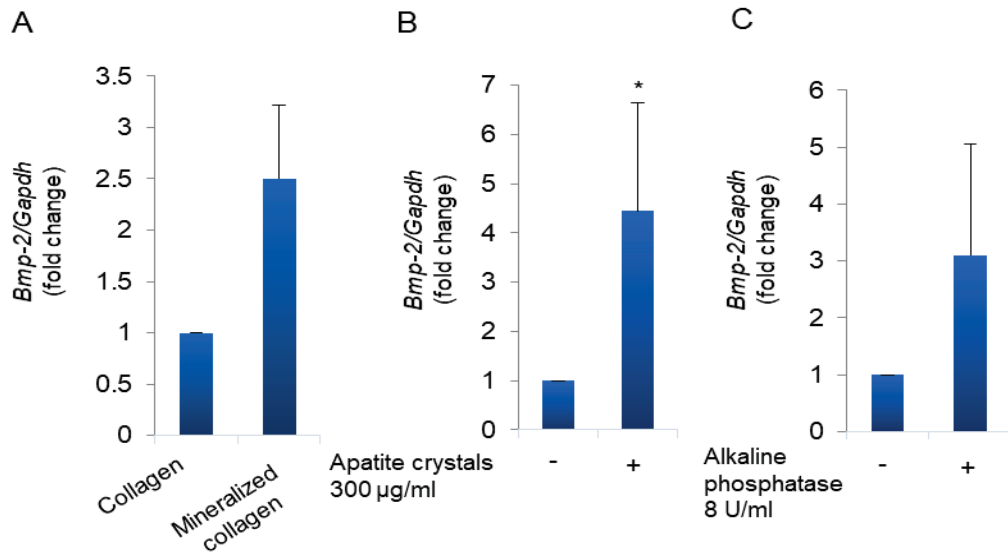


**Figure 23. The effect of ACs and exogenous alkaline phosphatase on *Bmp-2* gene expression in MOVAS.** *Bmp-2* mRNA levels were quantified after MOVAS cell culture on either mineralized or non-mineralized ACCs for 7 days (A); after MOVAS cell culture in the presence of different concentrations of ACs in suspension for 7 days at day 17 of stimulation (B), after MOVAS cell culture in the presence or absence of exogenous alkaline phosphatase for 7 days at day 17 of stimulation (C).

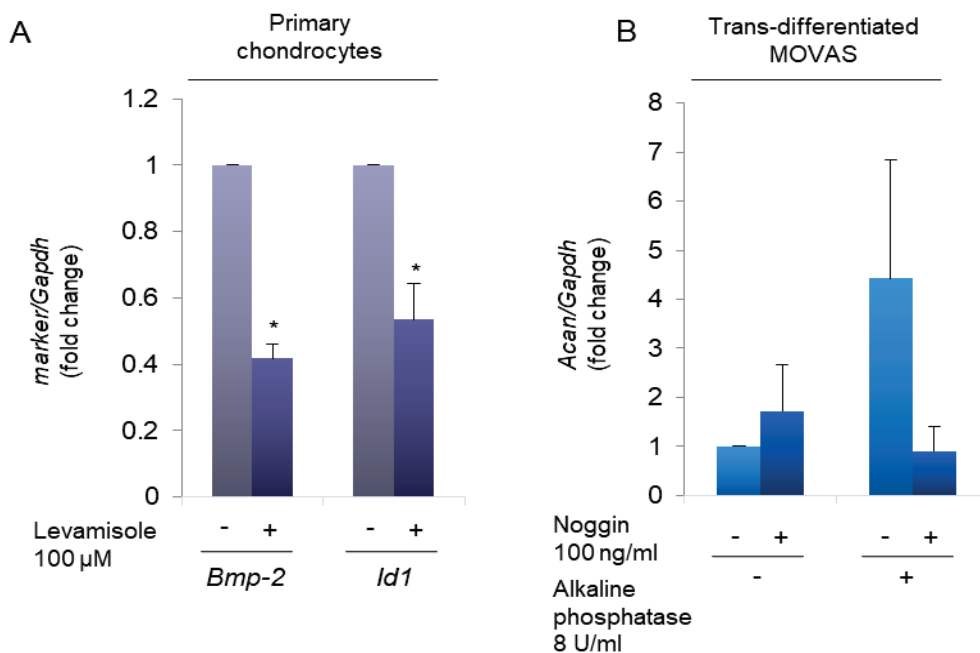


**Figure 24. Stimulation of *Acan* in MOVAS by BMP-2 activation mediated by TNAP.** Primary chondrocytes were stimulated for mineralization in the presence of 50 µg/ml AA and 10 mM β-GP for 10 days with or without 100 µM levamisole, followed by quantification of *Bmp-2* and *Id1* mRNA levels (A). MOVAS at day 17 of stimulation were treated with or without exogenous alkaline phosphatase for 7 days, in the presence or absence of the BMP-2 antagonist noggin (B).

Finally, we used noggin, an antagonist of BMP-2 activity to demonstrate that alkaline phosphatase activity stimulates aggrecan expression by stimulating BMP-2 (Fig. 24B).

#### 4.2.4. Study of ACs cytotoxicity

Then, we were interested how crystals generated by TNAP may affect gene expression by the cells. One of the possible mechanisms is activation of inflammasome complex leading to caspase-1 maturation which mediates the secretion of IL-1 $\beta$  (Martinon *et al.*, 2009). As already mentioned, NLRP3 inflammasome was shown to be required for atherogenesis and could be activated by crystalline structures (Dewell *et al.*, 2010; Rajamäki *et al.*, 2010). Interestingly, IL-1 $\beta$  has been shown recently to induce BMP-2 expression in human VSMCs (Ikeda *et al.*, 2012). Moreover, several reports indicate that this activation may involve cell death mechanisms caused by crystals (Ewence *et al.*, 2008; Cullen *et al.*, 2015).

In order to study the cytotoxic effect of ACs on non-differentiated and trans-differentiated MOVAS, we treated both at confluence with different concentrations of crystals and with or without TNF- $\alpha$ .

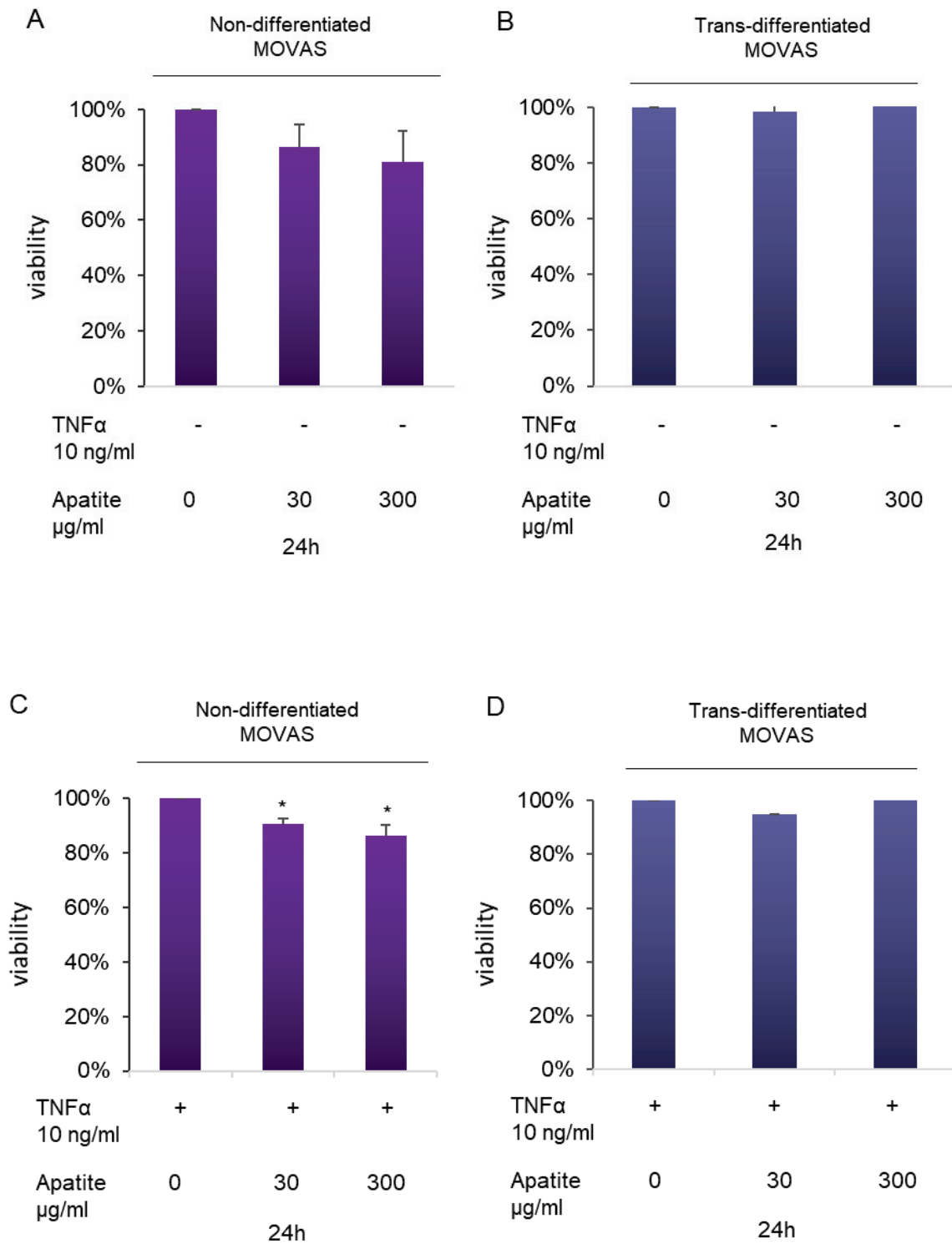


**Figure 25. Study of the effect of apatite ACs on MOVAS proliferation.** Cell proliferation quantified by MTT test in non-differentiated MOVAS (A) or cells trans-differentiated during 17 days (B) and cultured in the presence (+) or absence (-) of TNF- $\alpha$  and ACs at different concentrations.

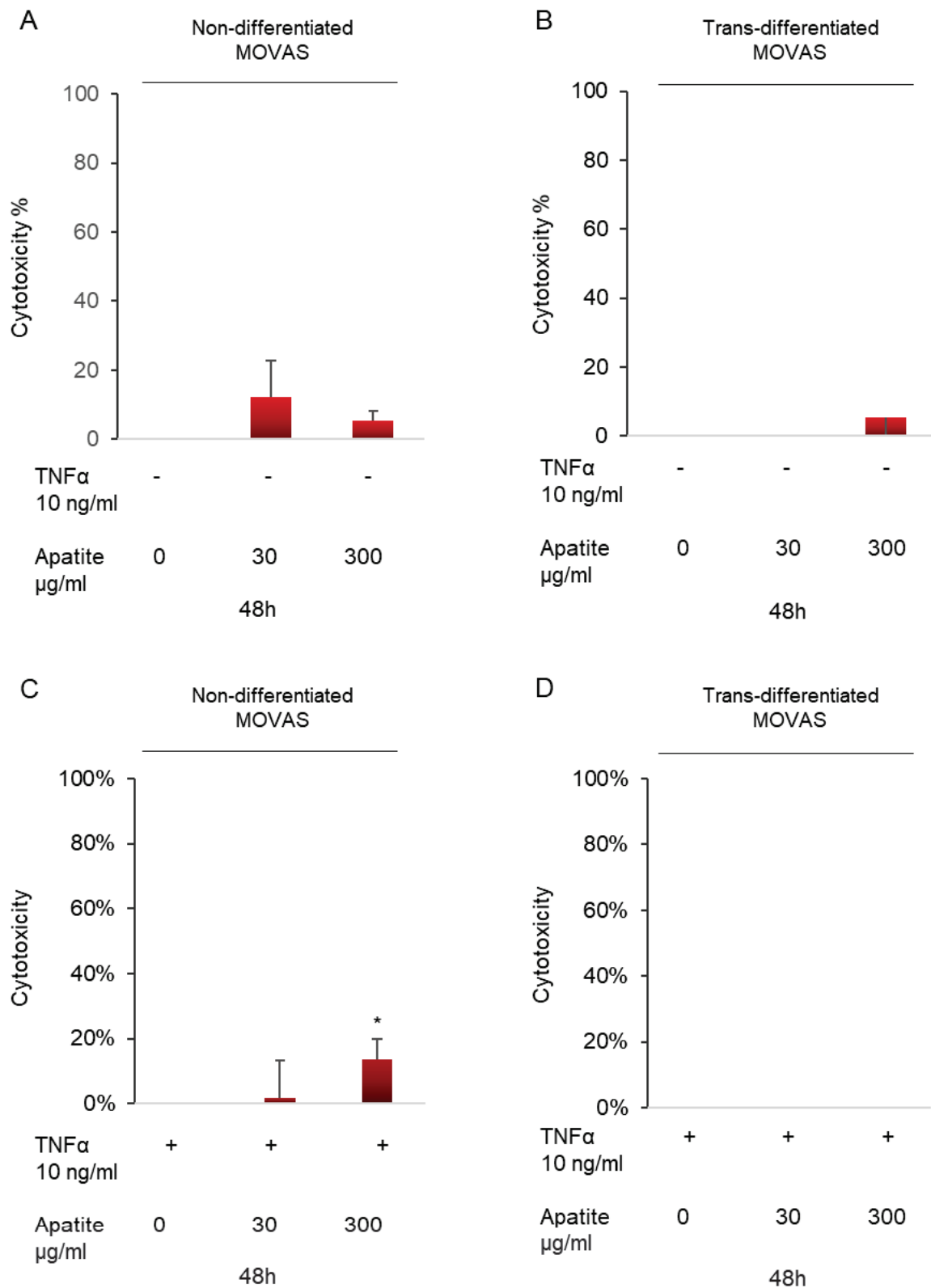


**Figure 26. Study of the cytotoxic effect of ACs on MOVAS.** Cytotoxicity of ACs measured by LDH assay in non-differentiated MOVAS (A) or cells trans-differentiated during 17 days (B) and cultured in the presence (+) or absence (-) of TNF- $\alpha$  and ACs at different concentrations.



Interestingly, we observed a dose-dependent decrease of non-differentiated MOVAS viability after 24 h of treatment with ACs (**Fig. 25A**) as well as the cytotoxic effect of ACs at the dose of 300 µg/ml after 48 h of treatment (**Fig. 26A**). In the case of trans-differentiated cells, apatite crystals did not affect cell viability and did not exert any cytotoxic effect (**Fig. 25B, Fig. 26B**).

### **4.3. TNAP and annexin localization and function in MV-mediated mineralization of MOVAS**

#### **4.3.1. TNAP localization in MOVAS**

Previously, several studies have been performed to visualize TNAP in human and murine bone tissues (Hoshi *et al.*, 1997; Morris *et al.*, 1992; Lencel *et al.*, 2011). In mineralizing cells, TNAP is anchored to the plasma membrane and to the outer layer of the matrix vesicle membrane via glycosylphosphatidylinositol (GPI). However, TNAP subcellular distribution in smooth muscle cells is poorly characterized, that is why we were interested in TNAP localization in MOVAS. After labelling TNAP with specific fluorescent antibody, we obtained a specific signal on the cell membrane in cells stimulated for mineralization and cultured on the surface of collagen (**Fig. 27**). Thus, we observed that TNAP localization in MOVAS is similar to that observed in human osteoblasts (Morris *et al.*, 1992). In resting cells, TNAP distribution on plasma membrane was regular (**Fig. 27C, arrows**), whereas in MOVAS stimulated for mineralization, we observed TNAP-enriched clusters seen in the apical region (**Fig. 27D, arrows**), being possible sites of MV biogenesis.

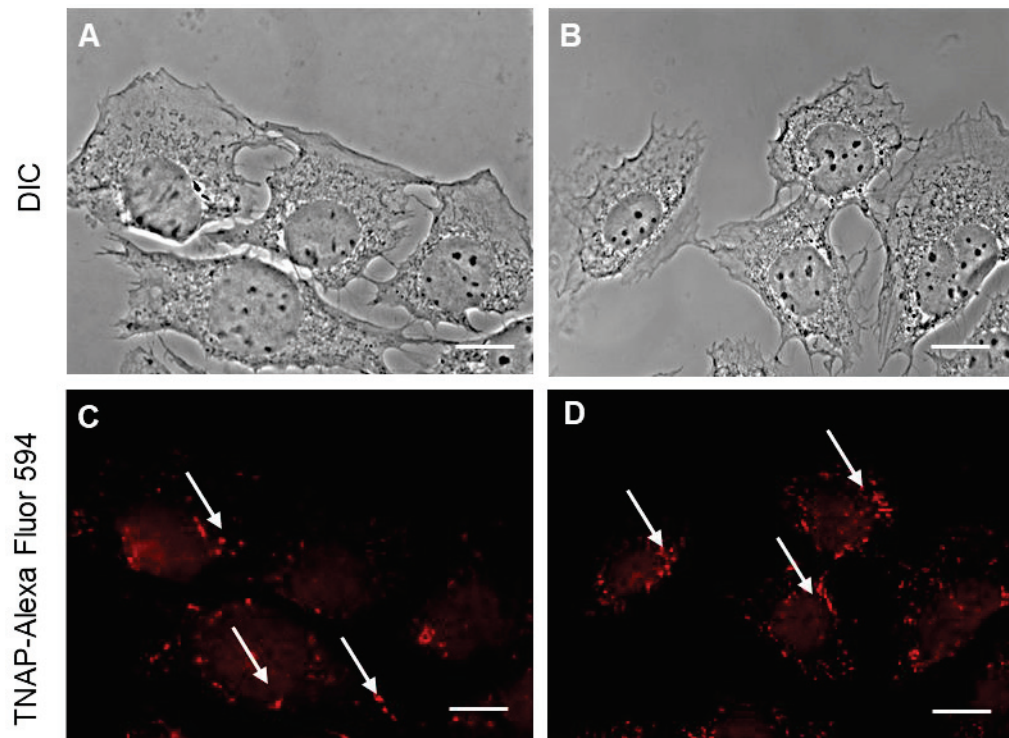


**Figure 27. TNAP localization in MOVAS.** MOVAS cells were visualized after 4 days of culture on collagen-coated coverslips in the presence (**B, D**) or absence (**A, C**) of 50  $\mu\text{g/ml}$  AA and 10 mM  $\beta\text{-GP}$ . TNAP was immunostained with anti-TNAP primary antibody followed by labelling with Alexa Fluor 594 secondary antibody (**arrows**). Representative photos were shown. Magnification 630 x, scale bar – 10  $\mu\text{m}$ .

#### 4.3.2. Morphology of MOVAS and released MVs

TEM analysis of MOVAS VSMC morphology revealed that 4 days of culture in mineralizing conditions were sufficient to stimulate MOVAS cells to release exosomes. More precisely, we observed vesicular structures, most probably MVs, budding from the plasma membrane of MOVAS stimulated for mineralization (**Fig. 28B**), in contrast to resting conditions where some vesicular structures are visible in the cytosol (**Fig. 28A**).

To study mineralization abilities of VSMC-derived MVs, collagen-free and collagen-attached, we applied two different strategies of MV isolation (described in Materials and methods section). Collagen-free MVs is a fraction of vesicles released by the cells to the culture medium, whereas collagen-attached MVs were isolated after collagenase digestion ECM produced by cell culture.

Concerning vesicle diameter, both fractions contained vesicles with the size between 30 and 100 nm (**Fig. 29E, F**) i.e., dimensions close to those released from growth plate chondrocytes whose minimum diameter is 30 nm and the average one is 200 nm (Zhang *et al.*,

2005). Moreover, it seems that our observations concerning murine MVs fit quite well with the findings of Reynolds and collaborators who determined that human VSMC-derived MVs had the diameter of less than 150 nm (Reynolds, 2004). Moreover, looking at TEM images, it is noticeable that the fractions of collagen-attached MVs (**Fig. 29D**) are enriched in electron dense material, in contrast to collagen-free MVs collected from the culture medium, which seem to be empty (**Fig. 29C**).

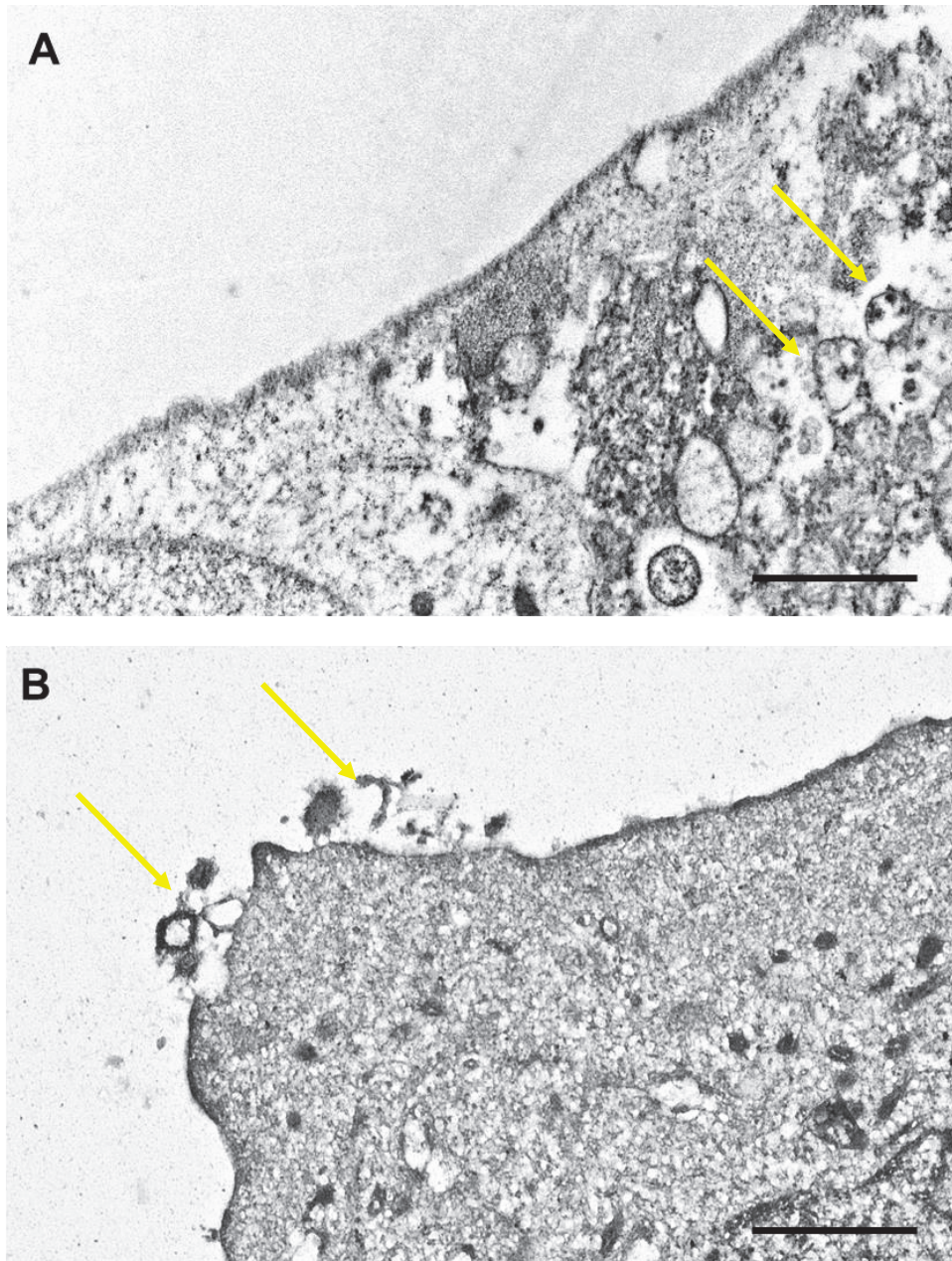


**Figure 28. Ultrastructure of MOVAS.** MOVAS cells were cultured in the presence (**B**) or absence (**A**) of 50 µg/ml AA and 10 mM β-GP for 4 days. Intracellular vesicles (**A, yellow arrows**) and extracellular vesicles (**B, yellow arrows**) were detected. Representative photos were shown. TEM images taken at 15,000 x magnification, scale bar – 2 µm.



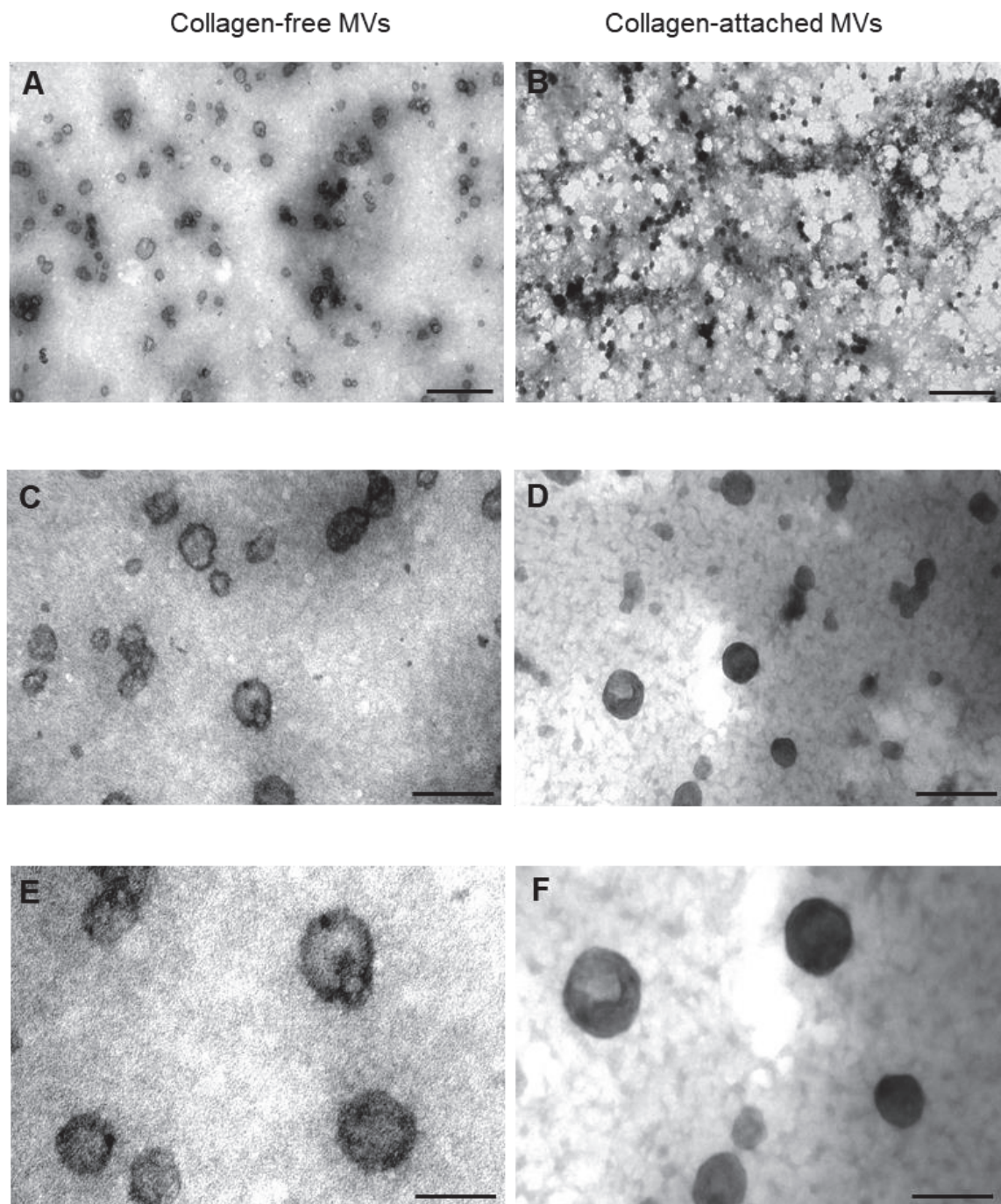


**Figure 29. Ultrastructure of collagen-free and collagen-attached MVs produced by trans-differentiated MOVAS.** MVs were isolated after culture of MOVAS in the presence of 50  $\mu\text{g/ml}$  AA and 10 mM  $\beta\text{-GP}$  for 21 days. Representative photos were shown. TEM images taken at: 50,000 x magnification, scale bar – 500 nm (**A, B**), 150,000 x magnification, scale bar – 200 nm (**C, D**), and 300,000 x magnification – scale bar – 100 nm (**E, F**).

### 4.3.3. The role of TNAP in MV-mediated mineralization

Different fractions of MOVAS cells and released MVs exhibited distinct protein patterns (**Fig. 30**). It is noticeable that whole cell lysates (WCLs) contain a broader range of protein sizes than both MV fractions. Also, after comparison of collagen-attached VSMC-derived MVs with bone collagenase-released MVs (Bechkoff *et al.*, 2008), their protein profiles are also quite different.

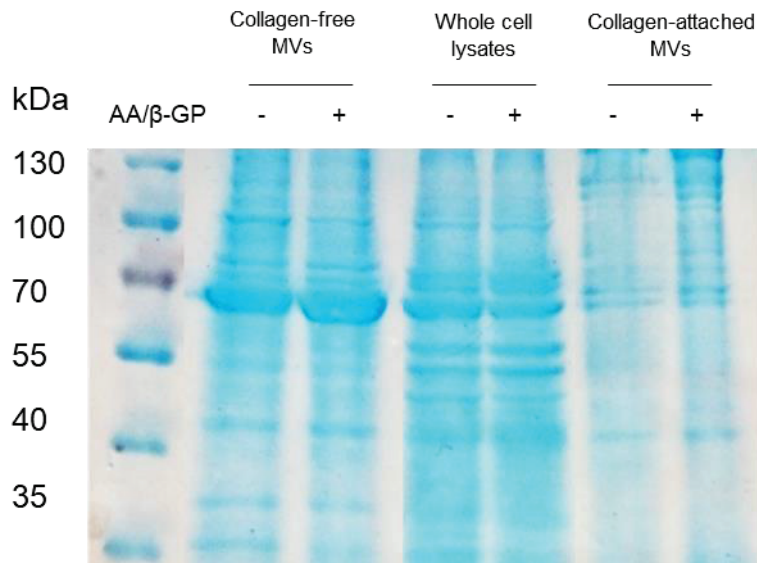


**Figure 30. Protein profiles of whole cell lysates (WCLs) and MVs of MOVAS.** Protein patterns were visualized after electrophoresis and staining of the gel with AMRESCO Protein Stain of WCLs as well as fractions of collagen-free and collagen-attached MVs of MOVAS cultured in the presence (+) or absence (-) of 50 µg/ml AA and 10 mM β-GP for 21 days. Representative gel was shown.

The presence of the active form of TNAP in different fractions of MOVAS was confirmed by the NBT/BCIP method (**Fig. 31**). Then, after measuring TNAP specific activity in WCLs and in the two different fractions of MVs, we observed that treatment in mineralizing conditions significantly stimulated TNAP activity in MVs that were attached to collagen by 2.5-fold and in WCLs, but not in collagen-free MVs (**Fig. 32**). Moreover, analysis of the protein content revealed that TNAP protein expression was increased by approximately 3-fold only in collagen-attached MVs after stimulation for mineralization (**Fig. 33**). Thus, our observations are analogous to the results of Chen and collaborators obtained in MVs originating from bovine VSMCs (Chen *et al.*, 2008) and with the previous studies showing that association

of MVs released by mineralizing cells with collagen is an important step in mineral expansion (Genge *et al.*, 2008; Kim and Kirsch, 2008).

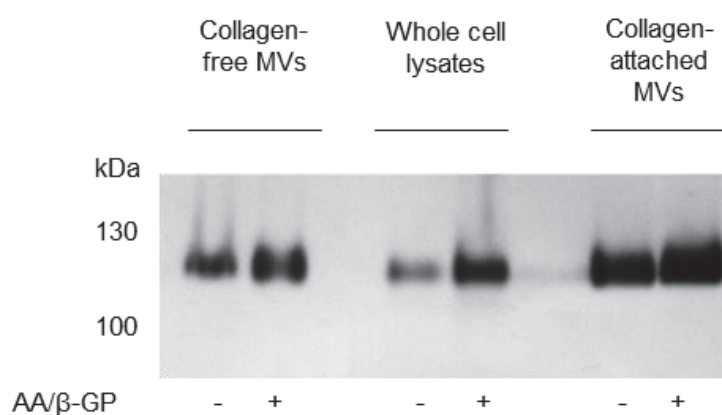


**Figure 31. The presence of the active form of TNAP in WCLs and MVs of trans-differentiated MOVAS stained by NBT/BCIP method.** Colorimetric analysis were performed after gel electrophoresis of WCLs as well as fractions of collagen-free and collagen-attached MVs of MOVAS cultured in the presence (+) or absence (-) of 50  $\mu\text{g/ml}$  AA and 10 mM  $\beta\text{-GP}$  for 21 days. Representative gel was shown.

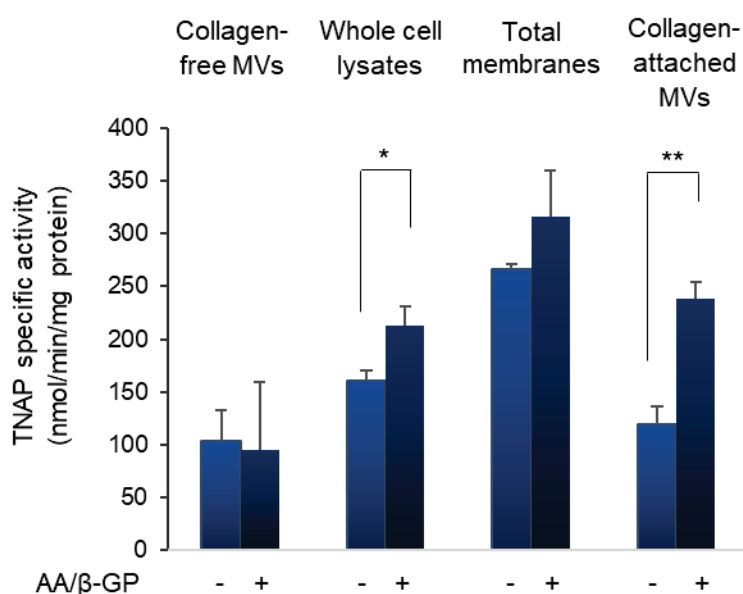


**Figure 32. Comparison of TNAP specific activity in different fractions of MOVAS and released MVs.** TNAP specific activity was measured in WCLs as well as in fractions of total membranes, collagen-free and collagen-attached MVs of MOVAS cultured in the presence (+) or absence (-) of 50  $\mu\text{g/ml}$  AA and 10 mM  $\beta\text{-GP}$  for 21 days.

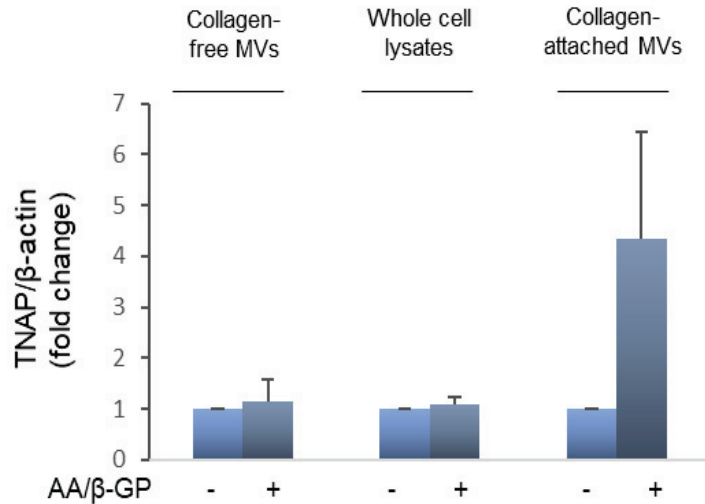


**Figure 33. The effect of trans-differentiation on TNAP protein content in WCLs of MOVAS and released MVs.** Western Blot analysis were performed after 21 days of MOVAS stimulation in the presence (+) or absence (-) of 50 µg/ml AA and 10 mM β-GP. Quantitative analysis of band optical density normalized to the β-actin were presented.

#### 4.3.4. Study of the role of cholesterol (Chol) in mineralization

Regarding a well-known role of Chol in the initiation of atherosclerosis, we were interested if there is any correlation between Chol content in VSMC-derived MVs and mineralization. An interesting study by Geng and collaborators revealed that Chol metabolism is implicated in mineralization by vascular cells (Geng *et al.*, 2011). It is known from the previous studies on physiological mineralization, that MVs originating from chondrocytes are enriched in Chol and several phospholipids, such as phosphatidylcholine (PC), PEA and PS (Damek-Poprawa *et al.*, 2006; Abdallah *et al.*, 2014). In general, vesicles released by mineralizing cells have similar lipid composition to the composition of plasma membrane, but in different proportions (Golub, 2009). Thus, we measured also Chol content in analyzed fractions of MOVAS and observed increased amount of Chol in the fraction of total membranes, but not in MVs. The level of Chol in total membranes exceeded significantly, by approximately 5-fold, its amount in WCLs and MVs (**Fig. 34**).



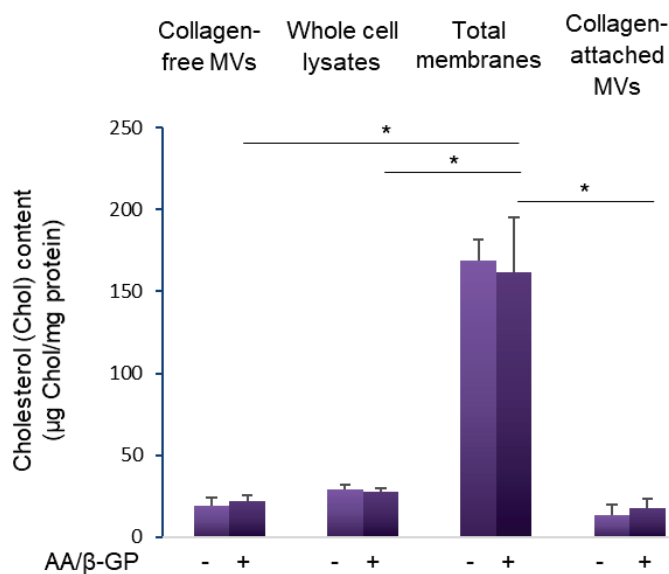


**Figure 34. Comparison of cholesterol (Chol) content in different fractions of MOVAS and released MVs.** Chol content was measured after 21 days of MOVAS stimulation in the presence (+) or absence (-) of 50 µg/ml AA and 10 mM β-GP. Chol content was measured by Amplex Red Cholesterol Assay and normalized to protein concentration.

#### 4.3.5. Localization of lipid rafts in MOVAS

Biological membranes are not homogeneous, but they are rather composed of highly organized lipid and protein complexes called lipid rafts. These membrane microdomains were shown to be enriched in Chol, PS and ganglioside 1 (GM1) (Moreno-Altamirano *et al.*, 2007). Gangliosides are a group of glycosphingolipids that have at least one sialic acid residue. The main function of membrane lipid raft microdomains is to organize signaling molecules into functional complexes for targeted transport of transmembrane and GPI-anchored proteins, that is why their protein composition is highly fluctuating. However, in mineralizing cells GPI-anchored TNAP was shown to associate with these domains. It is not clear whether lipid rafts and the process of MV budding from plasma membrane microvilli are related. As a next step, we considered GM1 and Chol as markers of lipid rafts and studied their intracellular distribution in VSMCs (**Fig. 35**). For better visualization of Chol and GM1 co-localization, filipin regular blue staining was replaced by red pseudocolor, indicating an area of co-localization by providing a yellow signal in combination with green staining of GM1. Interestingly, in resting cells we observed co-localization of Chol and GM1 on the plasma membrane (**Fig. 35G, arrows**), whereas in cells stimulated for mineralization there was a co-localization of lipid raft markers in the apical region of the cell (**Fig. 35H, arrows**), similarly to TNAP localization in MOVAS stimulated for mineralization, presented in **Fig. 27D**.

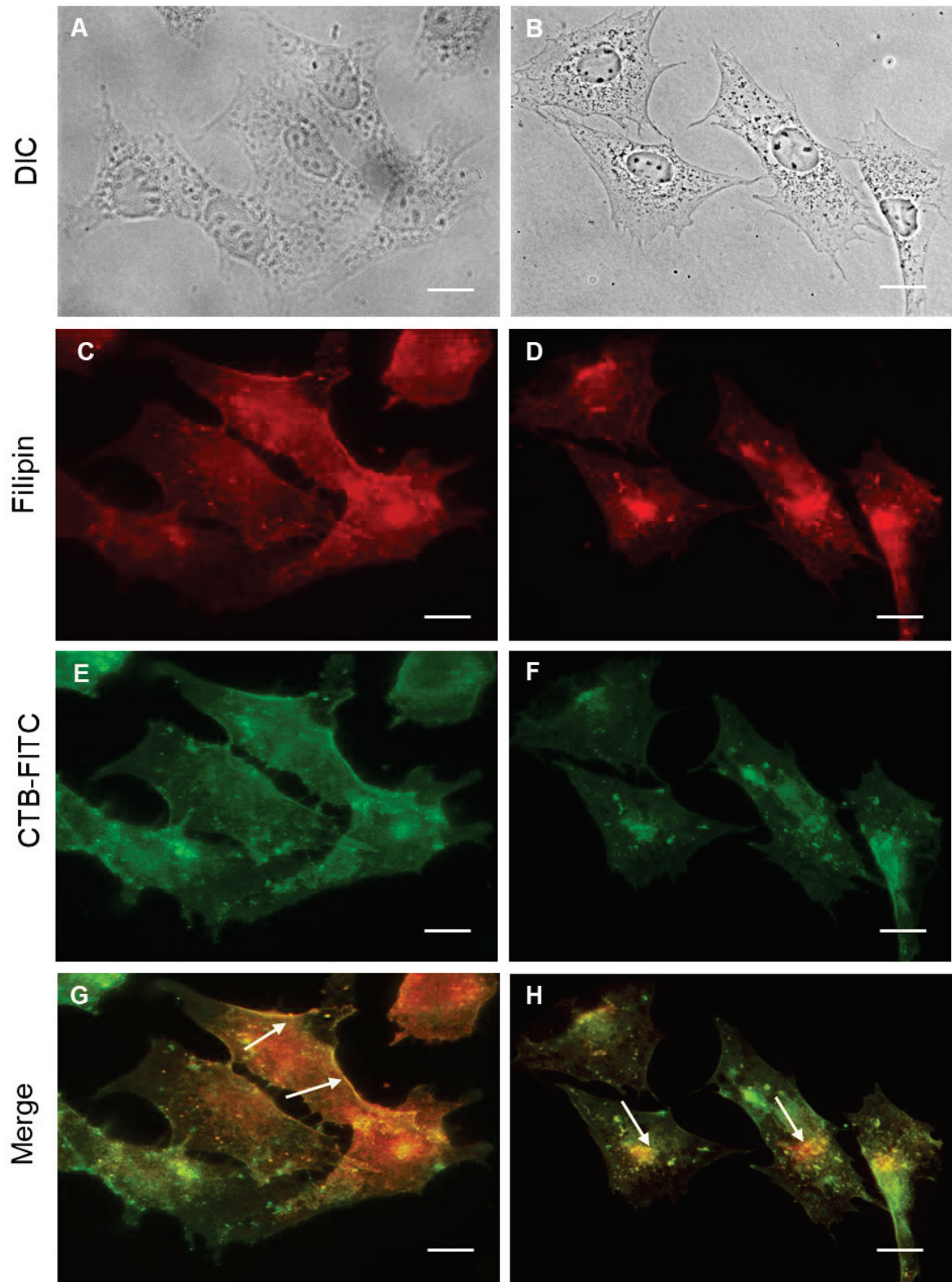


**Figure 35. Co-localization of Chol and GM1, markers of lipid rafts in MOVAS.** Chol was visualized by staining with filipin (regular blue color replaced by red pseudocolor), whereas GM1 was visualized by staining with Cholera toxin subunit B with FITC conjugate (green). MOVAS cells in resting conditions (A, C, E, G) and after 24 h of stimulation for mineralization (B, D, F, H) were presented. Representative photos were shown. Magnification – 630 x; scale bar – 10  $\mu$ m.

#### 4.3.6. Localization and function of annexins

Cellular annexins are normally present in the cytosol, however, in response to a rise in extracellular calcium, they may translocate to the plasma membrane (Monastyrskaya *et al.*, 2007). Indeed, both TNAP and annexin A2 (AnxA2) were shown to associate with lipid raft microdomains within plasma membrane of osteoblast-like cells (Gillette, 2003). After fluorescent staining of AnxA2 (**Fig. 36**) and AnxA6 (**Fig. 37**), in both cases we observed accumulation of annexin-enriched vesicular structures in a perinuclear region of trans-differentiated cells (**Fig. 36B and 37B, arrows**). Moreover, visualization of AnxA6 after overexpression of AnxA6 in living cells (**Fig. 38**) confirmed our observation of AnxA6 subcellular distribution by immunofluorescence.

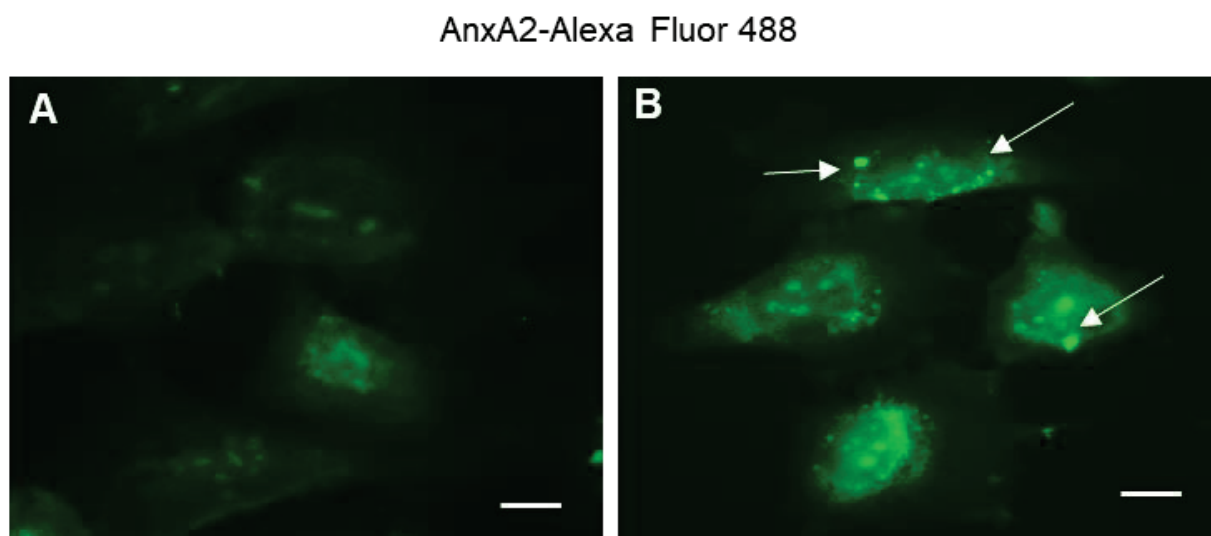


**Figure 36. Subcellular distribution of AnxA2 in MOVAS.** AnxA2 was visualized by immunofluorescence using an anti-AnxA2 primary antibody labelled with Alexa Fluor 488 secondary antibody after 24 h of stimulation in the presence (**A**) or absence (**B**) of AA and  $\beta$ -GP. GFP fluorescent filter was applied to image AnxA2 locations (**B, arrows**). Representative photos were shown. Magnification 630 x, scale bar – 10  $\mu$ m.

### AnxA6-Alexa Fluor 488

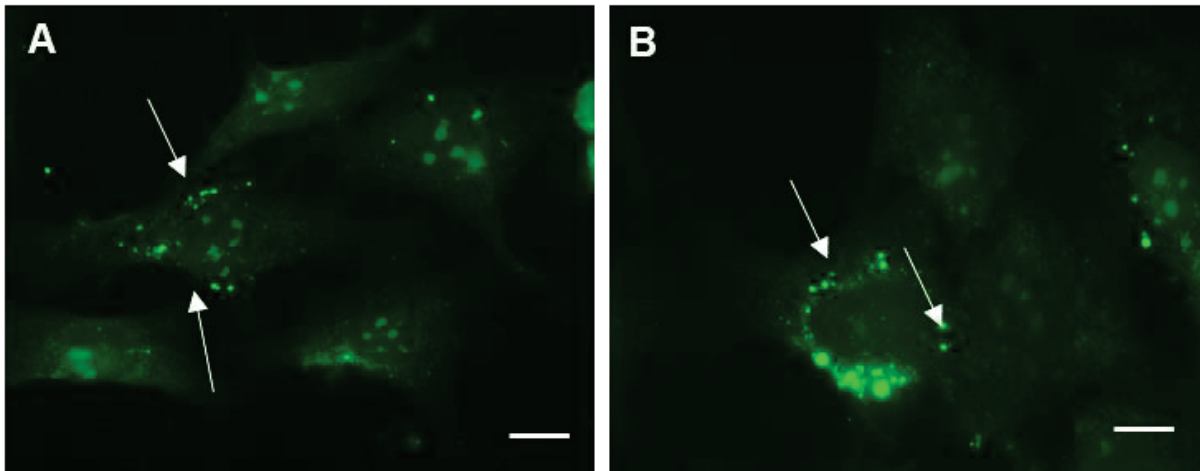


**Figure 37. Subcellular distribution of AnxA6 in MOVAS.** AnxA6 was visualized by immunofluorescence using anti-AnxA6 primary antibody labelled with Alexa Fluor 488 secondary antibody in cells cultured for 24 h in the presence (**B**) or absence of 50  $\mu\text{g/ml}$  AA and 10 mM  $\beta\text{-GP}$  (**A**). Fluorescent filter was applied to image AnxA6 locations (**A, B, arrows**). Representative photos were shown. Magnification 630x, scale bar – 10  $\mu\text{m}$ .

### AnxA6-EGFP-N3

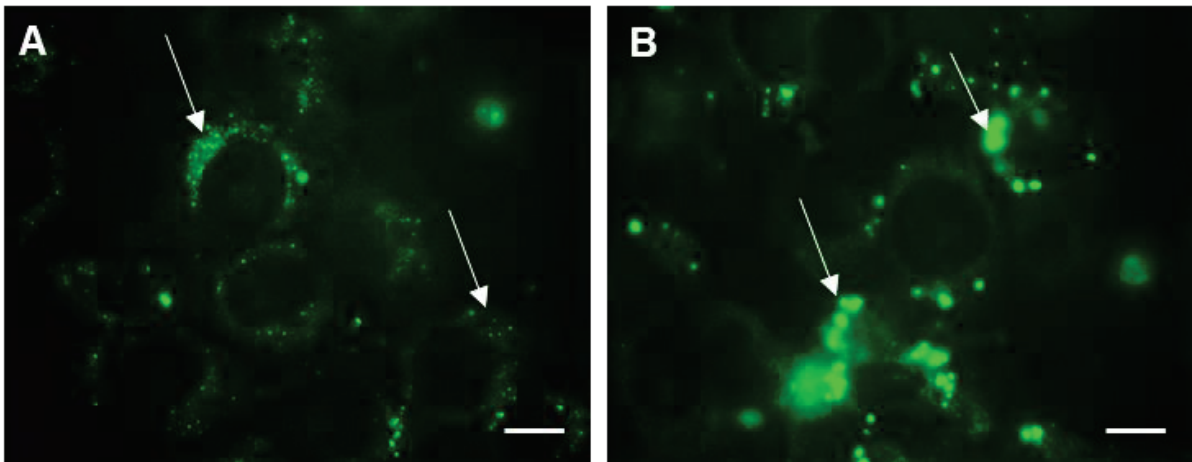


**Figure 38. Overexpression of AnxA6 in MOVAS.** MOVAS cells were transfected with a EGFP-N3 vector containing AnxA6 insert in resting conditions (**A**) and after 7 days of stimulation for mineralization in the presence of 50  $\mu\text{g/ml}$  AA and 10 mM  $\beta\text{-GP}$  (**B**). AnxA6 subcellular distribution was observed in living cells (**A, B, arrows**). Representative photos were shown. Magnification 630 x, scale bar – 10  $\mu\text{m}$ .

Apart from studying subcellular distribution of annexins, we compared also their protein content in MOVAS upon stimulation for mineralization (**Fig. 39**). Interestingly, we observed increased expression of AnxA2 in WCLs of trans-differentiated MOVAS, while the expression of AnxA6 was not changed in trans-differentiated cells in comparison to non-differentiated cells (**Fig. 39B**). Western Blot analysis revealed also the presence of AnxA2 in collagen-free and collagen-attached MVs and AnxA6 only in collagen-attached MVs of MOVAS (results not shown due to insufficient number of repetitions).

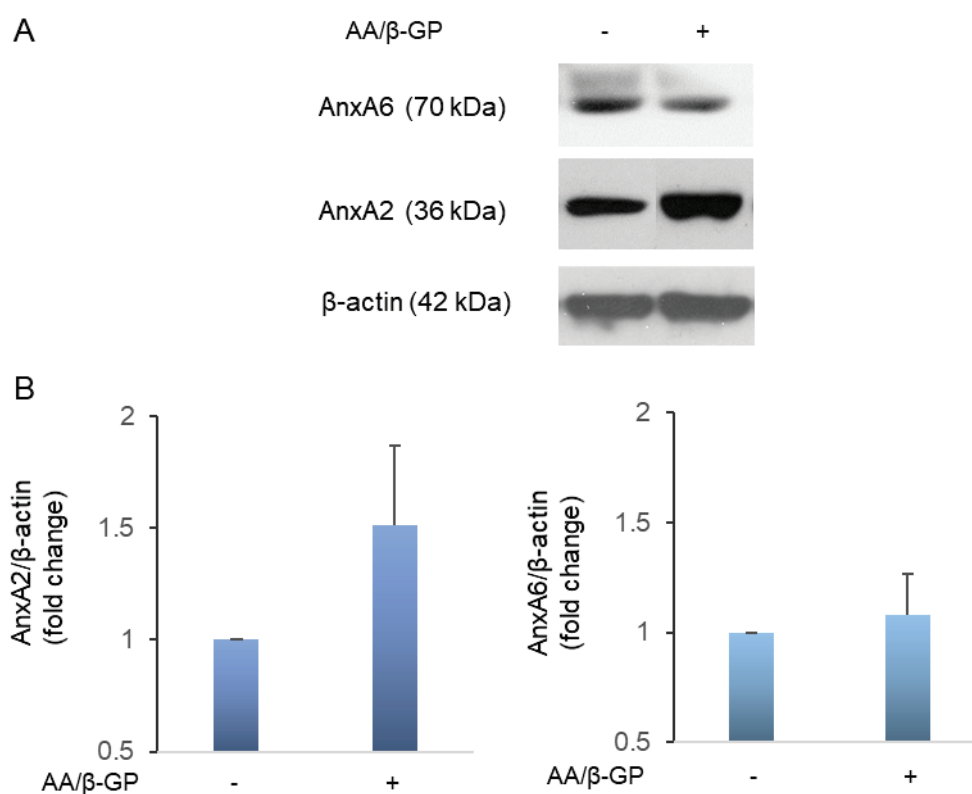


**Figure 39. The effect of trans-differentiation on AnxA2 and AnxA6 protein content in MOVAS WCLs.** Western Blot analysis were performed after 21 days of MOVAS stimulation in the presence (+) or absence (-) of 50  $\mu\text{g/ml}$  AA and 10 mM  $\beta\text{-GP}$ . The representative blots of three independent experiments were shown (**A**). Quantitative analysis of band optical density normalized to the  $\beta\text{-actin}$  were presented (**B**).

#### 4.3.7. MV chemical composition

As a next step, to study chemical composition of the vesicles, we carried out mapping of chemical elements and TEM X-ray microanalysis of collagen-free MVs (**Fig. 40**) and collagen-attached MVs (**Fig. 41**).



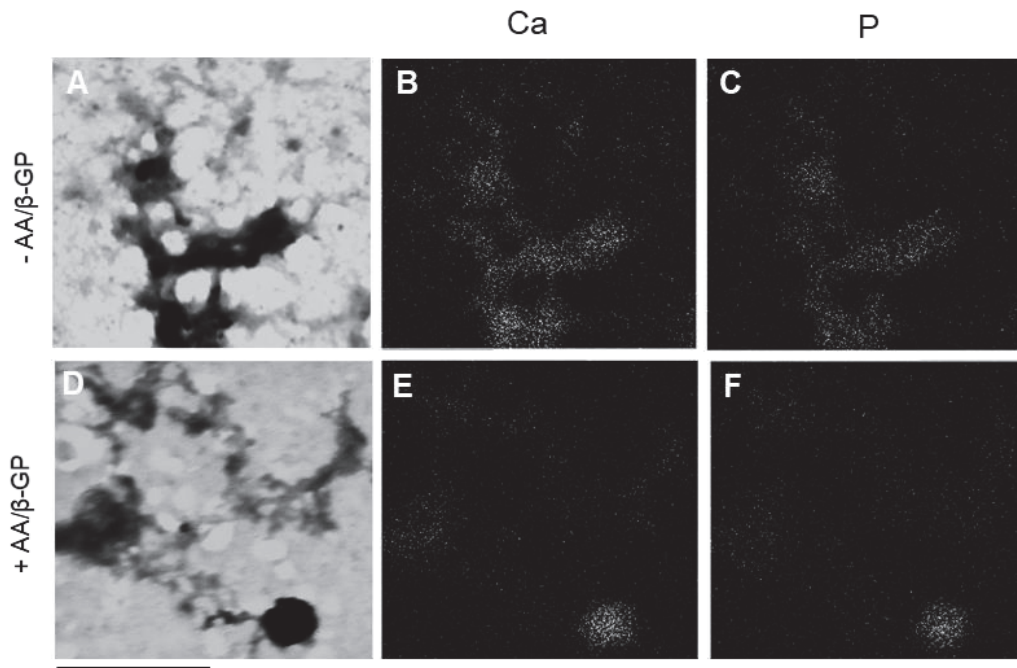


**Figure 40. Maps of collagen-free MV chemical composition.** TEM view of MV clusters (A, D). The maps of calcium (Ca) (B, E) and phosphate (P) (C, F) distribution in MVs were presented. MVs of non-differentiated MOVAS (A-C) and MVs of MOVAS trans-differentiated for 21 days were shown (D-F). Magnification 15,000 x, scale bar – 500 nm.

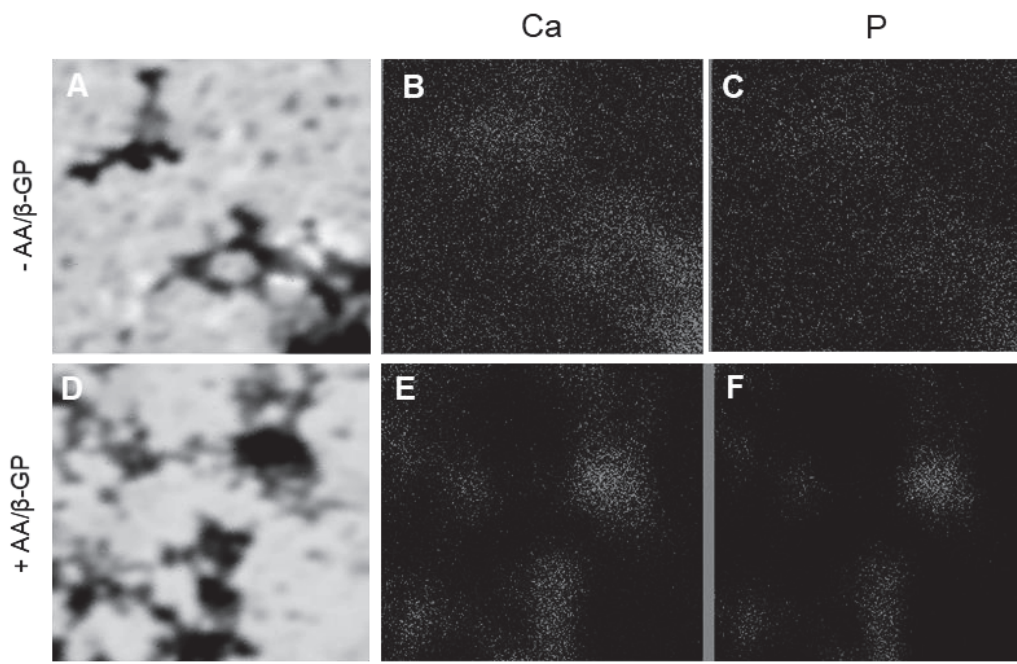


**Figure 41. Maps of collagen-attached MV chemical composition.** TEM view of MV clusters (A, D). The maps of calcium (Ca) (B, E) and phosphate (P) (C, F) were presented. MVs of non-differentiated MOVAS (A-C) and MVs of MOVAS trans-differentiated for 21 days were shown (D-F). Magnification 15,000 x, scale bar – 500 nm.

Interestingly, we detected Ca and P in both types of MVs. However, only in collagen-attached MVs released by trans-differentiated MOVAS, those elements perfectly co-localized with MV clusters (Fig. 41 E, F), in contrast to resting conditions, where both Ca and P were dispersed (Fig. 41B, C).

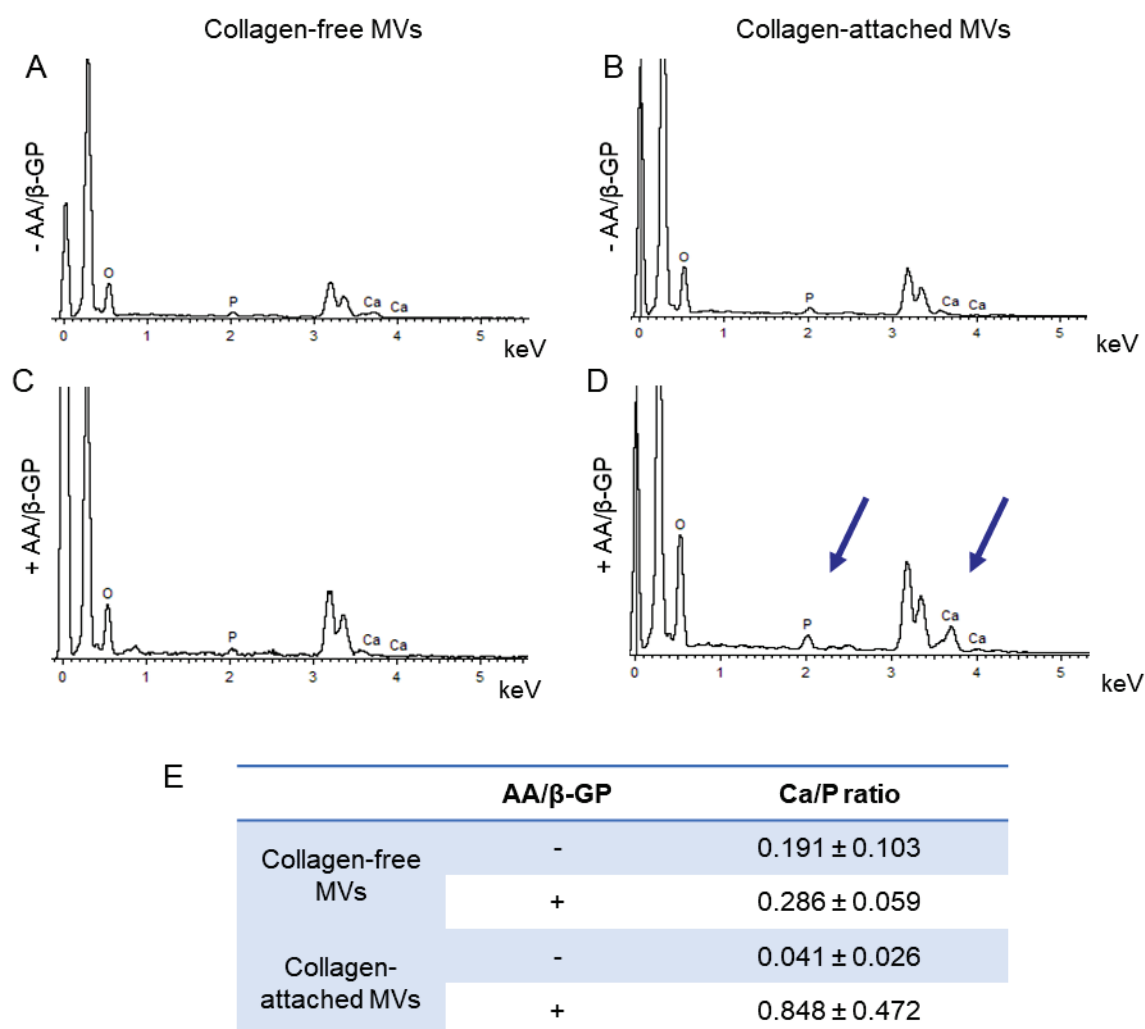


**Figure 42. Chemical composition of mineral produced by MVs derived from MOVAS.** Representative spectra obtained by TEM-EDX from collagen-free (A, C) and collagen-attached MVs (B, D). Both fractions of vesicles were isolated from MOVAS by differential ultracentrifugation after 21 days of treatment in the presence (+) or absence (-) of 50  $\mu$ g/ml AA and 10 mM  $\beta$ -GP. Increased levels of calcium (Ca) and phosphate (P) were indicated (D, arrows). Ca/P ratios of MVs were summarized in the table (E).

As a result of point measurements, we obtained peaks of P at the level of 2 keV and peaks of Ca between 3.5 and 4 keV. The spectrum between 3 and 3.5 keV represent uranium in the samples, which was used as a counterstain (Fig. 42A-D). Interestingly, we observed



increased levels of calcium (Ca) and phosphate (P) resulting in a Ca/P ratio close to 1 only in the case of collagen-attached MVs derived after stimulation for mineralization and collagenase digestion (**Fig. 42D, arrows, 42E**), whereas this ratio was lower in their collagen-free counterparts. This probably reflects an increased rate of calcium entry in MVs since intracellular calcium levels are normally much lower than the levels of  $P_i$ .

The Ca/P ratio of 1.67, calculated according to the formula of synthetic hydroxyapatite (HA) -  $Ca_{10}(PO_4)_6(OH)_2$  - does not specify the nature of biological apatite, which comprises several substitutions, with for instance  $CO_3^{2-}$  residues replacing either  $PO_4^{3-}$  or  $OH^-$  ions in apatite crystals. Moreover, biological apatites are calcium-deficient apatites in which calcium can be replaced by several other cations, such as fluorine or chlorine (Strzelecka-Kiliszek *et al.*, 2017). Our results indicate that the presence of collagen scaffold may be necessary for efficient mineral nucleation mediated by VSMC-derived MVs. Moreover, we would like to underline that collagenase digestion is an important step to obtain calcifying vesicles from trans-differentiated VSMCs.

# **Chapter V**

## **Discussion**

## Chapter 5. Discussion

Murshed and collaborators proposed the explanation of the phenomenon that physiological mineralization occurs exclusively in bone tissue. They indicated that co-expression of genes encoding two indispensable proteins, TNAP and collagen, is a specific feature of bone (Murshed, 2005). As a result of our collaboration with University of Lyon, we have shown recently that TNAP is necessary for differentiation of MSCs, the chondrocyte precursors, towards chondrocytes as well as for normal chondrocyte differentiation (Fakhry *et al.*, 2017). The fact that TNAP-deficient mice have disorganized growth plate is consistent with our observations (Narisawa *et al.*, 1997; Liu *et al.*, 2014).

Due to the clinical importance of VC, it is important to determine whether the proposed model may also relate to ectopic calcification. Accumulating data suggest that the type and location of calcifications rather than their extent are crucial for determination of atherosclerotic plaque stability (Ehara, 2004; Vengrenyuk *et al.*, 2010; Kelly-Arnold *et al.*, 2013). Microcalcifications are now considered as key determinants of acute cardiovascular complications. Those small but dangerous crystals seem to be particularly harmful when they are located in a fibrous cap (Vengrenyuk *et al.*, 2010; Kelly-Arnold *et al.*, 2013), where they may cause plaque rupture, even at the early stages of atherosclerosis. However, molecular mechanisms responsible for their formation are not yet elucidated.

### Origin of microcalcification

Several explanations were proposed to explain the origin of artery microcalcifications. Firstly, extracellular vesicles released by the cells during atherosclerosis have received particular attention. Interestingly, sortilin is a protein being recently characterized as a key regulator of VC, by the capacity to load TNAP to VSMC-derived MVs (Goettsch *et al.*, 2016). What is interesting is that smooth muscle cell calcification requires sortilin phosphorylation (Goettsch *et al.*, 2016). Thus, phosphorylation of sortilin is a potential therapeutic target for the formation of microcalcifications in the arteries.

Also, macrophages were proposed as cells able to release extracellular vesicles mediating crystal formation, similarly to MVs released by chondrocytes (New *et al.*, 2013). However, macrophages were shown to give rise to osteoclasts, but not to differentiate towards mineralizing cells. That is why this hypothesis requires further verification.

Another possibility is that microcalcification may form due to macrophage or VSMC apoptosis and/or necrosis. Indeed, the clearance of apoptotic bodies during atherogenesis

is impaired (Schrijvers, 2005), and they are abundantly present in atherosclerotic lesions. Thus, apoptotic bodies released by dying cells may serve as a nidus for calcification (Proudfoot *et al.*, 2000). However, this mechanism would be a difficult target for clinical treatment.

#### Involvement of TNAP in formation of microcalcification

Based on the results presented above as well as on the reports of other groups, we hypothesize, that TNAP may be involved in formation of microcalcifications. We have recently demonstrated that overexpression of TNAP was sufficient to induce mineralization in VSMCs (**Fig. 13**). Interestingly, this effect was not dependent on VSMCs trans-differentiation, since it occurred in A7R5 rat VSMCs which in our hands did not express any markers of osteoblast or chondrocyte differentiation.

TNAP-mediated induction of mineralization which we observed in VSMCs was very likely due to the hydrolysis of  $PP_i$ , as it is during *in vivo* mineralization (Hessle *et al.*, 2002). Moreover, it has been demonstrated that TNAP overexpression, specifically in VSMCs, was sufficient to induce artery calcification in mice (Sheen *et al.*, 2015). In addition, a very recent study revealed that TNAP overexpression accelerated coronary artery disease in mice (Romanelli *et al.*, 2017).

#### VSMC trans-differentiation and plasticity

VSMCs of the artery walls are not terminally differentiated, but they are able to modulate their phenotype in response to changing environment. In a mature blood vessel, VSMCs exhibit a “contractile” or differentiated (synthetic) phenotype characterized by the expression of contractile markers specific to smooth muscle, such as smooth muscle myosin heavy chain, smooth muscle  $\alpha$ -actin, h-caldesmon, and calponin, which are important for the regulation of the contraction (Rzucidlo *et al.*, 2007). Upon injury, VSMCs dedifferentiate and re-enter the cell cycle. Synthetic VSMCs demonstrate an increased rate of proliferation, migration, and synthesis of ECM. On the other hand, they are characterized by decreased expression of smooth muscle-specific contractile markers.

It was proposed that VSMC phenotypic plasticity may allow VSMC trans-differentiation towards osteoblasts or chondrocytes. Trans-differentiation is defined as the irreversible switch of one type of somatic cell to another. Natural trans-differentiation occurs in two steps: firstly, the cell dedifferentiates; and secondly, the natural developmental

programme is activated, allowing the cell to differentiate into a new lineage (Jopling *et al.*, 2011).

VSMCs, osteoblasts and chondrocytes derive from a common progenitor – mesenchymal stem cell. Commitment of MSCs towards VSMCs, osteoblasts or chondrocytes may be regulated by different factors. For instance, TGF- $\beta$  may stimulate both VSMC and chondrogenic differentiation of MSCs (Magne *et al.*, 2005). Remarkably, VSMCs were shown to lose their lineage markers, such as smooth muscle  $\alpha$ -actin, within 10 days of culture in mineralizing conditions. Conversely, the cells gained simultaneously an osteogenic phenotype as indicated by an increase in expression and DNA-binding activity of the Runx2 transcription factor (Steitz *et al.*, 2001).

#### Origin of macrocalcification

It is difficult to decide whether macrocalcification forms through the processes similar to endochondral or intramembranous ossification. Studies performed in *apoE*<sup>-/-</sup> mice indicated the presence of chondrocyte-like cells and collagen type II within atherosclerotic plaques, suggesting the role of endochondral ossification (Rosenfeld *et al.*, 2000; Rattazzi, 2005). However, some reports, (Herisson *et al.*, 2011), but not all (Aigner *et al.*, 2008), indicate the features of endochondral ossification in human lesions. Moreover, collagens type I and III, characteristic for intramembranous ossification, represent 90% of the total collagens present in human atherosclerotic plaques (Rekhter *et al.*, 1993) That is why in the literature those processes are defined as the consequence of trans-differentiation of VSMCs into osteochondrocyte-like cells. Nevertheless, in our hands, it is likely that TNAP activity stimulated MOVAS cells to trans-differentiate towards chondrocytes, not osteoblasts (**Fig. 20**).

#### Important role of apatite crystals generated by TNAP in regulation of trans-differentiation

In our opinion, the most important result of this PhD thesis is the effect of apatite crystals on VSMC gene expression. Indeed, we observed that treatment of those cells with alkaline phosphatase or apatite crystals, associated (ACCs) or not (ACs) to collagen, induced the expression of *Bmp-2* and *Acan*. To our knowledge, stimulation of BMP-2 by apatite crystals in VSMCs has been already reported by two research groups (Sage *et al.*, 2011; Nahar-Gohad *et al.*, 2015).

BMP-2 is a strong inducer of ectopic calcification (Biver *et al.*, 2013). Therefore, crystals may stimulate VSMC trans-differentiation into chondrocyte-like cells in a large part

through a BMP-2 autocrine loop, analogically to differentiation of MSCs towards osteoblasts. Rawadi and collaborators proposed the mechanism regulating TNAP expression in MSCs (Rawadi *et al.*, 2003). Briefly, BMPs may act through cell surface receptors, activating Smad translocation to the nucleus, resulting in transcription of target genes. In parallel, Smads may activate Wnt/ $\beta$ -catenin cascade that stimulates the expression of TNAP. Indeed, we observed that noggin, BMP antagonist, blocked *Acan* expression induced by alkaline phosphatase (Fig. 23).

Stimulation of *Acan* indicated that MOVAS cells trans-differentiated into cells resembling chondrocytes upon treatment with apatite crystals. Aggrecan is the predominant proteoglycan expressed in growth plate cartilage, and mutations in the human *Acan* gene result in chondrodysplasias (Lauing *et al.*, 2014). The absence of functional aggrecan in mice also leads to chondrodysplasia with chondrocytes failing to differentiate properly towards hypertrophic cells (Lauing *et al.*, 2014). Importantly, in human atherosclerotic plaques, it was recently reported that crystals are mainly covered by GAGs (Duer *et al.*, 2008).

Nevertheless, our studies have one limitation - not all chondrocyte markers were increased in response to cell treatment with exogenous alkaline phosphatase and apatite crystals. Therefore, it is possible that in response to TNAP and crystals, VSMCs differentiate into cells with an intermediate phenotype between VSMCs and chondrocytes. This is much probable, since TNAP inhibition in primary chondrocytes reduced the expression of all chondrocyte markers that we have investigated.

#### TNAP induction and inflammation – cause or consequence

As already mentioned, induction of mineralization after TNAP overexpression was not dependent on VSMCs trans-differentiation (Fig. 13). Therefore, it is likely that TNAP activation in VSMCs, in response to inflammatory cytokines, is sufficient to induce microcalcification. Indeed, TNAP induction in the fibrous cap would not require VSMC trans-differentiation into osteoblasts or chondrocytes (Lencel *et al.*, 2011). This model is coherent with the fact that TNAP activity and calcification associate with inflammation in early atherosclerosis of *apoE*<sup>-/-</sup> mice (Aikawa *et al.*, 2007). In atherosclerotic patients, inflammation was shown to precede calcification at the same location (Abdelbaky *et al.*, 2013). Therefore, TNAP activation by inflammatory cytokines within a fibrous cap may represent a crucial event during atherogenesis.

In addition, we observed the apatite crystals generated by TNAP may induce cell necrosis. Besides, this effect was more pronounced in non-differentiated than differentiated MOVAS. Moreover, ACCs seemed to exert a cytotoxic effect as well, since we observed that cells cultured on their surface were able to survive no longer than 7 days. These findings are consistent with a dramatic increase of *Acan* gene expression in response to TNAP overexpression in non-differentiated A7R5 rat VSMCs (Fakhry *et al.*, 2017). Moreover, our results are in agreement with the previous observation that apatite crystals induced vascular smooth muscle cell death (Ewence *et al.*, 2008). It was shown before that crystalline structures may activate NLRP3 inflammasome and promote IL-1 $\beta$  secretion by triggering necrosis (Cullen *et al.*, 2015). However, further investigation is necessary to elucidate whether necrosis caused by apatite crystals stimulate the release of inflammatory cytokines by VSMCs. Nevertheless, inflammation may be both the cause and the consequence of VC in the context of atherosclerosis. Inflammatory cytokines may induce VC by the activation of TNAP, whereas subsequent generation of apatite crystals may result in increased secretion of IL-1 $\beta$ , stimulating the inflammatory response.

#### Possible association of microcalcifications with collagen

In atherosclerotic plaques, the precise location of microcalcifications and their possible association with collagen are issues that are still debatable. However, it seems that the amount of collagen is a critical factor for atherosclerotic plaque stability. Vulnerable atherosclerotic lesions usually contain a thin and collagen-poor fibrous cap (Fukumoto, 2004). Interestingly, it was shown that calcium phosphate crystals taken up by fibroblasts may cause various consequences, such as for example increased production of matrix metalloproteinases (MMPs) (Morgan and McCarthy, 2002). MMPs are enzymes released also by macrophages within the plaque that decrease its thickness by collagen degradation. On the other hand, advanced lesions contain macrocalcifications together with a thick fibrous cap rich in collagen type I produced by VSMCs (Rekhter *et al.*, 1993). Macrocalcifications are thought to be responsible for advanced plaque stabilization and to serve as a barrier towards further inflammation (Pugliese *et al.*, 2015).

As mentioned above, VSMC-derived MVs enriched in TNAP may be implicated in formation of microcalcifications. As a result of our work, membrane-bound TNAP was visualized for the first time on the surface of VSMCs in mineralizing conditions. Also, we observed crystalline and vesicle structures that pinched off from plasma membrane



of MOVAS, suggesting membranous origin of VSMC-derived MVs. Moreover, we demonstrated that VSMC-derived MVs deposited in the vicinity of collagen fibrils exhibited increased TNAP activity and had the ability to produce minerals with Ca/P ratio close to that of biological apatite. According to previous findings, vesicle binding to collagen is an important step during normal bone formation. Our results suggest that, similarly as in the case of typical mineralizing cells, increased TNAP activity and association of VSMC-derived MVs with collagen are required for their ability to mineralize. Therefore, our results indicate that the dual requirement of TNAP and collagen may refer also to VC.

In MOVAS VSMCs, we observed vesicular structures enriched in annexins, most probably transport vesicles being in charge of annexin translocation towards plasma membrane during early mineralization, necessary for MV biogenesis (Cmoch *et al.*, 2011). This translocation may proceed in response to elevation of intracellular calcium, as demonstrated by the group of Shanahan in human aortic VSMCs (Kapustin *et al.*, 2011). Unfortunately, we did not detect annexins in the proximity of cellular plasma membrane, most probably due to the lack of additional stimulation by 2.7 mM Ca (Kapustin *et al.*, 2011). We do not apply additional stimulation by calcium to avoid its non-physiological effect on the cells. Nevertheless, our results suggest an important role of AnxA2 in early mineralization. Possibly, the role of AnxA2 is more pronounced at the cellular level, before MV formation, whereas AnxA6 is mostly implicated in MV-mediated mineralization, as indicated by Kapustin and collaborators (Kapustin *et al.*, 2011).

#### The role of cholesterol in vascular calcification

The mechanism through which Chol stimulates mineralization remains unknown. Excess Chol may provoke lipotoxicity that leads to ER stress, similarly to saturated fatty acids (Freigang *et al.*, 2013). In VSMCs, excess saturated fatty acids accumulate in the ER, triggering ER stress, leading to activation of ATF4 transcription factor, VSMC trans-differentiation and subsequent calcification (Masuda *et al.*, 2015). Another possibility is that Chol may modulate membrane dynamics leading to MV release. It was shown that Chol stimulates TNAP and mineralization in a dose-dependent manner in VSMCs (Liu *et al.*, 2016). Conversely, stimulation of Chol efflux, inhibition of HMG-CoA reductase and the lack of LDL receptor, alone or in combination, appear to decrease VSMC differentiation and calcification.

An interesting study by Geng and collaborators revealed that Chol metabolism is implicated in mineralization by vascular cells (Geng *et al.*, 2011). They observed that VSMCs

isolated from LDL receptor null (*Ldlr*<sup>-/-</sup>) mice, characterized by impaired Chol uptake, had lower levels of intracellular Chol and less osteogenic differentiation compared to WT cells (Geng *et al.*, 2011). However, based on our analysis of Chol content in trans-differentiated MOVAS and released MVs, it is difficult to draw conclusions concerning the effect of Chol on VSMC mineralization. We observed increased level of Chol in the membranous fractions, but not in MVs, in contrast to cholesterol-enriched chondrocyte MVs. Nevertheless, similar localization of lipid raft markers, Chol and GM1, as well as TNAP in the apical region of mineralizing cells, indicates a possible role of lipid rafts in MV biogenesis. Therefore, further investigation is necessary for better understanding of the stimulatory effect of Chol on VC.

## Concluding remarks

Atherosclerotic plaque calcification ranges from early, diffuse microcalcifications to a bone-like tissue formed in a process resembling endochondral ossification. Regarding the fact that early plaque microcalcifications were reported as structures being particularly harmful for plaque stability, solving the mechanisms responsible for their formation appears crucial.

- Based on our observations, we proposed a mechanism of TNAP-mediated stimulation of vascular calcification. Our findings are coherent with the model recently proposed by Chatrou and collaborators (Chatrou *et al.*, 2015). They observed that microcalcifications were present before “osteochondrocytes” in human atherosclerotic plaques and hypothesized that they may be the cause and not the consequence of VSMC trans-differentiation. In addition, we propose that TNAP activation by inflammatory cytokines in VSMCs, subsequent PP<sub>i</sub> hydrolysis and generation of apatite crystals, represents a particularly important mechanism responsible for the formation of microcalcifications. Our findings indicated that apatite crystals stimulate chondrogenesis through an activation of BMP-2 that may initiate trans-differentiation of VSMCs.
- We detected membrane-bound TNAP on the surface of VSMCs cultured in mineralizing conditions. We have also demonstrated that collagen-attached VSMC-derived MVs had higher TNAP activity and produced more apatite crystals than their collagen-free counterparts. Therefore, our results suggest that, similarly as in the case of typical mineralizing cells, increased TNAP activity and association of VSMC-derived MVs with collagen are required for their ability to mineralize.

## References

- Abdallah, D., Hamade, E., Merhi, R.A., Bassam, B., Buchet, R., and Mebarek, S. (2014). Fatty acid composition in matrix vesicles and in microvilli from femurs of chicken embryos revealed selective recruitment of fatty acids. *Biochem Biophys Res Commun* 446, 1161–1164.
- Abdelbaky, A., Corsini, E., Figueroa, A.L., Fontanez, S., Subramanian, S., Ferencik, M., Brady, T.J., Hoffmann, U., and Tawakol, A. (2013). Focal arterial inflammation precedes subsequent calcification in the same location: a longitudinal FDG-PET/CT study. *Circ Cardiovasc Imaging* 6, 747–754.
- Abela, G.S., and Aziz, K. (2005). Cholesterol crystals cause mechanical damage to biological membranes: a proposed mechanism of plaque rupture and erosion leading to arterial thrombosis. *Clin Cardiol* 28, 413–420.
- Abela, G.S., Aziz, K., Vedre, A., Pathak, D.R., Talbott, J.D., and Dejong, J. (2009). Effect of cholesterol crystals on plaques and intima in arteries of patients with acute coronary and cerebrovascular syndromes. *Am J Cardiol* 103, 959–968.
- Addison, W.N., Azari, F., Sørensen, E.S., Kaartinen, M.T., and McKee, M.D. (2007). Pyrophosphate Inhibits Mineralization of Osteoblast Cultures by Binding to Mineral, Up-regulating Osteopontin, and Inhibiting Alkaline Phosphatase Activity. *J Biol Chem* 282, 15872–15883.
- Aigner, T., Neureiter, D., Câmpean, V., Soder, S., and Amann, K. (2008). Expression of cartilage-specific markers in calcified and non-calcified atherosclerotic lesions. *Atherosclerosis* 196, 37–41.
- Aikawa, E., Nahrendorf, M., Figueiredo, J.-L., Swirski, F.K., Shtatland, T., Kohler, R.H., Jaffer, F.A., Aikawa, M., and Weissleder, R. (2007). Osteogenesis Associates With Inflammation in Early-Stage Atherosclerosis Evaluated by Molecular Imaging In Vivo. *Circulation* 116, 2841–2850.
- Anderson, H.C. (1967). Electron microscopic studies of induced cartilage development and calcification. *J Cell Biol* 35, 81–101.
- Anderson, H.C., Mulhall, D., and Garimella, R. (2010). Role of extracellular membrane vesicles in the pathogenesis of various diseases, including cancer, renal diseases, atherosclerosis, and arthritis. *Lab Invest* 90, 1549–1557.
- Balcerzak, M., Hamade, E., Zhang, L., Pikula, S., Azzar, G., Radisson, J., Bandorowicz-Pikula, J., and Buchet, R. (2003). The roles of annexins and alkaline phosphatase in mineralization process. *Acta Biochim Pol* 50, 1019–1038.
- Balcerzak, M., Malinowska, A., Thouverey, C., Sekrecka, A., Dadlez, M., Buchet, R., and Pikula, S. (2008). Proteome analysis of matrix vesicles isolated from femurs of chicken embryo. *Proteomics* 8, 192–205.
- Bandorowicz-Pikuła, J. (2007). [Annexins--proteins involved in organization and function of biological membranes--from *Arabidopsis thaliana* to *Homo sapiens*]. *Postepy Biochem* 53, 143–153.

- Barquera, S., Pedroza-Tobías, A., Medina, C., Hernández-Barrera, L., Bibbins-Domingo, K., Lozano, R., and Moran, A.E. (2015). Global Overview of the Epidemiology of Atherosclerotic Cardiovascular Disease. *Arch Med Res* 46, 328–338.
- Bechkoff, G., Radisson, J., Bessueille, L., Bouchekioua-Bouzaghrou, K., and Buchet, R. (2008). Distinct actions of strontium on mineral formation in matrix vesicles. *Biochem Biophys Res Commun* 373, 378–381.
- Belluoccio, D., Grskovic, I., Niehoff, A., Schlötzer-Schrehardt, U., Rosenbaum, S., Etich, J., Frie, C., Pausch, F., Moss, S.E., Pöschl, E., et al. (2010). Deficiency of annexins A5 and A6 induces complex changes in the transcriptome of growth plate cartilage but does not inhibit the induction of mineralization. *J Bone Mineral Res* 25, 141–153.
- Bessueille, L., and Magne, D. (2015). Inflammation: a culprit for vascular calcification in atherosclerosis and diabetes. *Cell Mol Life Sci* 72, 2475–2489.
- Bessueille, L., Fakhry, M., Hamade, E., Badran, B., and Magne, D. (2015). Glucose stimulates chondrocyte differentiation of vascular smooth muscle cells and calcification: A possible role for IL-1 $\beta$ . *FEBS Letters* 589, 2797–2804.
- Biver, E., Hardouin, P., and Caverzasio, J. (2013). The “bone morphogenic proteins” pathways in bone and joint diseases: Translational perspectives from physiopathology to therapeutic targets. *Cytokine Growth Factor Rev* 24, 69–81.
- Bobryshev, Y.V., Killingsworth, M.C., Lord, R.S.A., and Grabs, A.J. (2008). Matrix vesicles in the fibrous cap of atherosclerotic plaque: possible contribution to plaque rupture. *J Cell Mol Med* 12, 2073–2082.
- Bonewald, L.F. (2011). The amazing osteocyte. *J Bone Miner Res* 26, 229–238.
- Brachvogel, B., Dikschas, J., Moch, H., Welzel, H., von der Mark, K., Hofmann, C., and Pöschl, E. (2003). Annexin A5 Is Not Essential for Skeletal Development. *Mol Cell Biol* 23, 2907–2913.
- Brånén, L., Hovgaard, L., Nitulescu, M., Bengtsson, E., Nilsson, J., and Jovinge, S. (2004). Inhibition of tumor necrosis factor- $\alpha$  reduces atherosclerosis in apolipoprotein E knockout mice. *ATVB* 24, 2137–2142.
- Briolay, A., Jaafar, R., Nemoz, G., and Bessueille, L. (2013). Myogenic differentiation and lipid-raft composition of L6 skeletal muscle cells are modulated by PUFAs. *Biochim Biophys Acta* 1828, 602–613.
- Brunet, L.J., McMahon, J.A., McMahon, A.P., and Harland, R.M. (1998). Noggin, cartilage morphogenesis, and joint formation in the mammalian skeleton. *Science* 280, 1455–1457.
- Buchet, R., Millán, J.L., and Magne, D. (2013a). Multisystemic functions of alkaline phosphatases. *Phosphatase Modulators* 27–51.
- Buchet, R., Pikula, S., Magne, D., and Mebarek, S. (2013b). Isolation and characteristics of matrix vesicles. *Methods Mol Biol* 1053, 115–124.

- Caron, M.M.J., Emans, P.J., Cremers, A., Surtel, D.A.M., Coolen, M.M.E., van Rhijn, L.W., and Welting, T.J.M. (2013). Hypertrophic differentiation during chondrogenic differentiation of progenitor cells is stimulated by BMP-2 but suppressed by BMP-7. *Osteoarthritis Cartilage* 21, 604–613.
- Carter, D.R., and Wong, M. (2003). Modelling cartilage mechanobiology. *Philos Trans R Soc Lond B Biol Sci* 358, 1461–1471.
- Chamberlain, J., Francis, S., Brookes, Z., Shaw, G., Graham, D., Alp, N.J., Dower, S., and Crossman, D.C. (2009). Interleukin-1 regulates multiple atherogenic mechanisms in response to fat feeding. *PLoS ONE* 4, e5073.
- Chatrou, M.L.L., Cleutjens, J.P., van der Vusse, G.J., Roijers, R.B., Mutsaers, P.H.A., and Schurgers, L.J. (2015). Intra-Section Analysis of Human Coronary Arteries Reveals a Potential Role for Micro-Calcifications in Macrophage Recruitment in the Early Stage of Atherosclerosis. *PLOS ONE* 10, e0142335.
- Chen, N.X., O'Neill, K.D., Chen, X., and Moe, S.M. (2008). Annexin-Mediated Matrix Vesicle Calcification in Vascular Smooth Muscle Cells. *J Bone Miner Res* 23, 1798–1805.
- Cheung, J.O.P., Grant, M.E., Jones, C.J.P., Hoyland, J.A., Freemont, A.J., and Hillarby, M.C. (2003). Apoptosis of terminal hypertrophic chondrocytes in an in vitro model of endochondral ossification. *J Pathol* 201, 496–503.
- Church, L.D., Cook, G.P., and McDermott, M.F. (2008). Primer: inflammasomes and interleukin 1beta in inflammatory disorders. *Nat Clin Pract Rheumatol* 4, 34–42.
- Ciancaglini P, Yadav MC, Simão AM, Narisawa S, Pizauro JM, Farquharson C, Hoylaerts MF, Millán JL (2010). Kinetic analysis of substrate utilization by native and TNAP-, NPP1-, or PHOSPHO1-deficient matrix vesicles. *J Bone Miner Res* 25(4):716-723.
- Clarke, B. (2008). Normal Bone Anatomy and Physiology. *Clin J Am Soc Nephrol* 3, S131–S139.
- Clarke, M., and Bennett, M. (2006). The emerging role of vascular smooth muscle cell apoptosis in atherosclerosis and plaque stability. *Am J Nephrol* 26, 531–535.
- Clarke, E.M., Thompson, R.C., Allam, A.H., Wann, L.S., Lombardi, G.P., Sutherland, M.L., Sutherland, J.D., Cox, S.L., Soliman, M.A.-T., el-Maksoud, G.A., et al. (2014). Is atherosclerosis fundamental to human aging? Lessons from ancient mummies. *J Cardiol* 63, 329–334.
- Cmoch, A., Strzelecka-Kiliszek, A., Palczewska, M., Groves, P., and Pikula, S. (2011). Matrix vesicles isolated from mineralization-competent Saos-2 cells are selectively enriched with annexins and S100 proteins. *Biochem Biophys Res Commun* 412, 683–687.
- Criqui, M.H., Denenberg, J.O., Ix, J.H., McClelland, R.L., Wassel, C.L., Rifkin, D.E., Carr, J.J., Budoff, M.J., and Allison, M.A. (2014). Calcium Density of Coronary Artery Plaque and Risk of Incident Cardiovascular Events. *JAMA* 311, 271.

- Cullen, S.P., Kearney, C.J., Clancy, D.M., and Martin, S.J. (2015). Diverse Activators of the NLRP3 Inflammasome Promote IL-1 $\beta$  Secretion by Triggering Necrosis. *Cell Rep* *11*, 1535–1548.
- Damek-Poprawa, M., Golub, E., Otis, L., Harrison, G., Phillips, C., and Boesze-Battaglia, K. (2006). Chondrocytes Utilize a Cholesterol-Dependent Lipid Translocator To Externalize Phosphatidylserine. *Biochemistry* *45*, 3325–3336.
- Debray, J., Chang, L., Marquès, S., Pellet-Rostaing, S., Le Duy, D., Mebarek, S., Buchet, R., Magne, D., Popowycz, F., and Lemaire, M. (2013). Inhibitors of tissue-nonspecific alkaline phosphatase: Design, synthesis, kinetics, biomineralization and cellular tests. *Bioorg Med Chem* *21*, 7981–7987.
- Deckelbaum, R.J. (2010). n-6 and n-3 Fatty Acids and Atherosclerosis: Ratios or Amounts? *ATVB* *30*, 2325–2326.
- Demer, L.L., and Tintut, Y. (2008). Vascular Calcification: Pathobiology of a Multifaceted Disease. *Circulation* *117*, 2938–2948.
- Devlin, C.M., Kuriakose, G., Hirsch, E., and Tabas, I. (2002). Genetic alterations of IL-1 receptor antagonist in mice affect plasma cholesterol level and foam cell lesion size. *PNAS* *99*, 6280–6285.
- Doherty, T.M., Fitzpatrick, L.A., Inoue, D., Qiao, J.-H., Fishbein, M.C., Detrano, R.C., Shah, P.K., and Rajavashisth, T.B. (2004). Molecular, Endocrine, and Genetic Mechanisms of Arterial Calcification. *Endocr Rev* *25*, 629–672.
- Dong, Y.-F., Soung, D.Y., Schwarz, E.M., O’Keefe, R.J., and Drissi, H. (2006). Wnt induction of chondrocyte hypertrophy through the Runx2 transcription factor. *J Cell Physiol* *208*, 77–86.
- Duer, M.J., Friscic, T., Proudfoot, D., Reid, D.G., Schoppet, M., Shanahan, C.M., Skepper, J.N., and Wise, E.R. (2008). Mineral Surface in Calcified Plaque Is Like That of Bone: Further Evidence for Regulated Mineralization. *ATVB* *28*, 2030–2034.
- Duewell, P., Kono, H., Rayner, K.J., Sirois, C.M., Vladimer, G., Bauernfeind, F.G., Abela, G.S., Franchi, L., Nuñez, G., Schnurr, M., et al. (2010). NLRP3 inflammasomes are required for atherogenesis and activated by cholesterol crystals. *Nature* *464*, 1357–1361.
- Duval, E., Leclercq, S., Elissalde, J.-M., Demoor, M., Galéra, P., and Boumédiene, K. (2009). Hypoxia-inducible factor 1alpha inhibits the fibroblast-like markers type I and type III collagen during hypoxia-induced chondrocyte redifferentiation: hypoxia not only induces type II collagen and aggrecan, but it also inhibits type I and type III collagen in the hypoxia-inducible factor 1alpha-dependent redifferentiation of chondrocytes. *Arthritis Rheum* *60*, 3038–3048.
- Dweck, M.R., Aikawa, E., Newby, D.E., Tarkin, J.M., Rudd, J.H.F., Narula, J., and Fayad, Z.A. (2016). Noninvasive Molecular Imaging of Disease Activity in Atherosclerosis. *Circ Res* *119*, 330–340.
- Ehara, S. (2004). Spotty Calcification Typifies the Culprit Plaque in Patients With Acute Myocardial Infarction: An Intravascular Ultrasound Study. *Circulation* *110*, 3424–3429.



- Eisman JA, Bouillon R (2014). Vitamin D: direct effects of vitamin D metabolites on bone: lessons from genetically modified mice. *Bonekey Rep* 3:499.
- Ewence, A.E., Bootman, M., Roderick, H.L., Skepper, J.N., McCarthy, G., Epple, M., Neumann, M., Shanahan, C.M., and Proudfoot, D. (2008). Calcium Phosphate Crystals Induce Cell Death in Human Vascular Smooth Muscle Cells: A Potential Mechanism in Atherosclerotic Plaque Destabilization. *Circ Res* 103, e28–e34.
- Fakhry M, Hamade E, Badran B, Buchet R, Magne D. (2013). Molecular mechanisms of mesenchymal stem cell differentiation towards osteoblasts. *World J Stem Cells*. 5(4):136-148.
- Fakhry M, Roszkowska M, Briolay A, Bougault C, Guignandon A, Diaz-Hernandez JI, Diaz-Hernandez M, Pikula S, Buchet R, Hamade E, Badran B, Bessueille L, Magne D. (2017) TNAP stimulates vascular smooth muscle cell trans-differentiation into chondrocytes through calcium deposition and BMP-2 activation: Possible implication in atherosclerotic plaque stability. *Biochim Biophys Acta* 1863(3):643-653.
- Fedde, K.N., Blair, L., Silverstein, J., Coburn, S.P., Ryan, L.M., Weinstein, R.S., Waymire, K., Narisawa, S., Millán, J.L., MacGregor, G.R., et al. (1999). Alkaline phosphatase knock-out mice recapitulate the metabolic and skeletal defects of infantile hypophosphatasia. *J Bone Miner Res* 14, 2015–2026.
- Feng, B., Yao, P.M., Li, Y., Devlin, C.M., Zhang, D., Harding, H.P., Sweeney, M., Rong, J.X., Kuriakose, G., Fisher, E.A., et al. (2003). The endoplasmic reticulum is the site of cholesterol-induced cytotoxicity in macrophages. *Nat Cell Biol* 5, 781–792.
- Fitzpatrick, L.A., Severson, A., Edwards, W.D., and Ingram, R.T. (1994). Diffuse calcification in human coronary arteries. Association of osteopontin with atherosclerosis. *J Clin Invest* 94, 1597–1604.
- Freigang, S., Ampenberger, F., Weiss, A., Kanneganti, T.-D., Iwakura, Y., Hersberger, M., and Kopf, M. (2013). Fatty acid-induced mitochondrial uncoupling elicits inflammasome-independent IL-1 $\alpha$  and sterile vascular inflammation in atherosclerosis. *Nat Immunol* 14, 1045–1053.
- Fukumoto, Y. (2004). Genetically Determined Resistance to Collagenase Action Augments Interstitial Collagen Accumulation in Atherosclerotic Plaques. *Circulation* 110, 1953–1959.
- Fukumoto, S., and Martin, T.J. (2009). Bone as an endocrine organ. *Trends Endocrinol Metab* 20, 230–236.
- Gazzerro, E., Gangji, V., and Canalis, E. (1998). Bone morphogenetic proteins induce the expression of noggin, which limits their activity in cultured rat osteoblasts. *J Clin Invest* 102, 2106–2114.
- GBD 2013 Mortality and Causes of Death Collaborators (2015). Global, regional, and national age-sex specific all-cause and cause-specific mortality for 240 causes of death, 1990-2013: a systematic analysis for the Global Burden of Disease Study 2013. *Lancet* 385, 117–171.
- Genetos, D.C., Wong, A., Weber, T.J., Karin, N.J., and Yellowley, C.E. (2014). Impaired Osteoblast Differentiation in Annexin A2- and -A5-Deficient Cells. *PLoS ONE* 9, e107482.

- Geng, Y.J., and Libby, P. (1995). Evidence for apoptosis in advanced human atheroma. Colocalization with interleukin-1 beta-converting enzyme. *Am J Pathol* *147*, 251–266.
- Geng, Y., Hsu, J.J., Lu, J., Ting, T.C., Miyazaki, M., Demer, L.L., and Tintut, Y. (2011). Role of Cellular Cholesterol Metabolism in Vascular Cell Calcification. *J Biol Chem* *286*, 33701–33706.
- Genge, B.R., Wu, L.N.Y., and Wuthier, R.E. (2007). Kinetic analysis of mineral formation during in vitro modeling of matrix vesicle mineralization: Effect of annexin A5, phosphatidylserine, and type II collagen. *Anal Biochem* *367*, 159–166.
- Genge, B.R., Wu, L.N.Y., and Wuthier, R.E. (2008). Mineralization of Annexin-5-containing Lipid-Calcium-Phosphate Complexes: modulation by varying lipid composition and incubation with cartilage collagens. *J Biol Chem* *283*, 9737–9748.
- Gericke, A., Qin, C., Spevak, L., Fujimoto, Y., Butler, W.T., Sørensen, E.S., and Boskey, A.L. (2005). Importance of phosphorylation for osteopontin regulation of biomineralization. *Calcif Tissue Int* *77*, 45–54.
- Gerke, V., and Moss, S.E. (2002). Annexins: From Structure to Function. *Physiol Rev* *82*, 331–371.
- Getz, G.S., and Reardon, C.A. (2009). Apoprotein E as a lipid transport and signaling protein in the blood, liver, and artery wall. *J Lipid Res* *50*, S156–S161.
- Gillette JM, Nielsen-Preiss SM. (2004). The role of annexin 2 in osteoblastic mineralization. *J Cell Sci* *117*(Pt 3):441-449.
- Glass, C.K., and Witztum, J.L. (2001). Atherosclerosis: the road ahead. *Cell* *104*, 503–516.
- Goettsch, C., Hutcheson, J.D., Aikawa, M., Iwata, H., Pham, T., Nykjaer, A., Kjolby, M., Rogers, M., Michel, T., Shibasaki, M., et al. (2016). Sortilin mediates vascular calcification via its recruitment into extracellular vesicles. *J Clin Invest* *126*, 1323–1336.
- Goldring, M.B., Tsuchimochi, K., and Ijiri, K. (2006). The control of chondrogenesis. *J Cell Biochem* *97*, 33–44.
- Golub, E.E. (2009). Role of matrix vesicles in biomineralization. *Biochim Biophys Acta* *1790*, 1592–1598.
- Gosset, M., Berenbaum, F., Thirion, S., and Jacques, C. (2008). Primary culture and phenotyping of murine chondrocytes. *Nat Protoc* *3*, 1253–1260.
- Grebe, A., and Latz, E. (2013). Cholesterol crystals and inflammation. *Curr Rheumatol Rep* *15*, 313.
- Greenland, P., Smith, S.C., and Grundy, S.M. (2001). Improving coronary heart disease risk assessment in asymptomatic people: role of traditional risk factors and noninvasive cardiovascular tests. *Circulation* *104*, 1863–1867.
- Grskovic, I., Kutsch, A., Frie, C., Groma, G., Stermann, J., Schlötzer-Schrehardt, U., Niehoff, A., Moss, S.E., Rosenbaum, S., Pöschl, E., et al. (2012). Depletion of annexin A5, annexin A6,

and collagen X causes no gross changes in matrix vesicle-mediated mineralization, but lack of collagen X affects hematopoiesis and the Th1/Th2 response. *J Bone Miner Res* 27, 2399–2412.

Hahn, C., and Schwartz, M.A. (2009). Mechanotransduction in vascular physiology and atherogenesis. *Nat Rev Mol Cell Biol* 10, 53–62.

Hale, J.E., and Wuthier, R.E. (1987). The mechanism of matrix vesicle formation. Studies on the composition of chondrocyte microvilli and on the effects of microfilament-perturbing agents on cellular vesiculation. *J Biol Chem* 262, 1916–1925.

Halling Linder, C., Narisawa, S., Millán, J.L., and Magnusson, P. (2009). Glycosylation differences contribute to distinct catalytic properties among bone alkaline phosphatase isoforms. *Bone* 45, 987–993.

Hansson GK (2005). Inflammation, atherosclerosis, and coronary artery disease. *N Engl J Med* 352(16):1685-1695.

Harada, S., Matsumoto, T., and Ogata, E. (1991). Role of ascorbic acid in the regulation of proliferation in osteoblast-like MC3T3-E1 cells. *J Bone Miner Res* 6, 903–908.

Harrington, E.K., Lunsford, L.E., and Svoboda, K.K.H. (2004). Chondrocyte terminal differentiation, apoptosis, and type X collagen expression are downregulated by parathyroid hormone. *Anat Rec A Discov Mol Cell Evol Biol* 281, 1286–1295.

Herisson, F., Heymann, M.-F., Chétiveaux, M., Charrier, C., Battaglia, S., Pilet, P., Rouillon, T., Krempf, M., Lemarchand, P., Heymann, D., et al. (2011). Carotid and femoral atherosclerotic plaques show different morphology. *Atherosclerosis* 216, 348–354.

Hessle, L., Johnson, K.A., Anderson, H.C., Narisawa, S., Sali, A., Goding, J.W., Terkeltaub, R., and Millán, J.L. (2002). Tissue-nonspecific alkaline phosphatase and plasma cell membrane glycoprotein-1 are central antagonistic regulators of bone mineralization. *PNAS* 99, 9445–9449.

Hjorten, R., Hansen, U., Underwood, R.A., Telfer, H.E., Fernandes, R.J., Krakow, D., Sebald, E., Wachsmann-Hogiu, S., Bruckner, P., Jacquet, R., et al. (2007). Type XXVII collagen at the transition of cartilage to bone during skeletogenesis. *Bone* 41, 535–542.

Hornung, V., Bauernfeind, F., Halle, A., Samstad, E.O., Kono, H., Rock, K.L., Fitzgerald, K.A., and Latz, E. (2008). Silica crystals and aluminum salts activate the NALP3 inflammasome through phagosomal destabilization. *Nat Immunol* 9, 847–856.

Hoshi, K., Amizuka, N., Oda, K., Ikehara, Y., and Ozawa, H. (1997). Immunolocalization of tissue non-specific alkaline phosphatase in mice. *Histochem Cell Biol* 107, 183–191.

Huang, H., Virmani, R., Younis, H., Burke, A.P., Kamm, R.D., and Lee, R.T. (2001). The impact of calcification on the biomechanical stability of atherosclerotic plaques. *Circulation* 103, 1051–1056.

Hutcheson, J.D., Maldonado, N., and Aikawa, E. (2014). Small entities with large impact: microcalcifications and atherosclerotic plaque vulnerability. *Curr Opin Lipidol* 25, 327–332.

- Hutcheson, J.D., Goettsch, C., Bertazzo, S., Maldonado, N., Ruiz, J.L., Goh, W., Yabusaki, K., Faits, T., Bouten, C., Franck, G., et al. (2016). Genesis and growth of extracellular-vesicle-derived microcalcification in atherosclerotic plaques. *Nat Mater* 15, 335–343.
- Idelevich, A., Rais, Y., and Monsonego-Ornan, E. (2011). Bone Gla Protein Increases HIF-1 - Dependent Glucose Metabolism and Induces Cartilage and Vascular Calcification. *ATVB* 31, e55–e71.
- Ikeda, K., Souma, Y., Akakabe, Y., Kitamura, Y., Matsuo, K., Shimoda, Y., Ueyama, T., Matoba, S., Yamada, H., Okigaki, M., et al. (2012). Macrophages play a unique role in the plaque calcification by enhancing the osteogenic signals exerted by vascular smooth muscle cells. *Biochem Biophys Res Commun* 425, 39–44.
- Irkle, A., Vesey, A.T., Lewis, D.Y., Skepper, J.N., Bird, J.L.E., Dweck, M.R., Joshi, F.R., Gallagher, F.A., Warburton, E.A., Bennett, M.R., et al. (2015). Identifying active vascular microcalcification by <sup>18</sup>F-sodium fluoride positron emission tomography. *Nat Commun* 6, 7495.
- Isoda, K., Sawada, S., Ishigami, N., Matsuki, T., Miyazaki, K., Kusuhara, M., Iwakura, Y., and Ohsuzu, F. (2004). Lack of interleukin-1 receptor antagonist modulates plaque composition in apolipoprotein E-deficient mice. *ATVB* 24, 1068–1073.
- Jopling, C., Boue, S., and Belmonte, J.C.I. (2011). Dedifferentiation, transdifferentiation and reprogramming: three routes to regeneration. *Nat Rev Mol Cell Biol* 12, 79–89.
- Joshi, N.V., Vesey, A.T., Williams, M.C., Shah, A.S., Calvert, P.A., Craighead, F.H., Yeoh, S.E., Wallace, W., Salter, D., Fletcher, A.M., et al. (2014). <sup>18</sup>F-fluoride positron emission tomography for identification of ruptured and high-risk coronary atherosclerotic plaques: a prospective clinical trial. *The Lancet* 383, 705–713.
- Kapustin, A.N., Davies, J.D., Reynolds, J.L., McNair, R., Jones, G.T., Sidibe, A., Schurgers, L.J., Skepper, J.N., Proudfoot, D., Mayr, M., et al. (2011). Calcium Regulates Key Components of Vascular Smooth Muscle Cell-Derived Matrix Vesicles to Enhance Mineralization. *Circ Res* 109, e1–e12.
- Kellner-Weibel, G., Yancey, P.G., Jerome, W.G., Walser, T., Mason, R.P., Phillips, M.C., and Rothblat, G.H. (1999). Crystallization of free cholesterol in model macrophage foam cells. *ATVB* 19, 1891–1898.
- Kelly-Arnold, A., Maldonado, N., Laudier, D., Aikawa, E., Cardoso, L., and Weinbaum, S. (2013). Revised microcalcification hypothesis for fibrous cap rupture in human coronary arteries. *PNAS* 110, 10741–10746.
- Khan, R., Spagnoli, V., Tardif, J.-C., and L’Allier, P.L. (2015). Novel anti-inflammatory therapies for the treatment of atherosclerosis. *Atherosclerosis* 240, 497–509.
- Khavandgar, Z., Roman, H., Li, J., Lee, S., Vali, H., Brinckmann, J., Davis, E.C., and Murshed, M. (2014). Elastin Haploinsufficiency Impedes the Progression of Arterial Calcification in MGP-Deficient Mice: elastin content and vascular calcification. *J Bone Miner Res* 29, 327–337.

- Kiani, C., Chen, L., Wu, Y.J., Yee, A.J., and Yang, B.B. (2002). Structure and function of aggrecan. *Cell Res* 12, 19–32.
- Kim, H.J., and Kirsch, T. (2008). Collagen/Annexin V Interactions Regulate Chondrocyte Mineralization. *J Biol Chem* 283, 10310–10317.
- Kirii, H., Niwa, T., Yamada, Y., Wada, H., Saito, K., Iwakura, Y., Asano, M., Moriwaki, H., and Seishima, M. (2003). Lack of interleukin-1beta decreases the severity of atherosclerosis in ApoE-deficient mice. *ATVB* 23, 656–660.
- Kirsch, T., Ishikawa, Y., Mwale, F., and Wuthier, R.E. (1994). Roles of the nucleational core complex and collagens (types II and X) in calcification of growth plate cartilage matrix vesicles. *J Biol Chem* 269, 20103–20109.
- Kirsch, T., Harrison, G., Golub, E.E., and Nah, H.-D. (2000). The Roles of Annexins and Types II and X Collagen in Matrix Vesicle-mediated Mineralization of Growth Plate Cartilage. *J Biol Chem* 275, 35577–35583.
- Knudson, C.B., and Knudson, W. (2001). Cartilage proteoglycans. *Semin. Cell Dev Biol* 12, 69–78.
- Kramsch, D.M., Aspen, A.J., and Rozler, L.J. (1981). Atherosclerosis: Prevention by agents not affecting abnormal levels of blood lipids. *Science* 213, 1511–1512.
- Kronenberg, H.M. (2003). Developmental regulation of the growth plate. *Nature* 423, 332.
- Ladeiras-Lopes, R., Agewall, S., Tawakol, A., Staels, B., Stein, E., Mentz, R.J., Leite-Moreira, A., Zannad, F., and Koenig, W. (2015). Atherosclerosis: Recent trials, new targets and future directions. *Int J Cardiol* 192, 72–81.
- Lauing, K.L., Cortes, M., Domowicz, M.S., Henry, J.G., Baria, A.T., and Schwartz, N.B. (2014). Aggrecan is required for growth plate cytoarchitecture and differentiation. *Dev Biol* 396, 224–236.
- Le Du, M.-H., and Millan, J.L. (2002). Structural evidence of functional divergence in human alkaline phosphatases. *J Biol Chem* 277, 49808–49814.
- Lee, H.-L., Woo, K.M., Ryoo, H.-M., and Baek, J.-H. (2010). Tumor necrosis factor-alpha increases alkaline phosphatase expression in vascular smooth muscle cells via MSX2 induction. *Biochem Biophys Res Commun* 391, 1087–1092.
- Lee, N.K., Sowa, H., Hinoi, E., Ferron, M., Ahn, J.D., Confavreux, C., Dacquin, R., Mee, P.J., McKee, M.D., Jung, D.Y., et al. (2007). Endocrine Regulation of Energy Metabolism by the Skeleton. *Cell* 130, 456–469.
- Lencel, P., Delplace, S., Pilet, P., Leterme, D., Miellot, F., Sourice, S., Caudrillier, A., Hardouin, P., Guicheux, J., and Magne, D. (2011). Cell-specific effects of TNF- $\alpha$  and IL-1 $\beta$  on alkaline phosphatase: implication for syndesmophyte formation and vascular calcification. *Lab Invest* 91, 1434–1442.
- Li, X., and Cao, X. (2006). BMP signaling and skeletogenesis. *Ann NY Acad Sci* 1068, 26–40.

- Lin, J., Li, H., Yang, M., Ren, J., Huang, Z., Han, F., Huang, J., Ma, J., Zhang, D., Zhang, Z., et al. (2013). A Role of RIP3-Mediated Macrophage Necrosis in Atherosclerosis Development. *Cell Reports* 3, 200–210.
- Linton MF, Yancey PG, Davies SS, Jerome WGJ, Linton EF, Vickers KC. The Role of Lipids and Lipoproteins in Atherosclerosis. (2015) Dec 24. In: De Groot LJ, Chrousos G, Dungan K, Feingold KR, Grossman A, Hershman JM, Koch C, Korbonits M, McLachlan R, New M, Purnell J, Rebar R, Singer F, Vinik A, editors. *Endotext* [Internet]. South Dartmouth (MA): MDText.com, Inc.; 2000-.
- Little, C.B., Hughes, C.E., Curtis, C.L., Janusz, M.J., Bohne, R., Wang-Weigand, S., Taiwo, Y.O., Mitchell, P.G., Otterness, I.G., Flannery, C.R., et al. (2002). Matrix metalloproteinases are involved in C-terminal and interglobular domain processing of cartilage aggrecan in late stage cartilage degradation. *Matrix Biol* 21, 271–288.
- Liu, J., Nam, H.K., Campbell, C., Gasque, K.C. da S., Millán, J.L., and Hatch, N.E. (2014). Tissue-nonspecific alkaline phosphatase deficiency causes abnormal craniofacial bone development in the  $Alp^{1-/-}$  mouse model of infantile hypophosphatasia. *Bone* 67, 81–94.
- Liu, S., Guo, W., Han, X., Dai, W., Diao, Z., and Liu, W. (2016). Role of UBIAD1 in Intracellular Cholesterol Metabolism and Vascular Cell Calcification. *PloS One* 11, e0149639.
- Luo, G., Ducky, P., McKee, M.D., Pinero, G.J., Loyer, E., Behringer, R.R., and Karsenty, G. (1997). Spontaneous calcification of arteries and cartilage in mice lacking matrix gla protein. *Nature* 386, 78–81.
- Lusis, A.J. (2000). Atherosclerosis. *Nature* 407, 233–241.
- Ma, Y., Wang, W., Zhang, J., Lu, Y., Wu, W., Yan, H., and Wang, Y. (2012). Hyperlipidemia and Atherosclerotic Lesion Development in Ldlr-Deficient Mice on a Long-Term High-Fat Diet. *PLoS ONE* 7, e35835.
- Mackenzie NC, Zhu D, Longley L, Patterson CS, Kommareddy S, MacRae VE. (2011). MOVAS-1 cell line: a new in vitro model of vascular calcification. *Int J Mol Med*. 5:663-668.
- Magne, D., Julien, M., Vinatier, C., Merhi-Soussi, F., Weiss, P., and Guicheux, J. (2005). Cartilage formation in growth plate and arteries: from physiology to pathology. *BioEssays* 27, 708–716.
- Maldonado, N., Kelly-Arnold, A., Laudier, D., Weinbaum, S., and Cardoso, L. (2015). Imaging and analysis of microcalcifications and lipid/necrotic core calcification in fibrous cap atheroma. *Int J Cardiovasc Imaging* 31, 1079–1087.
- Malhotra, R., Burke, M.F., Martyn, T., Shakartzi, H.R., Thayer, T.E., O'Rourke, C., Li, P., Derwall, M., Spagnolli, E., Kolodziej, S.A., et al. (2015). Inhibition of Bone Morphogenetic Protein Signal Transduction Prevents the Medial Vascular Calcification Associated with Matrix Gla Protein Deficiency. *PLOS ONE* 10, e0117098.
- Martinon, F., Pétrilli, V., Mayor, A., Tardivel, A., and Tschopp, J. (2006). Gout-associated uric acid crystals activate the NALP3 inflammasome. *Nature* 440, 237–241.



- Masuda, M., Miyazaki-Anzai, S., Keenan, A.L., Okamura, K., Kendrick, J., Chonchol, M., Offermanns, S., Ntambi, J.M., Kuro-o, M., and Miyazaki, M. (2015). Saturated phosphatidic acids mediate saturated fatty acid-induced vascular calcification and lipotoxicity. *J Clin Invest* *125*, 4544–4558.
- Matsuo, N., Tanaka, S., Yoshioka, H., Koch, M., Gordon, M.K., and Ramirez, F. (2008). Collagen XXIV (Col24a1) gene expression is a specific marker of osteoblast differentiation and bone formation. *Connect. Tissue Res.* *49*, 68–75.
- Maxfield, F.R., and Tabas, I. (2005). Role of cholesterol and lipid organization in disease. *Nature* *438*, 612–621.
- McNamara, D.J. (2000). Dietary cholesterol and atherosclerosis. *Biochim Biophys Acta* *1529*, 310–320.
- Meir KS, Leitersdorf E. (2004). Atherosclerosis in the apolipoprotein-E-deficient mouse: a decade of progress. *ATVB* *6*:1006-1014.
- Millán, J.L. (2013). The Role of Phosphatases in the Initiation of Skeletal Mineralization. *Calcif Tissue Int* *93*, 299–306.
- Millán, J.L., and Whyte, M.P. (2016). Alkaline Phosphatase and Hypophosphatasia. *Calcif Tissue Int* *98*, 398–416.
- Minina, E., Kreschel, C., Naski, M.C., Ornitz, D.M., and Vortkamp, A. (2002). Interaction of FGF, Ihh/Pthlh, and BMP signaling integrates chondrocyte proliferation and hypertrophic differentiation. *Dev Cell* *3*, 439–449.
- Mintz, G.S., Popma, J.J., Pichard, A.D., Kent, K.M., Satler, L.F., Chuang, Y.C., Ditrano, C.J., and Leon, M.B. (1995). Patterns of calcification in coronary artery disease. A statistical analysis of intravascular ultrasound and coronary angiography in 1155 lesions. *Circulation* *91*, 1959–1965.
- Monastyrskaya, K., Babiychuk, E.B., Hostettler, A., Rescher, U., and Draeger, A. (2007). Annexins as intracellular calcium sensors. *Cell Calcium* *41*, 207–219.
- Moore, K.J., and Tabas, I. (2011). Macrophages in the Pathogenesis of Atherosclerosis. *Cell* *145*, 341–355.
- Moreno-Altamirano, M.M.B., Aguilar-Carmona, I., and Sánchez-García, F.J. (2007). Expression of GM1, a marker of lipid rafts, defines two subsets of human monocytes with differential endocytic capacity and lipopolysaccharide responsiveness. *Immunology* *120*, 536–543.
- Morgan, M.P., and McCarthy, G.M. (2002). Signaling mechanisms involved in crystal-induced tissue damage. *Curr Opin Rheumatol* *14*, 292–297.
- Morris, D.C., Masuhara, K., Takaoka, K., Ono, K., and Anderson, H.C. (1992). Immunolocalization of alkaline phosphatase in osteoblasts and matrix vesicles of human fetal bone. *Bone Miner* *19*, 287–298.

- Murphy, W.A., Nedden Dz, D. zur, Gostner, P., Knapp, R., Recheis, W., and Seidler, H. (2003). The iceman: discovery and imaging. *Radiology* 226, 614–629.
- Murshed M, Harmey D, Millán JL, McKee MD, Karsenty G. (2005). Unique coexpression in osteoblasts of broadly expressed genes accounts for the spatial restriction of ECM mineralization to bone. *Genes Dev* 19(9):1093-1104.
- Nahar-Gohad, P., Gohad, N., Tsai, C.-C., Bordia, R., and Vyavahare, N. (2015). Rat Aortic Smooth Muscle Cells Cultured on Hydroxyapatite Differentiate into Osteoblast-Like Cells via BMP-2–SMAD-5 Pathway. *Calcif Tissue Int* 96, 359–369.
- Nakashima, Y., Plump, A.S., Raines, E.W., Breslow, J.L., and Ross, R. (1994). ApoE-deficient mice develop lesions of all phases of atherosclerosis throughout the arterial tree. *Arterioscler Thromb* 14, 133–140.
- Narisawa, S., Harmey, D., Yadav, M.C., O’Neill, W.C., Hoylaerts, M.F., and Millán, J.L. (2007). Novel Inhibitors of Alkaline Phosphatase Suppress Vascular Smooth Muscle Cell Calcification. *J Bone Miner Res* 22, 1700–1710.
- Narisawa, S., Yadav, M.C., and Millán, J.L. (2013). In Vivo Overexpression of Tissue-Nonspecific Alkaline Phosphatase Increases Skeletal Mineralization and Affects the Phosphorylation Status of Osteopontin: TNAP affects bone mass and osteopontin phosphorylation. *J Bone Miner Res* 28, 1587–1598.
- Naumann, A., Dennis, J.E., Awadallah, A., Carrino, D.A., Mansour, J.M., Kastenbauer, E., and Caplan, A.I. (2002). Immunochemical and mechanical characterization of cartilage subtypes in rabbit. *J Histochem Cytochem* 50, 1049–1058.
- Neves, P.O., Andrade, J., and Monção, H. (2017). Coronary artery calcium score: current status. *Radiol Bras* 50, 182–189.
- New, S.E.P., Goettsch, C., Aikawa, M., Marchini, J.F., Shibasaki, M., Yabusaki, K., Libby, P., Shanahan, C.M., Croce, K., and Aikawa, E. (2013). Macrophage-Derived Matrix Vesicles: An Alternative Novel Mechanism for Microcalcification in Atherosclerotic Plaques. *Circ Res* 113, 72–77.
- Okura, Y., Brink, M., Itabe, H., Scheidegger, K.J., Kalangos, A., and Delafontaine, P. (2000). Oxidized low-density lipoprotein is associated with apoptosis of vascular smooth muscle cells in human atherosclerotic plaques. *Circulation* 102, 2680–2686.
- O’Neill, W.C., and Lomashvili, K.A. (2010). Recent progress in the treatment of vascular calcification. *Kidney Int* 78, 1232–1239.
- O’Neill, W.C., Lomashvili, K.A., Malluche, H.H., Faugere, M.-C., and Riser, B.L. (2011). Treatment with pyrophosphate inhibits uremic vascular calcification. *Kidney Int* 79, 512–517.
- Pearle, A.D., Warren, R.F., and Rodeo, S.A. (2005). Basic science of articular cartilage and osteoarthritis. *Clin Sports Med* 24, 1–12.
- Perrier, A., Dumas, V., Linossier, M.T., Fournier, C., Jurdic, P., Rattner, A., Vico, L., and Guignandon, A. (2010). Apatite content of collagen materials dose-dependently increases pre-osteoblastic cell deposition of a cement line-like matrix. *Bone* 47, 23–33.

- Persy, V.P., and McKee, M.D. (2011). Prevention of vascular calcification: is pyrophosphate therapy a solution? *Kidney Int* 79, 490–493.
- Pilz, S., Scharnagl, H., Tiran, B., Seelhorst, U., Wellnitz, B., Boehm, B.O., Schaefer, J.R., and März, W. (2006). Free fatty acids are independently associated with all-cause and cardiovascular mortality in subjects with coronary artery disease. *J Clin Endocrinol Metab* 91, 2542–2547.
- Pizette, S., and Niswander, L. (2000). BMPs are required at two steps of limb chondrogenesis: formation of prechondrogenic condensations and their differentiation into chondrocytes. *Dev Biol* 219, 237–249.
- Price, P.A., Faus, S.A., and Williamson, M.K. (1998). Warfarin causes rapid calcification of the elastic lamellae in rat arteries and heart valves. *ATVB* 18, 1400–1407.
- Proudfoot, D., Skepper, J.N., Hegyi, L., Bennett, M.R., Shanahan, C.M., and Weissberg, P.L. (2000). Apoptosis Regulates Human Vascular Calcification In Vitro : Evidence for Initiation of Vascular Calcification by Apoptotic Bodies. *Circ Res* 87, 1055–1062.
- Przybylska, D., Janiszewska, D., Goździk, A., Bielak-Zmijewska, A., Sunderland, P., Sikora, E., and Mosieniak, G. (2016). NOX4 downregulation leads to senescence of human vascular smooth muscle cells. *Oncotarget* 7, 66429–66443.
- Pugliese, G., Iacobini, C., Fantauzzi, C.B., and Menini, S. (2015). The dark and bright side of atherosclerotic calcification. *Atherosclerosis* 238, 220–230.
- Rabinovitch, A.L., and Anderson, H.C. (1976). Biogenesis of matrix vesicles in cartilage growth plates. *Fed Proc* 35, 112–116.
- Rader, D.J., and Daugherty, A. (2008). Translating molecular discoveries into new therapies for atherosclerosis. *Nature* 451, 904–913.
- Rajamäki, K., Lappalainen, J., Öörni, K., Välimäki, E., Matikainen, S., Kovanen, P.T., and Eklund, K.K. (2010). Cholesterol Crystals Activate the NLRP3 Inflammasome in Human Macrophages: A Novel Link between Cholesterol Metabolism and Inflammation. *PLoS ONE* 5, e11765.
- Rattazzi M, Bennett BJ, Bea F, Kirk EA, Ricks JL, Speer M, Schwartz SM, Giachelli CM, Rosenfeld ME. (2005). Calcification of advanced atherosclerotic lesions in the innominate arteries of ApoE-deficient mice: potential role of chondrocyte-like cells. *ATVB* 7:1420-1425.
- Rawadi, G., Vayssiere, B., Dunn, F., Baron, R., and Roman-Roman, S. (2003). BMP-2 controls alkaline phosphatase expression and osteoblast mineralization by a Wnt autocrine loop. *J Bone Miner Res* 18, 1842–1853.
- Rekhter, M.D., Zhang, K., Narayanan, A.S., Phan, S., Schork, M.A., and Gordon, D. (1993). Type I collagen gene expression in human atherosclerosis. Localization to specific plaque regions. *Am J Pathol* 143, 1634.
- Reynolds JL, Joannides AJ, Skepper JN, McNair R, Schurgers LJ, Proudfoot D, Jahnke-Dechent W, Weissberg PL, Shanahan CM. (2004). Human vascular smooth muscle cells undergo vesicle-mediated calcification in response to changes in extracellular calcium and

phosphate concentrations: a potential mechanism for accelerated vascular calcification in ESRD. *J Am Soc Nephrol* 15(11):2857-2867.

Ricard-Blum, S. (2011). The Collagen Family. *Cold Spring Harb Perspect in Biol* 3, a004978–a004978.

Riser, B.L., Barreto, F.C., Rezg, R., Valaitis, P.W., Cook, C.S., White, J.A., Gass, J.H., Maizel, J., Louvet, L., Druke, T.B., et al. (2011). Daily peritoneal administration of sodium pyrophosphate in a dialysis solution prevents the development of vascular calcification in a mouse model of uraemia. *Nephrol Dial Transplant* 26, 3349–3357.

Roijers, R.B., Debernardi, N., Cleutjens, J.P.M., Schurgers, L.J., Mutsaers, P.H.A., and van der Vusse, G.J. (2011). Microcalcifications in Early Intimal Lesions of Atherosclerotic Human Coronary Arteries. *Am J Pathol* 178, 2879–2887.

Romanelli, F., Corbo, A., Salehi, M., Yadav, M.C., Salman, S., Petrosian, D., Rashidbaigi, O.J., Chait, J., Kuruvilla, J., Plummer, M., et al. (2017). Overexpression of tissue-nonspecific alkaline phosphatase (TNAP) in endothelial cells accelerates coronary artery disease in a mouse model of familial hypercholesterolemia. *PLoS ONE* 12, e0186426.

Rosenfeld, M.E., Polinsky, P., Virmani, R., Kauser, K., Rubanyi, G., and Schwartz, S.M. (2000). Advanced atherosclerotic lesions in the innominate artery of the ApoE knockout mouse. *ATVB* 20, 2587–2592.

Rosenson, R.S. (2004). Statins in atherosclerosis: lipid-lowering agents with antioxidant capabilities. *Atherosclerosis* 173, 1–12.

Ross, R. (1993). The pathogenesis of atherosclerosis: a perspective for the 1990s. *Nature* 362, 801–809.

Rzucidlo, E.M., Martin, K.A., and Powell, R.J. (2007). Regulation of vascular smooth muscle cell differentiation. *J Vasc Surg* 45, A25–A32.

Sage, A.P., Lu, J., Tintut, Y., and Demer, L.L. (2011). Hyperphosphatemia-induced nanocrystals upregulate the expression of bone morphogenetic protein-2 and osteopontin genes in mouse smooth muscle cells in vitro. *Kidney Int* 79, 414–422.

von Scheidt, M., Zhao, Y., Kurt, Z., Pan, C., Zeng, L., Yang, X., Schunkert, H., and Lusis, A.J. (2017). Applications and Limitations of Mouse Models for Understanding Human Atherosclerosis. *Cell Metab* 25, 248–261.

Schrijvers DM, De Meyer GR, Kockx MM, Herman AG, Martinet W. (2005). Phagocytosis of apoptotic cells by macrophages is impaired in atherosclerosis. *ATVB* 6:1256-1261.

Schurgers, L.J., Uitto, J., and Reutelingsperger, C.P. (2013). Vitamin K-dependent carboxylation of matrix Gla-protein: a crucial switch to control ectopic mineralization. *Trends Mol Med* 19, 217–226.

Sekrecka, A., Balcerzak, M., Thouverey, C., Buchet, R., and Pikula, S. (2007). Rola aneksyn w procesie mineralizacji. *Postepy Biochem* 53, 159–163.

- Sergienko, E., Su, Y., Chan, X., Brown, B., Hurder, A., Narisawa, S., and Millan, J.L. (2009). Identification and Characterization of Novel Tissue-Nonspecific Alkaline Phosphatase Inhibitors with Diverse Modes of Action. *J Biomol Screen* 14, 824–837.
- Sheen, C.R., Kuss, P., Narisawa, S., Yadav, M.C., Nigro, J., Wang, W., Chhea, T.N., Sergienko, E.A., Kapoor, K., Jackson, M.R., et al. (2015). Pathophysiological Role of Vascular Smooth Muscle Alkaline Phosphatase in Medial Artery Calcification: Role of TNAP in Medial Vascular Calcification. *J Bone Miner Res* 30, 824–836.
- Shioi A, Katagi M, Okuno Y, Mori K, Jono S, Koyama H, Nishizawa Y. (2002) Induction of bone-type alkaline phosphatase in human vascular smooth muscle cells: roles of tumor necrosis factor-alpha and oncostatin M derived from macrophages. *Circ Res.* 91(1):9-16.
- Shoulders, M.D., and Raines, R.T. (2009). Collagen structure and stability. *Annu Rev Biochem* 78, 929–958.
- Sidique, S., Ardecky, R., Su, Y., Narisawa, S., Brown, B., Millán, J.L., Sergienko, E., and Cosford, N.D.P. (2009). Design and synthesis of pyrazole derivatives as potent and selective inhibitors of tissue-nonspecific alkaline phosphatase (TNAP). *Bioorg Med Chem Lett* 19, 222–225.
- Simons, K., and Ikonen, E. (2000). How cells handle cholesterol. *Science* 290, 1721–1726.
- Skålén, K., Gustafsson, M., Rydberg, E.K., Hultén, L.M., Wiklund, O., Innerarity, T.L., and Borén, J. (2002). Subendothelial retention of atherogenic lipoproteins in early atherosclerosis. *Nature* 417, 750–754.
- Small, D.M. (1988). George Lyman Duff memorial lecture. Progression and regression of atherosclerotic lesions. Insights from lipid physical biochemistry. *Arteriosclerosis* 8, 103–129.
- Sary H.C. Chandler AB, Dinsmore RE, Fuster V, Glagov S, Insull W Jr, Rosenfeld ME, Schwartz CJ, Wagner WD, Wissler RW. A definition of advanced types of atherosclerotic lesions and a histological classification of atherosclerosis. A report from the Committee on Vascular Lesions of the Council on Arteriosclerosis, American Heart Association. *Arterioscler Thromb Vasc Biol.* 1995 Sep;15(9):1512-31.
- Sary, H.C. (2000). Natural history of calcium deposits in atherosclerosis progression and regression. *Z Kardiol* 89 *Suppl* 2, 28–35.
- Steinberg, D. (2004). Thematic review series: The Pathogenesis of Atherosclerosis. An interpretive history of the cholesterol controversy: part I. *J Lipid Res* 45, 1583–1593.
- Steitz, S.A., Speer, M.Y., Curinga, G., Yang, H.-Y., Haynes, P., Aebersold, R., Schinke, T., Karsenty, G., and Giachelli, C.M. (2001). Smooth Muscle Cell Phenotypic Transition Associated With Calcification: Upregulation of Cbfa1 and Downregulation of Smooth Muscle Lineage Markers. *Circ Res* 89, 1147–1154.
- Strzelecka-Kiliszek, A., Bozycki, L., Mebarek, S., Buchet, R., and Pikula, S. (2017). Characteristics of minerals in vesicles produced by human osteoblasts hFOB 1.19 and osteosarcoma Saos-2 cells stimulated for mineralization. *J Inorg Biochem* 171, 100–107.

- Sun, Y., Byon, C.H., Yuan, K., Chen, J., Mao, X., Heath, J.M., Javed, A., Zhang, K., Anderson, P.G., and Chen, Y. (2012). Smooth Muscle Cell-Specific Runx2 Deficiency Inhibits Vascular Calcification: Novelty and Significance. *Circ Res* *111*, 543–552.
- Sweeney, E., Roberts, D., Corbo, T., and Jacenko, O. (2010). Congenic mice confirm that collagen X is required for proper hematopoietic development. *PLoS ONE* *5*, e9518.
- Tabas, I. (2010). The Role of Endoplasmic Reticulum Stress in the Progression of Atherosclerosis. *Circ Res* *107*, 839–850.
- Tabas, I., Williams, K.J., and Boren, J. (2007). Subendothelial Lipoprotein Retention as the Initiating Process in Atherosclerosis: Update and Therapeutic Implications. *Circulation* *116*, 1832–1844.
- Takagi, H., Asano, Y., Yamakawa, N., Matsumoto, I., and Kimata, K. (2002). Annexin 6 is a putative cell surface receptor for chondroitin sulfate chains. *J Cell Sci* *115*, 3309–3318.
- Tamminen, M., Mottino, G., Qiao, J.H., Breslow, J.L., and Frank, J.S. (1999). Ultrastructure of early lipid accumulation in ApoE-deficient mice. *ATVB* *19*, 847–853.
- Tangirala, R.K., Jerome, W.G., Jones, N.L., Small, D.M., Johnson, W.J., Glick, J.M., Mahlberg, F.H., and Rothblat, G.H. (1994). Formation of cholesterol monohydrate crystals in macrophage-derived foam cells. *J Lipid Res* *35*, 93–104.
- Tesch, W., Vandenbos, T., Roschgr, P., Fratzl-Zelman, N., Klaushofer, K., Beertsen, W., and Fratzl, P. (2003). Orientation of Mineral Crystallites and Mineral Density During Skeletal Development in Mice Deficient in Tissue Nonspecific Alkaline Phosphatase. *J Bone Miner Res* *18*, 117–125.
- Thacker, S.G., Zarzour, A., Chen, Y., Alcicek, M.S., Freeman, L.A., Sviridov, D.O., Demosky, S.J., and Remaley, A.T. (2016). High-density lipoprotein reduces inflammation from cholesterol crystals by inhibiting inflammasome activation. *Immunology* *149*, 306–319.
- Thouverey, C., Strzelecka-Kiliszek, A., Balcerzak, M., Buchet, R., and Pikula, S. (2009). Matrix vesicles originate from apical membrane microvilli of mineralizing osteoblast-like Saos-2 cells. *J Cell Biochem* *106*, 127–138.
- Thouverey, C., Malinowska, A., Balcerzak, M., Strzelecka-Kiliszek, A., Buchet, R., Dadlez, M., and Pikula, S. (2011). Proteomic characterization of biogenesis and functions of matrix vesicles released from mineralizing human osteoblast-like cells. *J Proteomics* *74*, 1123–1134.
- Tintut, Y., Patel, J., Parhami, F., and Demer, L.L. (2000). Tumor necrosis factor-alpha promotes in vitro calcification of vascular cells via the cAMP pathway. *Circulation* *102*, 2636–2642.
- Towler, D.A. (2005). Inorganic Pyrophosphate: A Paracrine Regulator of Vascular Calcification and Smooth Muscle Phenotype. *ATVB* *25*, 651–654.
- Tripathy, D., Mohanty, P., Dhindsa, S., Syed, T., Ghanim, H., Aljada, A., and Dandona, P. (2003). Elevation of free fatty acids induces inflammation and impairs vascular reactivity in healthy subjects. *Diabetes* *52*, 2882–2887.



- Uchida, Y., Maezawa, Y., Uchida, Y., Hiruta, N., Shimoyama, E., and Kawai, S. (2013). Localization of Oxidized Low-Density Lipoprotein and Its Relation to Plaque Morphology in Human Coronary Artery. *PLoS One* 8.
- Umlauf, D., Frank, S., Pap, T., and Bertrand, J. (2010). Cartilage biology, pathology, and repair. *Cell Mol Life Sci* 67, 4197–4211.
- Urist, M.R., and Strates, B.S. (1971). Bone morphogenetic protein. *J Dent Res* 50, 1392–1406.
- Vengrenyuk, Y., Kaplan, T.J., Cardoso, L., Randolph, G.J., and Weinbaum, S. (2010). Computational stress analysis of atherosclerotic plaques in ApoE knockout mice. *Ann Biomed Eng* 38, 738–747.
- Virmani, R., Burke, A.P., Kolodgie, F.D., and Farb, A. (2002). Vulnerable plaque: the pathology of unstable coronary lesions. *J Interv Cardiol* 15, 439–446.
- Walsh, M.C., and Choi, Y. (2014). Biology of the RANKL-RANK-OPG System in Immunity, Bone, and Beyond. *Front Immunol* 5, 511.
- Wang, C., Harris, W.S., Chung, M., Lichtenstein, A.H., Balk, E.M., Kupelnick, B., Jordan, H.S., and Lau, J. (2006). n-3 Fatty acids from fish or fish-oil supplements, but not alpha-linolenic acid, benefit cardiovascular disease outcomes in primary- and secondary-prevention studies: a systematic review. *Am J Clin Nutr* 84, 5–17.
- Wen, C., Yang, X., Yan, Z., Zhao, M., Yue, X., Cheng, X., Zheng, Z., Guan, K., Dou, J., Xu, T., et al. (2013). Nalp3 inflammasome is activated and required for vascular smooth muscle cell calcification. *Int J Cardiol* 168, 2242–2247.
- Wen, H., Gris, D., Lei, Y., Jha, S., Zhang, L., Huang, M.T.-H., Brickey, W.J., and Ting, J.P.-Y. (2011). Fatty acid-induced NLRP3-ASC inflammasome activation interferes with insulin signaling. *Nat Immun* 12, 408–415.
- Williams, K.J., and Tabas, I. (1995). The response-to-retention hypothesis of early atherogenesis. *ATVB* 15, 551–561.
- Wu, L.N., Yoshimori, T., Genge, B.R., Sauer, G.R., Kirsch, T., Ishikawa, Y., and Wuthier, R.E. (1993). Characterization of the nucleational core complex responsible for mineral induction by growth plate cartilage matrix vesicles. *J Biol Chem* 268, 25084–25094.
- Wuthier, R.E., Chin, J.E., Hale, J.E., Register, T.C., Hale, L.V., and Ishikawa, Y. (1985). Isolation and characterization of calcium-accumulating matrix vesicles from chondrocytes of chicken epiphyseal growth plate cartilage in primary culture. *J Biol Chem* 260, 15972–15979.
- Xiao, Z., Blonder, J., Zhou, M., and Veenstra, T.D. (2009). Proteomic analysis of extracellular matrix and vesicles. *J Proteomics* 72, 34–45.
- Yadav, M.C., Simão, A.M.S., Narisawa, S., Huesa, C., McKee, M.D., Farquharson, C., and Millán, J.L. (2011). Loss of skeletal mineralization by the simultaneous ablation of PHOSPHO1 and alkaline phosphatase function: A unified model of the mechanisms of initiation of skeletal calcification. *J Bone Miner Res* 26, 286–297.

- Yamashita, T., Sasaki, N., Kasahara, K., and Hirata, K. (2015). Anti-inflammatory and immune-modulatory therapies for preventing atherosclerotic cardiovascular disease. *J Cardiol* 66, 1–8.
- Ylönen, R., Kyrönlähti, T., Sund, M., Ilves, M., Lehenkari, P., Tuukkanen, J., and Pihlajaniemi, T. (2005). Type XIII collagen strongly affects bone formation in transgenic mice. *J Bone Miner Res* 20, 1381–1393.
- Yoshida, C.A., Yamamoto, H., Fujita, T., Furuichi, T., Ito, K., Inoue, K., Yamana, K., Zanma, A., Takada, K., Ito, Y., et al. (2004). Runx2 and Runx3 are essential for chondrocyte maturation, and Runx2 regulates limb growth through induction of Indian hedgehog. *Genes Dev* 18, 952–963.
- Yuan, Q., Jiang, Y., Zhao, X., Sato, T., Densmore, M., Schüler, C., Erben, R.G., McKee, M.D., and Lanske, B. (2014). Increased osteopontin contributes to inhibition of bone mineralization in FGF23-deficient mice. *J Bone Miner Res* 29, 693–704.
- Zhang, L., Balcerzak, M., Radisson, J., Thouverey, C., Pikula, S., Azzar, G., and Buchet, R. (2005). Phosphodiesterase activity of alkaline phosphatase in ATP-initiated  $\text{Ca}^{2+}$  and phosphate deposition in isolated chicken matrix vesicles. *J Biol Chem* 280, 37289–37296.

# **Annex**



## TNAP stimulates vascular smooth muscle cell trans-differentiation into chondrocytes through calcium deposition and BMP-2 activation: Possible implication in atherosclerotic plaque stability



Maya Fakhry<sup>a,b,1</sup>, Monika Roszkowska<sup>a,c,1</sup>, Anne Briolay<sup>a</sup>, Carole Bougault<sup>a</sup>, Alain Guignandon<sup>d</sup>, Juan Ignacio Diaz-Hernandez<sup>e</sup>, Miguel Diaz-Hernandez<sup>e</sup>, Slawomir Pikula<sup>c</sup>, René Buchet<sup>a</sup>, Eva Hamade<sup>b</sup>, Bassam Badran<sup>b</sup>, Laurence Bessueille<sup>a</sup>, David Magne<sup>a,\*</sup>

<sup>a</sup> Univ Lyon, University Lyon 1, ICBMS, UMR CNRS 5246, F-69622 Lyon, France

<sup>b</sup> Lebanese University, Laboratory of Cancer Biology and Molecular Immunology, EDST-PRASE, Hadath-Beirut, Lebanon

<sup>c</sup> Laboratory of Biochemistry of Lipids, Department of Biochemistry, Nencki Institute of Experimental Biology of Polish Academy of Sciences, Warsaw, Poland

<sup>d</sup> Univ Lyon, Université Jean Monnet Saint-Etienne, LBTO, UMR INSERM 1059, F-42023 Saint-Etienne, France

<sup>e</sup> Universidad Complutense de Madrid, Facultad de Veterinaria, Dpt. Bioquímica y Biología Molecular IV, Madrid, Spain

### ARTICLE INFO

#### Article history:

Received 29 July 2016

Received in revised form 12 November 2016

Accepted 4 December 2016

Available online 6 December 2016

#### Keywords:

Tissue-nonspecific alkaline phosphatase

Microcalcification

Inorganic pyrophosphate

Vascular calcification

VSMCs

Chondrocytes

### ABSTRACT

Atherosclerotic plaque calcification varies from early, diffuse microcalcifications to a bone-like tissue formed by endochondral ossification. Recently, a paradigm has emerged suggesting that if the bone metaplasia stabilizes the plaques, microcalcifications are harmful. Tissue-nonspecific alkaline phosphatase (TNAP), an ectoenzyme necessary for mineralization by its ability to hydrolyze inorganic pyrophosphate (PP<sub>i</sub>), is stimulated by inflammation in vascular smooth muscle cells (VSMCs). Our objective was to determine the role of TNAP in trans-differentiation of VSMCs and calcification. In rodent MOVAS and A7R5 VSMCs, addition of exogenous alkaline phosphatase (AP) or TNAP overexpression was sufficient to stimulate the expression of several chondrocyte markers and induce mineralization. Addition of exogenous AP to human mesenchymal stem cells cultured in pellets also stimulated chondrogenesis. Moreover, TNAP inhibition with levamisole in mouse primary chondrocytes dropped mineralization as well as the expression of chondrocyte markers. VSMCs trans-differentiated into chondrocyte-like cells, as well as primary chondrocytes, used TNAP to hydrolyze PP<sub>i</sub>, and PP<sub>i</sub> provoked the same effects as TNAP inhibition in primary chondrocytes. Interestingly, apatite crystals, associated or not to collagen, mimicked the effects of TNAP on VSMC trans-differentiation. AP and apatite crystals increased the expression of BMP-2 in VSMCs, and TNAP inhibition reduced BMP-2 levels in chondrocytes. Finally, the BMP-2 inhibitor noggin blocked the rise in aggrecan induced by AP in VSMCs, suggesting that TNAP induction in VSMCs triggers calcification, which stimulates chondrogenesis through BMP-2. Endochondral ossification in atherosclerotic plaques may therefore be induced by crystals, probably to confer stability to plaques with microcalcifications.

© 2016 Elsevier B.V. All rights reserved.

### 1. Introduction

The majority of deaths in western countries are due to cardiovascular events, mainly caused by atherosclerosis. The most dangerous complication of atherosclerosis is the rupture of a vulnerable plaque [1], however it is not yet understood what characterizes the unstable plaque. Since a single culprit lesion among many arterial segments affected by atherosclerosis can cause an acute syndrome, deciphering what renders a plaque unstable is essential. In this regard, the presence

of calcium is probably one of the most important factors affecting plaque stability. Clinically, calcium accumulation measured as a calcium score, has indeed emerged a strong independent predictor of acute cardiovascular events [2].

We have known for a long time that human atherosclerotic plaques are progressively ossified by a tissue which histologically appears nearly undistinguishable from bone, with the presence of osteocytes and bone marrow (reviewed in [3]). In atherosclerotic *Apolipoprotein (Apo)E*-deficient mice, calcium accumulates in plaques by a process similar to endochondral ossification, as revealed by the presence of chondrocyte-like cells and the expression of a type II collagen-rich matrix [4,5]. In this mouse model of atherosclerosis, VSMCs are the cells responsible for calcification, after their trans-differentiation into chondrocyte- and osteoblast-like cells [6]. In human atherosclerosis, it remains controversial

\* Corresponding author at: ICBMS UMR CNRS 5246, University of Lyon 1, Bâtiment Raulin, 43 Bd du 11 novembre 1918, 69622 Villeurbanne Cedex, France.

E-mail address: [david.magne@univ-lyon1.fr](mailto:david.magne@univ-lyon1.fr) (D. Magne).

<sup>1</sup> Both authors contributed equally.

whether plaque calcification also occurs through endochondral ossification, since some findings [7], but not all [8], indicated features of growth plate cartilage in human plaques. Although the calcium score identifies a patient at risk [2], it is increasingly recognized that bone metaplasia is an adaptive process triggered to stabilize a plaque [9]. This apparent paradox is now explained by the fact that an individual with heavily calcified plaques is also likely to have other poorly calcified, unstable plaques [3].

Unfortunately, recently published data have complicated this simple model. Intravascular ultrasound analysis in particular, revealed that it is not merely the presence of calcium *per se* that determines plaque stability, but rather the size and the extent of the calcium deposits [10]. The culprit segments of acute myocardial infarction patients generally contain numerous small calcium deposits, whereas those of stable angina pectoris patients contain fewer, but larger ones [10]. In this regard, diffuse microcalcifications, with the size less than 10  $\mu\text{m}$ , have been observed in type I lesions, before chondrocytes or osteoblasts can be detected in the plaques [11,12]. It is suggested that these microcalcifications are much more dangerous than is the bone metaplasia in advanced plaques. An interesting *in silico* analysis proposed that microcalcifications are particularly dangerous when they are located in the fibrous cap [13]. More recently, a histology and 2.1- $\mu\text{m}$  high-resolution  $\mu\text{CT}$  analysis of 22 nonruptured human atherosclerotic plaques revealed that nearly all fibrous caps contain microcalcifications with a size between 0.5 and 5  $\mu\text{m}$ , and that those that will grow above 5  $\mu\text{m}$  will be particularly harmful [14]. In light of these recent data, understanding how microcalcifications form and determining their impact appears crucial.

We recently formulated the hypothesis that tissue-nonspecific alkaline phosphatase (TNAP) activation in VSMCs is sufficient to induce vascular calcification [15]. TNAP is an ectoenzyme necessary for bone mineralization, by its capacity to hydrolyze the constitutive mineralization inhibitor inorganic pyrophosphate ( $\text{PP}_i$ ) (reviewed in [16]). TNAP is activated in VSMCs by the inflammatory cytokines tumor necrosis factor- $\alpha$  and interleukin-1 $\beta$ , which are major players in atherosclerotic plaque development [17–21]. Very recently, the group of Millan demonstrated that TNAP overexpression, specifically in VSMCs, was sufficient to induce arterial calcification [22]. It remains however unknown whether calcification induced by TNAP in VSMCs is dependent or not on VSMC trans-differentiation, and what the cellular effects of crystals are. In this regard, our objectives were to determine the effects of TNAP activation in VSMCs, from calcification to chondrocyte trans-differentiation, and to investigate the involved molecular mechanisms.

## 2. Materials and methods

### 2.1. Cell cultures

Mouse MOVAS VSMCs were purchased from ATCC (Molsheim, France). Rat A7R5 VSMCs were provided from PRASE-EDST, Beirut, Lebanon. Human primary mesenchymal stem cells (MSCs) were purchased from Lonza (Walkersville, USA). Murine primary chondrocytes were extracted from newborn mice as already published in details [23]. Animal experimentations were conducted according to French and European laws and approved by our local ethic committee (approval numbers A 69266 0501 and BH2012-63). Cell experiments were made on primary chondrocytes extracted from 4- to 6-day old newborn litters from SWISS mice (Janvier labs), after decapitation. The animal procedures were performed conform to the guidelines from Directive 2010/63/EU of the European Parliament on the protection of animals used for scientific purposes. Cells were routinely cultured in DMEM medium (4.5 g/L glucose) supplemented with 10% (v/v) fetal bovine serum (FBS), penicillin (100 U/mL), streptomycin (100  $\mu\text{g}/\text{mL}$ ), 20 mmol/L HEPES, and 2 mmol/L L-glutamine. To support the growth of MSCs, fibroblast growth factor-2 (2 ng/mL) was added to their culture medium. All cells were cultured in the presence of 50  $\mu\text{g}/\text{mL}$  ascorbic acid to

accelerate collagen secretion. MOVAS trans-differentiation was accelerated with 10  $\mu\text{g}/\text{mL}$  insulin with transferrin and sodium selenite (Sigma) as previously published [24,25]. Only where indicated, mineralization was stimulated with 10 mM of  $\beta$ -glycerophosphate ( $\beta$ -GP) in MOVAS and chondrocytes, and with 3 mM inorganic phosphate ( $\text{P}_i$ ) in A7R5. MSCs were induced to differentiate into chondrocytes in pellet cultures (500,000 cells per tube in 1 mL) with FBS-free DMEM in the presence of bovine insulin (10  $\mu\text{g}/\text{mL}$ ) and TGF- $\beta$ 1 (10 ng/mL) as previously published [18].

### 2.2. Alkaline phosphatase (AP) addition and TNAP overexpression

Bovine intestinal alkaline phosphatase from Sigma was used. In parallel, TNAP expressing plasmid or the corresponding empty vector (pIRES2-EGFP) have been prepared as described previously [26]. A7R5 cells were transfected at 80% confluence using lipofectamine reagent (Life Technologies), and transfected cells were selected within 7 additional days with G418 (800  $\mu\text{g}/\text{mL}$ ).

### 2.3. RNA extraction, reverse transcription, and quantitative polymerase chain reaction (RT-qPCR)

Total RNA was extracted using the NucleoSpin RNA II kit (Macherey-Nagel) following the manufacturer's protocol. 1  $\mu\text{g}$  of RNA was retrotranscribed into cDNA with Superscript II (Life Technologies) and quantitative PCR was performed using a LightCycler system (Roche Diagnostics). Primers and PCR conditions are given in Table 1. The obtained products were verified by sequencing. Relative quantification was performed using the  $2^{-\Delta\Delta\text{Ct}}$  method by RelQuant LightCycler software 4.1 (Roche Diagnostics, Meylan, France). *Gapdh* (glyceraldehyde-3-phosphate dehydrogenase) gene was used as reference gene.

### 2.4. Measurement of ATP- and $\text{PP}_i$ hydrolysis

At confluence, MOVAS and chondrocytes were differentiated in the presence of 50  $\mu\text{g}/\text{mL}$  ascorbic acid and 10 mM  $\beta$ -GP. Cultures were stopped on day 21 for VSMCs and on day 7 for primary chondrocytes and cells were fixed with 4% formaldehyde and incubated in HEPES buffer (pH = 7.0) containing  $\text{MgCl}_2$  (1 mM) and the substrate (10  $\mu\text{M}$  ATP or 20  $\mu\text{M}$   $\text{PP}_i$ ) at room temperature. Aliquots were taken at different time points and the  $\text{P}_i$  release was determined by Malachite Green assay as described elsewhere [27]. The results were expressed as  $\mu\text{M}$   $\text{P}_i$  by comparing to a standard curve of  $\text{P}_i$  and initial reaction rates were determined from the curves representing  $\text{P}_i$  concentrations versus time.

### 2.5. Preparation of mineralized collagen, apatite crystals and calcium pyrophosphate dihydrate (CPPD) crystals

MOVAS cells were seeded at their confluence density on collagen type I matrices, either unmineralized or mineralized with apatite as described earlier, and cultured in DMEM with ascorbic acid [28]. Briefly, 0.1 mg/mL calf skin type I collagen was coated in 6-well plates and incubated or not with intestinal AP, phosvitin (0.13 mg/mL) and calcium  $\beta$ -GP (6 mM). Calcification was determined with alizarin red staining and crystals were analyzed with Fourier transform infrared (FTIR) spectroscopy, using a Thermo Scientific Nicolet iS10 spectrometer (64 scans at 4  $\text{cm}^{-1}$  resolution). In parallel, apatite crystals were prepared starting from a solution of sodium phosphate (0.4 M, pH = 7.2), which was added to DMEM to reach a final concentration of 10 mM inorganic phosphate. The solution was incubated for 24 h at 37 °C. Crystals that formed in these conditions were collected after series of centrifugation at 3000g and washing steps in fresh medium. Crystals were then sonicated for 10 min in 10 mL, centrifuged at 3000g and dried. Calcium pyrophosphate dihydrate (CPPD) crystals were prepared similarly by mixing a solution of  $\text{PP}_i$  at 100  $\mu\text{M}$  with DMEM (1.8 mM calcium). MOVAS VSMCs and primary chondrocytes were treated respectively with

**Table 1**

Summary of primers used. Shown are the primer sequences (F: forward; R: reverse), annealing temperatures (Ta), base pair (bp) lengths of the corresponding PCR products, and GenBank accession numbers (Acan: aggrecan; Bmp-2: bone morphogenetic protein-2; Col2a1: collagen type II,  $\alpha 1$  chain; Col10a1: collagen type X,  $\alpha 1$  chain; Gapdh: glyceraldehyde phosphate dehydrogenase; Id1: inhibitor or DNA binding 1; Ocn: osteocalcin; Opn: osteopontin; Osx: osterix).

Gene	GenBank	Ta (°C)	Sequences	Lengths (bp)
<i>mAcan</i>	NM_007424.2	60	F: 5'-GTGCGGTACCAGTGCCTGA-3' R: 5'-GGGTCTGTGCAGGTGATTTCG-3'	104
<i>mBmp-2</i>	NM_007553	60	F: 5'-TGAAGTGGCCATTAGAG-3' R: 5'-TGACGCTTTTCTCGTTTGTG-3'	165
<i>mCol2a1</i>	NM_031163.3	60	F: 5'-GGCAACAGCAGGTTACAT-3' R: 5'-ATGGGTGCGATGCAATAA-3'	131
<i>mCol10a1</i>	NM_009925.4	60	F: 5'-CAAACGGCCTCTACTCTCTGA-3' R: 5'-CGATGGAATTGGTGGAAAG-3'	129
<i>mGapdh</i>	NM_001289726.1	60	F: 5'-GGCATTGCTCAATGACAA-3' R: 5'-TGTGAGGAGATGCTCAGTG-3'	200
<i>mId1</i>	NM_010495.3	60	F: 5'-GCGAGATCAGTGCCTTG-3' R: 5'-GAGTCCATCTGGTCCCTCAG-3'	97
<i>mOcn</i>	NM_001037939.2	60	F: 5'-AAGCAGGAGGCAATAAGGT-3' R: 5'-CGTTTGTAGGCGGTCTTCA-3'	364
<i>mOpn</i>	NM_001204203.1	60	F: 5'-CTTCACTCCAATCGTCCCTA-3' R: 5'-GCTCTCTTTGGAATGCTCAAGT-3'	305
<i>mOsx</i>	NM_130458.3	60	F: 5'-AGGCACAAAGAAGCCATACG-3' R: 5'-GCCAGGAAATGAGTGAGG-3'	170
<i>mRunx2</i>	NM_009820.5	62	F: 5'-GCCGGGAATGATGAGAACTA-3' R: 5'-GGACCGTCCACTGTCACTTT-3'	200
<i>rAcan</i>	NM_022190.1	60	F: 5'-CTCTGCCTCCGTTGAAAC-3' R: 5'-TGAAGTGCCTGCATCTATGT-3'	157
<i>rCol10a1</i>	XM_008773017.1	60	F: 5'-TTCACAAAGAGCGGACAGAGA-3' R: 5'-TCAAATGGGATGGAGCA-3'	143
<i>rGapdh</i>	NM_017008.4	60	F: 5'-GCAAGTCAACGGCAGAC-3' R: 5'-GCCAGTAGACTCCACGACA-3'	140

apatite crystals after 17 days of differentiation and CPPD after 10 days of differentiation, as described above.

## 2.6. Analytical methods

For the determination of TNAP activity using p-nitrophenyl phosphate (pNPP) as substrate [29], cells were harvested in 0.2% Nonidet P-40 and disrupted by sonication. TNAP specific activity was expressed as nmol of p-nitrophenol formed/min/mg of protein. Calcium deposition was determined by alizarin red staining (2% solution at pH 4.2) for 5 min and quantified at 570 nm after extracting the stain with 100 mM cetylpyridinium chloride for 2 h. For alcian blue staining of sulfated glycosaminoglycans (GAGs), cells were rinsed with PBS followed by fixation in methanol at  $-20^{\circ}\text{C}$  for 5 min. Staining was performed with 0.1% alcian blue solution in 0.1 M HCl overnight at room temperature. For quantification, after washing, the bound stain was extracted with 6 M guanidine HCl for 8 h, and absorbance was measured at 620 nm.

## 2.7. Statistical analysis

Experiments were performed in triplicates and repeated independently at least three times. Results are expressed as mean  $\pm$  the standard error of the mean (SEM). For statistical analysis, depending on the nature of distribution, a two tailed un-paired Student *t*-test or Mann-Whitney test was performed (Instat program, version 3.10.0.0). According to this rule, all tests were performed with Student *t*-test except the test concerning Fig. 2A, which was realized with Mann-Whitney. The differences between groups were considered significant with \* at  $p < 0.05$ , \*\* at  $p < 0.01$  and \*\*\* at  $p < 0.001$ .

## 3. Results

### 3.1. TNAP stimulates VSMC trans-differentiation into chondrocytes

The role of TNAP during VSMC trans-differentiation was first investigated using murine MOVAS VSMCs, which had been shown to trans-differentiate into chondrocytes and mineralize their extracellular

matrix (ECM) upon being cultured with ascorbic acid and  $\beta$ -GP [25]. In our hands, MOVAS cells expressed the chondrocyte markers aggrecan and type II collagen after 14 days of culture, and the hypertrophic markers type X collagen and osteocalcin after 21 days, when they also showed increased TNAP activity and mineralization ([25] and data not shown). Hence, we chose to treat these VSMCs with high levels of purified alkaline phosphatase (AP, 8 units per mL) on day 17, which is a few days before the onset of endogenous TNAP activity on day 21. Cells were treated with AP for 7 days in the absence of  $\beta$ -GP to avoid a non-physiological rise of  $P_i$  levels due to  $\beta$ -GP hydrolysis. When cells were cultured under these conditions, we observed an up-regulation of the mRNA encoding the early chondrocyte marker aggrecan, and of the late ones - type X collagen and osteocalcin after AP treatment (Fig. 1A). Aggrecan is a proteoglycan in which chondroitin sulfate and keratan sulfate GAG chains are attached to a protein core, creating a highly negatively-charged molecule that enables hydration of the cartilage tissue as well as binding of growth factors [30]. Type X collagen is widely used as a marker of hypertrophic chondrocytes, although its physiological role is not yet elucidated [31]. Osteocalcin is a abundant carboxylated protein associated with bone crystals, and after its release in the blood during bone resorption, a hormone that regulates glucose homeostasis [32]. Since osteocalcin is also expressed by osteoblasts, we sought to investigate whether VSMCs also trans-differentiate in osteoblasts after AP treatment. We measured the levels of the osteoblast-specific transcription factor osterix, which did not increase but instead decreased in the presence of AP, suggesting that VSMCs trans-differentiated into chondrocytes and not osteoblasts (Fig. 1A). To strengthen these results obtained with MOVAS VSMCs, we used A7R5 VSMCs, which in our hands were unable to trans-differentiate into chondrocytes in the presence of ascorbic acid and either  $\beta$ -GP or  $P_i$  (data not shown). Interestingly, overexpression of TNAP in these cells resulted in a dramatic increase in *Acan* levels (Fig. 1B) and in a significant stimulation of calcium accumulation in the matrix (Fig. 1C).

### 3.2. TNAP is necessary for normal chondrocyte differentiation

We next explored the involvement of alkaline phosphatase in normal chondrocyte differentiation. To address this issue, we first used



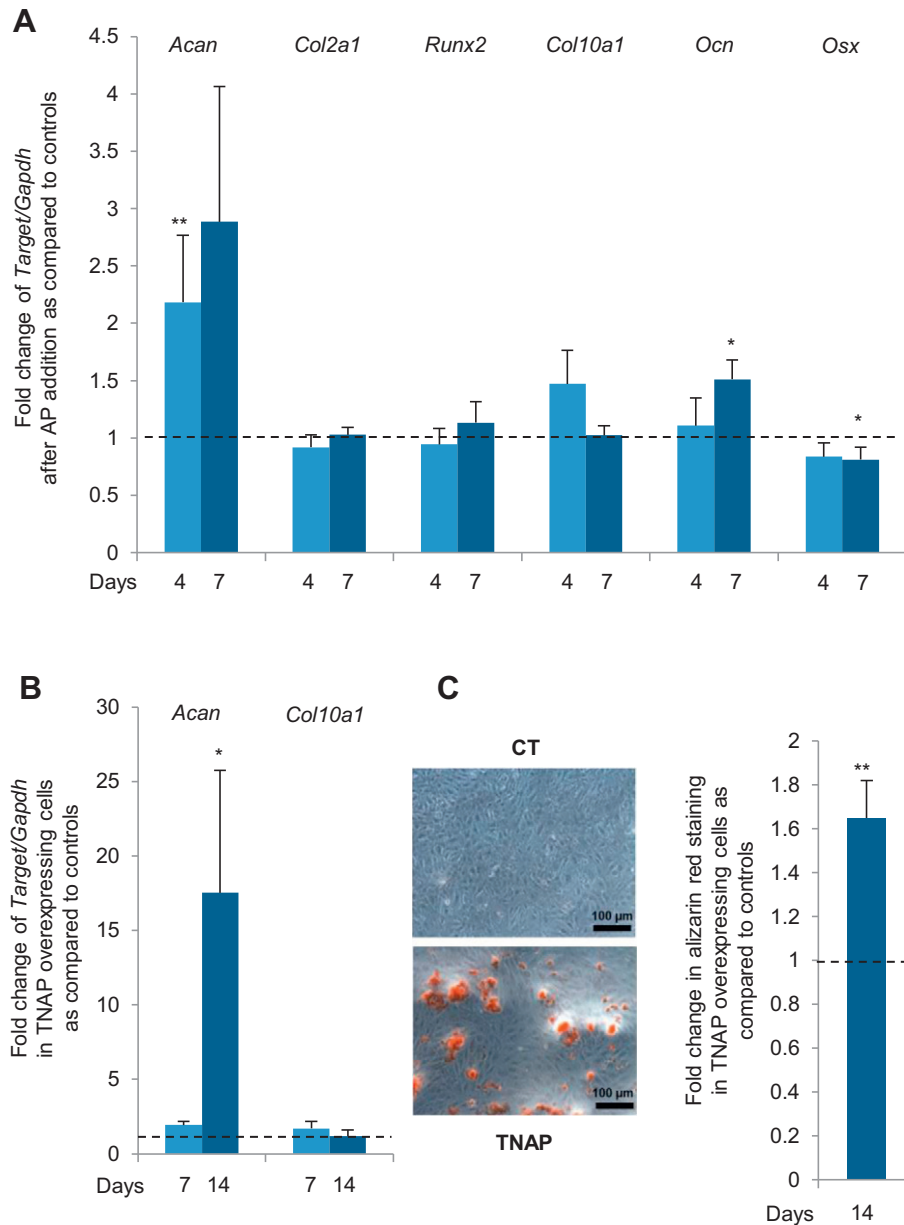


**Fig. 1.** Alkaline phosphatase activity stimulates chondrocyte differentiation and mineralization from VSMCs. MOVAS cells were cultured from confluence to day 17 with ascorbic acid and  $\beta$ -GP. On day 17,  $\beta$ -GP was removed and 8 U/mL of AP were added. (A) mRNA levels were quantified by RT-qPCR after 4 and 7 days of treatment, and normalized with *Gapdh* mRNA levels. (B and C) A7R5 cells stably overexpressing TNAP were cultured for 7 and 14 days. The levels of *Acan* and *Col10a1* were measured by RT-qPCR (B) and alizarin red staining was performed and quantified (C). \* indicates a statistical difference with  $p < 0.05$  and \*\* indicates a statistical difference with  $p < 0.01$ .

human MSCs as a model of chondrocyte precursors, and allowed them to commit towards chondrocytes in pellets in the presence of insulin and TGF- $\beta$ 1 [18], with or without exogenous AP. As shown in Fig. 2A, exogenous AP was sufficient to significantly increase the deposition of sulfated GAGs during chondrocyte differentiation of MSCs. We next sought to investigate whether inhibition of endogenous TNAP in hypertrophic chondrocytes impacts chondrocyte differentiation. To address this assumption, we isolated murine primary chondrocytes and differentiated them to hypertrophy by culturing from confluence for 10 days in the presence ascorbic acid. In these conditions, hypertrophic differentiation was demonstrated by a 30-fold increase in TNAP activity as compared to freshly isolated primary articular chondrocytes (Fig. 2B). In these cells, inhibiting TNAP activity with the well-known TNAP inhibitor levamisole significantly reduced the deposition of sulfated GAGs and dropped the mRNA levels of *Acan* as well as those of the hypertrophic markers *Col10a1* and *Ocn* (Fig. 2B).

### 3.3. Trans-differentiated VSMCs and chondrocytes use TNAP to hydrolyze $PP_i$

We then suspected that TNAP stimulates chondrogenesis through hydrolysis of ATP and/or that of  $PP_i$ . Indeed, TNAP has been shown to dephosphorylate ATP to accelerate axonal growth in neuron cultures [26], and genetic depletion of  $PP_i$  in mouse promotes chondrogenesis in arteries in addition to vascular calcification [33]. VSMCs induced to trans-differentiate into chondrocytes for 21 days were able to hydrolyze exogenously added ATP and  $PP_i$  (Fig. 3A). In these cells, levamisole dramatically dropped the release of  $P_i$  from exogenously added  $PP_i$  whereas it showed no effect on ATP hydrolysis (Fig. 3A). Similarly, hypertrophic chondrocytes were also able to hydrolyze exogenously added ATP and  $PP_i$  and levamisole inhibited the hydrolysis of  $PP_i$  but not that of ATP (Fig. 3B). These results indicate that trans-differentiated VSMCs as well as primary chondrocytes used TNAP to hydrolyze exogenous  $PP_i$ .

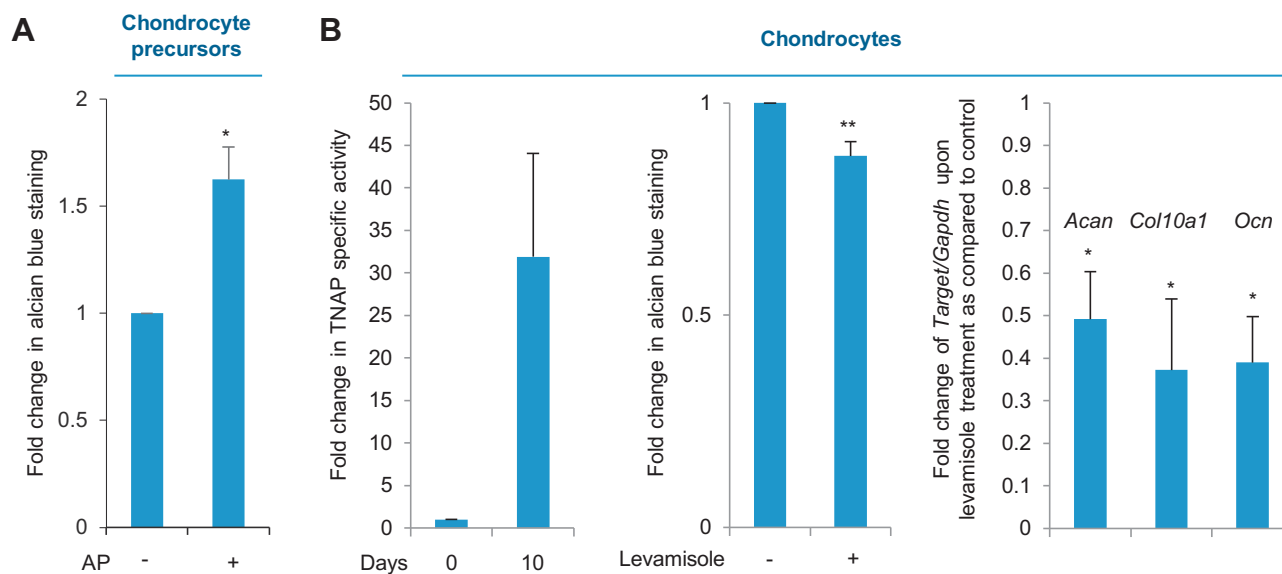


**Fig. 2.** Alkaline phosphatase activity stimulates chondrogenesis. Human MSCs used as chondrocyte precursors were cultured in pellets and treated with or without 8 U/mL of AP for 14 days, before alcian blue staining was performed (A). (B) Primary mouse chondrocytes were extracted and cultured as detailed in the [Materials and methods](#) section, and at confluence (day 0), were cultured for 10 additional days in the presence of 50  $\mu\text{g}/\text{mL}$  of ascorbic acid. On day 0 and 10, alkaline phosphatase activity was measured. Levamisole was added at 100  $\mu\text{M}$  to the medium from day 0 to day 10, and the deposition of sulfated GAGs was assessed with alcian blue on day 10. In parallel, we determined mRNA levels on day 10 with RT-qPCR. \* indicates a statistical difference with  $p < 0.05$ ; \*\* indicates a statistical difference with  $p < 0.01$ .

In contrast, both cell types probably used other enzymes than TNAP to hydrolyze ATP.

#### 3.4. $\text{PP}_i$ inhibits chondrocyte differentiation and calcification

To investigate a possible role of  $\text{PP}_i$  hydrolysis in the stimulation of chondrocyte differentiation by TNAP, we treated primary chondrocytes with doses of  $\text{PP}_i$  increasing from 2 to 100  $\mu\text{M}$ . Interestingly, treatment of primary chondrocytes with  $\text{PP}_i$  mimicked the inhibitory effects of levamisole on gene expression (as shown in [Fig. 2B](#)), with a pronounced dose-dependent decrease in the mRNA levels of early chondrocyte markers *Acan* and *Col2a1*, and a decrease in hypertrophic chondrocyte markers *Col10a1* ([Fig. 4A](#)) and TNAP ([Fig. 4B](#)). We next questioned whether this inhibitory effect of exogenous  $\text{PP}_i$  on chondrocyte differentiation was direct or secondary to the well-known role of  $\text{PP}_i$  in the inhibition of mineralization. In chondrocytes allowed to mineralize their extracellular matrix by addition of  $\beta\text{-GP}$ , we checked that treatment with  $\text{PP}_i$  reduced calcium deposition ([Fig. 4C](#)). Surprisingly, inhibition by 100  $\mu\text{M}$  of  $\text{PP}_i$  appeared less pronounced than that by 20  $\mu\text{M}$ , although the difference was not significant ([Fig. 4C](#)). FTIR analysis of crystals formed in cultures treated with 100  $\mu\text{M}$   $\text{PP}_i$  revealed the presence of a mixture of apatite crystals and crystals of calcium pyrophosphate dihydrate (CPPD) ([Fig. 4D](#)) [34]. In contrast, cultures untreated and those treated with 20  $\mu\text{M}$   $\text{PP}_i$  only revealed the presence of apatite (data not shown). This means that the lower inhibition of calcium accumulation in cultures treated with 100  $\mu\text{M}$  of  $\text{PP}_i$  as compared with 20  $\mu\text{M}$   $\text{PP}_i$  was due to the precipitation of CPPD crystals.

In these conditions, to be sure that the decrease in chondrocyte markers ([Fig. 4A](#)) was indeed due to  $\text{PP}_i$  and was not due to CPPD crystals, we investigated the effects of synthetic CPPD crystals on chondrocytes. [Fig. 4E](#) clearly indicates that in contrast to  $\text{PP}_i$ , CPPD crystals had no effect on the levels of *aggrecan* mRNA ([Fig. 4E](#)). As a positive control of genes regulated by high  $\text{PP}_i$  levels [35] and calcium phosphate crystals [36,37], we investigated the expression of the calcification inhibitor osteopontin. We observed that *Opn* mRNA levels were strongly increased when  $\text{PP}_i$  was added at the dose of 100  $\mu\text{M}$ , the same dose that induces CPPD crystal formation, but were not changed at the dose of 20  $\mu\text{M}$  ([Fig. 4F](#)). Moreover, CPPD crystals also increased *Opn* levels to the same extent than that achieved with 100  $\mu\text{M}$   $\text{PP}_i$ , the dose that

induces CPPD formation ([Fig. 4G](#)). This demonstrates that CPPD crystals but not  $\text{PP}_i$  were involved in upregulation of *Opn* levels. Collectively, the results of [Figs. 3 and 4](#) strongly suggest that TNAP stimulates chondrocyte differentiation through  $\text{PP}_i$  hydrolysis.

#### 3.5. TNAP stimulates VSMC trans-differentiation through $\text{PP}_i$ hydrolysis, the subsequent crystal formation, and the induction of BMP-2

We then questioned whether TNAP stimulates VSMC trans-differentiation into chondrocyte-like cells through the generation of apatite crystals induced by  $\text{PP}_i$  hydrolysis. To answer this question, we first prepared dishes coated with collagen, either left unmineralized or mineralized by addition of alkaline phosphatase ([Fig. 5A](#)). FTIR analysis of the  $\nu_1\nu_3\text{PO}_4$  domain between 1200 and 900  $\text{cm}^{-1}$  and of the  $\nu_1\text{CO}_3$  domain at 870  $\text{cm}^{-1}$  revealed that the crystals in mineralized collagen consisted of a carbonated apatite ([Fig. 5A](#)), virtually identical in organization and composition to the carbonated apatite that forms in the cartilage growth plate [38] and atherosclerotic plaques [39]. We then cultured VSMCs on these unmineralized or mineralized synthetic collagen matrices for 7 days. Interestingly, we observed a significant increase of *Acan* levels when VSMCs were cultured on mineralized collagen as compared to unmineralized collagen ([Fig. 5B](#)). Similarly, VSMCs treated with apatite crystals in suspension, without collagen, also showed the same 2-fold increase in *Acan* levels ([Fig. 5C](#)).

In order to begin in identifying the factors involved in the effects of TNAP and crystals on chondrocyte gene expression, we focused on bone morphogenetic protein-2 (BMP-2), one of the most potent anabolic growth factor known so far [40]. BMP-2 is expressed in human atherosclerotic plaques after calcification has been initiated [12] and its expression is induced by hydroxyapatite crystals in cultured VSMCs [37]. We observed that *Bmp-2* expression was increased when VSMCs were cultured on mineralized collagen as compared with unmineralized collagen, and that apatite crystals were also able to stimulate *Bmp-2* expression ([Fig. 6A](#)). In addition, we observed an increase in *Bmp-2* levels in response to exogenous AP ([Fig. 6A](#)). Furthermore, we observed that hypertrophic chondrocytes treated with levamisole had decreased levels of *Bmp-2* and of its transcriptional target *Id1*, suggesting a loss of BMP-2 activity upon inhibition of TNAP ([Fig. 6B](#)). Finally, we used

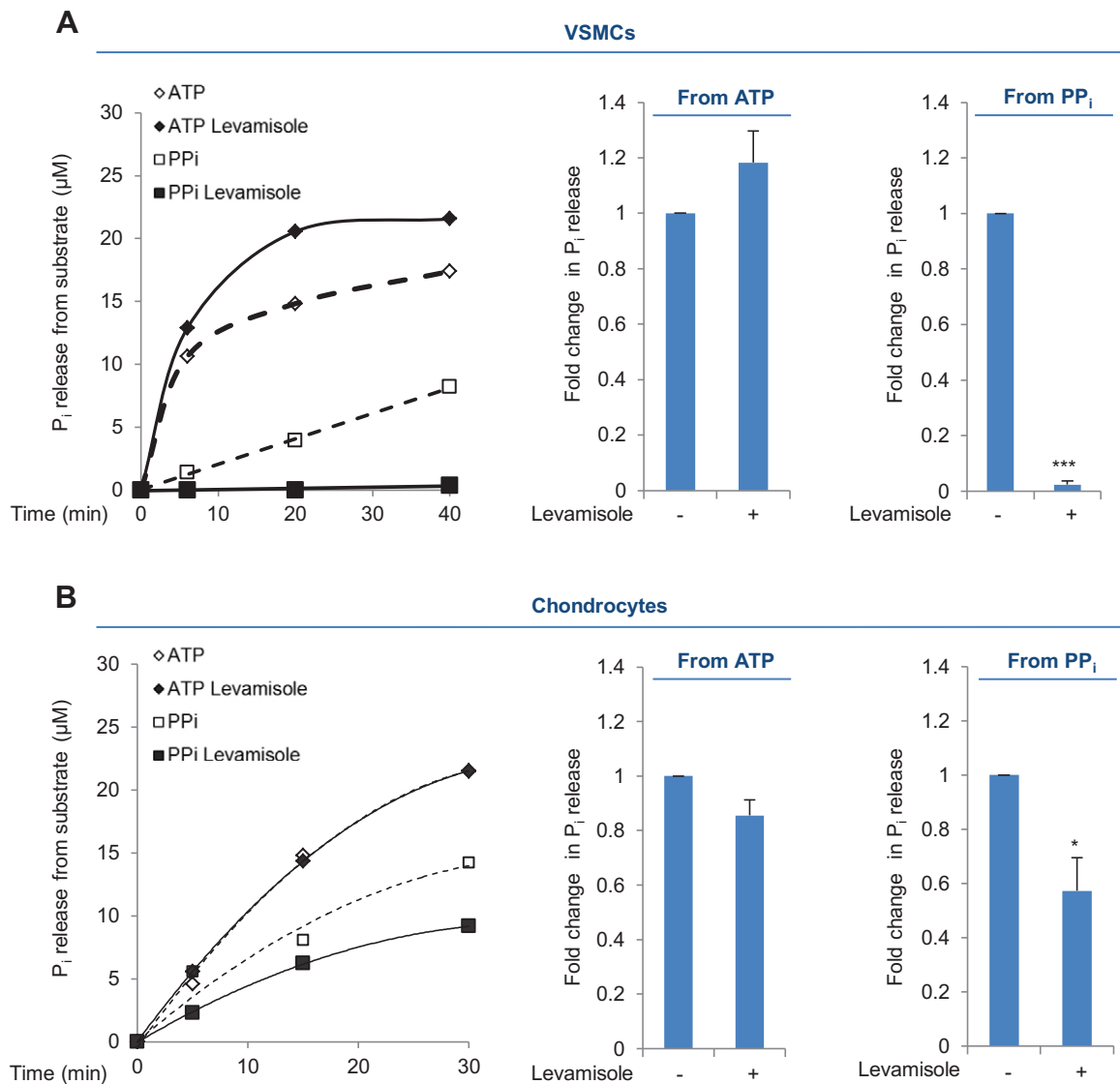


**Fig. 3.** VSMCs trans-differentiated into chondrocyte-like cells and primary chondrocytes use TNAP to hydrolyze  $PP_i$ . MOVAS cells or chondrocytes were cultured as detailed in the [Materials and methods](#) section, and after fixation,  $PP_i$  or ATP hydrolysis into  $P_i$  was measured at different time points in VSMCs (A) and primary chondrocytes (B) by the Malachite green assay in the presence or absence of 100  $\mu$ M levamisole (left panels, one representative experiment is shown). The ratio between the initial reaction rates measured in the presence versus in the absence of levamisole is represented in the right panels (mean of three independent experiments). \* indicates a statistical difference with  $p < 0.05$ ; \*\*\* indicates a statistical difference with  $p < 0.001$ .

the BMP-2 inhibitor Noggin to demonstrate that alkaline phosphatase activity stimulates aggrecan expression by stimulating BMP-2 (Fig. 6D).

#### 4. Discussion

It is increasingly recognized today that the type and location rather than the extent of calcifications are important to determine atherosclerotic plaque stability [10,13,14], and several reports indicate that microcalcifications, measuring less than a single cell size, seem to be particularly harmful when they are located in the fibrous cap [13,14]. These microcalcifications are formed early in human plaque development, probably as soon as in type I lesions, before chondrocyte-like cells or osteoblast-like cells can be detected [11,12]. Therefore, the process similar to endochondral ossification that occurs in atherosclerotic plaques [4,5] is probably not the mechanism leading to the nucleation of the first crystals in the plaques. The fact that these early microcalcifications that form before chondrocyte differentiation have not been reported in a number of studies is probably due to their small size, that renders them hardly detectable by von Kossa and alizarin red stainings [12,41].

Despite the fact that microcalcifications are now considered as crucial determinants of plaque stability and future cardiovascular complications [3,10,13,14], the molecular mechanisms responsible for their formation as well as their effects on VSMCs remain quite obscure. It has been proposed that macrophages release exosomes, which induce crystal formation in a similar manner as matrix vesicles released from chondrocytes [42]. This has however to be confirmed, since it would probably be a unique case where calcification is triggered by macrophages, which in skeletal tissues give rise to bone-resorbing osteoclasts, but not mineralizing cells. Alternatively, it is possible that microcalcification occurs in association with macrophage or VSMC apoptosis and/or necrosis. Indeed, the clearance of apoptotic bodies is impaired in atherosclerosis [43], where cells undergo secondary necrosis [44]. Dying cells may release apoptotic bodies, which in the absence of clearance mechanisms, may undergo necrosis and eventually constitute a nidus for calcification [45]. If this mechanism is indeed the main cause of microcalcification in atherosclerosis, it will probably be quite difficult to impact clinically.

On the other hand, different results from our laboratory and other groups suggest that a single enzyme, TNAP, is likely to play a significant

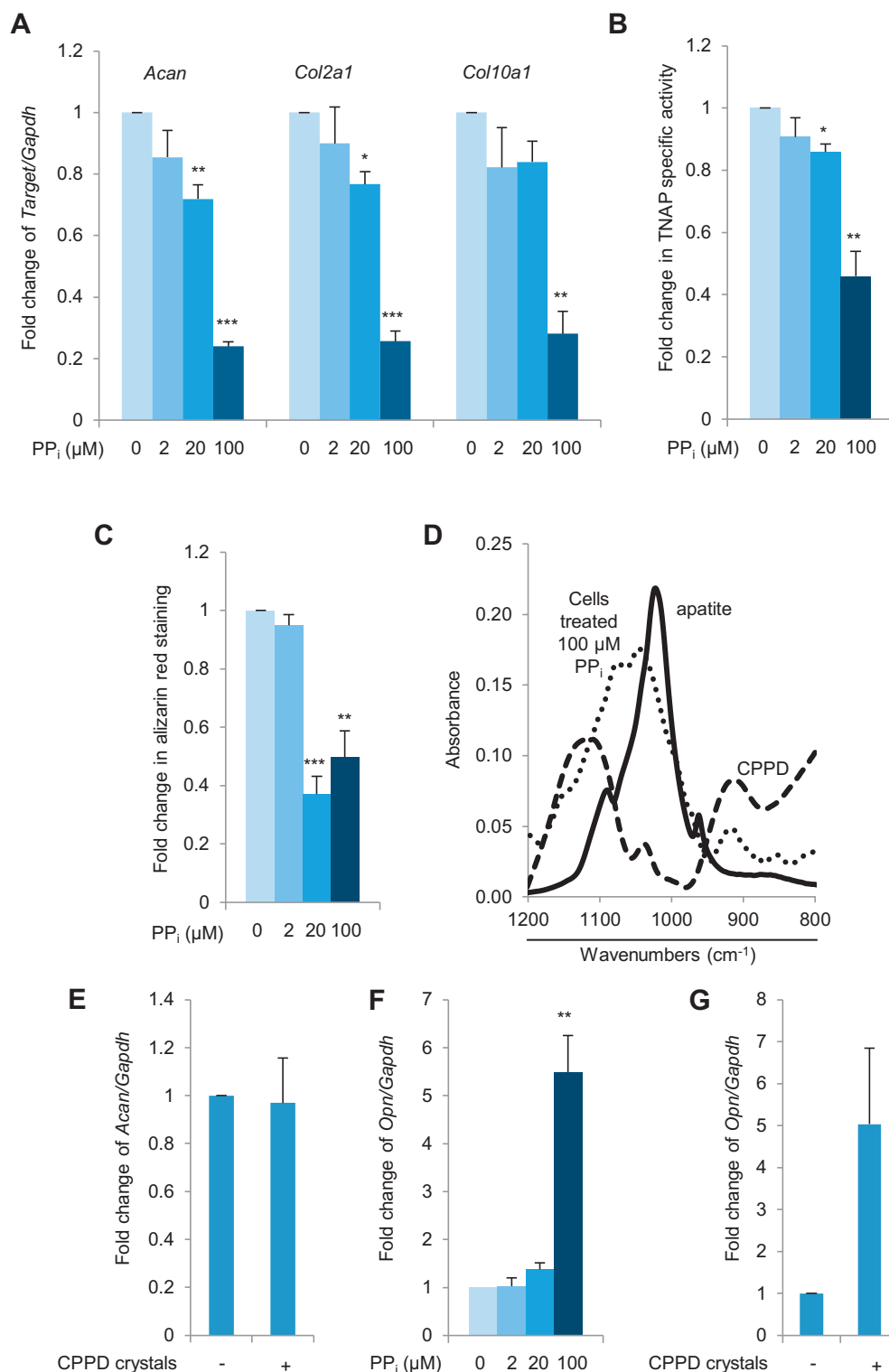


**Fig. 4.** PP<sub>i</sub> inhibits chondrocyte differentiation and mineralization. Primary mouse chondrocytes were cultured from confluence for 10 days in DMEM in the presence of 50 μg/mL ascorbic acid, with or without PP<sub>i</sub>. mRNA levels were quantified by RT-qPCR and normalized with *Gapdh* mRNA levels (A and F). Alkaline phosphatase activity was measured with pNPP as a substrate (B). Alizarin red was used to stain cells and quantify calcium deposits after extraction (C). The FTIR spectrum of crystals formed in cultures treated with 100 μM of PP<sub>i</sub> was compared with the spectra of synthetic apatite and CPPD crystals (D). Cells were treated with 300 μg/mL CPPD crystals for 7 days and mRNA levels were quantified by RT-qPCR (E and G). \* indicates a statistical difference with  $p < 0.05$ ; \*\* indicates a statistical difference with  $p < 0.01$ ; \*\*\* indicates a statistical difference with  $p < 0.001$ .

role in microcalcification. As its name indicates, tissue-nonspecific AP expression is not restricted to bone-forming cells, and TNAP plays other functions than mineralization [16]. Interestingly enough, TNAP is constitutively expressed at low levels in mesenchymal progenitors from many tissues [46,47], and is activated in VSMCs by TNF-α and IL-

1β [18–21]. If the pathophysiological aim of TNAP activation in VSMCs is not known, one of its consequences *in vivo* is induction of calcification [22]. In the present *in vitro* study, overexpression of TNAP in VSMCs was also sufficient to induce calcification. This induction of calcification by TNAP was not dependent on VSMCs trans-differentiation since it

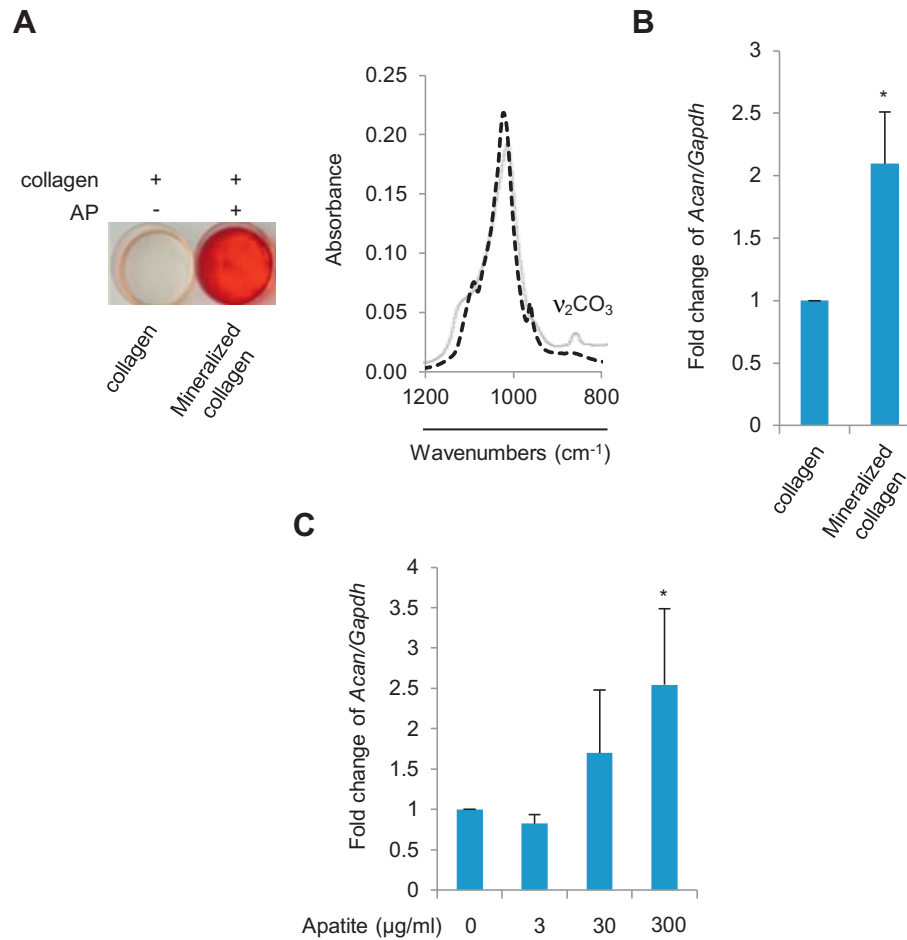


**Fig. 5.** Apatite crystals stimulate aggrecan expression in VSMCs. Unmineralized or mineralized collagen matrices were synthesized as described in the [Materials and methods](#) section. MOVAS cells were deposited on these collagens at a density corresponding to confluence in DMEM with ascorbic acid but in the absence of  $\beta$ -GP. (A) The presence of calcium in collagen matrices was determined with alizarin red staining and the nature of the crystals (grey spectrum) determined with FTIR spectroscopy as compared to synthetic hydroxyapatite (dotted dark spectrum). mRNA levels of *aggrecan* were quantified by RT-qPCR after 7 days of differentiation on collagen matrices (B) or in the presence of apatite crystals in suspension (C), and normalized with *Gapdh* mRNA levels. \* indicates a statistical difference with  $p < 0.05$ .

occurred not only in MOVAS VSMCs that trans-differentiate into chondrocytes in culture, but also in A7R5 VSMCs, which in our hands did not express any marker of osteoblasts or chondrocytes. This induction of mineralization by TNAP in the absence of bone cell differentiation is not really surprising since the group of Karsenty demonstrated that mineralization *in vivo* and *in vitro* merely requires the coexpression of TNAP and a fibrillar collagen [48]. Up to thirteen types of collagen are present in the normal vascular wall, with type I collagen accounting for about 65% of the total collagen content [49]. Moreover, the amount of type I collagen secreted by VSMCs increases in atherosclerotic plaques, in particular in the fibrous cap [49]. Therefore, activation of TNAP in VSMCs by inflammation is likely sufficient to induce microcalcification, especially in the fibrous cap, with no requirement of VSMC trans-differentiation into osteoblasts or chondrocytes [15,22,48]. This model is coherent with the fact that TNAP activity and calcification associate with inflammation in early atherosclerosis of *ApoE*-deficient mice [41]. In atherosclerotic patients also, inflammation was shown to precede calcification at the same location [50]. Since inflammation and ongoing calcification appear to co-localize at sites of plaque rupture [51], TNAP activation may represent a dramatic event in atherosclerotic progression. The recent development of TNAP inhibitors [52,53] will be precious to investigate the impact of TNAP inhibition on atherosclerosis development. Alternatively, proteins involved in TNAP activation may also represent attractive targets. In this regard, sortilin was recently described as an important inducer of TNAP activation in extracellular vesicles, which is likely to play a dramatic role in calcification of

atherosclerotic plaques [54]. TNAP induction of calcification in our hands was very likely due to the hydrolysis of  $PP_i$ , as it is during *in vivo* mineralization [48,55]. Interestingly,  $PP_i$  deficiency due to mutations in the gene encoding the  $PP_i$ -producing enzyme ectonucleotide pyrophosphatase/phosphodiesterase-1 (NPP1) leads to severe, lethal arterial calcification [56], and  $PP_i$  supplementation has been tested with success to prevent vascular calcification associated with chronic kidney disease [57,58]. It will therefore also be interesting to determine the impact of  $PP_i$  administration on microcalcification and the progression of atherosclerosis in comparison to the effects of TNAP inhibitors.

In our opinion, the most interesting result in the present study is the effect of apatite crystals on VSMCs. Indeed, we observed that treatment of these cells with alkaline phosphatase or apatite crystals induced the expression of BMP-2 and several chondrocyte markers. To our knowledge, stimulation of BMP-2 by apatite crystals in VSMCs has already been reported by two groups [37,59]. BMP-2 is probably the most potent inducer of ectopic bone formation [40], being able to induce ectopic bone formation when implanted intramuscularly or subcutaneously into rodents [60,61]. It can therefore be reasonably hypothesized that crystals stimulate VSMC trans-differentiation in chondrocyte-like cells in a large part through a BMP-2 autocrine loop. This is supported by our observation that the BMP-2 inhibitor noggin blocked aggrecan expression induced by alkaline phosphatase. Aggrecan is a proteoglycan abundant in sulfated GAGs produced by chondrocytes. Interestingly, in mice deficient in the mineralization inhibitor matrix Gla protein, vascular calcification precedes chondrocyte differentiation, and aggrecan is

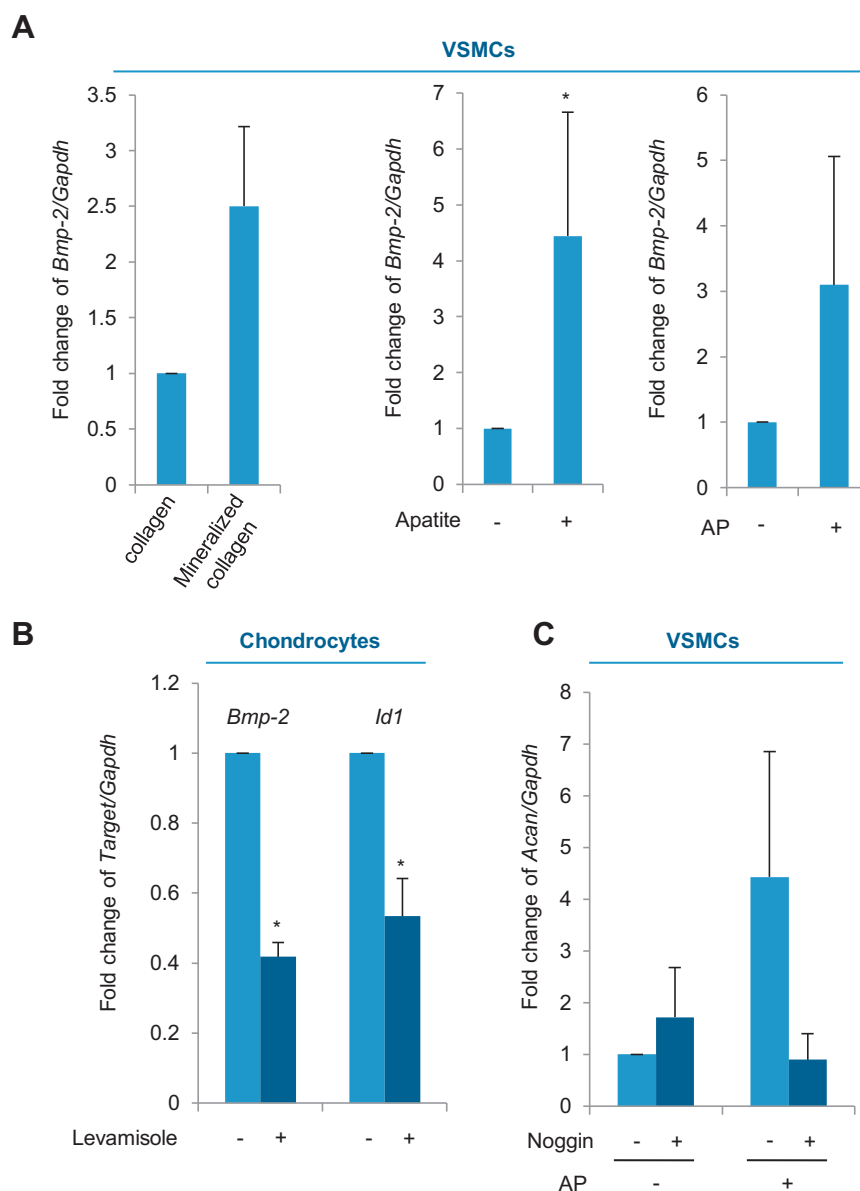


**Fig. 6.** Alkaline phosphatase stimulates aggrecan through BMP-2 activation in VSMCs. Unmineralized or mineralized collagen matrices were synthesized as described in the [Materials and methods](#) section. MOVAS cells were deposited on these collagens at a density corresponding to confluence, and cultured for 7 days in DMEM with ascorbic acid but in the absence of  $\beta$ -GP. To determine the effects of crystals in suspension and the effects of AP addition, MOVAS were cultured for 17 days in differentiation medium as detailed in the [Materials and Methods](#) section. (A) mRNA levels of *Bmp-2* were quantified by RT-qPCR after 7 days of culture on collagen matrices, 7 days of treatment with 300  $\mu$ g/mL apatite crystals in suspension, or 8 U/mL of AP and normalized with *Gapdh* mRNA levels. (B) Primary mouse chondrocytes were extracted and cultured as detailed in the [Materials and methods](#) section, and at confluence (day 0), were cultured for 10 additional days in the presence of 50  $\mu$ g/mL of ascorbic acid, with or without 100  $\mu$ M of levamisole. (C) MOVAS cells were cultured as detailed in the [Materials and methods](#) section for 17 days, and on day 17,  $\beta$ -GP was removed and 8 U/mL of AP were added or not, in the presence or absence of the BMP-2 inhibitor noggin (100 ng/mL, Immunotools). \* indicates a statistical difference with  $p < 0.05$ .

the first matrix protein to be detected, 5 days after crystal deposition [62]. In human atherosclerotic plaques, it was recently reported that crystals are mainly covered by GAGs [39], suggesting that the production of aggrecan and GAGs represent an adaptive mechanism used by VSMCs in response to microcalcification in the plaques. Yet the aim of such an adaptive GAG deposition is obscure. Proteoglycans including aggrecan are up-regulated at sites of intimal hyperplasia in atherosclerotic plaques [63], where they may bind and retain apolipoprotein-B containing lipoproteins, and stimulate chronic inflammation and the accumulation of macrophages. Because of its large size and large number of GAG modification sites, aggrecan has been hypothesized to have the greatest affinity for lipoproteins of all of the intimal proteoglycans [63]. Alternatively, since aggrecan expression is stimulated by apatite crystals, we speculate that it may also play a role in VSMC trans-

differentiation into chondrocytes in atherosclerosis [4,5]. Aggrecan is indeed the predominant chondroitin sulfate proteoglycan expressed in growth plate cartilage, and mutations in the *Acan* gene are the cause of chondrodysplasias [30]. The absence of functional aggrecan in mice also leads to chondrodysplasia with chondrocytes failing to differentiate properly and mature towards hypertrophic cells [30]. In our opinion, the role of aggrecan in atherosclerotic plaque development merits particular attention.

Our study has nevertheless one limitation. Not all chondrocyte markers were increased in response to TNAP and crystals. If *Acan* and *Ocn* were significantly up-regulated by TNAP for instance, the expression of *Col10a1* was increased but did not reach significance, and the expression of *Col2a1* encoding type II collagen was not changed. It is therefore possible that in response to TNAP and crystals, VSMCs



differentiate into cells with an intermediate phenotype between VSMCs and chondrocytes. Such an intermediate differentiation may also be due to the nature of the two VSMC lines we used that do not perfectly mimic primary cells. This is plausible since TNAP inhibition in primary chondrocytes reduced the expression of all chondrocyte markers we have investigated. Moreover, the fact that TNAP-deficient mice have disorganized growth plates [64,65] strengthens the notion that TNAP is required for chondrocyte differentiation.

In conclusion, our results and interpretation fit quite well with the model recently built by Chatrou and collaborators [12]. They observed that microcalcifications were present before “osteochondrocytes” in human atherosclerotic plaques and hypothesized that they may be the cause and not the consequence of VSMC trans-differentiation [12]. They proposed that a loss of functional matrix Gla protein may be involved in triggering microcalcification. Alternatively, or additionally, we propose that TNAP activation by inflammatory cytokines in VSMCs [18–21], and the subsequent hydrolysis of PPi, also represents a particularly important factor inducing plaque calcification.

### Conflict of interests

None declared.

### Transparency document

The Transparency document associated with this article can be found, in the online version.

### Acknowledgments

Maya Fakhry is a recipient of a PhD scholarship from the Lebanese National Council for Scientific Research (CNRS-L) and the Lebanese university; the research was supported by CNRS-L grant number 05-06 2014. Monika Roszkowska is a recipient of a scholarship granted by the Ministry of Foreign Affairs and International Development of France “Doctorat en Cotutelle 2014–2017”. Polish-French cooperation was supported by PHC Polonium 2015/2016 no. 33540RG granted by the Ministry of Science and Higher Education of Poland and the Ministry of Foreign Affairs in France.

### References

- [1] A.P. Burke, A. Farb, G.T. Malcom, Y. Liang, J.E. Smialek, R. Virmani, Plaque rupture and sudden death related to exertion in men with coronary artery disease, *JAMA* 281 (10) (1999) 921–926.
- [2] R. Vliegenthart, M. Oudkerk, A. Hofman, H.H. Oei, W. van Dijck, F.J. van Rooij, J.C. Witteman, Coronary calcification improves cardiovascular risk prediction in the elderly, *Circulation* 112 (4) (2005) 572–577.
- [3] G. Pugliese, C. Iacobini, C. Blasetti Fantauzzi, S. Menini, The dark and bright side of atherosclerotic calcification, *Atherosclerosis* 238 (2) (2015) 220–230.
- [4] M.E. Rosenfeld, P. Polinsky, R. Virmani, K. Kauser, G. Rubanyi, S.M. Schwartz, Advanced atherosclerotic lesions in the innominate artery of the ApoE knockout mouse, *Arterioscler. Thromb. Vasc. Biol.* 20 (12) (2000) 2587–2592.
- [5] M. Rattazzi, B.J. Bennett, F. Bea, E.A. Kirk, J.L. Ricks, M. Speer, S.M. Schwartz, C.M. Giachelli, M.E. Rosenfeld, Calcification of advanced atherosclerotic lesions in the innominate arteries of ApoE-deficient mice: potential role of chondrocyte-like cells, *Arterioscler. Thromb. Vasc. Biol.* 25 (7) (2005) 1420–1425.
- [6] Y. Sun, C.H. Byon, K. Yuan, J. Chen, X. Mao, J.M. Heath, A. Javed, K. Zhang, P.G. Anderson, Y. Chen, Smooth muscle cell-specific runx2 deficiency inhibits vascular calcification, *Circ. Res.* 111 (5) (2012) 543–552.
- [7] F. Herisson, M.F. Heymann, M. Chétiveaux, C. Charrier, S. Battaglia, P. Pilet, T. Rouillon, M. Krempf, P. Lemarchand, D. Heymann, Y. Gouëffic, Carotid and femoral atherosclerotic plaques show different morphology, *Atherosclerosis* 216 (2) (2011) 348–354.
- [8] T. Aigner, D. Neureiter, V. Câmpean, S. Soder, K. Amann, Expression of cartilage-specific markers in calcified and non-calcified atherosclerotic lesions, *Atherosclerosis* 196 (1) (2008) 37–41.
- [9] H. Huang, R. Virmani, H. Younis, A.P. Burke, R.D. Kamm, R.T. Lee, The impact of calcification on the biomechanical stability of atherosclerotic plaques, *Circulation* 103 (8) (2001) 1051–1056.
- [10] S. Ehara, Y. Kobayashi, M. Yoshiyama, K. Shimada, Y. Shimada, D. Fukuda, Y. Nakamura, H. Yamashita, H. Yamagishi, K. Takeuchi, T. Naruko, K. Haze, A.E. Becker, J. Yoshikawa, M. Ueda, Spotty calcification typifies the culprit plaque in patients with acute myocardial infarction: an intravascular ultrasound study, *Circulation* 110 (22) (2004) 3424–3429.
- [11] R.B. Roijers, N. Debernardi, J.P. Cleutjens, L.J. Schurgers, P.H. Mutsaers, G.J. van der Vusse, Microcalcifications in early intimal lesions of atherosclerotic human coronary arteries, *Am. J. Pathol.* 178 (6) (2011) 2879–2887.
- [12] M.L. Chatrou, J.P. Cleutjens, G.J. van der Vusse, R.B. Roijers, P.H. Mutsaers, L.J. Schurgers, Intra-section analysis of human coronary arteries reveals a potential role for micro-calcifications in macrophage recruitment in the early stage of atherosclerosis, *PLoS One* 10 (11) (2015), e0142335.
- [13] Y. Vengrenyuk, S. Carlier, S. Xanthos, L. Cardoso, P. Ganatos, R. Virmani, S. Einav, L. Gilchrist, S. Weinbaum, A hypothesis for vulnerable plaque rupture due to stress-induced debonding around cellular microcalcifications in thin fibrous caps, *Proc. Natl. Acad. Sci. U. S. A.* 103 (40) (2006) 14678–14683.
- [14] A. Kelly-Arnold, N. Maldonado, D. Laudier, E. Aikawa, L. Cardoso, S. Weinbaum, Revisited microcalcification hypothesis for fibrous cap rupture in human coronary arteries, *Proc. Natl. Acad. Sci. U. S. A.* 110 (26) (2013) 10741–10746.
- [15] P. Lencel, P. Hardouin, D. Magne, Do cytokines induce vascular calcification by the mere stimulation of TNAP activity? *Med. Hypotheses* 75 (6) (2010) 517–521.
- [16] R. Buchet, J.L. Millán, D. Magne, Multisystemic functions of alkaline phosphatases, *Methods Mol. Biol.* 1053 (2013) 27–51.
- [17] L. Bessueille, D. Magne, Inflammation: a culprit for vascular calcification in atherosclerosis and diabetes, *Cell. Mol. Life Sci.* (2015) 2475–2489.
- [18] P. Lencel, S. Delplace, P. Pilet, D. Leterme, F. Miellot, S. Sourice, A. Caudrillier, P. Hardouin, J. Guicheux, D. Magne, Cell-specific effects of TNF- $\alpha$  and IL-1 $\beta$  on alkaline phosphatase: implication for syndesmophyte formation and vascular calcification, *Lab. Invest.* 91 (10) (2011) 1434–1442.
- [19] Y. Tintut, J. Patel, F. Parhami, L.L. Demer, Tumor necrosis factor- $\alpha$  promotes in vitro calcification of vascular cells via the cAMP pathway, *Circulation* 102 (21) (2000) 2636–2642.
- [20] A. Shioi, M. Katagi, Y. Okuno, K. Mori, S. Jono, H. Koyama, Y. Nishizawa, Induction of bone-type alkaline phosphatase in human vascular smooth muscle cells: roles of tumor necrosis factor- $\alpha$  and oncostatin M derived from macrophages, *Circ. Res.* 91 (1) (2002) 9–16.
- [21] H.L. Lee, K.M. Woo, H.M. Ryoo, J.H. Baek, Tumor necrosis factor- $\alpha$  increases alkaline phosphatase expression in vascular smooth muscle cells via MSX2 induction, *Biochem. Biophys. Res. Commun.* 391 (1) (2010) 1087–1092.
- [22] C.R. Sheen, P. Kuss, S. Narisawa, M.C. Yadav, J. Nigro, W. Wang, T.N. Chhea, E.A. Sergienko, K. Kapoor, M.R. Jackson, M.F. Hoylaerts, A.B. Pinkerton, W.C. O'Neill, J.L. Millán, Pathophysiological role of vascular smooth muscle alkaline phosphatase in medial artery calcification, *J. Bone Miner. Res.* (2015) 824–836.
- [23] M. Gosset, F. Berenbaum, S. Thirion, C. Jacques, Primary culture and phenotyping of murine chondrocytes, *Nat. Protoc.* 3 (8) (2008) 1253–1260.
- [24] A. Idelevich, Y. Rais, E. Monsonego-Ornan, Bone Gla protein increases HIF-1 $\alpha$ -dependent glucose metabolism and induces cartilage and vascular calcification, *Arterioscler. Thromb. Vasc. Biol.* 31 (9) (2011) e55–e71.
- [25] L. Bessueille, M. Fakhry, E. Hamade, B. Badran, D. Magne, Glucose stimulates chondrocyte differentiation of vascular smooth muscle cells and calcification: a possible role for IL-1 $\beta$ , *FEBS Lett.* (2015) 2797–2804.
- [26] M. Díez-Zaera, J.I. Díaz-Hernández, E. Hernández-Álvarez, H. Zimmermann, M. Díaz-Hernández, M.T. Miras-Portugal, Tissue-nonspecific alkaline phosphatase promotes axonal growth of hippocampal neurons, *Mol. Biol. Cell* 22 (7) (2011) 1014–1024.
- [27] K.W. Harder, P. Owen, L.K. Wong, R. Aebersold, I. Clark-Lewis, F.R. Jirik, Characterization and kinetic analysis of the intracellular domain of human protein tyrosine phosphatase beta (HPTP beta) using synthetic phosphopeptides, *Biochem. J.* 298 (Pt 2) (1994) 395–401.
- [28] A. Perrier, V. Dumas, M.T. Linossier, C. Fournier, P. Jurdic, A. Rattner, L. Vico, A. Guignandon, Apatite content of collagen materials dose-dependently increases pre-osteoblastic cell deposition of a cement line-like matrix, *Bone* 47 (1) (2010) 23–33.
- [29] J. Ding, O. Ghali, P. Lencel, O. Broux, C. Chauveau, J.C. Devedjian, P. Hardouin, D. Magne, TNF- $\alpha$  and IL-1 $\beta$  inhibit RUNX2 and collagen expression but increase alkaline phosphatase activity and mineralization in human mesenchymal stem cells, *Life Sci.* 84 (15–16) (2009) 499–504.
- [30] K.L. Lauing, M. Cortes, M.S. Domowicz, J.G. Henry, A.T. Baria, N.B. Schwartz, Aggrecan is required for growth plate cytoarchitecture and differentiation, *Dev. Biol.* 396 (2) (2014) 224–236.
- [31] R. Rosati, G.S. Horan, G.J. Pinero, S. Garofalo, D.R. Keene, W.A. Horton, E. Vuorio, B. de Crombrugge, R.R. Behringer, Normal long bone growth and development in type X collagen-null mice, *Nat. Genet.* 8 (2) (1994) 129–135.
- [32] N.K. Lee, H. Sowa, E. Hinoi, M. Ferron, J.D. Ahn, C. Confavreux, R. Dacquin, P.J. Mee, M.D. McKee, D.Y. Jung, Z. Zhang, J.K. Kim, F. Mauvais-Jarvis, P. Ducy, G. Karsenty, Endocrine regulation of energy metabolism by the skeleton, *Cell* 130 (3) (2007) 456–469.
- [33] K. Johnson, M. Polewski, D. van Etten, R. Terkeltaub, Chondrogenesis mediated by PPI depletion promotes spontaneous aortic calcification in NPP1 $^{-/-}$  mice, *Arterioscler. Thromb. Vasc. Biol.* 25 (4) (2005) 686–691.
- [34] R. Garimella, X. Bi, H.C. Anderson, N.P. Camacho, Nature of phosphate substrate as a major determinant of mineral type formed in matrix vesicle-mediated in vitro mineralization: an FTIR imaging study, *Bone* 38 (6) (2006) 811–817.
- [35] W.N. Addison, F. Azari, E.S. Sørensen, M.T. Kaartinen, M.D. McKee, Pyrophosphate inhibits mineralization of osteoblast cultures by binding to mineral, up-regulating osteopontin, and inhibiting alkaline phosphatase activity, *J. Biol. Chem.* 282 (21) (2007) 15872–15883.
- [36] S. Khoshniat, A. Bourguine, M. Julien, M. Petit, P. Pilet, T. Rouillon, M. Masson, M. Gatiou, P. Weiss, J. Guicheux, L. Beck, Phosphate-dependent stimulation of MGP

- and OPN expression in osteoblasts via the ERK1/2 pathway is modulated by calcium, *Bone* 48 (4) (2011) 894–902.
- [37] A.P. Sage, J. Lu, Y. Tintut, L.L. Demer, Hyperphosphatemia-induced nanocrystals up-regulate the expression of bone morphogenetic protein-2 and osteopontin genes in mouse smooth muscle cells in vitro, *Kidney Int.* 79 (4) (2011) 414–422.
- [38] D. Magne, G. Bluteau, C. Fauchoux, G. Palmer, C. Vignes-Colombeix, P. Pilet, T. Rouillon, J. Caverzasio, P. Weiss, G. Duculsi, J. Guicheux, Phosphate is a specific signal for ATDC5 chondrocyte maturation and apoptosis-associated mineralization: possible implication of apoptosis in the regulation of endochondral ossification, *J. Bone Miner. Res.* 18 (8) (2003) 1430–1442.
- [39] M.J. Duer, T. Frisčić, D. Proudfoot, D.G. Reid, M. Schoppert, C.M. Shanahan, J.N. Skepper, E.R. Wise, Mineral surface in calcified plaque is like that of bone: further evidence for regulated mineralization, *Arterioscler. Thromb. Vasc. Biol.* 28 (11) (2008) 2030–2034.
- [40] E. Biver, P. Hardouin, J. Caverzasio, The “bone morphogenic proteins” pathways in bone and joint diseases: translational perspectives from physiopathology to therapeutic targets, *Cytokine Growth Factor Rev.* 24 (1) (2013) 69–81.
- [41] E. Aikawa, M. Nahrendorf, J.L. Figueiredo, F.K. Swirski, T. Shtatland, R.H. Kohler, F.A. Jaffer, M. Aikawa, R. Weissleder, Osteogenesis associates with inflammation in early-stage atherosclerosis evaluated by molecular imaging in vivo, *Circulation* 116 (24) (2007) 2841–2850.
- [42] S.E. New, C. Goetsch, M. Aikawa, J.F. Marchini, M. Shibasaki, K. Yabusaki, P. Libby, C.M. Shanahan, K. Croce, E. Aikawa, Macrophage-derived matrix vesicles: an alternative novel mechanism for microcalcification in atherosclerotic plaques, *Circ. Res.* 113 (1) (2013) 72–77.
- [43] D.M. Schrijvers, G.R. De Meyer, M.M. Kockx, A.G. Herman, W. Martinet, Phagocytosis of apoptotic cells by macrophages is impaired in atherosclerosis, *Arterioscler. Thromb. Vasc. Biol.* 25 (6) (2005) 1256–1261.
- [44] H. Kono, K.L. Rock, How dying cells alert the immune system to danger, *Nat. Rev. Immunol.* 8 (4) (2008) 279–289.
- [45] D. Proudfoot, J.N. Skepper, L. Hegyi, M.R. Bennett, C.M. Shanahan, P.L. Weissberg, Apoptosis regulates human vascular calcification in vitro: evidence for initiation of vascular calcification by apoptotic bodies, *Circ. Res.* 87 (11) (2000) 1055–1062.
- [46] D. Estève, J. Galitzky, A. Bouloumié, C. Fonta, R. Buchet, D. Magne, Multiple functions of MSCA-1/TNAP in adult mesenchymal progenitor/stromal cells, *Stem Cells Int.* 2016 (2016) 1815982.
- [47] K. Štefková, J. Procházková, J. Pacherník, Alkaline phosphatase in stem cells, *Stem Cells Int.* 2015 (2015) 628368.
- [48] M. Murshed, D. Harmey, J.L. Millán, M.D. McKee, G. Karsenty, Unique coexpression in osteoblasts of broadly expressed genes accounts for the spatial restriction of ECM mineralization to bone, *Genes Dev.* 19 (9) (2005) 1093–1104.
- [49] M.D. Reikter, K. Zhang, A.S. Narayanan, S. Phan, M.A. Schork, D. Gordon, Type I collagen gene expression in human atherosclerosis. Localization to specific plaque regions, *Am. J. Pathol.* 143 (6) (1993) 1634–1648.
- [50] A. Abdelbaky, E. Corsini, A.L. Figueroa, S. Fontanez, S. Subramanian, M. Ferencik, T.J. Brady, U. Hoffmann, A. Tawakol, Focal arterial inflammation precedes subsequent calcification in the same location: a longitudinal FDG-PET/CT study, *Circ. Cardiovasc. Imaging* 6 (5) (2013) 747–754.
- [51] N.V. Joshi, A.T. Vesey, M.C. Williams, A.S. Shah, P.A. Calvert, F.H. Craighead, S.E. Yeoh, W. Wallace, D. Salter, A.M. Fletcher, E.J. van Beek, A.D. Flapan, N.G. Uren, M.W. Behan, N.L. Cruden, N.L. Mills, K.A. Fox, J.H. Rudd, M.R. Dweck, D.E. Newby, (18)F-fluoride positron emission tomography for identification of ruptured and high-risk coronary atherosclerotic plaques: a prospective clinical trial, *Lancet* (2013) 705–713.
- [52] J. Debray, L. Chang, S. Marquès, S. Pellet-Rostaing, D. Le Duy, S. Mebarek, R. Buchet, D. Magne, F. Popowycz, M. Lemaire, Inhibitors of tissue-nonspecific alkaline phosphatase: design, synthesis, kinetics, biomineralization and cellular tests, *Bioorg. Med. Chem.* (2013) 7981–7987.
- [53] S. Narisawa, D. Harmey, M.C. Yadav, W.C. O'Neill, M.F. Hoylaerts, J.L. Millán, Novel inhibitors of alkaline phosphatase suppress vascular smooth muscle cell calcification, *J. Bone Miner. Res.* 22 (11) (2007) 1700–1710.
- [54] C. Goetsch, J.D. Hutcheson, M. Aikawa, H. Iwata, T. Pham, A. Nykjaer, M. Kjolby, M. Rogers, T. Michel, M. Shibasaki, S. Hagita, R. Kramann, D.J. Rader, P. Libby, S.A. Singh, E. Aikawa, Sortilin mediates vascular calcification via its recruitment into extracellular vesicles, *J. Clin. Invest.* 126 (4) (2016) 1323–1336.
- [55] L. Hesse, K.A. Johnson, H.C. Anderson, S. Narisawa, A. Sali, J.W. Goding, R. Terkeltaub, J.L. Millan, Tissue-nonspecific alkaline phosphatase and plasma cell membrane glycoprotein-1 are central antagonistic regulators of bone mineralization, *Proc. Natl. Acad. Sci. U. S. A.* 99 (14) (2002) 9445–9449.
- [56] F. Rutsch, S. Vaingankar, K. Johnson, I. Goldfine, B. Maddux, P. Schauer, H. Kalhoff, K. Sano, W.A. Boisvert, A. Superti-Furga, R. Terkeltaub, PC-1 nucleoside triphosphate pyrophosphohydrolase deficiency in idiopathic infantile arterial calcification, *Am. J. Pathol.* 158 (2) (2001) 543–554.
- [57] W.C. O'Neill, K.A. Lomashvili, H.H. Malluche, M.C. Faugere, B.L. Riser, Treatment with pyrophosphate inhibits uremic vascular calcification, *Kidney Int.* 79 (5) (2011) 512–517.
- [58] B.L. Riser, F.C. Barreto, R. Rezg, P.W. Valaitis, C.S. Cook, J.A. White, J.H. Gass, J. Maizel, L. Louvet, T.B. Drueke, C.J. Holmes, Z.A. Massy, Daily peritoneal administration of sodium pyrophosphate in a dialysis solution prevents the development of vascular calcification in a mouse model of uraemia, *Nephrol. Dial. Transplant.* 26 (10) (2011) 3349–3357.
- [59] P. Nahar-Gohad, N. Gohad, C.C. Tsai, R. Bordia, N. Vyavahare, Rat aortic smooth muscle cells cultured on hydroxyapatite differentiate into osteoblast-like cells via BMP-2-SMAD-5 pathway, *Calcif. Tissue Int.* 96 (4) (2015) 359–369.
- [60] M.R. Urist, Bone: formation by autoinduction, *Science* 150 (3698) (1965) 893–899.
- [61] M.R. Urist, B.S. Strates, Bone morphogenetic protein, *J. Dent. Res.* 50 (6) (1971) 1392–1406.
- [62] Z. Khavandgar, H. Roman, J. Li, S. Lee, H. Vali, J. Brinckmann, E.C. Davis, M. Murshed, Elastin haploinsufficiency impedes the progression of arterial calcification in MGP-deficient mice, *J. Bone Miner. Res.* 29 (2) (2014) 327–337.
- [63] P. Talusan, S. Bedri, S. Yang, T. Kattapuram, N. Silva, P.J. Roughley, J.R. Stone, Analysis of intimal proteoglycans in atherosclerosis-prone and atherosclerosis-resistant human arteries by mass spectrometry, *Mol. Cell. Proteomics* 4 (9) (2005) 1350–1357.
- [64] J. Liu, H.K. Nam, C. Campbell, K.C. Gasque, J.L. Millán, N.E. Hatch, Tissue-nonspecific alkaline phosphatase deficiency causes abnormal craniofacial bone development in the *Alpl*( $-/-$ ) mouse model of infantile hypophosphatasia, *Bone* 67 (2014) 81–94.
- [65] S. Narisawa, N. Fröhlander, J.L. Millán, Inactivation of two mouse alkaline phosphatase and establishment of a model of infantile hypophosphatasia, *Dev. Dyn.* 208 (3) (1997) 432–446.



## Collagen promotes matrix vesicle-mediated mineralization by vascular smooth muscle cells

Monika Roszkowska<sup>a,b</sup>, Agnieszka Strzelecka-Kiliszek<sup>a</sup>, Laurence Bessueille<sup>b</sup>, René Buchet<sup>b</sup>, David Magne<sup>b</sup>, Sławomir Pikula<sup>a,\*</sup>

<sup>a</sup> Laboratory of Biochemistry of Lipids, Department of Biochemistry, Nencki Institute of Experimental Biology of Polish Academy of Sciences, Warsaw, Poland

<sup>b</sup> Univ Lyon, University Lyon 1, ICBMS, UMR CNRS 5246, F-69622 Lyon, France

### ARTICLE INFO

#### Keywords:

Annexins  
Atherosclerosis  
Matrix vesicles  
Tissue-nonspecific alkaline phosphatase  
Vascular calcification  
Vascular smooth muscle cells

### ABSTRACT

Vascular calcification (VC) is a hallmark of atherosclerotic plaques. Calcification of advanced plaques shares common features with endochondral ossification of long bones and appears to be protective. On the other hand, microcalcification of early plaques, which is poorly understood, is thought to be harmful. Tissue-nonspecific alkaline phosphatase (TNAP) and collagen are the two proteins necessary for physiological mineralization. Here, we demonstrate the presence of membrane-bound TNAP, detected by immunofluorescence, that seems to form clusters on the plasma membrane of vascular smooth muscle cells (VSMCs) cultured in mineralizing conditions. We observed that TNAP activity and mineralization were increased when VSMCs were cultured in the presence of ascorbic acid (AA) and  $\beta$ -glycerophosphate ( $\beta$ -GP). Increased TNAP activity was observed in whole cell lysates, total membrane fractions and, more particularly, in matrix vesicles (MVs). We have shown that TNAP-enriched MVs released from VSMCs subjected to collagenase contained more apatite-like mineral than the less TNAP-rich/TNAP-enriched vesicles isolated without collagenase treatment. These results suggest a role for collagen in promoting calcification induced by TNAP in atherosclerotic plaques.

### 1. Introduction

It has been known for decades that advanced atherosclerotic plaques undergo endochondral-like ossification resulting in formation of macrocalcifications, which in advance lesions strongly resemble bone tissue. Ossified plaques consist of carbonated apatite associated with collagen, very similar in organization and composition to the crystals formed by cartilage growth plate [1]. More recently, microcalcifications, measuring  $< 10 \mu\text{m}$  in diameter, have been observed within the fibrous caps of early lesions, before the appearance of chondrocyte or osteoblast phenotypes in vascular smooth muscle cells (VSMCs) within the plaque [2]. An interesting study revealed that nearly all fibrous caps contain microcalcifications, and that those with a diameter above  $5 \mu\text{m}$  are particularly harmful [3]. Moreover, based on *in silico* analysis, it was proposed that microcalcifications are particularly harmful when located in a thin fibrous cap [4]. Finally, the culprit segments of vessels of acute myocardial infarction patients generally contain such microcalcifications, whereas those of stable angina pectoris patients contain macrocalcifications [5].

Deciphering when and where microcalcification begins in atherosclerotic plaques is therefore crucial. Two proteins appear to be

necessary for normal mineralization: a fibrillar collagen and TNAP [6]. VSMCs normally secrete type I collagen. Tissue-nonspecific alkaline phosphatase (TNAP) overexpression in VSMCs *in vitro* and *in vivo* triggers vascular calcification [7–9]. We therefore aimed at determining the molecular mechanisms of VSMC mediated mineralization, with a particular focus on collagen and TNAP.

TNAP is an enzyme playing a key role during physiological mineralization mediated by chondrocytes and osteoblasts that deposit calcium phosphate crystals in the extracellular matrix (ECM) [10–12]. TNAP regulates mineralization by hydrolyzing a constitutive mineralization inhibitor - inorganic pyrophosphate ( $\text{PP}_i$ ) [13].  $\text{PP}_i$  is a small molecule that binds to the arising calcium phosphate crystals and prevents further incorporation of phosphate [14]. Early stages of mineralization take place in nanostructures called matrix vesicles (MVs) that are released by mineralizing cells and serve as nucleation sites for apatite synthesis [15].

Besides TNAP, other proteins may play an important role in calcification. For instance, annexins, the calcium- and phospholipid-binding proteins, are engaged in calcium homeostasis of mineralizing cells and in the influx of  $\text{Ca}^{2+}$  to MVs [16]. The large variety of annexins present in MVs and their ability to bind to different sides of biological

\* Corresponding author.

E-mail address: [s.pikula@nencki.gov.pl](mailto:s.pikula@nencki.gov.pl) (S. Pikula).

<https://doi.org/10.1016/j.jinorgbio.2018.05.007>

Received 1 February 2018; Received in revised form 20 April 2018; Accepted 16 May 2018

Available online 18 May 2018

0162-0134/ © 2018 Elsevier Inc. All rights reserved.

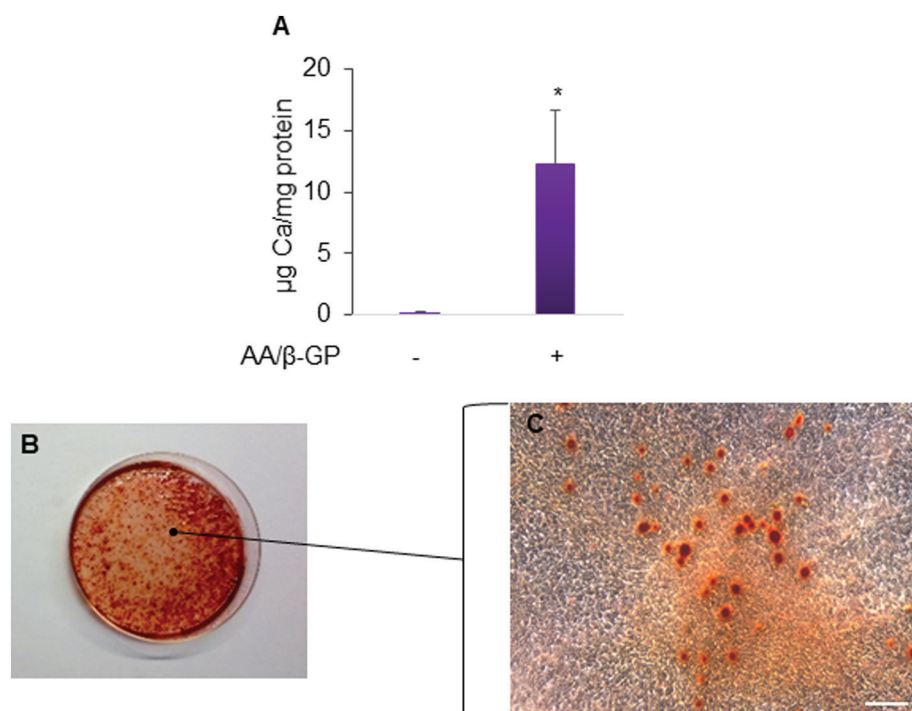


**Fig. 1.** Mineralization of MOVAS. A) Total calcium concentration measured by calcium colorimetric assay in MOVAS cells after 21 days of osteogenic stimulation in the presence of  $50 \mu\text{g mL}^{-1}$  AA and 10 mM  $\beta$ -GP,  $n = 4 \pm \text{SEM}$ . B) Calcium deposits produced by MOVAS stained with Alizarin Red S after 21 days of stimulation for mineralization in the presence of  $50 \mu\text{g mL}^{-1}$  AA and 10 mM  $\beta$ -GP, C) microscopic view of calcium deposits produced by trans-differentiated MOVAS taken by Zeiss Axiovert light microscope at  $100\times$  magnification, scale bar -  $100 \mu\text{m}$ . \* indicates a statistical difference with  $p < 0.05$ .

membranes suggest that they serve different functions during the mineralization process [17]. Initiation of mineralization during endochondral ossification is a multistep process that correlates with specific interactions of Annexin A5 (AnxA5) and collagens [18]. In addition, lack of AnxA6 in MVs, which initiate the mineralization process in growth plate cartilage, resulted in reduced TNAP activity and  $\text{Ca}^{2+}$  and  $\text{P}_i$  content and in an inability to form apatite-like crystals *in vitro* [19].

Sortilin is a protein that has been recently characterized as a key regulator of vascular cell calcification due to its capacity to load TNAP into extracellular vesicles [20,21]. Interestingly, mice deficient in the gene encoding this protein, *Sort1*, have decreased arterial calcification while normal bone formation is not affected.

There are several reports indicating that MVs are necessary for the progression of smooth muscle cell calcification [22–25]. Here we further delineate the localization of TNAP activity in VSMCs and in MVs and determine the requirement of collagen for the ability of MVs to calcify.

## 2. Materials and methods

### 2.1. Cell culture and treatment

Murine MOVAS VSMC cell line was purchased from ATCC (Molsheim, France). The cells were routinely cultured in Dulbecco's Modified Eagle Medium (DMEM) containing  $4.5 \text{ g L}^{-1}$  glucose and supplemented with 10% fetal bovine serum (FBS),  $100 \text{ U mL}^{-1}$  penicillin,  $100 \mu\text{g mL}^{-1}$  streptomycin, 20 mM 4-(2-hydroxyethyl)-1-piperazineethanesulfonic acid (HEPES) and 2 mM L-glutamine at  $37^\circ\text{C}$  in a humidified atmosphere containing 5%  $\text{CO}_2$ . MOVAS cells were seeded at a density of  $4000 \text{ cells cm}^{-2}$ . At confluence, trans-differentiation into mineralization-competent cells was induced by cell treatment with  $50 \mu\text{g mL}^{-1}$  ascorbic acid (AA, Sigma) and 10 mM  $\beta$ -glycerophosphate ( $\beta$ -GP, Sigma).

### 2.2. Immunofluorescence

To analyze TNAP, AnxA2, AnxA6 and cholesterol localization in

MOVAS, the cells were seeded at low concentration ( $1000 \text{ cells cm}^{-2}$ ) on coverslips coated with  $30 \mu\text{g mL}^{-1}$  Collagen Type I from rat tail (Sigma) and cultured in the presence of AA and  $\beta$ -GP for 1–4 days to initiate trans-differentiation. The cells were washed with PBS and fixed with 3% paraformaldehyde for 20 min at room temperature (RT). After washing with PBS, the cells were incubated with 50 mM  $\text{NH}_4\text{Cl}$  in PBS for 10 min at RT. In the case of AnxA2 and AnxA6, permeabilization step was included using 0.1% Triton X-100 in PBS for 5 min on ice. Afterwards, the cells were washed with TBS and subjected to blocking stage (5% FBS in TBS) for 1 h. The samples were incubated for 1.5 h at RT with rabbit anti-TNAP, mouse anti-AnxA2 or mouse anti-AnxA6 primary antibody (Abcam) prepared in 0.5% FBS in TBS supplemented with 0.05% Tween (TBST). Then, the cells were washed several times with TBST and incubated for 1 h at RT with anti-mouse Alexa Fluor 488 or anti-rabbit Alexa Fluor 594 secondary antibody prepared in 0.5% FBS in TBST. For visualization of cholesterol, the cells were incubated with filipin (Sigma) at the concentration of  $25 \mu\text{g mL}^{-1}$ . After extensive washing several times with TBST and once in TBS, coverslips were mounted with Mowiol 4–88 (Calbiochem), supplemented with 1,4-diazabicyclo[2.2.2]octane (DABCO, Sigma) on microscope slides. Images were taken by Zeiss AxioObserver Z.1 fluorescence microscope at the  $630\times$  magnification with appropriate fluorescent filter.

### 2.3. Isolation of total membranes and MVs

Membrane fractions were isolated according to Briolay and collaborators [26]. Briefly, MOVAS cells ( $25 \times 10^6$  cells) were disrupted in a Potter homogenizer (40 strokes) on ice in a TNE buffer consisting of 25 mM Tris-HCl, 150 mM NaCl and 5 mM EDTA (pH 7.5), supplemented with  $10 \mu\text{g mL}^{-1}$  of protease inhibitor cocktail (Sigma). The homogenate was then centrifuged at 900g for 10 min at  $4^\circ\text{C}$ . The supernatant was collected and then centrifuged at  $100,000\text{g}$  for 45 min at  $4^\circ\text{C}$  in an Optima L-100 XP ultracentrifuge (Beckman Coulter). After ultracentrifugation, the pellet containing crude membrane fraction (plasma membrane and cytoplasmic vesicular structures) was resuspended in  $200 \mu\text{L}$  of TNE buffer.

Isolation of VSMC-derived vesicles was performed according to the procedures described earlier [22,27]. The vesicles isolated from culture



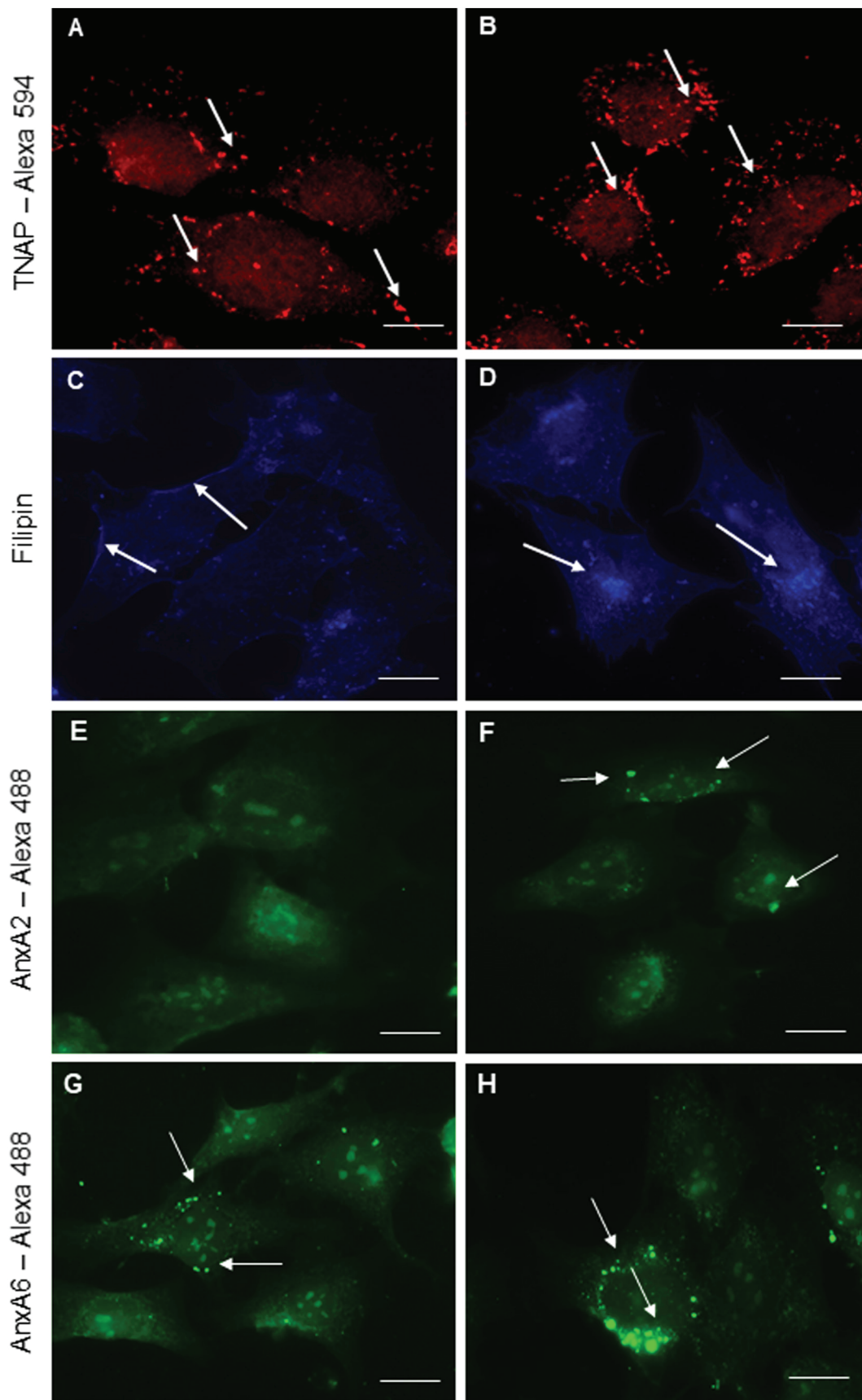
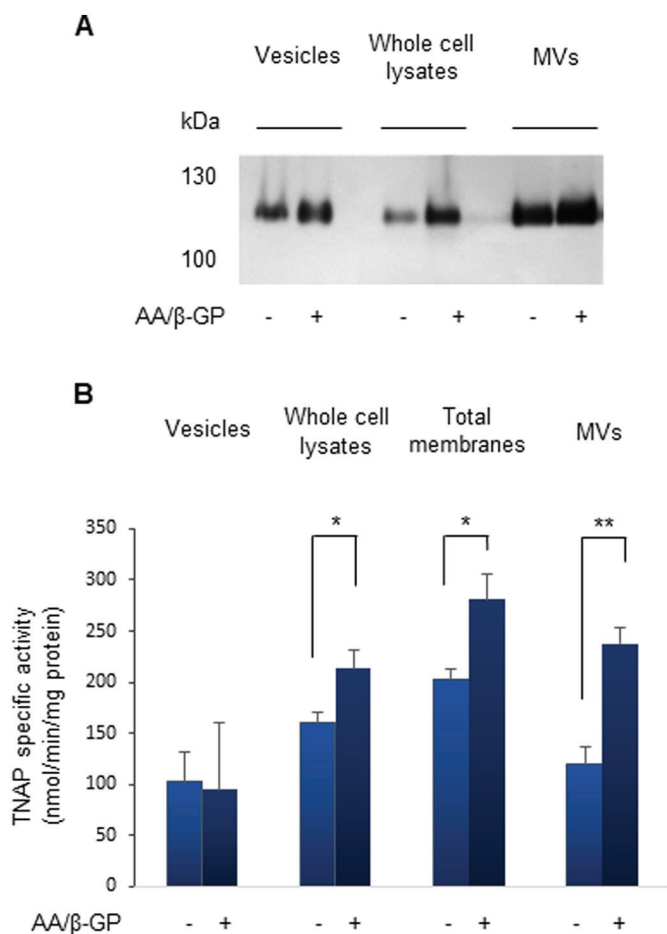


Fig. 2. TNAP, cholesterol and annexin localization in MOVAS. TNAP localization in MOVAS in MOVAS grown on collagen-coated coverslips (A, B, arrows). TNAP was immunostained with anti-TNAP primary antibody conjugated with Alexa Fluor 594 secondary antibody. Cholesterol was visualized by staining with filipin (C, D arrows) whereas AnxA2 (F, arrows) and AnxA6 (G, H, arrows) were immunostained with anti-AnxA2 and anti-AnxA6 primary antibodies, respectively, both conjugated with Alexa Fluor 488 secondary antibody. Cells were cultured in the presence (B, D, F, H) or absence (A, C, E, G) of  $50 \mu\text{g mL}^{-1}$  AA and  $10 \text{ mM } \beta\text{-GP}$  for 1–4 days. Magnification  $630\times$ , scale bar –  $10 \mu\text{m}$ .



**Fig. 3.** TNAP activity in different fractions of MOVAS cells and extracellular vesicles. (A) TNAP activity in whole cell lysates (WCLs), total membrane fractions as well as vesicles and MVs of non-differentiated (–AA/β-GP) or trans-differentiated (+AA/β-GP) MOVAS was assessed on the gel after electrophoresis using the NBT/BCIP method. (B) TNAP specific activity was measured based on p-nitrophenol hydrolysis in different fractions of MOVAS and in collagen-attached and collagen-free extracellular vesicles,  $n = 3 \pm \text{SEM}$ . \* indicates a statistical difference with  $p < 0.05$ ; \*\* indicates a statistical difference with  $p < 0.01$ .

medium without collagenase digestion were referred to as ‘collagen-free vesicles’, whereas collagen-attached vesicles obtained after collagenase digestion were called ‘MV’s’.  $1 \times 10^8$  of MOVAS cells were seeded on 100 mm culture dishes. At confluence, the cells were cultured for 21 days in the presence or absence of osteogenic factors, AA and β-GP. Afterwards, the culture medium was collected, centrifuged ( $1000 \times g$ , 30 min,  $4^\circ\text{C}$ , to remove apoptotic bodies) and subjected to ultracentrifugation ( $100,000 \times g$ , 30 min,  $4^\circ\text{C}$ ). The pellet containing vesicles was resuspended in synthetic cartilage lymph (SCL, pH 7.4), composed of 100 mM NaCl, 12.7 mM KCl, 1.42 mM  $\text{NaH}_2\text{PO}_4$ , 1.83 mM  $\text{NaHCO}_3$ , 0.57 mM  $\text{MgCl}_2$ , 0.57 mM  $\text{Na}_2\text{SO}_4$ , 5.55 mM D-glucose, 63.5 mM sucrose, and 16.5 mM HEPES and stored at  $-20^\circ\text{C}$  [28].

To obtain the fraction of collagen-attached vesicles, so-called MVs, the cells were rinsed with PBS and incubated in digestion buffer containing  $0.5 \text{ mg mL}^{-1}$  collagenase from *Clostridium histolyticum* (Sigma), 120 mM NaCl, 10 mM KCl, 250 mM sucrose and 20 mM Tris-HCl pH 7.4 for 3 h at  $37^\circ\text{C}$ . The cells were scraped, centrifuged ( $800 \times g$ , 30 min,  $4^\circ\text{C}$ , to remove cell debris) and subjected to ultracentrifugation ( $30,000 \times g$ , 30 min,  $4^\circ\text{C}$ , to separate basolateral membranes and microsomes). The supernatant was ultracentrifuged ( $250,000 \times g$ , 30 min,  $4^\circ\text{C}$ ) to collect the vesicles. The pellet containing MVs was resuspended in SCL and stored at  $-20^\circ\text{C}$ .

#### 2.4. Analytical methods

Calcium deposition was determined by alizarin red staining. Briefly, cells were washed with PBS and incubated with 2% Alizarin Red S (ARS, pH 4.2, Sigma) for 5 min at RT. After several washes, the photos were taken with a Zeiss Axiovert 40C light microscope.

Total calcium concentration was measured by a colorimetric calcium assay. The cells were washed with PBS and incubated overnight in 0.6 M HCl at RT. Then, the supernatants were collected. After decalcification, cells were washed three times with PBS, solubilized with 0.1 N NaOH/0.1% SDS and the collected supernatants were incubated for 5 min with 2-amino-2-methyl-1-propanol and o-cresolphthalein complexone reagent. Absorbance was measured at 570 nm. The protein content was determined by a Bi-Cinchoninic Acid (BCA) Protein Assay (Thermo Scientific). The calcium content in the cell layer was normalized to protein content.

For determination of TNAP activity based on the amount of p-nitrophenol (pNP) released after dephosphorylation of p-nitrophenyl phosphate (pNPP), the cells were collected in 0.1% Triton X-100 and disrupted by sonication ( $2 \times 10 \text{ s}$ , 20% power) using a S-250D digital sonifier (Branson Ultrasonic). Then, cell lysates were centrifuged ( $500 \times g$ , 5 min,  $4^\circ\text{C}$ ). Each supernatant was incubated with Alkaline Phosphatase Yellow (pNPP) Liquid Substrate (Sigma) at  $37^\circ\text{C}$  and the absorbance was measured at 450 nm in a Spectra Max M5e multi-detection reader (Molecular Devices). TNAP specific activity was expressed as nmoles of p-nitrophenol (pNP) formed per min and normalized relative to protein amount assessed by the BCA Protein Assay (Thermo Scientific).

#### 2.5. Nitroblue tetrazolium and bromo-chloro-indolyl phosphate (NBT/BCIP) method

The samples were prepared in mild denaturing conditions, in a buffer containing 60 mM Tris-HCl pH 6.8 and 2% SDS. Samples containing  $10 \mu\text{g}$  protein were loaded onto 7.5% SDS–polyacrylamide gels. After electrophoresis, the gels were incubated in a buffer composed of 100 mM Tris-HCl pH 9.0, 150 mM NaCl, 1 mM  $\text{MgCl}_2$ ,  $33 \mu\text{g mL}^{-1}$  nitroblue tetrazolium (NBT, Promega) and  $16.5 \mu\text{g mL}^{-1}$  bromo-chloro-indolyl phosphate (BCIP, Promega) at  $37^\circ\text{C}$  until the bands became clearly visible. The gels were photographed using InGenius LHR Gel Imaging System (Syngene).

#### 2.6. Transmission electron microscopy (TEM) and X-ray microanalysis (TEM-EDX)

Cell cultures were washed in PBS and fixed with 5 mL of 3% paraformaldehyde/1% glutaraldehyde mixture in 100 mM sodium phosphate buffer pH 7.2 for 1 h at RT. After washing, samples were postfixed with 2 mL of 1% osmium tetroxide in 100 mM sodium phosphate buffer, pH 7.2, for 20 min at RT in the dark. Then, the samples were dehydrated in a graded ethanol solution series at RT: 25% for 5 min, 50% for 10 min, 75% for 15 min, 90% for 20 min and finally in absolute ethanol once for 30 min and then for 12 h. The cells were mechanically scraped and centrifuged at  $130 g$  for 1 min. Pellets were suspended and incubated for 30 min at RT in mixtures of the LR White resin (Polysciences Inc.)/absolute ethanol at volume ratios of 1: 2 and 1: 1. Finally, samples were infiltrated twice with pure LR White resin for 1 h at RT, moved to gelatin capsules and polymerized at  $56^\circ\text{C}$  for 48 h. Sections ( $700 \text{ \AA}$ ) were cut using an LKB Nova ultramicrotome and placed on formvar coated and carbon-labelled 300 Mesh nickel grids (Agar Scientific Ltd.).

Suspensions of collagen-free vesicles or MVs were dropped on nickel grids. The sample-covered grids were dried for 30 min at RT. Both vesicle fractions and cell slices were negatively stained with 2.5% uranyl acetate solution in ethanol for 15 min at RT, protected from light. Finally, the grids were rinsed with 50% ethanol, deionized  $\text{H}_2\text{O}$  and dried for 24 h. Prepared fractions were observed under a JEM-1400



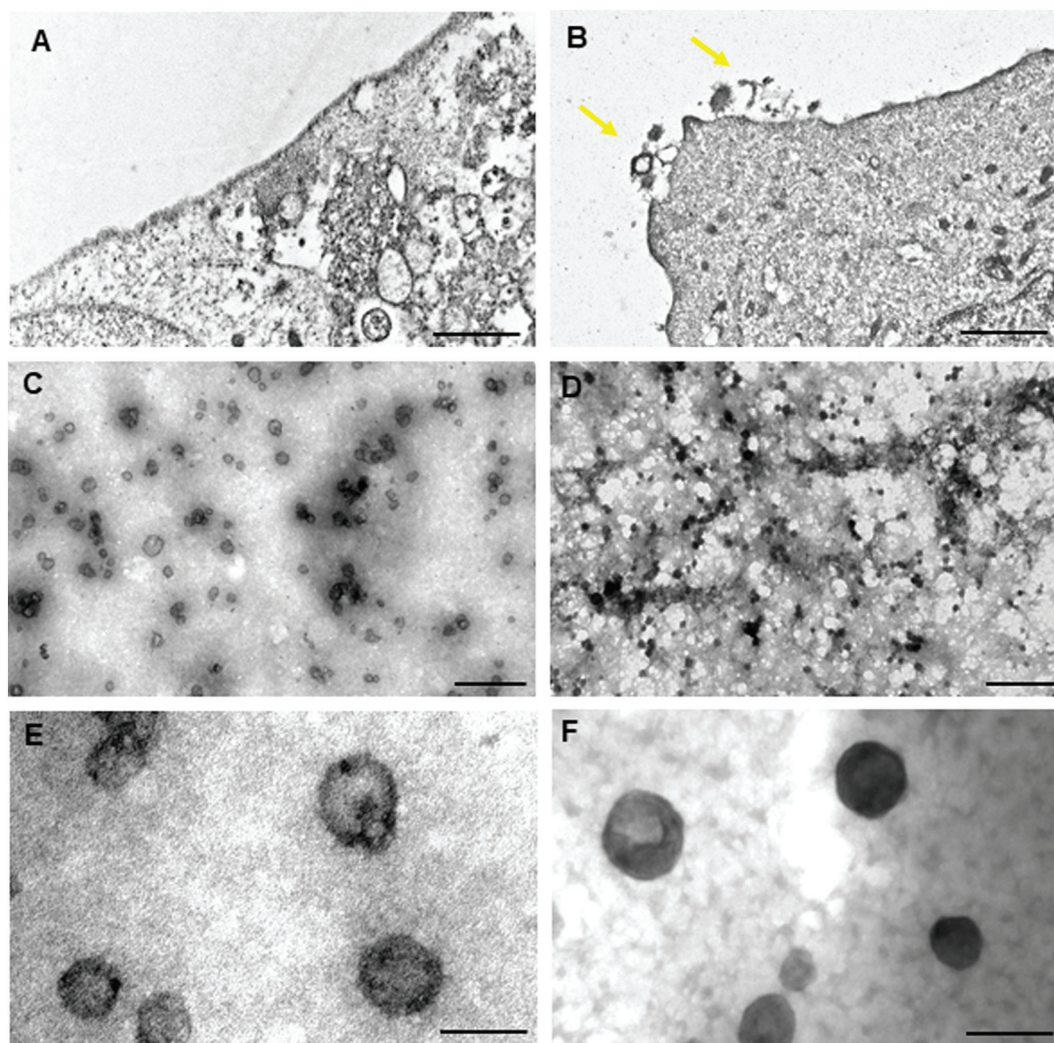


**Fig. 4.** Ultrastructure of MOVAS and extracellular vesicles. MOVAS morphology analyzed after 4 days of stimulation in the presence (B) or absence (A) of 50 µg/ml AA and 10 mM β-GP. Collagen-free MVs (C, E) and collagen-attached MVs obtained after collagenase digestion (D, F). Both fractions of vesicles were isolated from MOVAS by differential ultracentrifugation after 21 days of stimulation in the presence of 50 µg mL<sup>-1</sup> AA and 10 mM β-GP. TEM images were taken after negative staining. (A, B) magnification 15,000×, scale bar – 2 µm; (C, D) magnification 50,000×, scale bar - 500 nm; (E, F) magnification 300,000×, scale bar - 100 nm.

transmission electron microscope (TEM, JEOL Co.) equipped with an energy-dispersive full range X-ray microanalysis system (EDS INCA Energy TEM, Oxford Instruments), tomographic holder and 11 Megapixel TEM Camera MORADA G2 (EMSIS GmbH). Images were taken at magnifications between 40,000× and 150,000×. Point measurements of MV chemical components were performed using X-ray microanalysis based on the amount of elements: carbon (C), oxygen (O), calcium (Ca) and phosphorus (P) expressed as atomic % of the sum of all elements of the Periodic Table detected in the sample (expressed as 100%). After performing spectral and compositional analysis, Ca/P ratio was calculated for each point measurement. Mapping of Ca and P distribution in collagen-free or MVs was performed by use of EDX INCA Software.

### 2.7. Statistical analysis

For statistical analysis, a two tailed un-paired Student *t*-test was applied using Origin Software.

## 3. Results

### 3.1. Ability of MOVAS cells to mineralize

We checked if, in our hands, MOVAS cells had the ability to

mineralize, as previously published [29]. After 21 days of trans-differentiation we observed extensive calcium deposition in trans-differentiated cells (Fig. 1B, C). Moreover, calcium content determined by colorimetric assay was significantly increased in trans-differentiated cells (Fig. 1A). Thus, we confirmed that MOVAS cells are able to mineralize in a typical osteogenic medium.

### 3.2. Localization of TNAP

In cells, TNAP is anchored to the plasma membrane and to the outer layer of the matrix vesicle membrane *via* glycosylphosphatidylinositol (GPI) [10]. There were several findings on localization of TNAP in murine and human bone tissue [30–32]. However, TNAP subcellular localization in smooth muscle cells, especially with respect to the apical side of cells and to collagen, is poorly characterized. According to our observations, subcellular location of TNAP in MOVAS is similar as in the case of typical mineralizing cells. After staining TNAP with fluorescent antibody we observed a specific signal on the cell membrane in cells stimulated for mineralization and cultured on the surface of collagen (Fig. 2A, B). TNAP-enriched clusters seen in the apical region (Fig. 2B) of trans-differentiated MOVAS are possible sites of MV biogenesis. We observed accumulation of cholesterol in similar localization, suggesting a possible role of cholesterol-enriched lipid rafts in the

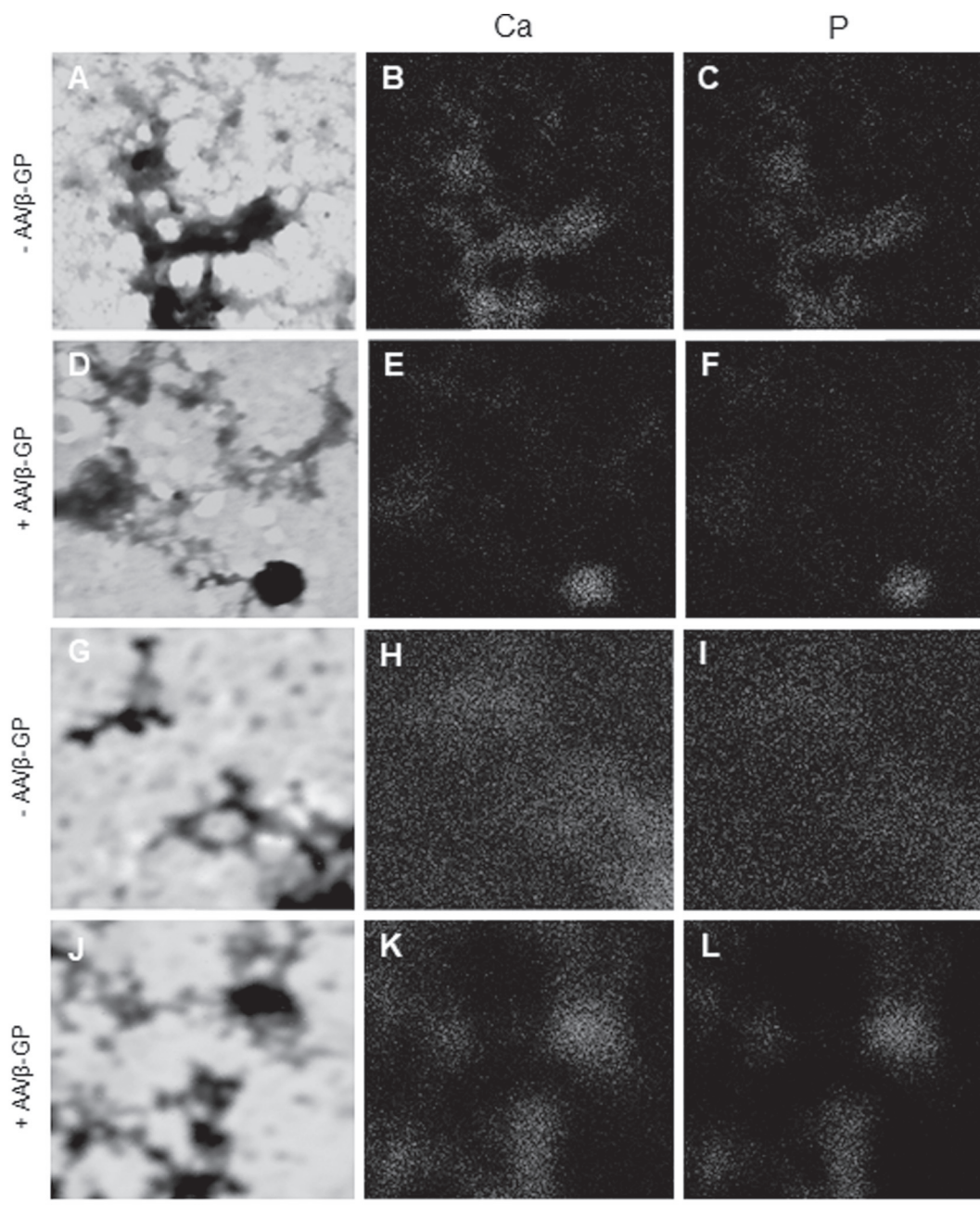


**Fig. 5.** Maps of vesicle and MV chemical composition. TEM view of vesicle (A, D) and MV clusters (G, J). The maps of calcium (Ca) (B, E, H, K) and phosphate (P) (C, F, I, L) distribution in MVs of non-differentiated (–AA/β-GP) or trans-differentiated MOVAS (+AA/β-GP). Magnification 15,000 $\times$ , scale bar – 500 nm.

process of MV sorting and release (Fig. 2D) [33]. Moreover, we detected annexins, AnxA2 (Fig. 2F) and AnxA6 (Fig. 2H), in a perinuclear region of trans-differentiated MOVAS. However, we did not detect annexins in the proximity of the plasma membrane, most probably due to the lack of additional stimulation by calcium.

### 3.3. Specific activity of TNAP in membrane fractions, vesicles and MVs

Collagen-free MVs are vesicles released by cells to the culture medium, whereas collagen-attached MVs can be isolated only after collagenase digestion of cells and ECM produced by them.

Using the NBT/BCIP method, we observed that TNAP was active in MOVAS whole cell lysates (WCLs) and both in released vesicles and in MVs (Fig. 3A). TNAP activity was increased in all fractions of MOVAS subjected to osteogenic treatment (addition of 50  $\mu\text{g mL}^{-1}$  AA and

10 mM  $\beta$ -GP) as compared to non-treated cells (Fig. 3A). Using pNPP as substrate, we observed significant increase in TNAP specific activity in WCLs, total membranes and in MVs (by 2.5-fold) in treated MOVAS as compared to untreated cells, in contrast to vesicles in which TNAP activity remained low (Fig. 3B). Thus, our observations are analogous to the results of Chen and collaborators reporting that VSMC-derived MVs had significantly increased ability to calcify on collagen compared with other secreted vesicles [22] and with the previous findings on MVs isolated from growth plate cartilage showing that association of MVs released by mineralizing cells with collagen is an important step in mineral expansion [18,34].

### 3.4. Vesicle formation from MOVAS cells

MOVAS cells produced vesicular structures both in the absence and



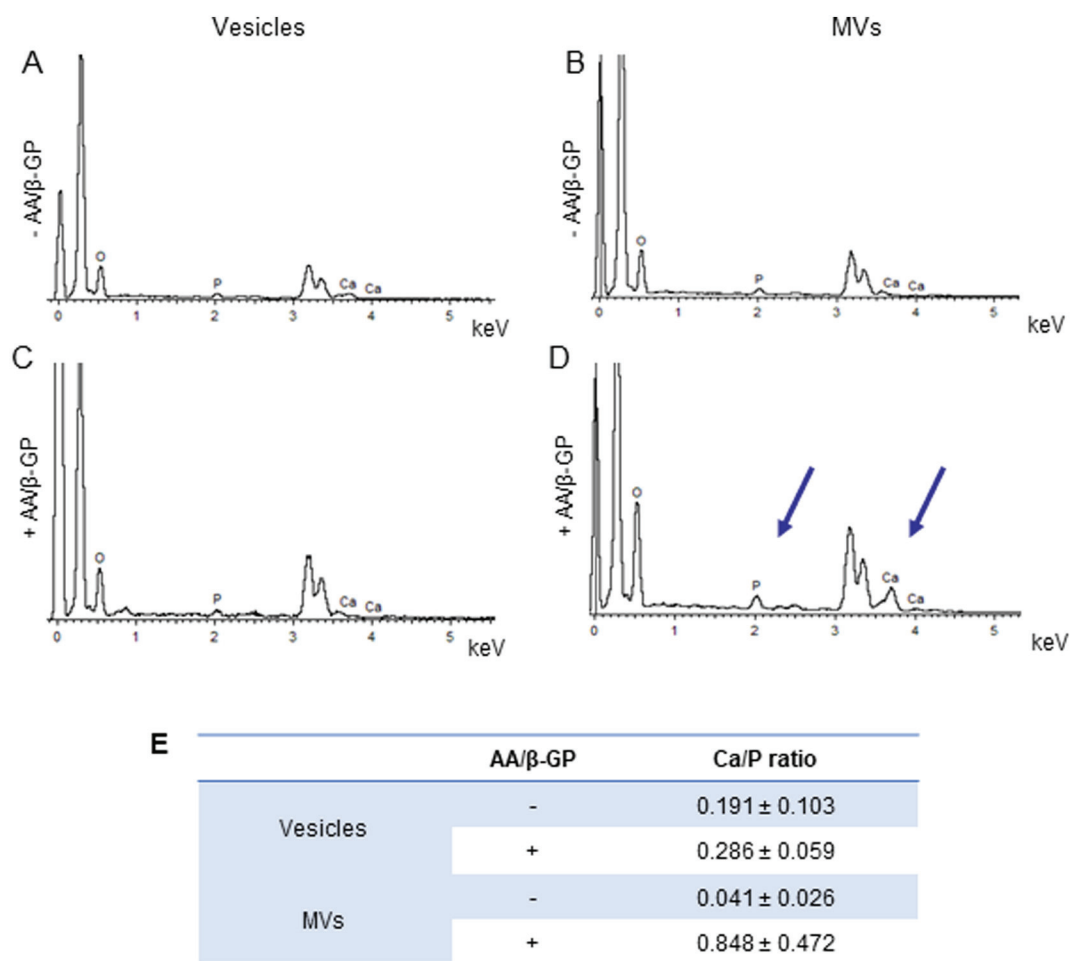


**Fig. 6.** Chemical composition of crystals produced by vesicles and MVs derived from MOVAS. Representative spectra obtained by TEM X-ray microanalysis of vesicles (A, C) and MVs (B, D). Vesicles and MVs were isolated from non-differentiated (–AA/β-GP) or trans-differentiated MOVAS (+AA/β-GP). Increased levels of calcium and phosphate are indicated (D, arrows). Ca/P ratios of vesicles and MVs are summarized in the table (E);  $n = 3$ . ± SEM.

presence of 50 μg/mL AA and 10 mM β-GP (Fig. 4A and B). We observed vesicles budding from the plasma membrane of MOVAS stimulated for mineralization (Fig. 4B, arrows). Concerning vesicle size, both fractions contained vesicles between 30 and 100 nm in diameter *i.e.*, smaller than MVs isolated from growth plate chondrocytes or from osteoblast-like Saos-2 cells that are around 100–300 nm in diameter [15]. Our observations concerning murine vesicles fit quite well with the findings of Reynolds and collaborators who determined that human VSMC-derived vesicles were < 150 nm in diameter [35]. Moreover, looking at TEM images, it is noticeable that the fractions of collagen-attached vesicles, so-called MVs (Fig. 4D, F) are enriched in the dark phase of mineral, in contrast to collagen-free vesicles collected from the culture medium (Fig. 4C, E).

### 3.5. Chemical composition of vesicles

We carried out mapping of chemical elements and TEM X-ray microanalysis of vesicle fractions. We detected Ca and P in both types of vesicles, collagen-free and MVs, however, those elements perfectly colocalized only in MVs isolated after collagenase treatment (Fig. 5 K, L).

We obtained peaks of P at the level of 2 keV and peaks of Ca between 3.5 and 4 keV. The spectrum between 3 and 3.5 keV represent uranium in the samples, which was used as a counterstain. Quantitative analysis revealed increased Ca and P levels resulting in a Ca/P ratio close to 1 only in the case of MVs of trans-differentiated MOVAS (Fig. 6D), whereas this ratio was lower in collagen-free vesicles. This probably reflects an increased rate of calcium entry into mineralizing

MVs since intracellular calcium levels are normally much lower than the levels of  $P_i$ . The Ca/P ratio of 1.67, calculated according to the formula of synthetic HA -  $Ca_{10}(PO_4)_6(OH)_2$  - does not specify the nature of biological apatite, which comprises several substitutions with, for instance,  $CO_3^{2-}$  residues replacing either  $PO_4^{3-}$  or  $OH^-$  ions in apatite crystals. Moreover, biological apatites are calcium-deficient apatites in which calcium can be replaced by several other cations. Finally, the composition and organization of crystals in mineralized tissues change profoundly during tissue aging, rendering the Ca/P ratios variable during crystal formation and maturation [36,37]. Our results confirm that the presence of collagen scaffold is necessary for efficient mineral nucleation mediated by VSMC-derived MVs. Moreover, we would like to underline that collagenase digestion is a necessary step to obtain calcifying vesicles from trans-differentiated VSMCs.

### 4. Discussion

Physiological mineralization in flat bones is a direct consequence of a process called intramembranous ossification. Conversely, long bones are formed through endochondral ossification, in which a cartilage template is being replaced by bone over time. These processes are maintained by mineralization-competent cells, such as osteoblasts and hypertrophic chondrocytes, respectively.

According to Murshed and collaborators [6] the mineralization process occurs exclusively in bone tissue due to co-expression of genes encoding two indispensable proteins - TNAP and collagen. Given the clinical importance of vascular calcification it is important to determine

whether this dual requirement is also true in vascular pathological calcification. In atherosclerotic plaques in particular, the precise location of microcalcifications and their possible association with collagen is still debated.

Vascular mineralization strongly resembles the process of endochondral ossification mediated by growth plate chondrocytes. Both processes are characterized by an increase in TNAP activity, ability to mineralize and to release MVs. Besides, chondrocyte- and VSMC-derived MVs share several common features such as enrichment in TNAP, ability to accumulate calcium and phosphate, annexins and collagen binding properties. This is indicative of analogies between the early events regulating VC and endochondral ossification [15].

Association of VSMC-derived MVs with collagen revealed that these vesicles were able to mineralize, in contrast to collagen-free vesicles, which do not induce mineralization. TNAP can bind to collagen [38], enabling the hydrolysis of  $PP_i$  at the site of mineralization. It was shown that the interaction of collagen type II and collagen type X with annexin A5 *in vitro* stimulates the uptake of  $Ca^{2+}$  ions by MVs and subsequent mineralization [18]. Moreover, selective removal of collagens from MV surface significantly reduced their ability to take up  $Ca^{2+}$  [34]. Collagen serves as a scaffold for the subsequent deposition of apatite crystals generated by MVs.

The amount of collagen is also a critical factor for atherosclerotic plaque stability. Vulnerable atherosclerotic lesions usually contain a thin and collagen-poor fibrous cap [39]. Matrix metalloproteinases, including collagenases, are enzymes released by macrophages within the plaque that decrease its thickness by collagen degradation. On the other hand, advanced plaques contain macrocalcifications together with a thick fibrous cap that stabilize the plaque and serve as a barrier towards further inflammation [40]. In this context, it will be important to investigate whether collagen is associated or not with microcalcifications, which are harmful for plaque stability.

In summary, we demonstrated that VSMC-derived MVs deposited in the vicinity of collagen fibrils exhibited increased TNAP activity and had the ability to accumulate calcium and phosphorus with an increased Ca/P ratio as compared to non-mineralizing vesicles, suggesting the deposition of apatite-like mineral.

## Abbreviations

AA	Ascorbic acid
AnxA2	Annexin A2
AnxA5	Annexin A5
AnxA6	Annexin A6
AR-S	Alizarin Red S
$\beta$ -GP	$\beta$ -glycerophosphate
BCA	Bi-Cinchoninic Acid
BCIP	5-bromo-4-chloro-3'-indolylphosphate p-toluidine salt
DMEM	Dulbecco's Modified Eagle Medium
ECM	Extracellular matrix
FBS	Foetal bovine serum
GPI	glycosylphosphatidylinositol
HEPES	4-(2-hydroxyethyl)-1-piperazineethanesulfonic acid
MV	Matrix vesicle
NBT	Nitro-blue tetrazolium chloride
PBS	Phosphate buffer saline
pNP	p-nitrophenol
pNPP	p-nitrophenyl phosphate
$PP_i$	Inorganic pyrophosphate
RT	Room temperature
SCL	Synthetic cartilage lymph
TEM	Transmission electron microscopy
TNAP	Tissue-nonspecific alkaline phosphatase
VC	Vascular calcification
VSMC	Vascular smooth muscle cell

## Acknowledgements

This work was supported by the MICROEXPLORATION grant from ERA-NET for Cardiovascular Diseases - Joint Transnational Call 2017 for David Magne from University Lyon 1, ICBMS, UMR CNRS and ERA-CVD/MICROEXPLORATION/4/2018 (NCBR) for Slawomir Pikula from Nencki Institute of Experimental Biology of Polish Academy of Sciences. Monika Roszkowska is a recipient of a scholarship "Doctorat en Cotutelle 2014–2017" granted by the French Government and the French Embassy in Poland. Polish-French cooperation was supported by PHC Polonium 2015/2016 no. 33540RG granted by the French Government and the French Embassy in Poland.

We would like to acknowledge the Laboratory of Electron Microscopy of the Nencki Institute for the excellent assistance in performing TEM and TEM-EDX analysis.

## References

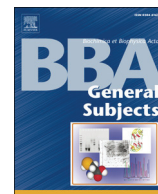
- [1] M.J. Duer, T. Friscić, D. Proudfoot, D.G. Reid, M. Schoppet, C.M. Shanahan, J.N. Skepper, E.R. Wise, *Arterioscler. Thromb. Vasc. Biol.* 28 (11) (2008) 2030–2034.
- [2] M.L.L. Chatrou, J.P. Cleutjens, G.J. van der Vusse, R.B. Roijers, P.H.A. Mutsaers, L.J. Schurgers, *PLoS One* 10 (2015) e0142335.
- [3] A. Kelly-Arnold, N. Maldonado, D. Laudier, E. Aikawa, L. Cardoso, S. Weinbaum, *Proc. Natl. Acad. Sci. U. S. A.* 110 (26) (2013) 10741–10746.
- [4] S. Ehara, *Circulation* 110 (2004) 3424–3429.
- [5] Y. Vengrenyuk, T.J. Kaplan, L. Cardoso, G.J. Randolph, S. Weinbaum, *Ann. Biomed. Eng.* 38 (2010) 738–747.
- [6] M. Murshed, D. Harmey, J.L. Millán, M.D. McKee, G. Karsenty, *Genes Dev.* 19 (9) (2005) 1093–1104.
- [7] C.R. Sheen, P. Kuss, S. Narisawa, M.C. Yadav, J. Nigro, W. Wang, T.N. Chhea, E.A. Sergienko, K. Kapoor, M.R. Jackson, M.F. Hoylaerts, A.B. Pinkerton, W.C. O'Neill, J.L. Millán, *J. Bone Miner. Res.* 30 (5) (2015) 824–836.
- [8] M. Fakhry, M. Roszkowska, A. Briolay, C. Bougault, A. Guignandon, J.I. Diaz-Hernandez, M. Diaz-Hernandez, S. Pikula, R. Buchet, E. Hamade, B. Badran, L. Bessueille, D. Magne, *Biochim. Biophys. Acta* 863 (3) (2017) 643–653.
- [9] F. Romanelli, A. Corbo, M. Salehi, S. Mc Yadav, D. Petrosian Salman, O.J. Rashidbaigi, J. Chait, J. Kuruvilla, M. Plummer, I. Radichev, K.B. Margulies, A.M. Gerdes, A.B. Pinkerton, J.L. Millán, A.Y. Savinov, O.V. Savinova, *PLoS One* 12 (10) (2017) e0186426.
- [10] R. Buchet, J.L. Millán, D. Magne, *Methods Mol. Biol.* 1053 (2013) 27–51.
- [11] S. Narisawa, M.C. Yadav, J.L. Millán, *J. Bone Miner. Res.* 28 (2013) 1587–1598.
- [12] W. Tesch, T. Vandebos, P. Roschgr, N. Fratzi-Zelman, K. Klaushofer, W. Beertens, P. Fratzi, *J. Bone Miner. Res.* 18 (2003) 117–125.
- [13] L. Hesse, K.A. Johnson, H.C. Anderson, S. Narisawa, A. Sali, J.W. Goding, R. Terkeltaub, J.L. Millán, *Proc. Natl. Acad. Sci. U. S. A.* 99 (2002) 9445–9449.
- [14] C. Thouverey, G. Bechkoff, S. Pikula, R. Buchet, *Osteoarthritis Cartil.* 17 (2009) 64–72.
- [15] M. Bottini, S. Mebarek, K.L. Anderson, A. Strzelecka-Kiliszek, L. Bozycki, A.M.S. Simão, M. Bolean, P. Ciancaglini, J.B. Pikula, S. Pikula, D. Magne, N. Volkman, D. Hanein, J.L. Millán, R. Buchet, *Biochim. Biophys. Acta* 1862 (3) (2017) 532–546.
- [16] D.C. Genetos, A. Wong, T.J. Weber, N.J. Karin, C.E. Yellowley, *PLoS One* 9 (2014) e107482.
- [17] A. Sekrecka, M. Balcerzak, C. Thouverey, R. Buchet, S. Pikula, *Postepy Biochem.* 53 (2007) 159–163.
- [18] T. Kirsch, G. Harrison, E.E. Golub, H.D. Nah, *J. Biol. Chem.* 275 (45) (2000) 35577–35583.
- [19] T. Minashima, W. Small, S.E. Moss, T. Kirsch, *J. Biol. Chem.* 287 (2012) 14803–14815.
- [20] C. Goettsch, J.D. Hutcheson, M. Aikawa, H. Iwata, T. Pham, A. Nykjaer, M. Kjolby, M. Rogers, T. Michel, M. Shibasaki, S. Hagita, R. Kramann, D.J. Rader, P. Libby, S.A. Singh, E. Aikawa, *J. Clin. Invest.* 126 (4) (2016) 1323–1336.
- [21] C. Goettsch, H. Iwata, J.D. Hutcheson, C.J. O'Donnell, R. Chapurlat, N.R. Cook, M. Aikawa, P. Szulc, E. Aikawa, *Arterioscler. Thromb. Vasc. Biol.* 37 (5) (2017) 1005–1011.
- [22] N.X. Chen, K.D. O'Neill, X. Chen, S.M. Moe, *J. Bone Miner. Res.* 23 (11) (2008) 1798–1805.
- [23] Y.V. Bobryshev, M.C. Killingsworth, R.S. Lord, A.J. Grabs, *J. Cell. Mol. Med.* 12 (5B) (2008) 2073–2082.
- [24] A.N. Kapustin, J.D. Davies, J.L. Reynolds, R. Mcnair, G.T. Jones, A. Sidibe, L.J. Schurgers, J.N. Skepper, D. Proudfoot, M. Mayr, C.M. Shanahan, *Circ. Res.* 109 (1) (2011) e1–12.
- [25] J.D. Hutcheson, C. Goettsch, T. Pham, M. Iwashita, M. Aikawa, S.A. Singh, E. Aikawa, *J. Extracell. Vesicles.* 3 (2014) 25129.
- [26] A. Briolay, R. Jaafar, G. Nemoz, L. Bessueille, *Biochim. Biophys. Acta* 1828 (2013) 602–613.
- [27] R.E. Wuthier, *Biochim. Biophys. Acta* 409 (1) (1975) 128–143.
- [28] R. Buchet, S. Pikula, D. Magne, S. Mebarek, *Methods Mol. Biol.* 1053 (2013) 115–124.

- [29] L. Bessueille, M. Fakhry, E. Hamade, B. Badran, D. Magne, *FEBS Lett.* 589 (2015) 2797–2804.
- [30] D.C. Morris, K. Masuhara, K. Takaoka, K. Ono, H.C. Anderson, *Bone Miner.* 19 (3) (1992) 287–298.
- [31] K. Hoshi, N. Amizuka, K. Oda, Y. Ikehara, H. Ozawa, *Histochem. Cell Biol.* 107 (3) (1997) 183–191.
- [32] P. Lencel, S. Delplace, P. Pilet, D. Leterme, F. Miellot, S. Sourice, A. Caudrillier, P. Hardouin, J. Guicheux, D. Magne, *Lab. Investig.* 91 (10) (2011) 1434–1442.
- [33] M. Roszkowska, A. Strzelecka-Kiliszek, D. Magne, S. Pikula, L. Bessueille, *Postepy Biochem.* 62 (2016) 511–517.
- [34] B.R. Genge, L.N. Wu, R.E. Wuthier, *J. Biol. Chem.* 283 (15) (2008) 9737–9748.
- [35] J.L. Reynolds, A.J. Joannides, J.N. Skepper, R. Mcnair, L.J. Schurgers, D. Proudfoot, W. Jahnen-Dechent, P.L. Weissberg, C.M. Shanahan, *J. Am. Soc. Nephrol.* 15 (11) (2004) 2857–2867.
- [36] D. Magne, P. Weiss, J.M. Boulter, O. Laboux, G. Daculsi, *J. Bone Miner. Res.* 16 (4) (2001) 750–777.
- [37] D. Magne, P. Pilet, P. Weiss, G. Daculsi, *Bone* 29 (6) (2001) 547–552.
- [38] F. Vittur, N. Stagni, L. Moro, B. de Bernard, *Experientia* 40 (1984) 836–837.
- [39] Y. Fukumoto, J.O. Deguchi, P. Libby, E. Rabkin-Aikawa, Y. Sakata, M.T. Chin, C.C. Hill, P.R. Lawler, N. Varo, F.J. Schoen, S.M. Krane, M. Aikawa, *Circulation* 110 (14) (2004) 1953–1959.
- [40] G. Pugliese, C. Iacobini, C.B. Fantauzzi, S. Menini, *Atherosclerosis* 238 (2015) 220–230.



Contents lists available at ScienceDirect

Biochimica et Biophysica Acta

journal homepage: [www.elsevier.com/locate/bbagen](http://www.elsevier.com/locate/bbagen)

## Review

# Functions of Rho family of small GTPases and Rho-associated coiled-coil kinases in bone cells during differentiation and mineralization



Agnieszka Strzelecka-Kiliszek<sup>a</sup>, Saida Mebarek<sup>b,c,d,e,f,g</sup>, Monika Roszkowska<sup>a,b,c</sup>, René Buchet<sup>b,c,d,e,f,g</sup>, David Magne<sup>b,c,d,e,f,g</sup>, Sławomir Pikula<sup>a,\*</sup>

<sup>a</sup> Department of Biochemistry, Nencki Institute of Experimental Biology, Polish Academy of Sciences, 3 Pasteura Str., 02-093 Warsaw, Poland

<sup>b</sup> ICBMS, UMR CNRS 5246, University of Lyon 1, Bâtiment Raulin, 43 Bd du 11 novembre 1918, 69622 Villeurbanne Cedex, France

<sup>c</sup> Université de Lyon, 69622 Villeurbanne Cedex, France

<sup>d</sup> Université Lyon 1, 69622 Villeurbanne Cedex, France

<sup>e</sup> INSA de Lyon, 69621 Villeurbanne Cedex, France

<sup>f</sup> CPE Lyon, 69616 Villeurbanne Cedex, France

<sup>g</sup> ICBMS CNRS UMR 5246, 69622 Villeurbanne Cedex, France

## ARTICLE INFO

## Article history:

Received 26 August 2016

Received in revised form 2 February 2017

Accepted 6 February 2017

Available online 08 February 2017

## Keywords:

Bone cells

Differentiation

Mineralization

ROCK

Signal transduction

Vesicles

## ABSTRACT

**Background:** Members of Rho-associated coiled-coil kinases (ROCKs) are effectors of Rho family of small GTPases. ROCKs have multiple functions that include regulation of cellular contraction and polarity, adhesion, motility, proliferation, apoptosis, differentiation, maturation and remodeling of the extracellular matrix (ECM).

**Scope of the review:** Here, we focus on the action of RhoA and RhoA effectors, ROCK1 and ROCK2, in cells related to tissue mineralization: mesenchymal stem cells, chondrocytes, preosteoblasts, osteoblasts, osteocytes, lining cells and osteoclasts.

**Major conclusions:** The activation of the RhoA/ROCK pathway promotes stress fiber formation and reduces chondrocyte and osteogenic differentiations, in contrast to that in mesenchymal stem cells which stimulated the osteogenic and the chondrogenic differentiation. The effects of Rac1 and Cdc42 in promoting chondrocyte hypertrophy and of Rac1, Rac2 and Cdc42 in osteoclast are discussed. In addition, members of the Rho family of GTPases such Rac1, Rac2, Rac3 and Cdc42, acting upstream of ROCK and/or other protein effectors, may compensate the actions of RhoA, affecting directly or indirectly the actions of ROCKs as well as other protein effectors. **General significance:** ROCK activity can trigger cartilage degradation and affect bone formation, therefore these kinases may represent a possible therapeutic target to treat osteoarthritis and osseous diseases. Inhibition of Rho/ROCK activity in chondrocytes prevents cartilage degradation, stimulate mineralization of osteoblasts and facilitate bone formation around implanted metals. Treatment with osteoprotegerin results in a significant decrease in the expression of Rho GTPases, ROCK1 and ROCK2, reducing bone resorption. Inhibition of ROCK signaling increases osteoblast differentiation in a topography-dependent manner.

© 2017 Elsevier B.V. All rights reserved.

## 1. Introduction

The mineralization process that occurs during bone ossification is a tightly regulated cascade of molecular events leading to the formation of a correct skeleton in adults [1]. The cells responsible for mineraliza-

tion are osteoblasts, odontoblasts, and hypertrophic chondrocytes. Mineralization-competent cells produce extracellular matrix (ECM) principally composed of fibrillar collagen, in which they subsequently deposit hydroxyapatite (HA) [2]. Mineralization-competent cells are enriched in tissue-nonspecific alkaline phosphatase (TNAP) [3,4].

**Abbreviations:** AGC, protein kinase A, G, and C families (PKA, PKC, PKG) of cytoplasmic serine/threonine kinases; AnxA, vertebrate annexin; ALP, alkaline phosphatase; ANK, progressive ankylosis protein; BMP, bone morphogenetic protein; BSP, bone sialoprotein; CHOL, cholesterol; CysD, cysteine-rich domain; DMPK, dystrophica myotonin protein kinase; ECM, extracellular matrix; HA, hydroxyapatite; LIMK, LIM kinase; LPA, lysophosphatidic acid; MAPK, mitogen-activated protein kinase; MARCKS, myristoylated alanine-rich C kinase substrate; MLC, myosin light chain; MLCK, myosin light chain kinase; MMP, matrix metalloproteinase; MVs, matrix vesicles; NPP1, nucleotide pyrophosphatase phosphodiesterase 1; OCN, osteocalcin; OPN, osteopontin; P<sub>i</sub>, inorganic phosphate; PHD, Pleckstrin homology domain; PI3-K, phosphoinositide 3-kinase; PLA, PLC, PLD, phospholipase A, C, D; PP<sub>i</sub>, inorganic pyrophosphate; PS, phosphatidylserine; PTH, parathyroid hormone; RANKL, receptor activator of nuclear factor- $\kappa$ B ligand; RBD, Rho-binding domain; ROCK, Rho-associated coiled-coil kinase; SM, sphingomyelin; TNAP, tissue non-specific alkaline phosphatase.

\* Corresponding author.

E-mail address: [s.pikula@nencki.gov.pl](mailto:s.pikula@nencki.gov.pl) (S. Pikula).



Pathological mineralization gives rise to a large group of diseases, affecting not only skeletal (bones and joints) but also non-skeletal tissues [5,6]. They are manifested by HA crystal deposition, often mediated by matrix vesicles (MVs) [3], in the soft tissues of tendons and/or ligaments (calcific tendinitis and ankylosing spondylitis) [7], in articular cartilage (some cases of osteoarthritis) [8], in arterial media (vascular calcification induced by chronic kidney disease (CKD) [9–11] or by type 2 non-insulin-dependent diabetes mellitus [12,13]) and in atherosclerosis [14,15]. Recent discoveries in the field of bone, growth plates and periodontal biology indicate participation of the Rho family of small GTPases and Rho-associated, coiled-coil containing protein kinases (ROCK) in cytoskeletal reorganization and differentiation towards osteogenic cells as well as in cell growth and cell death that may affect matrix remodeling [16,17].

The review is divided into three main parts. The first chapter is focused on bone cell biology; the second is centered on functions of Rho family of small GTPases and Rho-associated kinases and the third concerns the function of RhoA and Rho-associated kinases ROCK1 and ROCK2 during bone formation.

## 2. Bone cell biology

Bone-forming cells (osteoblasts) and chondrocytes originate from mesenchymal stem cells [18,19] while hematopoietic stem cells give rise to bone-resorbing cells (osteoclasts) [20] (Fig. 1). Bone tissue is continuously renewed due to concerted action of osteoblasts that build the bone and by osteoclasts (OCs) that resorb it. In young adults, the resorbed bone material is precisely replaced in both location and mass by a newly formed tissue. With aging, the coupling becomes unbalanced with increasing bone resorption resulting in a net loss of the bone tissue, as in osteoporosis [21–23] or aberrant accumulation calcification as in the case of osteopetrosis. The cells communicate with each other to regulate bone repair and adaptation to changes.

### 2.1. Mesenchymal stem cells

Mesenchymal stem cells (MSCs) have the capacity to differentiate into fibroblasts, myoblasts, chondrocytes, osteoblasts or adipocytes [18,19] (Fig. 1). Flattened and spread human MSCs undergo osteogenesis, while unspread, round cells become adipocytes. Wnt/ $\beta$ -catenin/TCF signaling stimulates bone formation and suppresses adipogenesis. The

propensity of bone marrow MSCs to differentiate into adipocytes at the expense of osteoblasts is a critical factor leading to bone loss and osteoporosis [24].

### 2.2. Intramembranous (osteoblasts) and endochondral ossification (chondrocytes)

During intramembranous ossification, which is the mechanism responsible for the embryonic development of flat bones and for natural healing of bone fractures, mature osteoblasts synthesize and secrete large amounts of type I collagen, noncollagenous proteins, enzymes and growth factors, which comprise major components of the bone matrix that later becomes mineralized [23].

Approximately 60 to 80% of osteoblasts die via apoptosis [25,26]. The remaining osteoblasts become either lining cells or osteocytes [23] (Fig. 1). In contrast to bone forming osteoblasts and bone resorbing osteoclasts, chondrocytes have multiple functions, for example, formation and removal of cartilaginous tissues (hyaline articular cartilage). Chondrogenesis may progress in two different directions in the developing bone. One route leads to the formation of long bone via endochondral ossification, (at the primary and secondary centers of ossification, and in the growth plate) and the second route leads to stable hyaline articular cartilage and provides a frictionless surface facilitating load transfer [27]. MSCs, primary chondrocytes and chondrocyte cell lines may serve as tools for *in vitro* experiments in cartilage research and repair [27]. Coordinated proliferation and differentiation of growth plate cells is required for normal growth and development of the skeleton [28]. Chondrocytes participate in the synthesis of extracellular matrix proteins, production and activation of matrix degrading proteins and, in some cases, matrix calcification. Chondrocytes are responsible for the growth and maintenance of the growth plate [28].

Disruption of chondrocyte proliferation and/or differentiation by gene mutations commonly results in chondrodysplasias that are characterized by skeletal deformities and reduced growth [29–31].

### 2.3. Osteocytes

Osteocytes represent 95% of all bone cells. Osteocyte life span is 1–50 years while for osteoblasts it is only around 1–200 days. The life span of lining cells is 1–10 years, whereas for osteoclasts it is merely 1–25 days [32]. Osteocytes, which sense mechanical signals or micro-

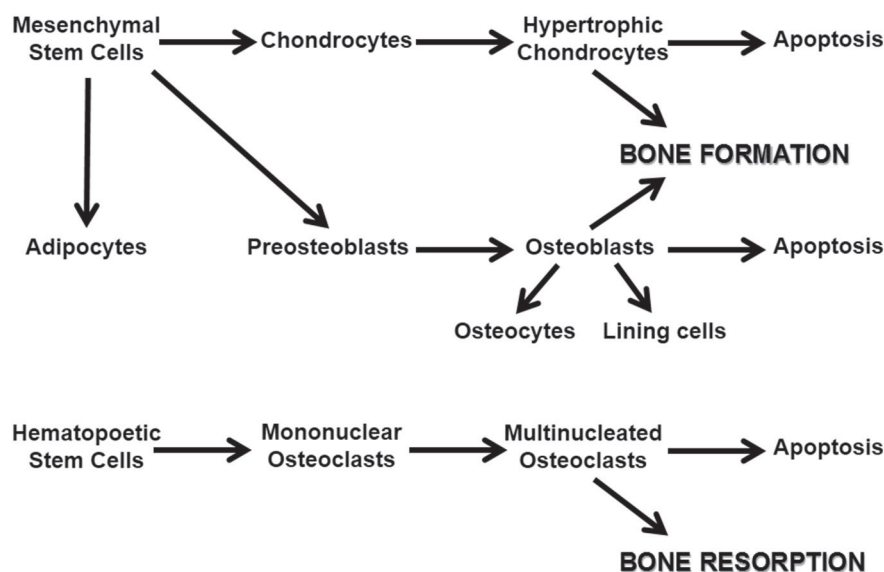


**Fig. 1.** Origin of osteoblasts, osteoclasts and chondrocytes. Mesenchymal stem cells are the source of adipocytes, chondrocytes and preosteoblasts. Osteoblasts and hypertrophic chondrocytes are able to mineralize. Hypertrophic chondrocytes and a population of osteoblasts die during apoptosis. A part of osteoblasts become osteocytes and lining cells. Hematopoietic stem cells are the source of mononuclear osteoclasts. They mature as multinucleated osteoclasts and can resorb bone once activated by RANKL.

damages in bone, regulate bone metabolism by communicating with other bone cells [33,34]. This function is served by dendrites that maintain communication by gap junctions, forming an interconnected signaling network in bone canaliculi. Osteocytes are generally considered to inhibit bone resorption [35]. They not only affect bone remodeling by controlling osteoclast formation via production of the receptor activator of nuclear factor- $\kappa$ B ligand (RANKL), but also regulate osteoblast formation via production of sclerostin [36]. Osteocytes are the main source of the RANKL required for osteoclast formation [37]. The signals produced by mechanical forces are transmitted by integrins and a signalosome comprising actin filaments, microtubules, the focal adhesion kinase FAK, and Src kinases. Osteocytes interact with the extracellular matrix through integrins [38,39], which tether them to the canalicular wall [40].

#### 2.4. Osteoclasts

During osteoclastogenesis, osteoclasts (OCs) derived from hematopoietic stem cells (Fig. 1) become multinucleated and stimulated by macrophage colony-stimulating factor (M-CSF) and RANKL [20]. OCs grown on non-mineralized support undergo extensive morphological changes to form podosome clusters and, subsequently, podosome rings, which fuse into a podosome belt [41,42]. Differentiated OCs grown on mineralized support polarize and reorganize their membrane into four regions: the sealing zone (SZ), the ruffled border (RB), the basolateral domain (BD) or free membrane domain (FM) and the functional secretory domain (FSD) [23,43]. Multinucleated OCs, when attached to calcified tissues, become polarized and resorb the bone by forming a resorption lacuna, wherein HA is dissolved due to the acidic environment in the sealed zone. Furthermore, the extracellular bone matrix is degraded by acidic proteases, such as cathepsin K, matrix metalloproteinases, such as MMP-9, conjointly with tartrate resistant acid phosphatase, which also contributes to bone resorption. Multinucleated OCs migrate along the surface of the bones to continue bone resorption, until they die by apoptosis [20].

#### 2.5. Cell adhesion to extracellular matrix

Bone mineralization induced by mineral competent cells requires not only HA deposition but also formation of ECM. Cell adhesion to ECM is initiated through direct interaction of integrin extracellular domains with the extracellular matrix, which leads to clustering of integrins, their recruitment to the focal adhesion complexes, and tyrosine phosphorylation of FAK [44–46]. Focal complexes at the leading edge direct cell movement.

### 3. Bone ossification

Endochondral ossification is induced by chondrocyte maturation in the growth plate, vascular expansion in the surrounding tissues, osteoblast differentiation and osteogenesis in the perichondrium and the developing bone center [47]. During bone ossification, cells in the growth plate undergo a cascade of events that lead to terminal differentiation and mineralization [48,49]. The mineralization process is accompanied by rapid matrix remodeling and expression of mineralization-related genes, including those encoding TNAP,  $\text{Ca}^{2+}$  and phospholipid binding proteins belonging to the annexin family – AnxA (AnxA1, AnxA2, AnxA4, AnxA5, AnxA6 and AnxA11), extracellular matrix metalloproteinase degrading enzymes – MMPs (MMP-2, MMP-3, MMP-9, MMP-13), collagens (types I, II and X) [49–54]. The level of inorganic phosphate ( $\text{P}_i$ )-phospholipid complexes also increases. The mineralization process occurs by a series of biochemical processes facilitating the deposition of a solid phase composed of HA. Although calcium and phosphate ions can reach sufficient concentrations in extracellular fluids to become metastable, it is not always sufficient to form HA. Therefore, nucleation may be necessary to accelerate HA formation. The nucleation step occurs in the extracellular medium and/or in MVs [3,55,56]. In addition,

small-sized MVs can diffuse better than large cells through the collagen fibers to sustain and spread the mineralization process.

#### 3.1. Initial steps of mineralization occur in matrix vesicles

MVs are extracellular organelles produced by chondrocytes, osteoblasts and odontoblasts. Isolation of MVs from osteoblasts and chondrocytes as well as their main characteristics were reported [57–63]. MVs originate from microvilli-like protrusions of mineralization-competent cells such as chondrocytes [64] and osteoblasts [65]. The MV membrane is enriched in acidic phospholipids and certain proteins, particularly TNAP, nucleotide pyrophosphatase phosphodiesterase 1 (NPP1) and progressive ankylosis protein (ANK) [66–68]. TNAP, acting as a phosphomonoesterase, hydrolyzes free phosphate esters such as pyrophosphate, an inhibitor of HA formation. NPP1, by hydrolyzing ATP, produces  $\text{PP}_i$  while ANK transports  $\text{PP}_i$  from the intracellular (or from the lumen of MVs) to extracellular medium [69]. NPP1 and ANK are considered as enzymes antagonistic to TNAP since they contribute to an increase in extracellular  $\text{PP}_i$ , while TNAP hydrolyzes  $\text{PP}_i$ .

#### 3.2. Molecular mechanisms of mineralization

Physiological mineralization occurs in the ECM of skeletal tissues and its strict regulation is necessary for the formation, development and function (rearrangement and repair) of the skeleton. There are only few data in the literature concerning mechanisms that regulate MV release (as reviewed earlier [67–69]). The presence of vesicular trafficking molecules (e.g. Rab proteins) suggests that apical targeting is required for incorporation of specific lipids and proteins at the site of MV formation [66]. MV release from microvilli-like membranes may be driven by actions of actin-severing proteins (gelsolin, cofilin 1) and contractile motor proteins (myosins) [64,66]. However, questions concerning regulation and mechanisms of MV release, incorporation of proteins into MV membrane and influence of ECM factors on mineral formation still remain without answer.

The currently held mineralization mechanism postulates that ANK and NPP1 suppress mineralization by increasing the extracellular concentration of the calcification inhibitor,  $\text{PP}_i$ , while TNAP promotes mineralization by decreasing the concentration of  $\text{PP}_i$  [70–72]. Extracellular  $\text{PP}_i$  is formed from extracellular nucleoside triphosphates (NTP) by NPP1 in cells and in MVs or exported from cells and MVs through ANK; it is hydrolyzed to  $\text{P}_i$  by TNAP anchored to the cell plasma membrane and to the membrane of MVs.

Pathological mineralization such as vascular calcification resembles physiological mineralization [5,6]. Indeed, smooth muscle cells involved in vascular calcification behave as mineral competent cells – they are able to release MVs, are characterized by increased TNAP activity and produce collagen [5,73,74].

### 4. ROCK kinases as key enzymes participating in actomyosin skeletal reorganization

#### 4.1. Members of Rho family of small GTPases

Actomyosin cytoskeletal reorganization is essential for various cell activities, including changes in morphology, cell motility, adhesion and cytokinesis. Various extracellular stimuli induce changes in actin organization through signaling pathways that link the external stimuli to the machinery controlling actin polymerization and organization. Rho-family of small GTPases regulates cytoskeleton during cell migration, adhesion and cytokinesis [75]. The mammalian Rho-family of small GTPases is composed of 23 intracellular signaling molecules [75], the best documented of which are: Ras homolog gene family member A (RhoA), its two homologs, RhoB and RhoC, Ras-related C3 botulinum toxin substrate 1 (Rac; existing in three isoforms – Rac1, Rac2, and Rac3) and cell division control protein 42 (Cdc42). The Rho GTPases

act through downstream effectors such as Citron, mDia, ROCKs, rhophilin, rhotekin and PKN [75]. One Rho GTPase can target several downstream effector proteins [76]. Active RhoA can bind to ROCK, rhophilin and rhotekin triggering their activity, while Rac1 acts on Pak1 [77]. Several Rho-family GTPases can target the same effector, which may obscure knockout mouse phenotypes. For example, during vascular muscle contractility, RhoA, RhoB and RhoC can interact with the same effectors i.e., ROCKs [78]. To determine the function of RhoA, botulinum C3 exoenzyme, a specific inhibitor of Rho, is often used [76]. Rho GTPases are regulated through their expression level, stability and post-translational modifications. Prenylation at their C-terminus facilitates their association with the intracellular leaflet of cell membranes. The GTPases switch from an active GTP-bound state to an inactive GDP-bound state [78,79]. Guanine-nucleotide exchange factor (GEF) promotes the release of GDP in exchange of GTP, while GTPase activating protein (GAP) increases the intrinsic hydrolytic GTPase activity, which leads to GDP generation from GTP, whereby the GTPase becomes inactivated. GEFs fall into two families: Dbl and Dock proteins. There are eleven Dock1-related proteins in mammals [80–82] characterized by a unique DHR-2 (or CZH-2) domain that catalyzes nucleotide exchange on Rac1 or Cdc42 and a DHR-1 domain that tethers the GEFs to phosphatidylinositol(3,4,5) triphosphate-enriched membranes.

#### 4.2. Structures of ROCKs

ROCKs (i.e. Rho-associated coiled-coil kinases) are kinases activated by RhoA, RhoB and RhoC [83–86]. They belong to the AGC (the protein kinase A, G, and C families (PKA, PKC, PKG) of cytoplasmic serine/threonine kinases) super family of human kinome. The AGC super family comprises DMPK (dystrophica myotonin protein kinase) family of kinases to which ROCKs belong [86,87]. ROCKs trigger actin reorganization, formation of stress fibers, focal adhesion, smooth muscle contraction, increase cell motility, and induce changes in proliferation cell survival and tumor cell invasion [88–92]. There are two highly homologous isoforms of ROCK: ROCK1 (p160<sup>ROCK</sup> or ROK $\beta$ ) and ROCK2 (p164<sup>ROCK</sup>, ROK $\alpha$ ). ROCK1 and ROCK2 are collectively called ROCK or ROCK1/2. They have 65% of amino acids in common and more than 90% identity within their kinase domains [93,94]. Human ROCK1 consists of 1354 amino acid residues whereas ROCK-2 has 1388 amino acid residues [85]. ROCKs have an N-terminal kinase domain (KD), a coiled-coiled region, Rho-binding domain (RBD), a pleckstrin homology domain (PHD) and a cysteine-rich domain (CRD) at the C-terminal [95]. An autoinhibitory mechanism has been proposed for ROCKs. This mechanism involves an intramolecular interaction between KD and PHD in the absence of Rho binding [95]. Thus, the kinase activity is off when ROCKs are intramolecularly folded and switched on when Rho-GTP binds to RBD and disrupts the autoinhibitory interaction within ROCKs [96].

#### 4.3. Tissue expression and subcellular localization of ROCKs

The tissue distribution of the two ROCK enzymes differs: ROCK2 is preferentially expressed in brain and in muscles whereas ROCK1 is primarily expressed in the non-neuronal organs like liver, lung, kidneys, spleen and testis [93–97]. The PHD of ROCK2 binds to phosphatidylinositol (3,4,5) triphosphate and to phosphatidylinositol (4,5) biphosphate, while the PHD of ROCK1 does not [98], suggesting distinct subcellular distribution of ROCK1 and ROCK2. ROCK2 resides in the cytoplasm, is associated with the centrosome, co-localizes with actin and vimentin, and is present at the intercalated disk and Z-disk of striated cells [88,99–105]. ROCK1 co-localize with the centrosomes, plasma membrane, cell-cell contacts, cell adhesion sites and vesicles [105–108].

#### 4.4. Substrates and functions of ROCKs

ROCKs phosphorylate more than thirty substrates, among them, myosin phosphatase target subunit 1 (MYPT-1) [109–111], insulin

receptor substrate 1 (IRS-1) [112], myosin light chain 2 (MLC2) [109,113], LIM kinases (LIMK1, LIMK2) [114–118], ezrin/radixin/moesin (ERM) [119], adducin [120] and enzymes of the PI3-K/AKT pathway [121,122]. One of the most established function of ROCK is exemplified during activation of the RhoA/ROCK/MYPT1/MLC2 pathway in smooth muscle cells (Fig. 2). The contraction of smooth muscle and interaction of actin and myosin in non-muscle cells is triggered by RhoA effector, mostly ROCK2 [123] that directly phosphorylates MLC2 and MYPT-1. The phosphorylation of MYPT-1 at Thr697 and Thr855 inactivates the myosin light chain (MLC) phosphatase [110,122] (Fig. 2). Both phosphorylation of MLC2 and inhibition of MLC phosphatase by ROCK contribute to the accumulation of phosphorylated MLC2 (MLC2-P) and to the stimulation of actomyosin contractility (Fig. 2). During detachment of mouse embryonic fibroblasts, ROCK1 mediated destabilization of actin cytoskeleton through MLC2 phosphorylation while, in contrast, ROCK2 stabilized actin cytoskeleton via cofilin phosphorylation by activating LIMK [124] (Fig. 2). This illustrates that ROCK2 acts differently during contraction of smooth muscle cells, i.e., by stimulating actin contractility [123], and during regulation of stress-induced fiber disassembly and cell detachment [124], in the course of which it stabilizes the actin cytoskeleton. Differences in the activity [123–126] and therapeutic implications [83–85,127–134] between the two isoforms (ROCK1 and ROCK2) were reported. As reviewed in [126], functional differences between ROCK1 and ROCK2 were observed in adipocytes [135], cancer cells [136,137], endothelial cells [138–142], fibroblasts [98,135,143,144], smooth muscle cells [123,145], keratinocytes [146–148] and neurons [144]. Such differences in ROCK functions originate from their distinct localizations, distinct modes of activation by upstream GTPases, different regulatory mechanisms and different downstream targets [134,135]. The cell type, its maturation and differentiation state can also favor one specific ROCK-dependent signaling pathway over others.

#### 4.5. Mouse models of *Rock1* or *Rock2* deletions

The majority of homozygous deletions of *Rock1* or *Rock2* lead to high rates of embryonic and perinatal mortality [134]. The homozygous deletion of *Rock1* in mice (C57B1/6 background) produced newborns with open eyes. Around 90% of ROCK1<sup>-/-</sup> C57B1/6-mice later die from omphalocele (an abdominal wall muscle defect in which organs remain in a sac outside the abdomen), while the remaining mice develop normally except for eye defects [149]. The ROCK2<sup>-/-</sup> mice (mixed 129/SvJ-and-C57BL/6 background) die in utero due to placental dysfunction, intrauterine growth and fetal retardation [150], while newborn ROCK2<sup>-/-</sup> mice (C57BL/6 background) have open eyes and 99% die later due to omphalocele [151]. The survival rate of mutant mice depends of their origin, genetics and the extent to which one ROCK can substitute the other [134]. *Rock2* knockout in mice (C57B1/6 background) indicated that ROCK2 limits axonal growth after CNS trauma [152]. ROCK1 knockout in mice (C57BL/6–129/SvJ mixed background) causes insulin resistance [153]. Also, ROCK1 contributes to the development of cardiac fibrosis and induction of fibrogenic cytokines in cardiomyocytes in response to pathological stimuli [154]. A reduced neointima formation was found in *Rock1*<sup>±</sup> mice (C57BL/6 background) compared with that of WT or *Rock2*<sup>±</sup> mice [155], indicating that ROCK1 mediates leukocyte recruitment and neointima formation following vascular injury [155]. Increased recruitment and migration of macrophages and neutrophils were observed in ROCK1<sup>-/-</sup> mice (FVB background), showing that ROCK1 is negatively regulating macrophage and neutrophil function [156]. Several distinct and non-redundant functions of ROCK1 and ROCK2 were evidenced in knockout mouse models [134,149–156], reinforcing the view that each type of ROCK may orchestrate distinct downstream processes.

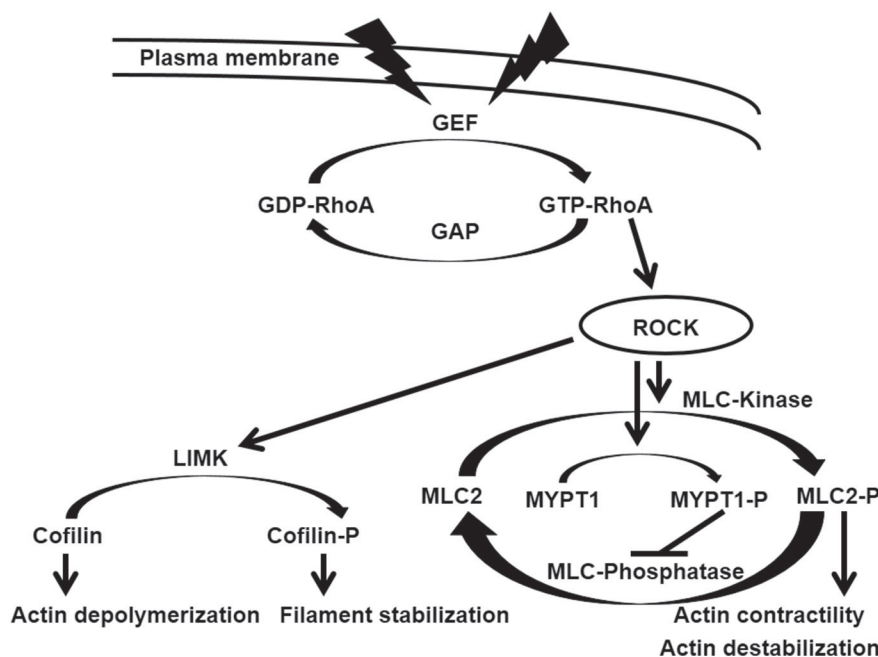


**Fig. 2.** Rho/ROCK/MLCK/MLC-P and Rho/ROCK/LIMK/Cofilin-P pathways. Rho GTPases are regulated through their expression level, stability and post-translational modifications. The Rho GTPases switch between an active GTP bound state and an inactive GDP bound state. Guanine-nucleotide exchange factor (GEF) promotes the release of GDP in exchange of GTP, while GTPase activating protein (GAP) increases the intrinsic hydrolytic activity that converts GTP into GDP, inactivating the GTPase. ROCK leads to an increase of myosin light chain (MLC) phosphorylation (MLC-P), activating myosin light chain kinase (MLCK) and inhibiting MLC phosphatase, and thereby inducing actomyosin-based contractility. ROCK directly phosphorylates and activates LIMK, which results in downstream phosphorylation and inactivation of the actin depolymerizing factor, cofilin leading to filament stabilization.

#### 4.6. Inhibitors of ROCK and their therapeutic applications

The research effort on inhibitors of ROCKs is powered by the awareness that ROCKs are involved in angiogenesis [157] cancer cell migration [132,133,157–159], erectile dysfunction [160], glaucoma [161], idiopathic pulmonary pathway [162], neurological disorders [163–165], spinal muscular atrophy [166] and vascular diseases [126,131]. Development of more selective ROCK inhibitors is highly encouraged by their beneficial effects at clinical levels and the prospect of curing a large variety of diseases [83,134,167,168]. The two most widely used inhibitors, fasudil (HA-1077, 5-(1,4-diazepane-1-sulfonyl) isoquinoline) and Y-27632 ((+)-(R)-trans-4-(1-aminoethyl)-N-(4-pyridyl)cyclohexane carboxamide) inhibit both ROCKs, and at higher concentrations inhibit also protein kinase C-related kinase 1, cAMP-activated protein kinase and AMP-activated kinase [126,134]. Both fasudil and Y-27632 (RKI-983 or SNJ-1656) are competitive with respect to ATP [169,170]. Y-27632 is a cell-permeable ROCK 1 inhibitor ( $K_i = 140$  nM), however, it also inhibits ROCK 2 with similar potency [169]. Fasudil has a  $K_i = 330$  nM [170], and its metabolite hydroxyfasudil is equally effective. As reviewed in [171], fasudil has been approved for human use in Japan to treat cerebral vasospasm since 1995 [172], while ripasudil (a close fasudil analog, also called K-115) entered clinical application in Japan to treat glaucoma in 2014 [173]. As reviewed in [171], AR-13324, a ROCK inhibitor, reached Phase 3 trial for treating glaucoma [174], while AMA 0076 [3-[2-(aminomethyl)-5-[pyridine-4-yl]carbonyl]phenyl]benzoate [175] and AR-12286 [2-(dimethylamino)-N(1-oxo-2H-isoquinolin-6-yl)-2-thiophen-3ylacetamide] reached Phase 2 trial [171]. Among the very few selective inhibitors, KD-025 (or SLx-2119) [2-(3-(4-((1H-indazol-5-yl)amino)quinazolin-2-yl)phenoxy)-N-isopropylacetamide] is selective for ROCK2 with  $IC_{50}$  value of 0.195 mM versus  $IC_{50}$  value of 24 mM for ROCK1 [176–178].

Simvastatin (1S,3R,7S,8S,8aR)-8[2-[(2R,4R)-4-hydroxy-6-oxotetrahydro-2H-pyran-2-yl]ethyl]-3,7-dimethyl-1,2,3,7,8,8a-hexahydronaphthalen-1yl-2,2-dimethylbutanoate) exerts cardioprotective effects and improves insulin resistance (IR). Its beneficial action can be attributed, at least in part, to inhibition of ROCKs and activation of PI3-K/Akt [121]. Other ROCK inhibitors such as GSK2699962A [N-3-[[2-(4-amino-1,2,5-oxadiazol-3-yl)-1-ethyl-1H-imidazo[4,5-c]pyridine-6-yl]oxy]phenyl]4-[[2-(4-morpholinyl)ethyl]oxy]benzamide] limit ROCK activity in the nM range [DOE]. Wf-536, a derivative of fasudil H1152 [(S)-(+)-2-methyl-1-[(4-methyl-5-isoquinolyl)sulfonyl]hexahydro-1H-1,4-diazepine] and RKI-1447 reduced progression of hepatocellular cancer, lung cancers, melanoma and breast cancers [179–182]. ROCK inhibitors, due to multiple therapeutic targets, have the potential to act synergistically on distinct pathways triggering the risk of side effects. So far, fasudil has been approved for clinical use since 1995, despite its lack of selectivity.

## 5. ROCKs action in bone

### 5.1. ROCKs and mesenchymal stem cells

A pioneer work on ROCKs involvement in human mesenchymal stem cell (hMSCs) differentiation was published 12 years ago [18]. The shape of hMSCs regulates their differentiation to adipocyte or osteoblast lineage, when RhoA signaling and cytoskeletal tension are intact. Interference with cell shape, RhoA signaling, ROCK activity, or cytoskeletal tension alters the fate of hMSCs [18].

RhoA-stimulated osteogenesis was conditional on the shape, while constitutive activation of ROCK induced osteogenesis independently of the cell shape [18]. The mechanism of cell shape acting as a mechanical cue to induce osteogenesis was substantiated by results of hMSCs treatment with bone morphogenetic protein 2 (BMP-2) [183]. BMP-2 is a cytokine that promotes osteogenesis [184,185]. The treatment of hMSCs with BMP-2 induces Rho/ROCK-mediated cell tension and nuclear



translocation of SMAD 1, which is responsible for BMP-2 induced osteogenesis [183]. Restricting cell spreading, reducing ROCK signaling, or inhibiting the cytoskeletal tension prevented the BMP-2 induced SMAD 1 phosphorylation, SMAD 1 dimerization with SMAD4, and SMAD 1 translocation into the nucleus [183] (Fig. 3).

The anabolic growth factor, Wnt5a, stimulates osteoblast differentiation of human progenitors through ROCK activity [186] (Fig. 3). Osteogenic differentiation of hMSCs increases matrix stiffness as evidenced by the level of type I collagen and osteocalcin (OCN), increase in ROCK, FAK and ERK 1/2 activities and in mineralization [187]. Inhibition of FAK, a mediator of osteogenic differentiation, and of ROCK, resulted in decreased expression of osteogenic markers during osteogenic induction. In addition, FAK affects osteogenic differentiation through ERK 1/2, while ROCK regulates both FAK and ERK 1/2. Furthermore,  $\alpha$ 2 integrin was upregulated on matrix stiffness during osteogenic induction and its knockdown by siRNA down-regulated osteogenic phenotype through activation of ROCK, FAK and ERK 1/2 [187].

These findings are consistent with the hypothesis that matrix rigidity affects intracellular signaling through ROCK-dependent mechanotransduction events mediated by integrins and is decisive for the fate of hMSCs. Alternatively, ROCKs may also be involved in induction of chondrogenesis in MSCs. In hMSCs stimulated by transforming growth factor- $\beta$ 1 (TGF- $\beta$ 1) to undergo chondrocyte differentiation (Fig. 3), inhibition of ROCKs with Y27632 blocked expression of the chondrogenic transcription factor Sox9, type I collagen, type II collagen and aggrecan together with inhibition of SMAD2/3 phosphorylation [188]. Thus, inhibition of ROCK in hMSCs prevented osteogenic [183] as well as chondrogenic [188] differentiation. Adherent and well-spread hMSCs stimulated with TGF $\beta$ 3 exhibited increased smooth muscle cell (SMC)-specific gene expression pattern. Cells cultured onto micropatterned substrates, which prevented cell spreading and flattening, were characterized by increased expression of chondrogenic genes [189]. Cells undergoing SMC differentiation have shown little change in RhoA but higher Rac1 activity than that of chondrogenic cells [189]. Rac1 activation prevented chondrogenesis, and was necessary and sufficient to promote SMC differentiation [189].

## 5.2. ROCKs and osteoblasts

Mesenchymal-to-epithelial transition (MET) in cultured osteosarcoma Saos-2 cells is induced by Pax 3 transcription factor and by alteration of signal transduction pathways that regulate cytoskeleton remodeling. Actomyosin contractility induced via RhoA/ROCK signaling is required for the formation of circumferential actin bundles, epithelial discoid cell shape and regulation of membrane protrusions in Saos-2 cells

[190]. An AMPK activator, 5-aminoimidazole-4-carboxamide- $\beta$ -D-ribo-nucleoside (AICAR), and fasudil hydrochloride stimulated endothelial nitric oxide synthase (eNOS), BMP-2, and OCN mRNA expression, and mineralization in osteoblastic MC3T3-E1 cells. Also, measurement of ROCKs activities revealed that addition of both AICAR and fasudil significantly suppressed phosphorylation of the myosin-binding subunit of myosin phosphatase, a ROCK substrate [191]. These findings indicate that both the AMPK activator and the ROCK inhibitor stimulate mineralization of osteoblasts which is consistent with other reports. Indeed, expression of a dominant-negative ROCK mutant in mouse stromal ST2 cells induced osteoblastic differentiation, whereas expression of a constitutively active ROCK mutant attenuated osteoblastic differentiation. The function of BMPs is modulated by RhoA and ROCK [192,193]. Addition of Y-27632 enhanced ectopic bone formation induced by BMP-2. RhoA/ROCK signaling negatively regulates BMP-induced osteoblastic differentiation (Fig. 4). The function of RhoA is also regulated by neogenin, a receptor for BMPs and an activator of RhoA. Knockdown of neogenin in mouse C2C12 myoblasts stimulated BMP-2-induced osteoblastic differentiation, whereas overexpression suppressed it [193]. Inhibition of Rac1 activated BMP-2-induced osteoblastic differentiation in C2C12 myoblasts [194]. It is not clear which effectors were affected by Rac1 [191–193]. In addition the RhoA/ROCK pathway is regulated by parathyroid hormone (PTH). PTH regulates hypoxia-inducible factor driven signaling through RhoA/ROCK in osteoblasts (Fig. 4), by disrupting the actin cytoskeleton and reducing stress fibers through a cAMP-dependent mechanism [195]. Taken together, these findings tend to suggest that inhibition of the RhoA/ROCK pathway stimulates osteoblastic differentiation (Fig. 4).

In bone, osteoblasts can sense and respond to mechanical loads to maintain and regenerate bone tissue. Osteoblasts can regulate their mechanosensitivity to continued load through P2Y2R-mediated activation of the RhoA signaling cascade, leading to actin stress fiber formation and increased cell stiffness [196]. P2X7R action induces NFATc1, PI3K/AKT, ROCK and VEGF pathways in osteoblasts promoting either primary tumor development or osteoblastic lesions [197]. Deletion of P2Y13R affects both osteoblasts and osteoclasts and leads to less trabecular bone in mice. Down-regulation of RhoA/ROCK signaling and a reduced ratio of RANKL/OPG may be the possible molecular mechanisms behind these alternations. These may affect the downstream ERK-MAPK signaling and leads to dysfunction and impaired differentiation of bone cells, particularly osteoblasts [198].

Rho levels are considerably higher in cells embedded in immobilized collagen gels compared to those in floating collagen gels that have not been subjected to mechanical stress [199]. Addition of Y-27632 to osteoblast-like MG-63 cells embedded in stress-relaxed collagen gels produced a dose-dependent inhibition of contraction [200]. The high

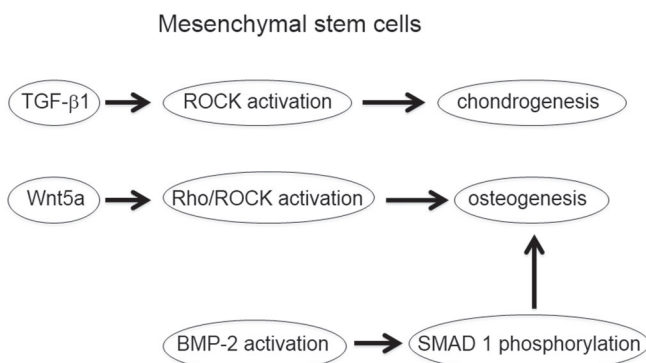


**Fig. 3.** Functions of Rho-associated coiled-coil kinases in human mesenchymal stem cells (hMSCs). The hMSCs stimulated by transforming growth factor- $\beta$ 1 (TGF- $\beta$ 1) undergo chondrocyte differentiation. Wnt5a, stimulates osteoblast differentiation of human progenitors through ROCK activity. The treatment of hMSCs with BMP-2 induces a Rho/ROCK-mediated cell tension which is responsible for BMP-2 induced osteogenesis.

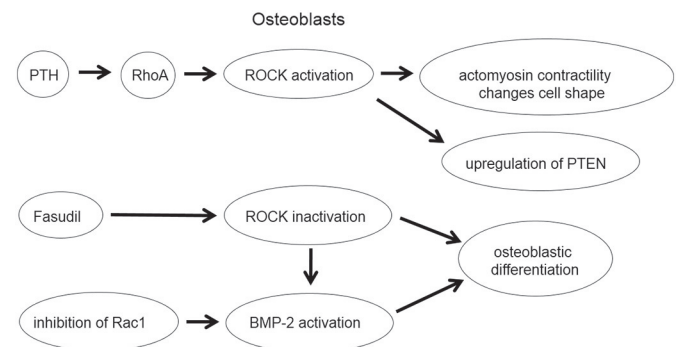


**Fig. 4.** Functions of Rho family of small GTPases and Rho-associated coiled-coil kinases in osteoblasts. ROCK upregulates the activity of phosphatase and tensin homolog (PTEN) and actomyosin contractility in osteoblasts. ROCK inhibitors (fasudil) stimulate mineralization of osteoblasts. The function of BMPs is modulated by RhoA and ROCK. RhoA/ROCK signaling negatively regulates BMP-induced osteoblastic differentiation. Inhibition of Rac1 activates BMP-2-induced osteoblastic differentiation in C2C12 myoblasts.

RhoA activity in cells poorly attached to substrates caused an increase in the activity of ROCK, that upregulated the activity of phosphatase and tensin homolog (PTEN) [201]. As a result, activated PTEN down regulated the activity and phosphorylation of PI3K/Akt, which are essential for cell proliferation. The RhoA-ROCK-PTEN pathway (Fig. 4) acts as a molecular switch to control cell proliferation and determine anchorage dependence. In cells that are poorly attached to substrates, its inhibition is sufficient to restore cell proliferation without the need for physico-chemical modification of the material surface [201]. Moreover, upregulation of PTEN may attenuate adhesion, migration and invasion capabilities of osteosarcoma cells [202].

Numerous miRNAs that regulate ROCK1 expression and activity have been identified in cancer tissues [203]. ROCK1 is a target of miR-145 [204], miR-335 [205] and miR-340 [206,207] in osteosarcoma. Decreased expression of miRNAs in cancer tissues leads to increased ROCK expression/activity and increased migration, invasion, or proliferation. This cell phenotype can be rescued by overexpression of miRNAs, inhibition of ROCK1 by Y27632 or ROCK1 siRNA [204,207].

### 5.3. ROCKs and chondrocytes

Rho GTPases in chondrocytes transduce the signals from extracellular matrix to the actin skeleton and control cellular activities such as cell cycle, gene expression and apoptosis [208]. Specific inhibitors such as ML141 for Cdc42, NSC23766 for Rac1, toxin C3 for RhoA and Y-27632 for ROCK are often employed to differentiate the activities of various members of Rho GTPases and ROCK. Rac1, Cdc42, and RhoA are present in chondrocytes and levels of active Rac1 and Cdc42 increase with maturation [209]. Mature chondrocytes are rounded or polygonal and display characteristic cortical actin organization, while the organization of actin stress fibers, at least *in vitro*, has been associated with de-differentiation of chondrocytes to a fibroblast-like phenotype [17,18]. Very often RhoA promotes stress fiber formation and inhibits chondrocyte differentiation [210,211] while, in contrast, Rac1 and Cdc42 promote chondrocyte hypertrophy [212–214] (Fig. 5). miRNAs may regulate Rho GTPase activities at least in part through regulating RhoA and RhoA/Rac1 cross-talk [215]. For example, miR-34a is upregulated by chondro-inhibition, whereas miR-34a knockdown stimulates transition of cells from a fibroblastoid morphology to a rounded or polygonal morphology. Rac1 regulates chondrocyte proliferation through Rac1-mediated ERK1/2 pathway [216–218]. Early and late chondrocyte proliferation can be initiated via Rac1-mediated p38 MAP kinases [219–221]. Rac1 and, to a lesser extent, Cdc42, transactivate MEKK1, which is, in turn, responsible for activation of mitogen-activated protein kinase 7 [222]. Rac1 accelerates osteoarthritis (OA) development [223]

and can promote cartilage matrix destruction by stimulating MMP-13 production [224], while inhibition of Rac1 by NSC23766 protects cartilage from OA in C57L/6 mice models of OA.  $\beta$ -Catenin might partially function downstream of activated Rac1 in modulating pathological changes in chondrocytes [223]. This is consistent with the previous finding that Rac1 can increase  $\beta$ -catenin activation and that Wnt/ $\beta$ -catenin and Rac1 signaling cross-talk in chondrocytes [209]. Furthermore, ofloxacin, was found to induce the juvenile rabbit joint chondrocyte apoptosis in three dimensional culture system, activating the EGFR-Vav2-Rac1 pathway [225].

The association of Cdc42 with actin cytoskeleton architecture and phenotypic expression is supported by the evidence from articular chondrocytes stimulation of which by either the catabolic cytokines, IL-1 or tumor necrosis factor, or by shear stress, activates MAP kinase subgroups JNK, p38, and ERK, which is consistent with signaling through Cdc42 [226–229]. Cdc42 is essential for chondrogenesis and interdigital programmed cell death during limb development [230] as well as for cartilage development during endochondral bone formation [231]. Treatment of chondrocytes from horse femoropatellar joints with insulin-like growth factor (IGF-1) induced a decrease in GTP-bound Cdc42 suggesting a link between the IGF-1 and Cdc42 signaling pathways [232,233]. Mutation in *Fgd1* which encodes a guanine nucleotide exchange factor results in faciogenital dysplasia. A loss of FGD1 activity disrupted Cdc42 signaling [234]. TGF- $\beta$ /Cdc42 signaling pathways were enhanced in small mother against decapentaplegic 3 (Smad3) gene knockout (Smad3(ex8/ex8)) mice, which display a phenotype similar to human OA [235].

RhoA promotes fibroblastoid cell shape and the formation of actin stress fibers. Overexpression of RhoA inhibited both early chondrogenesis and hypertrophic chondrocyte differentiation [17] (Fig. 5). Both inhibition of Rho by toxin C3 (a RhoA inhibitor) and inhibition of ROCKs by Y27632 in primary mouse chondrocytes increased cell spreading on a bone sialoprotein (BSP)-coated surface [236]. However, ROCK inhibition was not able to mimic all effects of Rho GTPase inhibition [236]. Rho inhibition by toxin C3, disturbed the actin cytoskeleton in chondrocytes leading to the loss of intracellular actin fibers and prominent filamentous actin structures at the cell periphery. This was not observed with ROCK inhibition in chondrocytes [236]. RhoA overexpression increased proliferation and delayed hypertrophic differentiation, as evidenced by decreased TNAP activity, mineralization, and expression of the hypertrophic markers: collagen X, BSP, and MMP-13 [237]. In contrast, inhibition of ROCKs by Y27632 diminished chondrocyte proliferation, accelerated hypertrophic differentiation and partially rescued the effects of RhoA overexpression in chondrogenic ATDC5 cells [237]. Expression of ROCK 1 was significantly increased in

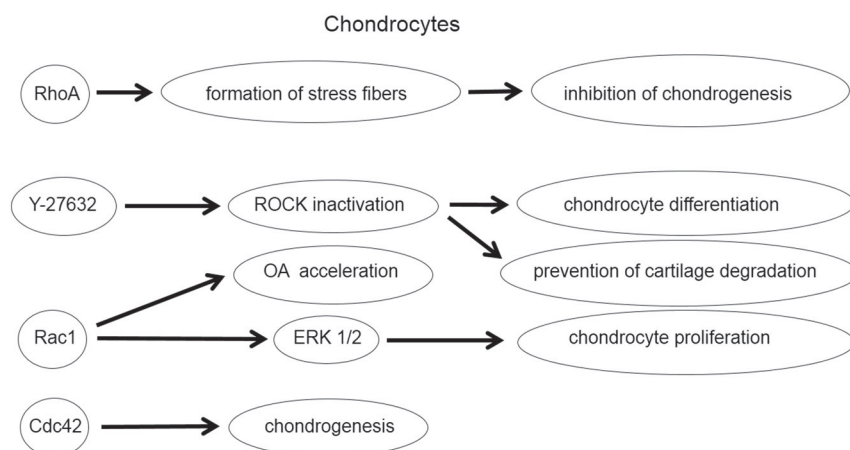


**Fig. 5.** Functions of Rho family of small GTPases and Rho-associated coiled-coil kinases in chondrocytes. RhoA activates the formation of stress fibers, which has been associated with differentiation of chondrocytes. Inhibition of ROCK by Y-27632 induces chondrocyte differentiation and prevents cartilage degradation. Rac-1 accelerates osteoarthritis (OA) and through ERK 1/2 pathway activates chondrocyte proliferation through ERK 1/2 pathway. Cdc42 favors chondrogenesis.



developmental dysplasia of the hip acetabulum chondrocytes compared to normal cells [238]. Inhibition of ROCK signaling by Y-27632 in ATDC5 cells produced spherical cells (a hallmark of differentiated chondrocytes), increased transcription of Sox9, and glycosaminoglycan accumulation [239]. RhoA overexpression inhibited the expression of collagen II, aggrecan, chondrogenic transcription factors L-Sox5 and Sox6 in these cells. ROCK inhibition by Y-27632 in ATDC5 cells resulted in an increase in all the above markers [239]. The RhoA/ROCK pathway suppresses glycosaminoglycan synthesis, a marker of early chondrogenic differentiation [239]. It was proposed that the RhoA/ROCK pathway repressed chondrogenic gene expression in general, likely through down-regulation of Sox9 levels [240]. ROCK inhibition in ATDC5 cells and primary chondrocytes in monolayer culture as well as in mesenchymal limb buds cells cultured in three-dimensional micromass cultures, all resulted in an increased level of Sox9 mRNA. However, chondrocytes in micromass cultures, in contrast to monolayer cultures, exhibited reduced expression of Sox9 target genes despite increased levels of Sox9 mRNA, which indicates that RhoA/ROCK signaling effects are dependent of the type of cells and type of culture [240]. Upon repeated passage, primary caudal sternal chondrocytes (isolated from 14-day-old chicken embryos) change their round shape to a fibroblast morphology [241]. The expression of collagen II, aggrecan, Sox9, Sox5, and Sox6 genes was lost between the P1 and P4 passage. This was correlated with an increase in total RhoA protein and active GTP-bound RhoA. There is an inverse correlation between the levels of active RhoA protein in a cell and the expression of both chondrogenic transcription factors and differentiation markers [241] (Fig. 5). Indeed, culture of dedifferentiated chondrocytes in alginate gel induces a precipitous loss of RhoA protein and a loss of stress fibers concomitant with re-expression of the chondrocyte differentiation program. ROCKs were shown to phosphorylate Ser181 of Sox9 confirming a link between ROCK and Sox-9 [242,243].

Recent findings suggest that inhibition of Rho/ROCK activity can prevent cartilage degradation (Fig. 5). Y-27632 prevents dedifferentiation of monolayer-cultured chondrocytes, and may help to maintain the chondrocytic phenotype *in vitro* for chondrocyte-based regeneration therapy [244]. Transforming growth factor- $\alpha$  (TGF $\alpha$ ) levels are increased in the synovium and synovial fluid of patients with OA or rheumatoid arthritis (RA) [245,246]. Upregulation of the catabolic activity of TGF- $\alpha$ , a strong stimulator of cartilage degradation, is prevented by ROCK inhibition by Y27632, RhoA inhibition by C3, p38 MAPK (mitogen activated protein kinase) inhibition by SB202190 and PI3K (phosphatidylinositol-4,5-bisphosphate 3-kinase) inhibition by LY294002 but not by MEK (MAPK/ERK kinase)/ERK (extracellular-signal-regulated kinase) inhibition by U0126 in rat chondrocytes and in osteochondral explants. The inhibition prevents excess type II collagen and aggrecan degradation by MMP-13 in response to TGF- $\alpha$  [247]. Stimulation of EGFR signaling in articular chondrocytes by TGF- $\alpha$  results in the activation of Rho/ROCK, MEK/ERK, PI3K and p38 MAPK pathways [247]. Disruption of chondrocyte proliferation and/or differentiation by gene mutations commonly results in chondrodysplasias [29–31].

Excessive mechanical stress on the cartilage can cause matrix degradation leading to OA [248]. Cyclic compression caused Rho activation, p38 MAPK phosphorylation and MMP-13 expression that were blocked by Y-27632 or SB202190 in bovine metacarpal phalangeal articular cartilage explants [248]. AS182802, a selective ROCK inhibitor, prevented cartilage damage induced by monoiodoacetate in rat model of OA, suggesting a possible clinical application for the treatment of OA [249]. Treatment with Y-27632 suppressed MMP-3 expression and increased that of aggrecan, indicating that ROCKs inhibition affected the balance between degradation and synthesis of cartilaginous extracellular matrix [250].

There is some experimental evidence of ROCKs action during cytoskeletal reorganization in chondrocytes. Ultrasound stimulation disrupted actin stress fibers of bovine chondrocytes seeded on 3D chitosan matrix in a ROCK dependent manner since this effect was sensitive

to Y-27632 [251]. Chondrocytes stimulated with leptin exhibited an epithelioid morphology with increased cellular spreading. Leptin activates the RhoA/ROCK/LIMK/cofilin pathway, resulting in cytoskeletal reorganization in chondrocytes [252]. As already mentioned [236], both the inhibition of RhoA by toxin C3 or ROCKs inhibition by Y-27632 in primary chondrocytes from mice increase cell spreading on BSP-coated surface, while only ROCK inhibition increase cell spreading on fibronectin. RhoA inhibition did not increase cell spreading on fibronectin indicating that Rho action is dependent on the surface type.

#### 5.4. ROCKs and osteocytes and lining cells

So far, there is no direct experimental evidence of Rho-associated coiled-coil containing kinase activities in osteocytes. As hypothesized, proteins which may be regulated by Rho kinases in osteocytes are focal adhesion kinases (FAK) and integrins [253]. Among FAK related proteins in osteocytes, there is proline-rich tyrosine kinase 2 (Pyk2) that induces reorganization of the cytoskeleton, cell detachment and apoptosis and may serve as an “off switch” to suppress the anabolic response of a bone subjected to mechanical load [254].

#### 5.5. ROCKs and osteoclasts

Different GTPases of the Rho family act at the subsequent steps of osteoclastogenesis i.e., during the fusion of mononuclear cells into multinucleated OCs, podosome organization, migration and polarization, consistent with the model that separates differentiation and podosome dynamics from osteoclast adhesion [255,256]. Activated Rac mediated lamellipodia formation and cytoskeletal reorganization in OCs [204–206,257–259] while Cdc42 stimulated filopodia formation and Rho GTPases-mediated retraction fiber assembly [260]. RhoA stimulated actin cable assembly and cell contraction while the Rho inhibitor, C3 transferase, induced the loss of actin cables. Bac1 macrophages have adhesion sites containing beta1 integrin, pp125FAK, paxillin, vinculin, and tyrosine phosphorylated proteins. The focal complexes were disassembled in cells injected with Cdc42 or Rac1 mutants [260]. Cdc42, Rac and RhoA regulate the formation of distinct actin filament-based structures. Cdc42 and Rac are also required for the attachment of adhesion sites to the extracellular matrix. As reviewed [41,42], Rac1 and Rac2 are essential for the formation of the podosome belt (PB) and for bone resorption [261–264] (Fig. 6). Deletion of both Rac1 and Rac2 in mature osteoclasts causes petroses, an age-dependent change in osteoclast number, and a reduced number of osteoblasts *in vivo*, which indicates that Rac1 and Rac2 are indispensable in skeletal metabolism [265]. Rac1, Rac2, Cdc42, RhoA and RhoU act during migration and fusion of mononuclear cells into multinucleated cells. In addition to Arf6 and Rab7, the same Rho GTPases (Rac1, Rac2, Cdc42, RhoA and RhoU) act during the formation of PB and the sealing zone (SZ) (Fig. 6). In contrast, only Cdc42, Rac1 and Rab7 are involved in polarization and bone resorption, while Cdc42 and Rac1 prevent osteoclast apoptosis [41,42]. Several mechanisms trigger the activation of Rho GTPases via RANKL, or via effectors such as Dock5, Par3, PIP2, etc. Dock5, is of particular interest since it is a target for intervention in osteoporosis treatment. Cytoskeleton has a complex relationship to vesicle trafficking regulated by Rab and Arf (ADP-ribosylation factor) GTPases. Dock proteins regulate actin cytoskeleton, cell adhesion and migration [266]. Dock family proteins, comprising 11 members in mammals, named Dock1 to Dock11, are exchange factors (GEF) for the Rho GTPases Rac and Cdc42 [266]. GEF Dock5 is essential for the formation of SZ *in vitro* and *in vivo*. Indeed, inhibition of Rac1 activation by Dock5 can reduce bone resorption by OCs. The expression of Dock5 is restricted mainly to OCs, and it is absent from osteoblasts. Therefore, development of Dock5 inhibitors appears to be an alternative approach to generate antiresorptive molecules that would target OC activity with reduced side effects [267]. Treatment with osteoprotegerin reduced bone resorption and caused a significant

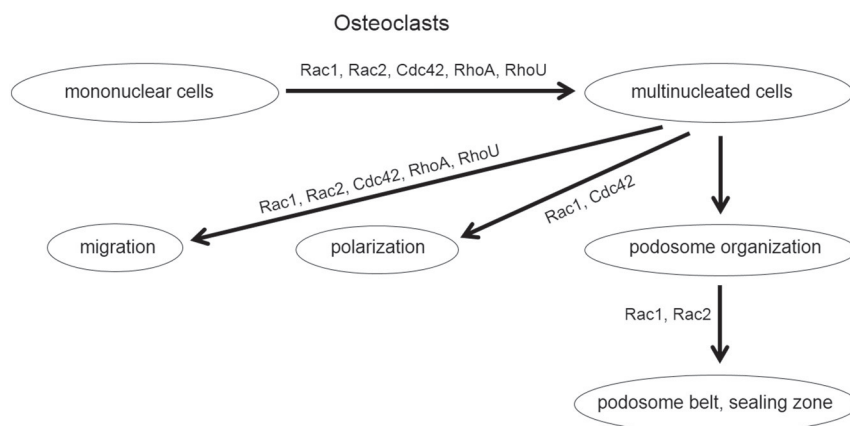


**Fig. 6.** Functions of Rho family of small GTPases in osteoclasts. Rac1, Rac2, Cdc42, RhoA, RhoU act during fusion of mononuclear cells into multinucleated cells and during migration. Rac1 and Cdc42 can induce polarization and bone resorption. Rac1 and Rac2 act during formation of podosome belt and sealing zone.

decrease in the expression of Dock5, MMP-9, Rho GTPases, ROCK1 and ROCK2 [268,269].

Primary RhoE-deficient OCs delivered evidence that RhoE stimulates OC migration and bone resorption by maintaining fast actin turnover in podosomes. Moreover, RhoE activated cofilin, a podosome component, by inhibiting its ROCK-mediated phosphorylation. In conclusion, the RhoE-ROCK-cofilin pathway promotes podosome dynamics and patterning, inducing OC migration, SZ formation, and bone resorption [270]. Bone metastasis in breast cancers is often accelerated by TGF- $\beta$  signalling that activates Rho and enhances the parathyroid hormone-like hormone (PTHrP) [271,272]. Such activation affects the osteoblast/osteoclast balance, resulting in an osteolytic vicinity of tumour cells [271]. Inhibition of Rho-ROCK, either by C3 treatment to inhibit RhoA or by Y27632 or fasudil treatments to inhibit ROCK, reduced PTHrP production and breast cancer bone metastasis *in vitro* and *in vivo* [271–273]. In osteoclasts, ADP is a powerful osteolytic agent acting via the P2Y<sub>1</sub> receptor [198,274]. Deletion of the P2Y<sub>13</sub> receptor leads to less trabecular bone in P2Y<sub>13</sub><sup>-/-</sup> mice, by affecting both osteoblasts and osteoclasts and by decreasing RhoA [274]. It was suggested that the decrease in RhoA/ROCK signaling reduces ERK activity, diminishes runt-related transcription factor 2 activity, and alters TNAP activity in osteoblasts [275]. Decrease in ERK action via RhoA/ROCK signaling impairs survival and induces apoptosis in osteoclasts by affecting the formation of a ruffled border and the maintenance of cell polarity [276, 277].

### 5.6. ROCKs and cell adhesion to extracellular matrix

Cell adhesion to ECM results in clustering of integrins in focal adhesions, which are sites of signal transduction and integration where signaling cascades are initiated [44]. Changes in osteoblast adhesion and reorganization of the F-actin cytoskeleton in response to altered topography occur prior to osteoblast differentiation and are regulated by Rac and RhoA (through ROCKs). During osteogenic differentiation matrix stiffness is regulated by integrin-mediated mechanotransduction and the ROCK-MAPK-ERK pathway [187]. Inhibition of RhoA and ROCKs in MC3T3-E1 cells cultured on collagen-functionalized poly(ethylene glycol) hydrogels decreased ERK activity, while active RhoA increased it. Inhibition of RhoA by C3 toxin and inhibition of ROCK by Y27632 together with downregulation of the MAPK pathway slowed down osteogenesis as evidenced by altered OCN and BSP gene expression, TNAP activity, and mineralization [275]. These findings suggest that ECM rigidity regulates osteogenic differentiation through MAPK activation downstream of the RhoA/ROCK signaling pathway [275]. When activated by kindlin-2, Rac induces cell adhesion, spreading and proliferation of osteoblasts [278]. Indeed, its inhibition reduced osteoblast-like MC3T3-E1 cell adhesion, spreading, and proliferation. Rac negatively

regulates TGF- $\beta$ -stimulated VEGF synthesis via inhibition of p38 MAP kinase in MC3T3-E1 cells [279]. Very often, focal contact formation and polymerization of actin at the cell periphery is regulated by Rac, while activation of RhoA/ROCK is linked to the formation of F-actin stress fibers and development of focal contacts into focal adhesions by modulating MLC phosphorylation. ROCK inhibitors stimulate migration of human cultured osteoblastic cells (HOB and Saos-2 cells) by regulating actomyosin activity [280]. Inhibition of ROCK signaling could improve bone formation around implanted metals [281]. ROCK inhibitors decrease MLC phosphorylation, and then induce actin reorganization and focal contact disassembly, as well as upregulation of MLCK levels. MLCK is active during stimulation of cell migration. As a consequence, osteoblasts change their shape and migrate more rapidly after ROCK inhibitor treatment. Other proteins and kinases such as focal adhesion kinase (FAK), Src, and/or paxillin may also be involved in the ROCK signaling pathway [280]. The RhoA/ROCK pathway is activated during mesenchymal stem cell and osteoblast orientation on nanometric surfaces. The RhoA/ROCK pathway regulates contact guidance of bone-related cells on metallic substrates to a varying extent depending on the cell type and dimensions of the substrate pattern [282].

### 6. Perspectives

The RhoA/ROCK pathway is the most investigated pathway [109–118] involving the Rho family of GTPases and their downstream effectors. Generally, the RhoA/ROCK pathway, as exemplified in Fig. 2, activates formation of stress fibers and actomyosin contraction in chondrocytes [17,18,210,211,251] and in osteoblasts [190,196]. Pharmacological inhibition of ROCK by Y27632 or by fasudil has been employed in hMSCs [188], chondrocytes [17,218,236,239,240,244,247, 251] osteoblasts [192,193,200,204,207], and in osteoclasts [271–273]. However, it does not allow to differentiate between the often distinct activities [98,128,135–148] of ROCK1 and ROCK2 [169,170]. The RhoA/ROCK pathway has been shown to decrease the expression of chondrogenic genes in chondrocytes [240], osteoblastic markers in MC3T3-E1 [191] and impair osteoblastic differentiation [191,193]. This is in contrast to hMSCs where inhibition of ROCK prevented the osteogenic [183] and chondrogenic [188] differentiation. These findings indicate that at an earlier stage of lineage commitment, as in the case of hMSCs, the RhoA/ROCK pathway is osteogenic or chondrogenic, while in differentiated osteoblasts and in chondrocytes, the RhoA/ROCK pathway acts to suppress osteoblastic and chondrogenic markers. Inhibitors of ROCKs in differentiated cells are expected to stimulate osteogenic markers and to restrict cell invasion. In this respect the proof of concept that inhibition of the ROCK by Y27632 or fasudil prevents cartilage degradation [244,248–250] and restricts cancer cell migration and invasion [204,207,271–273] have been reported. Treatment with

osteoprotegerin, which reduces bone resorption and causes a decrease in the level and activity of Rho GTPases, ROCK1 and ROCK2, suggests that inhibition of ROCK may also prevent osteoporosis [268,269]. Therefore, a local delivery of ROCK inhibitor targeting ROCK needs to be elaborated to bypass the systemic side effects of ROCK inhibitors. The RhoE/ROCK/cofilin pathway, which promotes podosome dynamics and patterning, stimulates OC migration, SZ formation, and bone resorption, [270] is in the focus of attention as a possible target of intervention in bone resorption, in the context of osteoporosis.

In addition, members of the Rho family of GTPases such Rac1, Rac2, Rac3 and Cdc42, which act upstream of ROCK and/or other protein effectors, regulate morphology, motility and adhesion of chondrocytes [209,212–214,216–221,230–232] and osseous cells [41,42,194,204–206,257–265]. They may compensate for the actions of RhoA, affecting directly or indirectly the actions of ROCKs and other protein effectors.

From a perspective point of view, there are still many unanswered questions concerning the possible effects of the RhoA/ROCK pathway activity in osseous and cartilage tissues, especially during bone formation. Of particular interest are the possible actions of RhoA/ROCK pathway during matrix vesicle release. We speculate that proteins of the submembranous cytoskeletal system, which are substrates for these kinases, such as non-muscle myosin II, may be considered as vesicular transport platforms that control different steps of receptor transport and sorting to different cellular organelles [237]. Also proteins and kinases of the cellular adhesion system such as FAK, vinculin, or paxillin may be involved in the ROCK signaling pathway and be responsible for the association of plasma membrane integrins with the actin cytoskeleton in cell-cell as well as cell-extracellular matrix contact sites [217,283]. Oncogenic perturbation (suppression) of the ROCK pathway via p120-dependent mechanisms ultimately resulted in constitutive activation of the actin severing protein, cofilin, whose activity was necessary but not sufficient to permit the transition to anchorage independence and, presumably, tumorigenicity. Regulation of membrane remodeling is also mediated in part by Arf GAPs (GTPase-activating proteins) that act as upstream regulators of the Rho family proteins and provide a scaffold for Rho effectors and exchange factors. With multiple functional elements, the Arf GAPs could integrate signals and biochemical activities that result in coordinated changes in actin and membranes necessary for a wide range of cellular functions [284]. The occurrence of vesicular trafficking molecules and of the on-site protein synthetic machinery suggests that cell polarization and apical targeting are required for the incorporation of specific lipids and proteins at the site of MV formation. MV release from Saos-2 cells was stimulated by inhibition of filament polymerization by cytochalasin D [65]. Probably the detachment of actin filaments leads to a drop in membrane tension, indispensable to MV formation. Moreover, MV release from microvilli-like membranes may be driven by actin-severing proteins (gelsolin, cofilin 1) and contractile motor proteins (myosins) [66].

## 7. Conclusions

Mineralization is a multifactorial and complex process that results in the deposition of mineral crystals in the extracellular matrix of various tissues. Ectopic calcification, occurring in many soft tissues including articular cartilage, cardiovascular tissues, kidney, ligaments, and tendons is a process that shares similarities with physiological formation of bones, teeth and certain areas of cartilage [285]. Therefore, understanding of factors and mechanisms of the Rho GTPase pathway that regulates the mineralization process is essential for the development of alternative therapeutic strategies to prevent or inhibit pathological mineralization and cartilage degradation.

## Conflict of interest

The authors declare no conflict of interest.

## Transparency document

The Transparency document associated with this article can be found, in online version.

## Acknowledgements

This research was supported by the Nencki Institute of Experimental Biology, Polish Academy of Sciences and by the Hubert Curien Partnership Programme between Governments of the Republic of Poland and the Republic of France POLONIUM (grant no 33540RG).

## References

- [1] S. Das, J.C. Crockett, Osteoporosis – a current view of pharmacological prevention and treatment, *Drug Des. Devel. Ther.* 7 (2013) 435–448.
- [2] H. Orimo, The mechanism of mineralization and the role of alkaline phosphatase in health and disease, *J. Nippon Med. Sch.* 77 (2010) 4–12.
- [3] H.C. Anderson, The role of matrix vesicles in physiological and pathological calcification, *Curr. Opin. Orthop.* 18 (2007) 428–433.
- [4] M. Whyte, Physiological role of alkaline phosphatase explored in hypophosphatasia, *Ann. N. Y. Acad. Sci.* 192 (2010) 190–200.
- [5] H.C. Andersen, D. Mulhall, R. Garimella, Role of extracellular membrane vesicles in the pathogenesis of various diseases, including cancer, renal diseases, atherosclerosis, and arthritis, *Lab. Invest.* 90 (2011) 1549–1557.
- [6] S. Mebarek, E. Hamade, C. Thouverey, J. Bandorowicz-Pikula, S. Pikula, D. Magne, R. Buchet, Ankylosingspondylarthritis, late osteoarthritis, vascular calcification, chondrocalcinosis and pseudo gout: Toward a possible drug therapy, *Curr. Med. Chem.* 18 (2011) 2196–2203.
- [7] H.W. Sampson, R.W. Davis, D.C. Dufner, Spondyloarthropathy in progressive ankylosis mice: ultrastructural features of the intervertebral disk, *Acta Anat. (Basel)* 141 (1991) 36–41.
- [8] S.Y. Ali, Apatite crystal nodules in arthritic cartilage, *Eur. J. Rheumatol. Inflamm.* 14 (1978) 115–119.
- [9] D. Magne, M. Julien, C. Vinatier, F. Merhi-Soussi, P. Weiss, J. Guicheux, Cartilage formation in growth plate and arteries: from physiology to pathology, *Bioessays* 27 (2005) 708–716.
- [10] J.S. Shao, J. Cai, D.A. Towler, Molecular mechanisms of vascular calcification: lessons learned from the aorta, *Arterioscler. Thromb. Vasc. Biol.* 26 (2006) 1423–1430.
- [11] S.E.P. New, E. Aikawa, Role of extracellular vesicles in *de novo* mineralization. An additional novel mechanism of cardiovascular calcification, *Arterioscler. Thromb. Vasc. Biol.* 33 (2013) 1753–1758.
- [12] J.E. Everhart, D.J. Pettitt, W.C. Knowler, F.A. Rose, P.H. Bennett, Medial arterial calcification and its association with mortality and complications of diabetes, *Diabetologia* 31 (1988) 16–23.
- [13] S. Lehto, L. Niskanen, M. Suhonen, T. Rönnemaa, M. Laakso, Medial artery calcification. A neglected harbinger of cardiovascular complications in non-insulin-dependent diabetes mellitus, *Arterioscler. Thromb. Vasc. Biol.* 16 (1996) 978–983.
- [14] G.S. Mintz, J.A. Kovach, S.P. Javier, A.D. Pichard, K.M. Kent, J.J. Popma, L.F. Salter, M.B. Leon, Mechanisms of lumen enlargement after excimer laser coronary angioplasty. An intravascular ultrasound study, *Circulation* 92 (1995) 3408–3414.
- [15] M. Jeziorska, C. McCollum, D.E. Woolley, Calcification in atherosclerotic plaque of human carotid arteries: associations with mast cells and macrophages, *J. Pathol.* 185 (1998) 10–17.
- [16] T. Yamamoto, Y. Ugawa, K. Yamashiro, M. Shimoe, K. Tomikawa, S. Hongo, S. Kochi, H. Ideguchi, H. Maeda, S. Takashiba, Osteogenic differentiation regulated by Rho-kinase in periodontal ligament cells, *Differentiation* 88 (2014) 33–41.
- [17] F. Beier, R.F. Loeser, Biology and pathology of Rho GTPase, PI-3 Kinase-A and MAP kinase signaling pathways in chondrocytes, *J. Cell. Biochem.* 110 (2010) 573–580.
- [18] R. McBeath, D.M. Pirone, C.M. Nelson, K. Bhadriraju, C.S. Chen, Cell shape, cytoskeletal tension, and RhoA regulate stem cell lineage commitment, *Dev. Cell* 6 (2004) 483–495.
- [19] M. Fakhry, E. Hamade, B. Badran, R. Buchet, D. Magne, Molecular mechanisms of mesenchymal stem cell differentiation towards osteoblasts, *World J Stem Cells* 5 (2013) 136–148.
- [20] S.L. Teitelbaum, Osteoclasts: what do they do and how do they do it? *Am. J. Pathol.* 170 (2007) 427–435.
- [21] T.J. Martin, N.A. Sims, Osteoclast-derived activity in the coupling of bone formation to resorption, *Trends Mol. Med.* 11 (2005) 76–81.
- [22] M.A. Karsdal, T.J. Martin, J. Bollerslev, C. Christiansen, K. Henriksen, Are nonresorbing osteoclasts sources of bone anabolic activity? *J. Bone Miner. Res.* 22 (2007) 487–494.
- [23] H. Zhao, Membrane trafficking in osteoblasts and osteoclasts: new avenues for understanding and treating skeletal diseases, *Traffic* 13 (2012) 1307–1314.
- [24] J. Li, X. Liu, B. Zuo, L. Zhang, The role of bone marrow microenvironment in governing the balance between osteoblastogenesis and adipogenesis, *Aging Dis.* 2015 (7) (2015) 514–525.
- [25] R.L. Jilka, R.S. Weinstein, A.M. Parfitt, S.C. Manolagas, Quantifying osteoblast and osteocyte apoptosis: challenges and rewards, *J. Bone Miner. Res.* 22 (2007) 1492–1501.
- [26] R.L. Jilka, B. Noble, R.S. Weinstein, Osteocyte apoptosis, *Bone* 54 (2013) 264–271.



- [27] A. Nazempour, B.J. Van Wie, Chondrocytes, mesenchymal stem cells, and their combination in articular cartilage regenerative medicine, *Ann. Biomed. Eng.* 44 (2016) 1325–1354.
- [28] X. Tang, L. Fan, M. Pei, L. Zeng, Z. Ge, Evolving concepts of chondrogenic differentiation: history, state-of-the-art and future perspectives, *Eur. Cell. Mater.* 30 (2015) 12–27.
- [29] S. Mundlos, B.R. Olsen, Heritable diseases of the skeleton. Part I: molecular insights into skeletal development—transcription factors and signaling pathways, *FASEB J.* 11 (1997) 125–132.
- [30] S. Mundlos, B.R. Olsen, Heritable diseases of the skeleton. Part II: molecular insights into skeletal development—matrix components and their homeostasis, *FASEB J.* 11 (1997) 227–233.
- [31] E. Zelzer, B.R. Olsen, The genetic basis for skeletal diseases, *Nature* 423 (2003) 343–348.
- [32] S.C. Manolagas, A.M. Parfitt, What old means to bone, *Trends Endocrinol. Metab.* 369–374 (2010).
- [33] G.Y. Rochefort, C.L. Benhamou, Osteocytes are not only mechanoreceptive cells, *Int. J. Numer. Methods Biomed. Eng.* 29 (2013) 1082–1088.
- [34] J.T. Compton, F.Y. Lee, A review of osteocyte function and the emerging importance of sclerostin, *J. Bone Joint Surg. Am.* 96 (2014) 1659–1668.
- [35] T. Komori, Mouse models for the evaluation of osteocyte functions, *J. Bone Metab.* 21 (2014) 55–60.
- [36] S.C. Manolagas, A.M. Parfitt, For whom the bell tolls: distress signals from long-lived osteocytes and the pathogenesis of metabolic bone diseases, *Bone* 54 (2013) 272–278.
- [37] J. Xiong, M. Piemontese, M. Onal, J. Campbell, J.J. Goellner, V. Dusevich, L. Bonewald, S.C. Manolagas, C.A. O'Brien, Osteocytes, not osteoblasts or lining cells, are the main source of the RANKL required for osteoclast formation in remodeling bone, *PLoS One* 10 (2015) e0138189.
- [38] A.R. Gohel, A.R. Hand, G.A. Gronowicz, Immunogold localization of beta 1-integrin in bone: effect of glucocorticoids and insulin-like growth factor 1 on integrins and osteocyte formation, *J. Histochem. Cytochem.* 43 (1995) 1085–1096.
- [39] E.M. Aarden, P.J. Nijweide, A. Plas, M.J. Alblas, E.J. Mackie, M.A. Horton, M.H. Helfrich, Adhesive properties of iso-lated chick osteocytes in vitro, *Bone* 18 (1996) 305–313.
- [40] L.D. You, S. Weinbaum, S.C. Cowin, M.B. Schaffler, Ultra-structure of the osteocyte process and its pericellular matrix, *Anat. Rec.* 278A (2004) 505–513.
- [41] H. Touaitahuata, E. Planus, C. Albiges-Rizo, A. Blangy, G. Pawlak, Podosomes are dispensable for osteoclast differentiation and migration, *Eur. J. Cell Biol.* 92 (2013) 139–149.
- [42] H. Touaitahuata, A. Blangy, V. Vives, Modulation of osteoclast differentiation and bone resorption by Rho GTPases, *Small GTPases* 5 (2014) e28119.
- [43] C. Itzstein, F.P. Coxon, M.J. Rogers, The regulation of osteoclast function and bone resorption by small GTPases, *Small GTPases* 2 (2011) 117–130.
- [44] S. Miyamoto, H. Teramoto, O.A.J.S. Coso, P.D. Burbello Gutkind, S.K. Akiyama, K.M. Yamada, Integrin function: molecular hierarchies of cytoskeletal and signaling proteins, *J. Cell Biol.* 131 (1995) 791–805.
- [45] J.T. Parsons, K.H. Martin, J.K. Slack, J.M. Taylor, S.A. Weed, Focal adhesion kinase: a regulator of focal adhesion dynamics and cell movement, *Oncogene* 19 (2000) 5606–5613.
- [46] P. Keely, L. Parise, R. Juliano, Integrins and GTPases in tumour cell growth, motility and invasion, *Trends Cell Biol.* 8 (1998) 101–106.
- [47] C. Maes, Signaling pathways effecting crosstalk between cartilage and adjacent tissues: seminars in cell and developmental biology: the biology and pathology of cartilage, *Semin. Cell Dev. Biol.* (2016) 30131–30138 (pii: S1084-9521).
- [48] B. de Crombrughe, V. Lefebvre, K. Nakashima, Regulatory mechanisms in the pathways of cartilage and bone formation, *Curr. Opin. Cell Biol.* 13 (2001) 721–727.
- [49] T. Kirsch, W. Wang, D. Pfander, Functional differences between growth plate apoptotic bodies and matrix vesicles, *J. Bone Miner. Res.* 18 (2003) 1872–1881.
- [50] N. Johansson, K. Airola, R. Grénman, A.L. Kariniemi, U. Saarialho-Kere, V.M. Kähäri, Expression of collagenase-3 (matrix metalloproteinase-13) in squamous cell carcinomas of the head and neck, *Am. J. Pathol.* 151 (1997) 499–508.
- [51] D. Pfander, B. Swoboda, T. Kirsch, Expression of early and late differentiation markers (proliferating cell nuclear antigen, syndecan-3, annexin VI, and alkaline phosphatase) by human osteoarthritic chondrocytes, *Am. J. Pathol.* 159 (2001) 1777–1783.
- [52] M. Inada, Y. Wang, M.H. Byrne, M.U. Rahman, C. Miyaura, C. Lopez-Otin, S.M. Krane, Critical roles for collagenase-3 (Mmp13) in development of growth plate cartilage and in endochondral ossification, *Proc. Natl. Acad. Sci. U. S. A.* 101 (2004) 17192–17197.
- [53] U. Rescher, D. Ruche, C. Ludwig, N. Zobiack, V. Gerke, Annexin 2 is a phosphatidylinositol (4,5)-bisphosphate binding protein recruited to actin assembly sites at cellular membranes, *J. Cell Sci.* 117 (2004) 3473–3480.
- [54] M. Balcerzak, A. Malinowska, C. Thouverey, A. Sekrecka, M. Dadlez, R. Buchet, S. Pikula, Proteome analysis of matrix vesicles isolated from femurs of chicken embryo, *Proteomics* 8 (2008) 192–205.
- [55] D.S. Howell, Articular cartilage calcification and matrix vesicles, *Curr. Rheumatol. Rep.* 4 (2002) 265–269.
- [56] H.C. Anderson, Matrix vesicles and calcification, *Curr. Rheumatol. Rep.* 5 (2003) 222–226.
- [57] H.C. Anderson, Isolation and characterization of calcifying matrix vesicles from epiphyseal cartilage, *Proc. Natl. Acad. Sci. U. S. A.* 167 (1970) 1513–1520.
- [58] R.J. Majeska, R.E. Wuthier, Studies on matrix vesicles isolated from chick epiphyseal cartilage. Association of pyrophosphatase and ATPase activities with alkaline phosphatase, *Biochim. Biophys. Acta* 60 (1975) 51–60.
- [59] R.E. Wuthier, R.E. Linder, G.P. Warner, S.T. Gore, T.K. Borg, Nonenzymatic method for isolation of matrix vesicles: characterization and initial studies on Ca and P orthophosphate metabolism, *Metab. Bone Dis. Relat. Res.* 1 (1978) 125–136.
- [60] E.L. Watkins, J.V. Stillo, R.E. Wuthier, Subcellular fractionation of epiphyseal cartilage: isolation of matrix vesicles and profiles of enzymes, phospholipids, calcium and phosphate, *Biochim. Biophys. Acta* 631 (1980) 289–304.
- [61] T. Kirsch, R.E. Wuthier, Stimulation of calcification of growth plate cartilage matrix vesicles by binding to type II and X collagens, *J. Biol. Chem.* 269 (1994) 11462–11469.
- [62] M. Balcerzak, J. Radisson, G. Azzar, D. Farlay, G. Boivin, S. Pikula, R. Buchet, A comparative analysis of strategies for isolation of matrix vesicles, *Anal. Biochem.* 361 (2007) 176–182.
- [63] R. Buchet, S. Pikula, D. Magne, S. Mebarek, Isolation and characteristics of matrix vesicles, *Methods Mol. Biol.* 1053 (2013) 115–124.
- [64] J.E. Hale, R.E. Wuthier, The mechanism of matrix vesicle formation. Studies on the composition of chondrocyte microvilli and on the effects of microfilament-perturbing agents on cellular vesiculation, *J. Biol. Chem.* 262 (1987) 1916–1925.
- [65] C. Thouverey, A. Strzelecka-Kiliszek, M. Balcerzak, R. Buchet, S. Pikula, Matrix vesicles originate from apical membrane microvilli of mineralizing osteoblast-like Saos-2 cells, *J. Cell. Biochem.* 106 (2009) 127–138.
- [66] C. Thouverey, A. Malinowska, M. Balcerzak, A. Strzelecka-Kiliszek, R. Buchet, M. Dadlez, S. Pikula, Proteomic characterization of biogenesis and functions of matrix vesicles released from mineralizing human osteoblast-like cells, *J. Proteomics* 74 (2011) 1123–1134.
- [67] E.E. Golub, Role of matrix vesicles in biomineralization, *Biochim. Biophys. Acta* 1790 (2009) 1592–1598.
- [68] R.E. Wuthier, G.F. Lipscomb, Matrix vesicles: structure, composition, formation and function in calcification, *Front. Biosci.* 16 (2011) 2812–2902.
- [69] I.M. Shapiro, W.J. Landis, M.V. Risbud, Matrix vesicles: are they anchored exosomes? *Bone* 79 (2015) 29–36.
- [70] L. Hesse, K.A. Johnson, H.C. Anderson, S. Narisawa, A. Sali, J.W. Goding, R. Terleitaub, J.L. Millan, Tissue-nonspecific alkaline phosphatase and plasma cell membrane glycoprotein-1 are central antagonistic regulators of bone mineralization, *Proc. Natl. Acad. Sci. U. S. A.* 99 (2002) 9445–9449.
- [71] D. Harmey, L. Hesse, S. Narisawa, K.A. Johnson, R. Terleitaub, J.L. Millan, Concerted regulation of inorganic pyrophosphate and osteopontin by Akp2, Enpp1, and Ank: an integrated model of the pathogenesis of mineralization disorders, *Am. J. Pathol.* 164 (2004) 1199–1209.
- [72] J.L. Millan, M.P. Whyte, Alkaline phosphatase and hypophosphatasia, *Calcif. Tissue Int.* 98 (2016) 398–416.
- [73] A.N. Kapustin, J.D. Davies, J.L. Reynolds, R. McNair, G.T. Jones, A. Sidibe, L.J. Schurgers, J.N. Skepper, D. Proudfoot, M. Mayr, C.M. Shanahan, Calcium regulates key components of vascular smooth muscle cell-derived matrix vesicles to enhance mineralization, *Circ. Res.* 109 (2011) e1–12.
- [74] J. Huang, H. Huang, M. Wu, J. Li, H. Xie, H. Zhou, E. Liao, Y. Peng, Connective tissue growth factor induces osteogenic differentiation of vascular smooth muscle cells through ERK signaling, *Int. J. Mol. Med.* 32 (2013) 423–429.
- [75] G. Watanabe, Y. Saito, P. Madaule, T. Ishizaki, K. Fujisawa, N. Morii, H. Mukai, Y. Ono, A. Kakizuka, S. Narumiya, Protein kinase N (PKN) and PKN-related protein rhophilin as targets of small GTPase Rho, *Science* 271 (1996) 645–648.
- [76] D. Thumke, S. Watanabe, S. Narumiya, Physiological roles of Rho and Rho effectors in mammals, *Eur. J. Cell Biol.* 92 (2013) 303–315.
- [77] G. Loirand, P. Pacaud, Involvement of Rho GTPases and their regulators in the pathogenesis of hypertension, *Small GTPases* 5 (2014) e983666.
- [78] S. Etienne-Manneville, A. Hall, Rho GTPases in cell biology, *Nature* 420 (2002) 629–635.
- [79] A. Hall, Rho GTPases and the actin cytoskeleton, *Science* 279 (1998) 509–514.
- [80] J.F. Cote, K. Vuori, Identification of an evolutionarily conserved super-family of DOCK180-related proteins with guanine nucleotide exchange activity, *J. Cell Sci.* 115 (2002) 4901–4913.
- [81] N. Meller, S. Merlot, C. Guda, CZH proteins: a new family of Rho-GEFs, *J. Cell Sci.* 118 (2005) 4937–4946.
- [82] V. Vives, M. Laurin, G. Cres, P. Larrousse, Z. Morichaud, D. Noel, J.F. Côté, A. Blangy, The Rac1 exchange factor Dock5 is essential for bone resorption by osteoclasts, *J. Bone Miner. Res.* 26 (2011) 1099–1110.
- [83] L. Julian, M.F. Olson, Rho-associated coiled-coil containing kinases (ROCK): structure, regulation, and functions, *Small GTPases* 5 (2014) e29846.
- [84] A.V. Schofield, O. Bernard, Rho-associated coiled-coil kinase (ROCK) signaling and disease, *Crit. Rev. Biochem. Mol. Biol.* 48 (2013) 301–316.
- [85] S. Hartmann, A.J. Ridley, S. Lutz, The function of Rho-associated kinases ROCK1 and ROCK2 in the pathogenesis of cardiovascular disease, *Front. Pharmacol.* 276 (2015) 1–16.
- [86] P. Pan, M. Shen, H. Yu, Y. Li, D. Li, T. Hou, Advances in the development of Rho-associated protein kinase (ROCK) inhibitors, *Drug Discov. Today* 18 (2013) 1323–1333.
- [87] L.R. Pearce, D. Komander, D.R. Alessi, The nuts and bolts of AGC protein kinases, *Nat. Rev. Mol. Cell Biol.* 11 (2010) 9–22.
- [88] T. Leung, E. Manser, L. Tan, L. Lim, A novel serine/threonine kinase binding the Ras-related RhoA GTPase which translocates the kinase to peripheral membranes, *J. Biol. Chem.* 270 (1995) 29051–29054.
- [89] T. Ishizaki, M. Maekawa, K. Fujisawa, K. Okawa, A. Iwamatsu, A. Fujita, N. Watanabe, Y. Saito, A. Kakizuka, N. Morii, S. Narumiya, The small GTP-binding protein Rho binds to and activates a 160 kDa Ser/Thr protein kinase homologous to myotonic dystrophy kinase, *EMBO J.* 15 (1996) 1885–1893.

- [90] T. Leung, X.Q. Chen, E. Manser, L. Lim, The p160 RhoA-binding kinase ROK alpha is a member of a kinase family and is involved in the reorganization of the cytoskeleton. *Mol. Cell Biol.* 16 (1996) 5313–5327.
- [91] M. Amano, K. Chihara, K. Kimura, Y. Fukata, N. Nakamura, Y. Matsuura, K. Kaibuchi, Formation of actin stress fibers and focal adhesions enhanced by Rho-kinase. *Science* 275 (1997) 1308–1311.
- [92] M. Amano, Y. Fukata, K. Kaibuchi, Regulation and functions of Rho-associated kinase. *Exp. Cell Res.* 261 (2000) 44–51.
- [93] O. Nakagawa, K. Fujisawa, T. Ishizaki, Y. Saito, K. Nakao, S. Narumiya, ROCK-I and ROCK-II, two isoforms of Rho-associated coiled-coil forming protein serine/threonine kinase in mice. *FEBS Lett.* 392 (1996) 189–193.
- [94] C. Hahmann, T. Schroeter, Rho-kinase inhibitors as therapeutics: from pan inhibition to isoform selectivity. *Cell. Mol. Life Sci.* 67 (2010) 171–177.
- [95] W. Wen, W. Liu, J. Yan, M. Zhang, Structure basis and unconventional lipid membrane binding properties of the PH-C1 tandem of rho kinases. *J. Biol. Chem.* 283 (2008) 26263–26273.
- [96] K. Riento, A.J. Ridley, Rocks: multifunctional kinases in cell behaviors. *Nat. Rev. Mol. Cell Biol.* 4 (2003) 446–456.
- [97] L. Julian, M.F. Olson, Rho-associated coiled-coil containing kinases (ROCK) structure, regulation and functions. *Small GTPases* 5 (2014) e229846.
- [98] A. Yoneda, H.A. Multhaupt, J.R. Couchman, The Rho kinases I and II regulate different aspects of myosin II activity. *J. Cell Biol.* 170 (2005) 443–453.
- [99] T. Matsui, M. Amano, T. Yamamoto, K. Chihara, M. Nakafuku, M. Ito, T. Nakano, K. Okawa, A. Iwamatsu, K. Kaibuchi, Rho-associated kinase, a novel serine/threonine kinase, as a putative target for small GTP binding protein Rho. *EMBO J.* 15 (1996) 2208–2216.
- [100] W.C. Sin, X.Q. Chen, T. Leung, L. Lim, RhoA-binding kinase alpha translocation is facilitated by the collapse of the vimentin. *Mol. Cell Biol.* 18 (1998) 6325–6339.
- [101] K. Katoh, Y. Kano, M. Amano, H. Onishi, K. Kaibuchi, K. Fujiwara, Rho-kinase – mediated contraction of isolated stress fibers. *J. Cell Biol.* 153 (2001) 569–584.
- [102] S. Kawabata, J. Usukura, N. Morone, M. Ito, A. Iwamatsu, K. Kaibuchi, M. Amano, Interaction of Rho-kinase with myosin II at stress fibers. *Genes Cells* 9 (2004) 653–660.
- [103] Z. Ma, M. Kana, K. Kawamura, K. Kaibuchi, K. Ye, K. Fukasawa, Interaction between ROCK II and nucleophosmin/B23 in the regulation of centrosome duplication. *Mol. Cell Biol.* 26 (2006) 9016–9034.
- [104] T. Tanaka, D. Nishimura, R.C. Wu, M. Amano, T. Iso, L. Kedes, H. Nishida, K. Kaibuchi, Y. Hamamori, Nuclear Rho kinase, ROCK2, targets p300 acetyltransferase. *J. Biol. Chem.* 281 (2006) 15320–15329.
- [105] M. Iizuka, K. Kimura, S. Wang, K. Kato, M. Amano, K. Kaibuchi, A. Mizoguchi, Distinct distribution and localization of Rho-kinase in mouse epithelial, muscle and neural tissues. *Cell Struct. Funct.* 37 (2012) 155–175.
- [106] V. Chevrier, M. Piel, N. Collomb, Y. Saoudi, R. Frank, M. Paintrand, S. Narumiya, M. Bornens, D. Job, The Rho-associated protein kinase p160ROCK is required for centrosome positioning. *J. Cell Biol.* 157 (2002) 807–817.
- [107] M.C. Glyn, J.G. Lawrenson, B.J. Ward, A Rho-associated kinase mitigates reperfusion-induced change in the shape of cardiac capillary endothelial cells in situ. *Cardiovasc. Res.* 57 (2003) 195–206.
- [108] P.J. Stroeken, B. Alvarez, J. Van Rheenen, Y.M. Wijnands, D. Geerts, K. Jalink, E. Roos, Integrin cytoplasmic domain-associated protein-1 (ICAP-1) interacts with the ROCK-I kinase at the plasma membrane. *J. Cell. Physiol.* 208 (2006) 620–628.
- [109] M. Amano, M. Ito, K. Kimura, Y. Fukata, K. Chihara, T. Nakano, Y. Matsuura, K. Kaibuchi, Phosphorylation and activation of myosin by Rho-associated kinase. *J. Biol. Chem.* 271 (1996) 20246–20249.
- [110] K. Kimura, M. Ito, M. Amano, K. Chihara, Y. Fukata, M. Nakafuku, B. Yamamori, J. Feng, T. Nakano, K. Okawa, A. Iwamatsu, K. Kaibuchi, Regulation of myosin phosphatase by Rho and Rho-associated kinase (Rho-kinase). *Science* 273 (1996) 245–248.
- [111] Y. Kawano, Y. Fukata, N. Oshiro, M. Amano, T. Nakamura, M. Ito, F. Matsumura, M. Inagaki, K. Kaibuchi, Phosphorylation of myosin-binding subunit (MBS) of myosin phosphatase by Rho-kinase in vivo. *J. Cell Biol.* 147 (1999) 1023–1038.
- [112] K.H. Chun, K. Araki, D.H. Lee, B.C. Oh, H. Huang, P.S. Park, S.W. Lee, J.M. Zabolotny, Y.B. Kim, Regulation of glucose transport by ROCK1 differs from that of ROCK2 and is controlled by actin polymerization. *Endocrinology* 153 (2012) 1649–1662.
- [113] Y. Kureishi, S. Kobayashi, M. Amano, K. Kimura, H. Kanaide, T. Nakano, K. Kaibuchi, M. Ito, Rho-associated kinase directly induces smooth muscle contraction through myosin light chain phosphorylation. *J. Biol. Chem.* 272 (1997) 12257–12260.
- [114] M. Maekawa, T. Ishizaki, S. Boku, N. Watanabe, A. Fujita, A. Iwamatsu, T. Obinata, K. Ohashi, K. Mizuno, S. Narumiya, Signaling from Rho to the actin cytoskeleton through protein kinases ROCK and LIM-kinase. *Science* 285 (1999) 895–898.
- [115] K. Ohashi, K. Nagata, M. Maekawa, T. Ishizaki, S. Narumiya, K. Mizuno, Rho-associated kinase ROCK activates LIM-kinase 1 by phosphorylation at threonine 508 within the activation loop. *J. Biol. Chem.* 275 (2000) 3577–3582.
- [116] T. Sumi, K. Matsumoto, T. Nakamura, Specific activation of LIM kinase 2 via phosphorylation of threonine 505 by ROCK, a Rho-dependent protein kinase. *J. Biol. Chem.* 276 (2001) 670–676.
- [117] T. Amano, K. Tanabe, T. Eto, S. Narumiya, K. Mizuno, LIM-kinase 2 induces formation of stress fibres, focal adhesions and membrane blebs, dependent on its activation by Rho-associated kinase-catalysed phosphorylation at threonine-505. *Biochem. J.* 354 (2001) 149–159.
- [118] T. Lin, L. Zeng, Y. Liu, K. DeFea, M.A. Schwartz, S. Chien, J.Y. Shyy, Rho-ROCK-LIMK-cofilin pathway regulates shear stress activation of sterol regulatory element binding proteins. *Circ. Res.* 92 (2003) 1296–1304.
- [119] T. Matsui, M. Maeda, Y. Doi, S. Yonemura, M. Amano, K. Kaibuchi, S. Tsukita, S. Tsukita, Rho-kinase phosphorylates COOH-terminal threonines of ezrin/radixin/moesin (ERM) proteins and regulates their head-to-tail association. *J. Cell Biol.* 140 (1998) 647–657.
- [120] Y. Fukata, N. Oshiro, N. Kinoshita, Y. Kawano, Y. Matsuoka, V. Bennett, Y. Matsuura, K. Kaibuchi, K. Kaibuchi, Phosphorylation of adducin by Rho-kinase plays a crucial role in cell motility. *J. Cell Biol.* 145 (1999) 347–361.
- [121] C.B. Li, X.X. Li, Y.G. Chen, H.Q. Gao, M.C. Bao, J. Zhang, P.L. Bu, Y. Zhang, X.P. Ji, Simvastatin exerts cardioprotective effects and inhibits the activity of Rho-associated protein kinase in rats with metabolic syndrome. *Clin. Exp. Pharmacol. Physiol.* 39 (2012) 759–764.
- [122] M. Uehata, T. Ishizaki, H. Satoh, T. Ono, T. Kawahara, T. Morishita, H. Tamakawa, Y. Yamagami, J. Inui, M. Maekawa, S. Narumiya, Calcium sensitization of smooth muscle mediated by a Rho-associated protein kinase in hypertension. *Nature* 389 (1997) 990–994.
- [123] Y. Wang, X.R. Zheng, N. Riddick, M. Bryden, W. Baur, X. Zhang, H.K. Surks, ROCK isoform regulation of myosin phosphatase and contractility in vascular smooth muscle cells. *Circ. Res.* 104 (2009) 531–540.
- [124] J. Shi, X. Wu, M. Surma, S. Vemula, L. Zhang, Y. Yang, R. Kapur, L. Wei, Distinct roles for ROCK1 and ROCK2 in the regulation of cell detachment. *Cell Death Dis.* 4 (2013) e483.
- [125] S. Mertsch, S. Thanos, Opposing signaling of ROCK1 and ROCK2 determines the switching of substrate specificity and the mode of migration of glioblastoma cells. *Mol. Neurobiol.* 49 (2014) 900–915.
- [126] J. Shi, L. Wei, L. Rho kinases in cardiovascular physiology and pathophysiology: the effect of fasudil. *J. Cardiovasc. Pharmacol.* 62 (2013) 341–354.
- [127] J. Wang, X. Liu, Y. Zhong, Rho/Rho-associated kinase pathway in glaucoma. *Int. J. Oncol.* 43 (2013) 1357–1367.
- [128] R.S. Mali, S. Kapur, R. Kapur, Role of Rho kinases in abnormal and normal hematopoiesis. *Curr. Opin. Hematol.* 21 (2014) 271–275.
- [129] N. Hensel, S. Rademacher, P. Claus, Chatting with the neighbors: crosstalk between Rho-kinase (ROCK) and other signaling pathways for treatment of neurological disorders. *Front. Neurosci.* 9 (2015) 198.
- [130] V.T. Chin, A.M. Nagrial, A. Chou, A.V. Biankin, A.J. Gill, P. Timpson, M. Pajic, Rho-associated kinase signaling and the cancer microenvironment: novel biological implications and therapeutic opportunities. *Expert Rev. Mol. Med.* 17 (2015) e17.
- [131] T. Shimizu, J.K. Liao, Rho kinases and cardiac remodeling. *Circ. J.* 80 (2016) 1491–1498.
- [132] L.M. Surma, S. Shi, N. Lambert-Cheatham, J. Shi, Novel insights into the roles of Rho kinase in cancer. *Arch. Immunol. Ther. Exp. (Warsz.)* 64 (2016) 259–278.
- [133] M. Morgan-Fisher, U.M. Wewer, A. Yoneda, Regulation of ROCK activity in cancer. *J. Histochem. Cytochem.* 61 (2013) 185–198.
- [134] G. Loirand, Rho kinases in health and diseases: from basic science to translational research. *Pharmacol. Rev.* 67 (2015) 1074–1095.
- [135] M. Noguchi, K. Hosoda, J. Fujikura, M. Fujimoto, H. Iwakura, T. Tomita, T. Ishii, N. Arai, M. Hirata, K. Ebihara, H. Masuzaki, H. Itoh, S. Narumiya, K. Nakao, Genetic and pharmacological inhibition of Rho-associated kinase II enhances adipogenesis. *J. Biol. Chem.* 282 (2007) 29574–29583.
- [136] N. Inaba, S. Ishizawa, M. Kimura, K. Fujioka, M. Watanabe, T. Shibasaki, Y. Manome, Effect of inhibition of the ROCK isoform on RT2 malignant glioma cells. *Anticancer Res* 30 (2010) 3509–3514.
- [137] D. Vigil, T.Y. Kim, A. Plachco, A.J. Garton, L. Castaldo, J.A. Pachter, H. Dong, X. Chen, B. Tokar, S.L. Campbell, C.J. Der, ROCK1 and ROCK2 are required for non-small cell lung cancer anchorage-independent growth and invasion. *Cancer Res.* 72 (2012) 5338–5347.
- [138] P.Y. Mong, Q. Wang, Activation of Rho kinase isoforms in lung endothelial cells during inflammation. *J. Immunol.* 182 (2009) 2385–2394.
- [139] B.A. Bryan, E. Dennstedt, D.C. Mitchell, T.E. Walshe, K. Noma, R. Loureiro, M. Saint-Geniez, J.P. Campaigniac, J.K. Liao, P.A. D'Amore, RhoA/ROCK signaling is essential for multiple aspects of VEGF-mediated angiogenesis. *FASEB J.* 24 (2010) 3186–3195.
- [140] H. Shimada, L.E. Rajagopalan, Rho kinase-2 activation in human endothelial cells drives lysophosphatidic acid-mediated expression of cell adhesion molecules via NF-kappaB p65. *J. Biol. Chem.* 285 (2010) 12536–12542.
- [141] J. Montalvo, C. Spencer, A. Hackathorn, K. Masterjohn, A. Perkins, C. Doty, A. Arumugam, P.P. Ongusaha, R. Lakshmanaswamy, J.K. Liao, D.C. Mitchell, B.A. Bryan, ROCK1 & 2 perform overlapping and unique roles in angiogenesis and angiosarcoma tumor progression. *Curr. Mol. Med.* 13 (2013) 205–219.
- [142] S. Boku, S. Nakagawa, H. Toda, A. Kato, N. Takamura, Y. Omiya, T. Inoue, T. Koyama, ROCK2 regulates bFGF-induced proliferation of SH-SY5Y cells through GSK-3 $\beta$  and  $\beta$ -catenin pathway. *Brain Res.* 1492 (2013) 7–17.
- [143] A. Yoneda, D. Ushakov, H.A. Multhaupt, J.R. Couchman, Fibronectin matrix assembly requires distinct contributions from Rho kinases I and -I. *Mol. Biol. Cell* 18 (2007) 66–75.
- [144] H. Darenfed, B. Dayanandan, T. Zhang, S.H. Hsieh, A.E. Fournier, C.A. Mandato, Molecular characterization of the effects of Y-27632. *Cell Motil. Cytoskeleton* 64 (2007) 97–109.
- [145] Y. Zhao, M. Lv, H. Lin, Y. Hong, F. Yang, Y. Sun, Y. Guo, Y. Cui, S. Li, Y. Gao, ROCK1 induces ERK nuclear translocation in PDGF-BB-stimulated migration of rat vascular smooth muscle cells. *IUBMB Life* 64 (2012) 194–202.
- [146] F.E. Lock, H.A. Hotchin, Distinct roles for ROCK1 and ROCK2 in the differential regulation of adhesion complex turnover by ROCK1 and ROCK2. *PLoS One* 4 (2009) e8190.
- [147] F.E. Lock, K.R. Ryan, N.S. Poulter, M. Parsons, N.A. Hotchin, Differential regulation of adhesion complex turnover by ROCK1 and ROCK2. *PLoS One* 7 (2012) e31423.
- [148] R. Kalaji, A.P. Wheeler, J.C. Erasmus, S.Y. Lee, R.G. Endres, L.P. Cramer, V.M. Braga, ROCK1 and ROCK2 regulate epithelial polarization and geometric cell shape. *Biol. Cell* 104 (2012) 435–451.

- [149] Y. Shimizu, D. Thumkeo, J. Keel, T. Ishizaki, H. Oshima, M. Oshima, Y. Noda, F. Matsumura, M.M. Taketo, S. Narumiya, ROCK-I regulates closure of the eyelids and ventral body wall by inducing assembly of actomyosin bundles, *J. Cell Biol.* 168 (2005) 941–953.
- [150] D. Thumkeo, J. Keel, T. Ishizaki, M. Hirose, K. Nonomura, H. Oshima, M. Oshima, M.M. Taketo, S. Narumiya, Targeted disruption of the mouse rho-associated kinase 2 gene results in intrauterine growth retardation and fetal death, *Mol. Cell Biol.* 23 (2003) 5043–5055.
- [151] D. Thumkeo, Y. Shimizu, S. Sakamoto, S. Yamada, S. Narumiya, ROCK-I and ROCK-II cooperatively regulate closure of eyelid and ventral body wall in mouse embryo, *Genes Cells* 10 (2005) 825–834.
- [152] P. Duffy, A. Schmandke, A. Schmandke, J. Sigworth, S. Narumiya, W.B. Cafferty, S.M. Strittmatter, Rho-associated kinase II (ROCKII) limits axonal growth after trauma within the adult mouse spinal cord, *J. Neurosci.* 29 (2009) 15266–15276.
- [153] D.H. Lee, J. Shi, N.H. Jeoung, M.S. Kim, J.M. Zabolotny, S.W. Lee, M.F. White, L. Wei, Y.B. Kim, Targeted disruption of ROCK1 causes insulin resistance in vivo, *J. Biol. Chem.* 284 (2009) 11776–11780.
- [154] Y.M. Zhang, J. Bo, G.E. Taffet, J. Chang, J. Shi, A.K. Reddy, L.H. Michael, M.D. Schneider, M.L. Entman, R.J. Schwartz, L. Wei, Targeted deletion of ROCK1 protects the heart against pressure overload by inhibiting reactive fibrosis, *FASEB J.* 20 (2006) 916–925.
- [155] K. Noma, Y. Rikitake, N. Oyama, G. Yan, P. Alcaide, P.Y. Liu, H. Wang, D. Ahl, N. Sawada, R. Okamoto, Y. Hiroi, K. Shimizu, F.W. Lusinskas, J. Sun, J.K. Liao, ROCK1 mediates leukocyte recruitment and neointima formation following vascular injury, *J. Clin. Invest.* 118 (2008) 1632–1644.
- [156] S. Vemula, J. Shi, P. Hanneman, L. Wei, R. Kapur, ROCK1 functions as a suppressor of inflammatory cell migration by regulating PTEN phosphorylation and stability, *Blood* 115 (2010) 1785–1796.
- [157] W. Chen, K. Mao, T. Hua-Huy, Y. Bei, Z. Liu, A.T. Dinh-Xuan, Fasudil inhibits prostate cancer-induced angiogenesis *in vitro*, *Oncol. Rep.* 32 (2014) 2795–2802.
- [158] V.T. Chhin, A.M. Nagrial, A. Chou, A.V. Biankin, A.J. Gill, P. Timpson, M. Pajic, Rho-associated kinase signaling and the cancer microenvironment: novel biological implications and therapeutic opportunities, *Expert Rev. Mol. Med.* 17 (2015) e17.
- [159] V.P. Kale, J.A. Hengst, D.H. Desai, S.G. Amin, J.K. Yun, The regulatory roles of ROCK and MRCK kinases in the plasticity of cancer cell migration, *Cancer Lett.* 361 (2015) 185–196.
- [160] N.A. Sopko, J.L. Hannan, T.J. Bivalacqua, Understanding and targeting the Rho kinase pathway in erectile dysfunction, *Nat. Rev. Urol.* 11 (2014) 622–628.
- [161] S.K. Wang, R.T. Chang, An emerging treatment option for glaucoma: Rho kinase inhibitors, *Clin. Ophthalmol.* 8 (2014) 883–890.
- [162] R.S. Knipe, A.M. Tager, J.K. Liao, The Rho kinases: critical mediators of multiple profibrotic processes and rational targets for new therapies for pulmonary fibrosis, *Pharmacol. Rev.* 67 (2015) 103–117.
- [163] N. Hensel, S. Rademacher, P. Claus, Chatting with the neighbors: crosstalk between Rho-kinase (ROCK) and other signaling pathways for treatment of neurological disorders, *Front. Neurosci.* 9 (2015) 198.
- [164] Y. Fujita, T. Yamashita, Axon growth inhibition by RhoA/ROCK in the central nervous system, *Front. Neurosci.* 8 (2014) 338.
- [165] H. Huang, D.H. Lee, J.M. Zabolotny, Y.B. Kim, Metabolic actions of Rho-kinase in periphery and brain, *Trends Endocrinol. Metab.* 24 (2013) 506–514.
- [166] E. Coque, C. Raoul, M. Bowerman, ROCK inhibition as a therapy for spinal muscular atrophy: understanding the repercussions on multiple cellular targets, *Front. Neurosci.* 8 (2014) 271.
- [167] S. Shah, J. Savjani, A review on ROCK-II inhibitors: from molecular modelling to synthesis, *Bioorg. Med. Chem. Lett.* 26 (2016) 2383–2391.
- [168] P. Pan, M. Shen, H. Yu, Y. Li, T. Hou, Advances in the development of Rho-associated protein kinase (ROCK) inhibitors, *Drug Discov. Today* 18 (2013) 1323–1333.
- [169] T. Asano, I. Ikegaki, S. Satoh, Y. Suzuki, M. Shibuya, M. Takayasu, H. Hidaka, Mechanism of action of a novel antivasospasm drug, HA1077, *J. Pharmacol. Exp. Ther.* 241 (1987) 1033–1040.
- [170] S. Narumiya, T. Ishizaki, M. Uehata, Use and properties of ROCK-specific inhibitor Y-27632, *Methods Enzymol.* 325 (2000) 273–284.
- [171] L. Wei, M. Surma, S. Shi, N. Lambert-Cheatham, J. Shi, Novel insights into the roles of Rho kinase in cancer, *Arch. Immunol. Ther. Exp. (Warsz.)* (2016).
- [172] E. Tachibana, T. Harada, M. Shibuya, K. Saito, M. Takayasu, Y. Suzuki, J. Yoshida, Intra-arterial infusion of fasudil hydrochloride for treating vasospasm following subarachnoid hemorrhage, *Acta Neurochir.* 141 (1999) 13–19.
- [173] H. Inazaki, S. Kobayashi, Y. Anzai, H. Satoh, S. Sato, M. Inoue, S. Yamane, K.J. Kadonosono, Efficacy of the additional use of ripasudil, a Rho-kinase inhibitor, Patients With Glaucoma Inadequately Controlled Under Maximum Medical Therapy, *Glaucoma*, Sep. 21 2016.
- [174] R.A. Lewis, B. Levy, N. Ramirez, C.C. Kocpozynski, D.W. Usner, G.D. Novack, PG324-CS201 Study Group. Fixed-dose combination of AR-13324 and latanoprost: a double-masked, 28-day, randomized, controlled study in patients with open-angle glaucoma or ocular hypertension, *Br. J. Ophthalmol.* 100 (2016) 339–344.
- [175] S. Van de Velde, T. Van Bergen, E. Vandewalle, N. Kindt, K. Castermans, L. Moons, I. Stalmans, Rho kinase inhibitor AMA0526 improves surgical outcome in a rabbit model of glaucoma filtration surgery, *Prog. Brain Res.* 220 (2015) 283–297.
- [176] M. Boerma, Q. Fu, J. Wang, D.S. Loose, A. Bartolozzi, J.L. Ellis, S. McGonigle, E. Paradisi, P. Sweetnam, L.M. Fink, M.C. Vozenin-Brotans, M. Hauer-Jensen, Comparative gene expression profiling in three primary human cell lines after treatment with a novel inhibitor of Rho kinase or atorvastatin, *Blood Coagul. Fibrinolysis* 19 (2008) 709–718.
- [177] J.H. Lee, Y. Zheng, D. von Bornstadt, Y. Wei, A. Balcioğlu, A. Daneshmand, N. Yalcin, E. Yu, F. Herisson, Y.B. Atalay, M.H. Kim, Y.J. Ahn, M. Balkaya, P. Sweetnam, O. Schueller, M.V. Poyurovsky, H.H. Kim, E.H. Lo, K.L. Furie, C. Ayata, Selective ROCK2 inhibition in focal cerebral ischemia, *Ann. Clin. Transl. Neurol.* 1 (2014) 2–14.
- [178] A. Zanin-Zhorov, R. Flynn, S.D. Waksal, B.R. Blazar, Isoform-specific targeting of ROCK proteins in immune cells, *Small GTPases* 7 (2016) 173–177.
- [179] M. Takamura, M. Sakamoto, T. Genda, T. Ichida, H. Asakura, S. Hirohashi, Inhibition of intrahepatic metastasis of human hepatocellular carcinoma by Rho-associated protein kinase inhibitor Y-27632, *Hepatology* 33 (2001) 577–581.
- [180] M. Nakajima, K. Hayashi, K. Katayama, Y. Amano, Y. Egi, M. Uehata, N. Goto, T. Kondo, Wf-536 prevents tumor metastasis by inhibiting both tumor motility and angiogenic actions, *Eur. J. Pharmacol.* 459 (2003) 113–120.
- [181] M. Nakajima, K. Hayashi, Y. Egi, K. Katayama, Y. Amano, M. Uehata, M. Ohtsuki, A. Fujii, K. Oshita, H. Kataoka, Effect of Wf-536, a novel ROCK inhibitor, against metastasis of B16 melanoma, *Cancer Chemother. Pharmacol.* 52 (2003) 319–324.
- [182] R.A. Patel, Y. Liu, B. Wang, R. Li, S.M. Sebti, Identification of novel ROCK inhibitors with anti-migratory and anti-invasive activities, *Oncogene* 33 (2014) 550–555.
- [183] Y.K. Wang, X. Yu, D.M. Cohen, M.A. Wozniak, M.T. Yang, L. Gao, J. Eyckmans, C.S. Chen, Bone morphogenetic protein-2-induced signaling and osteogenesis is regulated by cell shape, RhoA/ROCK, and cytoskeletal tension, *Stem Cells Dev.* 21 (2012) 1176–1186.
- [184] J.M. Wozney, V. Rosen, A.J. Celeste, L.M. Mitscock, M.J. Whitters, R.W. Kriz, R.M. Hewick, E.A. Wang, Novel regulators of bone formation: molecular clones and activities, *Science* 242 (1982) 1528–1534.
- [185] M.R. Urist, A. Mikulski, A. Lietze, Solubilized and insolubilized bone morphogenetic protein, *Proc. Natl. Acad. Sci. U. S. A.* 76 (1979) 1828–1832.
- [186] A. Santos, A.D. Bakker, J.M. de Bleeck-Hogervorst, J. Klein-Nulend, WNT5A induces osteogenic differentiation of human adipose stem cells via rho-associated kinase ROCK, *Cytotherapy* 12 (2010) 924–932.
- [187] Y.R. Shih, K.F. Tseng, H.Y. Lai, C.H. Lin, O.K. Lee, Matrix stiffness regulation of integrin-mediated mechanotransduction during osteogenic differentiation of human mesenchymal stem cells, *J. Bone Miner. Res.* 26 (2011) 730–738.
- [188] T. Xu, M. Wu, J. Feng, X. Lin, Z. Gu, RhoA/Rho kinase signaling regulates transforming growth factor- $\beta$ 1-induced chondrogenesis and actin organization of synovium-derived mesenchymal stem cells through interaction with the Smad pathway, *Int. J. Mol. Med.* 30 (2012) 1119–1125.
- [189] L. Gao, R. McBeath, C.S. Chen, Stem cell shape regulates a chondrogenic versus myogenic fate through Rac1 and N-cadherin, *Stem Cells* 28 (2010) 564–572.
- [190] O. Wiggan, A.E. Shaw, J.R. Bamburg, Essential requirement for Rho family GTPase signaling in Pax3 induced mesenchymal-epithelial transition, *Cell. Signal.* 18 (2006) 1501–1514.
- [191] I. Kanazawa, T. Yamaguchi, S. Yano, M. Yamauchi, T. Sugimoto, Activation of AMP-kinase and inhibition of Rho-kinase induce the mineralization of osteoblastic MC3T3-E1 cells through endothelial NOS and BMP-2 expression, *Am. J. Physiol. Endocrinol. Metab.* 296 (2008) 139–146.
- [192] H. Yoshikawa, K. Yoshioka, T. Nakase, K. Itoh, Stimulation of ectopic bone formation in response to BMP-2 by Rho kinase inhibitor: a pilot study, *Clin. Orthop. Relat. Res.* 467 (2009) 3087–3095.
- [193] M. Hagihara, M. Endo, K. Hata, C. Higuchi, K. Takaoka, H. Yoshikawa, T. Yamashita, Neogenin, a receptor for bone morphogenetic proteins, *J. Biol. Chem.* 286 (2011) 5157–5165.
- [194] M. Onishi, Y. Fujita, H. Yoshikawa, T. Yamashita, Inhibition of Rac1 promotes BMP-2 induced osteoblastic differentiation, *Cell Death Dis.* 27 (2013) e698.
- [195] A. Wong, G.G. Loots, C.E. Yellowley, A.C. Dosé, D.C. Genetos, Parathyroid hormone regulation of hypoxia-inducible factor signaling in osteoblastic cells, *Bone* 81 (2015) 97–103.
- [196] J. Gardinier, W. Yang, G.R. Madden, A. Kronbergs, V. Gangadharan, E. Adams, K. Czymmek, R.L. Duncan, P2Y2 receptors regulate osteoblast mechanosensitivity during fluid flow, *Am. J. Physiol. Cell Physiol.* 306 (2014) C1058–C1067.
- [197] E. Adinolfi, F. Amoroso, A.L. Giuliani, P2X7 receptor function in bone-related cancer, *J. Osteoporos.* 2012 (2012) 637863.
- [198] N. Wang, B. Robaye, A. Agrawal, T.M. Skerry, J.M. Boeynaems, A. Gartland, Reduced bone turnover in mice lacking the P2Y13 receptor of ADP, *Mol. Endocrinol.* 26 (2012) 142–152.
- [199] M.A. Wozniak, R. Desai, P.A. Solski, C.J. Der, P.J. Keely, ROCK-generated contractility regulates breast epithelial cell differentiation in response to the physical properties of a three-dimensional collagen matrix, *J. Cell Biol.* 163 (2003) 583–595.
- [200] J. Parreno, D.A. Hart, Molecular and mechano-biology of collagen gel contraction mediated by human MG-63 cells: involvement of specific intracellular signaling pathways and the cytoskeleton, *Biochem. Cell Biol.* 87 (2009) 895–904.
- [201] S. Yang, K.M. Kim, The RhoA-ROCK-PTEN pathway as a molecular switch for anchorage dependent cell behavior, *Biomaterials* 33 (2012) 2902–2915.
- [202] Y. Hu, S. Xu, W. Jin, Q. Yi, W. Wei, Effect of the PTEN gene on adhesion, invasion and metastasis of osteosarcoma cells, *Oncol. Rep.* 32 (2014) 1741–1747.
- [203] L. Wei, M. Surma, S. Shi, N. Lambert-Cheatham, J. Shi, Novel insights into the roles of Rho kinase in cancer, *Arch. Immunol. Ther. Exp. (Warsz.)* 64 (2016) 259–278.
- [204] E. Li, J. Zhang, T. Yuan, B. Ma, miR-145 inhibits osteosarcoma cells proliferation and invasion by targeting ROCK1, *Tumour Biol.* 35 (2014) 7645–7650.
- [205] Y. Wang, W. Zhao, Q. Fu, miR-335 suppresses migration and invasion by targeting ROCK1 in osteosarcoma cells, *Mol. Cell. Biochem.* 384 (2013) 105–111.
- [206] H. Cai, L. Lin, H. Cai, M. Tang, Z. Wang, Combined microRNA-340 and ROCK1 mRNA profiling predicts tumor progression and prognosis in pediatric osteosarcoma, *Int. J. Mol. Sci.* 15 (2014) 560–573.
- [207] X. Zhou, M. Wei, W. Wang, MicroRNA-340 suppresses osteosarcoma tumor growth and metastasis by directly targeting ROCK1, *Biochem. Biophys. Res. Commun.* 437 (2013) 653–658.



- [208] A. Woods, G. Wang, F. Beier, Regulation of chondrocyte differentiation by the actin skeleton and adhesive interactions, *J. Cell. Physiol.* 231 (2007) 1–8.
- [209] B.A. Kerr, T. Otani, E. Koyama, T.A. Freeman, M. Enomoto-Iwamoto, Small GTPase protein Rac-1 is activated with maturation and regulates cell morphology and function in chondrocytes, *Exp. Cell Res.* 314 (2008) 1301–1312.
- [210] G. Wang, F. Beier, Rac1/Cdc42 and RhoA GTPases antagonistically regulate chondrocyte proliferation, hypertrophy, and apoptosis, *J. Bone Miner. Res.* 20 (2005) 1022–1031.
- [211] K. Novakofski, A. Boehm, L. Fortier, The small GTPase Rho mediates articular chondrocyte phenotype and morphology in response to interleukin-1 alpha and insulin-like growth factor-I, *J. Orthop. Res.* 27 (2009) 58–64.
- [212] A. Woods, G. Wang, H. Dupuis, Z. Shao, F. Beier, Rac1 signaling stimulates N-cadherin expression, mesenchymal condensation, and chondrogenesis, *J. Biol. Chem.* 282 (2007) 23500–23508.
- [213] A. Woods, D. Pala, L. Kennedy, S. McLean, J.S. Rockel, G. Wang, A. Leask, F. Beier, Rac1 signaling regulates CTGF/CCN2 gene expression via TGFbeta/Smad signaling in chondrocytes, *Osteoarthritis Cartilage* 17 (2009) 406–413.
- [214] P.M. Jungmann, A.T. Mehlhorn, H. Schmal, H. Schillers, H. Oberleithner, N.P. Südkamp, Nanomechanics of human adipose-derived stem cells: small GTPases impact chondrogenic differentiation, *Tissue Eng. Part A* 18 (2012) 1035–1044.
- [215] D. Kim, J. Song, S. Kim, H.M. Park, C.H. Chun, J. Sonn, E.J. Jin, MicroRNA-34a modulates cytoskeletal dynamics through regulating RhoA/Rac1 cross-talk in chondroblasts, *J. Biol. Chem.* 287 (2012) 12501–12509.
- [216] K. Ren, F. Liu, Y. Huang, W. Liang, W. Cui, Q. Wang, W. Fan, Periodic mechanical stress activates integrin $\beta$ 1-dependent Src-dependent PLC $\gamma$ 1-independent Rac1 mitogenic signal in rat chondrocytes through ERK1/2, *Cell. Physiol. Biochem.* 30 (2012) 827–842.
- [217] W. Liang, K. Ren, F. Liu, W. Cui, Q. Wang, Z. Chen, W. Fan, Periodic mechanical stress stimulates the FAK mitogenic signal in rat chondrocytes through ERK1/2 activity, *Cell. Physiol. Biochem.* 32 (2013) 915–930.
- [218] J. Xiao, X. Chen, L. Xu, Y. Zhang, Q. Yin, F. Wang, Regulation of chondrocyte proliferation through GIT1-Rac1-mediated ERK1/2 pathway by PDGF, *Cell Biol. Int.* 38 (2014) 695–701.
- [219] G. Wang, A. Woods, H. Agoston, V. Ulici, M. Glogauer, F. Beier, Genetic ablation of Rac1 in cartilage results in chondrodysplasia, *Dev. Biol.* 306 (2007) 612–623.
- [220] J.W. Shim, K. Hamamura, A. Chen, Q. Wan, S. Na, H. Yokota, Rac1 mediates load-driven attenuation of mRNA expression of nerve growth factor beta in cartilage and chondrocytes, *J. Musculoskelet. Neuronal Interact.* 13 (2013) 372–379.
- [221] K. Hamamura, P. Zhang, L. Zhao, J.W. Shim, A. Chen, T.R. Dodge, Q. Wan, H. Shih, S. Na, C.C. Lin, H.B. Sun, H. Yokota, Knee loading reduces MMP13 activity in the mouse cartilage, *BMC Musculoskelet. Disord.* 14 (2013) 312.
- [222] Z.R. Healy, F. Zhu, J.D. Stull, K. Konstantopoulos, Elucidation of the signaling network of COX-2 induction in sheared chondrocytes: COX-2 is induced via Rac/MEKK1/MKK7/JNK2/c-Jun-C/EBPbeta-dependent pathway, *Am. J. Physiol. Cell Physiol.* 294 (2008) C1146–C1157.
- [223] S. Zhu, P. Lu, H. Liu, P. Chen, Y. Wu, Y. Wang, H. Sun, X. Zhang, Q. Xia, B.C. Heng, Y. Zhou, H.W. Ouyang, Inhibition of Rac1 activity by controlled release of NSC23766 from chitosan microspheres effectively ameliorates osteoarthritis development in vivo, *Ann. Rheum. Dis.* 74 (2015) 285–293.
- [224] D.L. Long, J.S. Willey, R.F. Loeser, Rac1 is required for matrix metalloproteinase 13 production by chondrocytes in response to fibronectin fragments, *Arthritis Rheum.* 65 (2013) 1561–1568.
- [225] Z.G. Sheng, W. Huang, Y.X. Liu, Y. Yuan, B.Z. Zhu, Ofloxacin induces apoptosis via  $\beta$ 1 integrin-EGFR-Rac1-Nox2 pathway in microencapsulated chondrocytes, *Toxicol. Appl. Pharmacol.* 267 (2013) 74–87.
- [226] J.H. Exton, Small GTPases minireview series, *J. Biol. Chem.* 273 (1992) 19923–21434.
- [227] Y. Geng, J. Valbracht, M. Lotz, Selective activation of the mitogen-activated protein kinase subgroups c-Jun NH<sub>2</sub> terminal kinase and p38 by IL-1 and TNF in human articular chondrocytes, *J. Clin. Invest.* 98 (1996) 2425–2430.
- [228] G. Jin, R.L. Sah, Y.-S. Li, M. Lotz, J.Y.-J. Shyy, S. Chien, Biomedical regulation of matrix metalloproteinase-9 in cultured chondrocytes, *J. Orthop. Res.* 18 (2000) 899–908.
- [229] K.D. Novakofski, C.J. Torre, L.A. Fortier, Interleukin-1 $\alpha$ , -6, and -8 decrease Cdc42 activity resulting in loss of articular chondrocyte phenotype, *J. Orthop. Res.* 30 (2012) 246–251.
- [230] R. Aizawa, A. Yamada, D. Suzuki, T. Limura, H. Kassai, T. Harada, M. Tsukasaki, G. Yamamoto, T. Tachikawa, K. Nakao, M. Yamamoto, A. Yamaguchi, A. Aiba, R. Kamijo, Cdc42 is required for chondrogenesis and interdigital programmed cell death during limb development, *Mech. Dev.* 129 (2012) 38–50.
- [231] W. Suzuki, A. Yamada, R. Aizawa, D. Suzuki, H. Kassai, T. Harada, M. Nakayama, R. Nagahama, K. Maki, S. Takeda, M. Yamamoto, A. Aiba, K. Baba, R. Kamijo, Cdc42 is critical for cartilage development during endochondral ossification, *Endocrinology* 156 (2015) 314–322.
- [232] L.A. Fortier, M.M. Deak, S.A. Semevolos, R.A. Cerione, Insulin-like growth factor-1 diminishes the activation status and expression of the small GTPase Cdc42 in articular chondrocytes, *J. Orthop. Res.* 22 (2004) 436–445.
- [233] L.A. Fortier, B.J. Miller, Signaling through the small G-protein Cdc42 is involved in insulin-like growth factor-1 resistance in aging articular chondrocytes, *J. Orthop. Res.* 24 (2006) 1765–1772.
- [234] J.L. Gorski, L. Estrada, C. Hu, Z. Liu, Skeletal-specific expression of Fgd1 during bone formation and skeletal defects in faciogenital dysplasia (FGDY; Aarskog syndrome), *Dev. Dyn.* 218 (2000) 573–586.
- [235] H. Wang, J. Zhang, Q. Sun, X. Yang, Altered gene expression in articular chondrocytes of Smad3(ex8/ex8) mice, revealed by gene profiling using microarrays, *J. Genet. Genomics* 34 (2007) 698–708.
- [236] K.S. Gill, F. Beier, H.A. Goldberg, Rho-ROCK signaling differentially regulates chondrocyte spreading on fibronectin and bone sialoprotein, *Am. J. Physiol. Cell Physiol.* 295 (2008) C38–C49.
- [237] G. Wang, A. Woods, S. Sabari, L. Pagnotta, L.-A. Stanton, F. Beier, RhoA/ROCK signaling suppresses hypertrophic chondrocyte differentiation, *J. Biol. Chem.* 279 (2004) 13205–13214.
- [238] X. Pei, Y. Mo, B. Ning, Z. Yuan, L. Peng, R. Ma, The role of TGF $\beta$ 1 stimulating ROCK 1 signal pathway to reorganize actin in a rat experimental model of developmental dysplasia of the hip, *Mol. Cell. Biochem.* 391 (2014) 1–9.
- [239] A. Woods, G. Wang, F. Beier, RhoA/ROCK signaling regulates Sox9 expression and actin organization during chondrogenesis, *J. Biol. Chem.* 280 (2005) 11626–11634.
- [240] A. Woods, F. Beier, RhoA/ROCK signaling regulates chondrogenesis in a context-dependent manner, *J. Biol. Chem.* 28 (2006) 13134–13140.
- [241] D. Kumar, A.B. Lassar, The transcriptional activity of Sox9 in chondrocytes is regulated by RhoA signaling and actin polymerization, *Mol. Cell. Biol.* 29 (2009) 4262–4273.
- [242] D.R. Haudenschild, D.D. D’Lima, M.K. Lotz, Dynamic compression of chondrocytes induces a Rho kinase-dependent reorganization of the actin cytoskeleton, *Biorheology* 45 (2008) 219–228.
- [243] D.R. Haudenschild, J. Chen, N. Pang, M.K. Lotz, D.D. D’Lima, Rho kinase-dependent activation of SOX9 in chondrocytes, *Arthritis Rheum.* 62 (2010) 191–200.
- [244] E. Matsumoto, T. Furumatsu, T. Kanazawa, M. Tamura, T. Ozaki, ROCK inhibitor prevents the dedifferentiation of human articular chondrocytes, *Biochem. Biophys. Res. Commun.* 420 (2012) 124–129.
- [245] A.L. Hallbeck, T.M. Walz, K. Briheim, et al., TGF-alpha and ErbB2 production in synovial joint tissue: increased expression in arthritic joints, *Scand. J. Immunol.* 34 (2005) 204–211.
- [246] C. Ritchlin, E. Dwyer, R. Bucala, et al., Sustained and distinctive patterns of gene activation in synovial fibroblasts and whole synovial tissue obtained from inflammatory synovitis, *Scand. J. Immunol.* 40 (1994) 292–298.
- [247] C.T. Appleton, S.E. Usmani, J.S. Mort, F. Beier, Rho/ROCK and MEK/ERK activation by transforming growth factor-alpha induces articular cartilage degradation, *Lab. Invest.* 90 (2010) 20–30.
- [248] K. Nakagawa, T. Teramura, T. Takehara, Y. Onodera, C. Hamanishi, M. Akagi, K. Fukuda, Cyclic compression-induced p38 activation and subsequent MMP13 expression requires Rho/ROCK activity in bovine cartilage explants, *Inflamm. Res.* 61 (2012) 1093–1100.
- [249] N. Takeshita, E. Yoshimi, C. Hatori, F. Kumakura, N. Seki, Y. Shimizu, Alleviating effects of AS1892802, a Rho kinase inhibitor, on osteoarthritic disorders in rodents, *J. Pharmacol. Sci.* 115 (2011) 481–489.
- [250] T. Furumatsu, E. Matsumoto-Ogawa, T. Tanaka, Z. Lu, T. Ozaki, ROCK inhibition enhances aggrecan deposition and suppresses matrix metalloproteinase-3 production in human articular chondrocytes, *Connect. Tissue Res.* 55 (2014) 89–95.
- [251] S. Noriega, G. Hasanova, A. Subramanian, The effect of ultrasound stimulation on the cytoskeletal organization of chondrocytes seeded in three-dimensional matrices, *Cells Tissues Organs* 197 (2013) 14–26.
- [252] J. Liang, J. Feng, W.K. Wu, J. Xiao, Z. Wu, D. Han, Y. Zhu, G. Qiu, Leptin-mediated cytoskeletal remodeling in chondrocytes occurs via the RhoA/ROCK pathway, *J. Orthop. Res.* 29 (2011) 369–374.
- [253] C.A. Heckman, H.K. Plummer 3rd., Filopodia as sensors, *Cell. Signal.* 25 (2013) 2298–2311.
- [254] J.M. Hum, R.N. Day, J.P. Bidwell, Y. Wang, F.M. Pavalko, Mechanical loading in osteocytes induces formation of a Src/Pyk2/MBD2 complex that suppresses anabolic gene expression, *PLoS One* 9 (2014) e-97942.
- [255] S. Hu, E. Planus, D. Georgess, C. Place, X. Wang, C. Albiges-Rizo, P. Jurdic, J.C. Geminard, Podosome rings generate forces that drive saltatory osteoclast migration, *Mol. Biol. Cell* 22 (2011) 3120–3126.
- [256] S. Hu, T. Biben, X. Wang, P. Jurdic, J.C. Geminard, Internal dynamics of actin structures involved in the cell motility and adhesion: modeling of the podosomes at the molecular level, *J. Theor. Biol.* 270 (2011) 25–30.
- [257] H. Sakai, Y. Chen, T. Itokawa, K.P. Yu, M.L. Zhu, K. Insogna, Activated c-Fms recruits Vav and Rac during CSF-1-induced cytoskeletal remodeling and spreading in osteoclasts, *Bone* 39 (2006) 1290–1301.
- [258] R. Faccio, S.L. Teitelbaum, K. Fujikawa, J. Chappel, A. Zallone, V.L. Tybulewicz, F.P. Ross, W. Swat, Vav3 regulates osteoclast function and bone mass, *Nat. Med.* 11 (2005) 284–290.
- [259] A. Fukuda, A. Hikita, H. Wakeyama, T. Akiyama, H. Oda, K. Nakamura, S. Tanaka, Regulation of osteoclast apoptosis and motility by small GTPase binding protein Rac1, *J. Bone Miner. Res.* 20 (2005) 2245–2253.
- [260] W.E. Allen, G.E. Jones, J.W. Pollard, A.J. Ridley, Rho, Rac and Cdc42 regulate actin organization and cell adhesion in macrophages, *J. Cell Sci.* 110 (1997) 707–720.
- [261] Y. Wang, D. Lebowitz, C. Sun, H. Thang, M.D. Grynaps, M. Glogauer, Identifying the relative contributions of rac1 and rac2 to osteoclastogenesis, *J. Bone Miner. Res.* 23 (2008) 260–270.
- [262] M. Croke, F.P. Ross, M. Korhonen, D.A. Williams, W. Zou, S.L. Teitelbaum, Rac deletion in osteoclasts causes severe osteopetrosis, *J. Cell Sci.* 124 (2011) 3811–3821.
- [263] T. Itokawa, M.L. Zhu, N. Troiano, J. Bian, T. Kawano, K. Insogna, Osteoclasts lacking Rac2 have defective chemotaxis and resorptive activity, *Calcif. Tissue Int.* 88 (2011) 75–86.
- [264] S.R. Goldberg, J. Georgiou, M. Glogauer, M.D. Grynaps, A 3D scanning confocal imaging method measures pit volume and captures the role of Rac in osteoclast function, *Bone* 51 (2012) 145–152.
- [265] M. Zhu, B.H. Sun, K. Saar, C. Simpson, N. Troiano, S.L. Dallas, L.M. Tiede-Lewis, E. Nevius, J.P. Pereira, R.S. Weinstein, S.M. Tommasini, K.L. Insogna, Deletion of Rac in mature osteoclasts causes osteopetrosis, an age-dependent change in osteoclast

- number and a reduced number of osteoblasts in vivo, *J. Bone Miner. Res.* 31 (2015) 864–873.
- [266] G. Gadea, A. Blangy, Dock-family exchange factors in cell migration and disease, *Eur. J. Cell Biol.* 93 (2014) 466–477.
- [267] V. Vives, M. Laurin, G. Cres, P. Larrousse, Z. Morichaud, D. Noel, J.F. Côté, A. Blangy, The Rac1 exchange factor Dock5 is essential for bone resorption by osteoclasts, *J. Bone Miner. Res.* 26 (2011) 1099–1110.
- [268] R. Song, J. Gu, X. Liu, J. Zhu, Q. Wang, Q. Gao, J. Zhang, L. Cheng, X. Tong, X. Qi, Y. Yuan, Z. Liu, Inhibition of osteoclast bone resorption activity through osteoprotegerin-induced damage of the sealing zone, *Int. J. Mol. Med.* 34 (2014) 856–862.
- [269] R. Song, X. Liu, J. Zhu, Q. Gao, Q. Wang, J. Zhang, D. Wang, L. Cheng, D. Hu, Y. Yuan, J. Gu, Z. Liu, RhoV mediates apoptosis of RAW264.7 macrophages caused by osteoclast differentiation, *Mol. Med. Rep.* 11 (2015) 1153–1159.
- [270] D. Georgess, M. Mazzorana, J. Terrado, C. Delprat, C. Chamot, R.M. Guasch, I. Pérez-Roger, P. Jurdic, I. Machuca-Gayet, Comparative transcriptomics reveals RhoE as a novel regulator of actin dynamics in bone-resorbing osteoclasts, *Mol. Biol. Cell* 25 (2014) 380–396.
- [271] Y. Wang, R. Lei, X. Zhuang, N. Zhang, H. Pan, G. Li, J. Hu, X. Pan, Q. Tao, D. Fu, J. Xiao, Y.E. Chin, Y. Kang, Q. Yang, G. Hu, DLC1-dependent parathyroid hormone-like hormone inhibition suppresses breast cancer bone metastasis, *J. Clin. Invest.* 124 (2014) 1646–1659.
- [272] N.S. Ruppender, A.R. Merkel, T.J. Martin, G.R. Mundy, J.A. Sterling, S.A. Guelcher, Matrix rigidity induces osteolytic gene expression of metastatic breast cancer cells, *PLoS One* 5 (2010) e15451.
- [273] S. Liu, R.H. Goldstein, E.M. Scepansky, M. Rosenblatt, Inhibition of rho-associated kinase signaling prevents breast cancer metastasis to human bone, *Cancer Res.* 69 (2009) 8742–8751.
- [274] N. Wang, B. Robaye, F. Gossiel, J.M. Boeynaems, A. Gartland, The P2Y13 receptor regulates phosphate metabolism and FGF-23 secretion with effects on skeletal development, *FASEB J.* 28 (2014) 2249–2259.
- [275] C.B. Khatiwala, P.D. Kim, S.R. Peyton, A.J. Putnam, ECM compliance regulates osteogenesis by influencing MAPK signaling downstream of RhoA and ROCK, *J. Bone Miner. Res.* 24 (2009) 886–889.
- [276] A.I. Idris, A. Idris, E. Mrak, I. Greig, F. Guidobono, S.H. Ralston, R. van 't Hof, ABD56 causes osteoclast apoptosis by inhibiting the NF $\kappa$ B and ERK pathways, *Biochem. Biophys. Res. Commun.* 371 (2008) 94–98.
- [277] H. Nakamura, A. Hirata, T. Tsuji, T. Yamamoto, Role of osteoclast extracellular signal-regulated kinase (ERK) in cell survival and maintenance of cell polarity, *J. Bone Miner. Res.* 18 (2003) 1198–1205.
- [278] G.Y. Jung, Y.J. Park, J.S. Han, Mediation of Rac1 activation by kindlin-2: an essential function in osteoblast adhesion, spreading, and proliferation, *J. Cell. Biochem.* 112 (2011) 2541–2548.
- [279] N. Yamamoto, T. Otsuka, A. Kondo, R. Matsushima-Nishiwaki, G. Kuroyanagi, O. Kozawa, H. Tokuda, Rac limits TGF- $\beta$ -induced VEGF synthesis in osteoblasts, *Mol. Cell. Endocrinol.* 405 (2015) 35–41.
- [280] X. Zhang, C. Li, H. Gao, H. Nabeka, T. Shimokawa, H. Wakisaka, S. Matsuda, N. Kobayashi, Rho kinase inhibitors stimulate the migration of human cultured osteoblastic cells by regulating actomyosin activity, *Cell. Mol. Biol. Lett.* 16 (2011) 279–295.
- [281] P.D. Prowse, C.G. Elliott, J. Hutter, D.W. Hamilton, Inhibition of Rac and ROCK signaling influence osteoblast adhesion, differentiation and mineralization on titanium topographies, *PLoS One* 8 (2013) e-58898.
- [282] A. Calzado-Martín, A. Méndez-Vilas, M. Multigner, L. Saldaña, J.L. González-Carrasco, M.L. González-Martín, N. Vilaboa, On the role of RhoA/ROCK signaling in contact guidance of bone-forming cells on anisotropic Ti6Al4V surfaces, *Acta Biomater.* 7 (2011) 1890–1901.
- [283] C. Li, S. Gao, T. Terashita, T. Shimokawa, H. Kawahara, S. Matsuda, N. Kobayashi, In vitro assays for adhesion and migration of osteoblastic cells (Saos-2) on titanium surfaces, *Cell Tissue Res.* 324 (2006) 369–375.
- [284] P.A. Randazzo, H. Inoue, S. Bharti, Arf GAPs as regulators of the actin cytoskeleton, *Biol. Cell* 99 (2007) 583–600.
- [285] T. Kirsch, Biomineralization — an active or passive process? *Connect. Tissue Res.* 53 (2012) 438–445.

### ABSTRACT

Vascular calcification accompanies the pathological process of atherosclerotic plaque formation. Artery calcification results from trans-differentiation of vascular smooth muscle cells (VSMCs) into cells resembling mineralization-competent cells such as osteoblasts and chondrocytes. The activity of tissue-nonspecific alkaline phosphatase (TNAP), a GPI-anchored enzyme necessary for physiological mineralization, is induced in VSMCs in response to inflammation. TNAP achieves its mineralizing function being anchored to plasma membrane of mineralizing cells and to the surface of their derived matrix vesicles (MVs), and numerous important reports indicate that membranes play a crucial role in initiating the crystal formation. In this review, we would like to highlight various functions of lipids and proteins associated to membranes at different stages of both physiological mineralization and vascular calcification, with an emphasis on the pathological process of atherosclerotic plaque formation.

### INTRODUCTION

Mineralization is a physiological process by which growth plate chondrocytes and osteoblasts deposit calcium phosphate crystals during endochondral and membranous ossification respectively. This process is initiated by TNAP activity [1,2]. Deficiency of this enzyme in human cells results in a severe disease called hypophosphatasia (HPP) causing *in utero* death of fetuses devoid of mineralized skeleton [3,4]. TNAP activity is necessary for physiological mineralization, but also probably for the induction of vascular calcification. Glycosylphosphatidylinositol (GPI)-anchored proteins such as TNAP may associate with lipid rafts, which are lipid membrane microdomains. In this article we would like to consider a possible role of lipid rafts in sorting and release of MVs as well as to discuss a stimulating effect of saturated fatty acids and cholesterol on vascular calcification.

### EARLY STEPS OF PHYSIOLOGICAL MINERALIZATION

#### BONE MINERALIZATION REQUIRES COEXPRESSION OF TNAP AND COLLAGEN

Physiological mineralization is regulated by the changes of inorganic phosphate ( $P_i$ ) and inorganic pyrophosphate ( $PP_i$ ) homeostasis.  $PP_i$  is a constitutive inhibitor of mineralization, which is hydrolyzed by TNAP [5]. According to Murshed and collaborators [1], mineralization process is restricted to bone tissue due to the unique co-expression of genes encoding two important proteins – TNAP and collagen type I. These molecules are necessary and sufficient to trigger the extracellular matrix (ECM) mineralization. In fact, this hypothesis can be helpful to understand also the process of soft tissue calcification that may occur in cells producing fibrillar collagen where ectopic expression of TNAP could be responsible for the occurrence of pathological mineralization.

#### MATRIX VESICLES RICH IN PHOSPHATASES AND ANNEXINS BIND TO COLLAGEN

Early stages of mineralization take place in MVs which are 30-1,000 nm-diameter structures [6,7]. Since TNAP is an ectoenzyme located on the surface of MVs, it may be, together with collagen fibrils, involved in crystal growth and multiplication outside MVs. It is therefore likely that other enzymes are present inside MVs to allow hydroxyapatite (HA) crystal nucleation. Phosphatase orphan 1 (phospho1) was proposed as a novel phosphatase providing  $P_i$ , as it is highly expressed in bone and MVs [8]. Phospho1 is able to cleave phosphatidylcholine (PC) and phosphatidylethanolamine (PE), the most abundant phosphomonoesters in cartilage. In contrast to TNAP, phospho1 is not able to hydrolyze  $PP_i$ . Interestingly, double ablation of *Phospho1* and *Alpl* (encoding TNAP), completely abolishes mineralization of osteoblast-derived MVs [9].

Monika Roszkowska<sup>1,2</sup>, ✉  
Agnieszka  
Strzelecka-Kiliszek<sup>1</sup>  
David Magne<sup>2</sup>  
Slawomir Pikula<sup>1</sup>  
Laurence Bessueille<sup>2</sup>

<sup>1</sup>Laboratory of Biochemistry of Lipids, Department of Biochemistry, Nencki Institute of Experimental Biology of Polish Academy of Sciences, 3 Pasteur St., 02-093 Warsaw, Poland  
<sup>2</sup>ICBMS, UMR CNRS 5246, University of Lyon 1; Bâtiment Raulin, 43 Bd du 11 novembre 1918; 69622 Villeurbanne Cedex, France

✉ e-mail: m.roszkowska@nencki.gov.pl

Received: June 16, 2016

Accepted: September 26, 2016

**Key words:** mineralization, vascular calcification, matrix vesicles, lipid rafts, cholesterol, fatty acids

**Abbreviations:** ACP – amorphous calcium phosphate; AnxA – annexin; ATF4 – activating transcription factor 4; Chol – cholesterol; ECM – extracellular matrix; ER – endoplasmic reticulum; FA – fatty acid; GPI – glycosylphosphatidylinositol; LDL – low density lipoprotein; MV – matrix vesicle; NC – nucleation core; PC – phosphatidylcholine; PE – phosphatidylethanolamine; PI – phosphatidylinositol; phospho1 – phosphatase orphan 1;  $P_i$  – inorganic phosphate;  $PP_i$  – inorganic pyrophosphate; PS – phosphatidylserine; CPLX – lipid-calcium-phosphate complex; PUFA – polyunsaturated fatty acid; TNAP – tissue-nonspecific alkaline phosphatase; VSMC – vascular smooth muscle cell

**Acknowledgements:** M. Roszkowska is a recipient of a scholarship granted by the Ministry of Foreign Affairs and International Development of France “Doctorat en Cotutelle 2014-2017”. Polish-French cooperation was supported by PHC Polonium Program 2015/2016 no. 33540RG granted by the Ministry of Science and Higher Education of Poland and the Ministry of Foreign Affairs and International Development of France.

Except from TNAP and phospho1, other important components highly expressed in MVs are annexins (AnxA) which are calcium- and lipid-binding proteins [10]. It has been shown previously [11] that in growth plate cartilage, MVs are able to bind type II and X collagen. This interaction seems to be mediated by AnxA5 resulting in the stimulation of Ca<sup>2+</sup> uptake and mineralization of MVs. Vesicle binding to collagen may play a crucial role in formation of the first mineral phase, regarding the fact that selective removal of collagens from the MV surface significantly reduced their ability to take up Ca<sup>2+</sup> [12]. Therefore, collagen may serve as a template for the subsequent deposition of HA crystals originating from MVs.

#### THE INITIATION OF MINERALIZATION IN MVs IS ASSOCIATED WITH THE MEMBRANES CONTAINING PHOSPHATIDYLSERINE

The internal layer of MVs is rich in phosphatidylserine (PS), a lipid that has a high affinity to Ca<sup>2+</sup> ions and is able to bind both calcium and phosphate. Early mineralization in MVs begins with the formation of membrane-anchored structures known as nucleation core (NC) [13]. NC consists of three key components: amorphous calcium phosphate (ACP), PS-lipid-calcium-phosphate complex (PS-CPLX) and AnxA5. ACP comprises nearly 90% of NC, however, *in vitro* studies on synthetic NCs revealed that ACP mediates only 20% of mineral formation [14]. Also, incorporation of PS was shown to significantly retard the induction time of mineral formation. Interestingly, AnxA5 is able to catalyze the mineral nucleation of CPLX, shortening the process by 10–20 fold, by transforming the weakly nucleating binary PS-CPLX into a ternary complex (PS-CPLX-AnxA5) with powerful nucleation activity [14].

Annexins are also thought to mediate Ca<sup>2+</sup> influx into MVs. Kirsch and collaborators demonstrated that if MVs isolated from non-mineralizing hypertrophic chondrocytes showed no significant Ca<sup>2+</sup> uptake, addition of exogenous AnxA2, AnxA5 and AnxA6, could restore these MVs' ability to take up Ca<sup>2+</sup> [11]. However, these proteins are not typical ion channels and they probably rather facilitate calcium binding than transport calcium through the membrane. Nevertheless, further investigation *in vivo* is needed to better understand the role of annexins in Ca<sup>2+</sup> influx into MVs.

In conclusion, membranes or more precisely membrane lipids could play an important role in mineralization. Therefore, better insight into the composition of membrane domains involved in MV formation and mineralization appears crucial.

#### LIPID RAFTS - MEMBRANE MICRODOMAINS RICH IN CHOLESTEROL AND SPHINGOLIPIDS

Biological membranes are not homogeneous lipid mixtures but they are rather composed of highly organized lipid and protein complexes called lipid rafts. The term lipid rafts, also referred to lipid microdomains, has been used to describe low-density membrane domains that are

rich in cholesterol (Chol) and sphingolipids and particular protein classes such as signaling and transport proteins [15]. Recently, there has been a great interest in different subtypes of lipid microdomains that can be distinguished according to their protein and lipid composition. Specialized microdomains termed 'caveolae' constitute a distinct subset of lipid rafts with morphologically defined cell surface invaginations that are rich in proteins of the caveolin family [16,17].

As mentioned above, lipid rafts are invariably characterized by their high content of Chol and sphingolipids. However, lipid rafts can differ in their composition depending on the cell type [18] and the way of their preparation. In general, lipid rafts were shown to be rich in Chol and glycosphingolipids, but often poor in glycerophospholipids [19-24]. Glycerophospholipids were represented by a high content of PE, PS and PC and a lower content of PI [23,25]. However, the phospholipid profile of lipid rafts may vary considerably. For example, platelets contain PS-enriched membrane rafts [26]. Moreover, in chondrocyte lipid rafts PS accounts for over 44% of the total phospholipids [27].

The fatty-acid side chains of lipid raft phospholipids tend to be more saturated than those in the surrounding membrane. The ratio of saturation-unsaturation of lipid raft fatty-acid side chains was assessed in numerous studies. It appears that the predominant fatty acids in lipid rafts are saturated (16:0, 18:0) and monounsaturated (18:1 n-9 and 18:1 n-7). PC mainly comprised saturated 16:0, while PE contained more 18:0 [20]. The higher content of 16:0 in PC and of 18:0 in PE is consistent with the known

Table 1. Comparison of the lipid composition of rafts and MVs [25,27,28]

Lipids	Lipid rafts (relative molar composition)	MVs
Chol	50	20
Sphingomyelin	30	5
Glycerophospholipids (relative molar composition)		
PC	52	52
PS	45	12
PE	20	20
PI	10	8
FAs (relative molar composition)		
palmitic acid (16:0)	24.1	35.34
palmitoleic acid (16:1n-7)	1.08	2.56
stearic acid (18:0)	22.05	13.06
oleic acid (18:1n-9)	17.64	27.25
PUFAs (relative molar composition)		
linoleic acid (18:2n-6)	0.85	7.58
arachidonic acid (20:4n-6)	3.7	5.61



**Table 2.** Comparison of the protein profiles of lipid rafts and MVs [40,47]

	Lipid rafts	MVs
<b>Enzymes</b>		
alkaline phosphatase	+	+
5'-nucleotidase	+	+
inorganic pyrophosphatase 1	+	+
phospho1	-	+
sphingomyelin phosphodiesterase 3	+	+
<b>Ca<sup>2+</sup> ion homeostasis</b>		
voltage dependent calcium channel	+	+
sorcin	-	+
<b>Annexins</b>		
AnxA1, AnxA2, AnxA4, AnxA5, AnxA6, AnxA7 and AnxA11	+	+
<b>Transport/channel proteins</b>		
Na <sup>+</sup> /K <sup>+</sup> ATPase	+	+
Kv3.1 potassium channel subunit	+	-
<b>Intravesicular pH</b>		
vacuolar H <sup>+</sup> -ATPase	+	+
SLC4A7	+	+
<b>ECM proteins</b>		
MMP-2	+	+
MMP-3	-	+
MMP-13	-	+
<b>Regulatory proteins</b>		
Ras GTPase-activating protein	+	+
protein kinase C	+	+
<b>Cytoskeletal proteins</b>		
vimentin, tropomyosin	+	+
filamin B	+	+
actin, tubulin	+	+
<b>Endocytosis</b>		
caveolin-1	+	+
flotillin-1	+	+
<b>TCR-associated signaling molecules</b>		
TCR-R	+	-
Lck	+	-
Calmodulin	+	+
<b>Heatshock proteins</b>		
HSP60	+	-
HSP90	+	+
<b>GTP-binding regulatory proteins</b>		
Gs(α)	+	-
Gi(α)-2	+	+
Gq	+	+
Gβ2	+	+
Gβ4	+	-
<b>Intrinsic membrane proteins</b>		
stomatin-like protein 2	+	+

predilection of these fatty acids for the sn-1 position of the corresponding glycerophospholipids [20]. A similar enrichment of 16:0 and 18:0 fatty acids in lipid rafts of various cell types was observed [22, 28,29].

**MATRIX VESICLES MEMBRANE COMPOSITION:  
THE SAME OR DIFFERENT FROM LIPID RAFTS?**

It has been suggested that MVs may originate from apical membrane microvilli [7] and exhibit a characteristic lipid composition that resembles that of lipid rafts (Tab. 1). The proportion of free cholesterol and the cholesterol/phospholipid ratio was nearly twice as high in lipid rafts as in MVs. MVs and microvilli obtained from Saos-2 osteosarcoma cell cultures were rich in Chol and

sphingolipids [30] as in the case of MVs produced by epiphyseal cartilage cells [31,32] or by hypertrophic chondrocytes [33]. The phospholipid composition of MVs presented mostly PC and PE, and, to a lesser extent, PS [27].

Fatty acid patterns of MVs were distinguishable from those of isolated cells, being generally richer in 16:0 and 18:1, and presenting lower content of 16:1 and 18:2 fatty acids (FAs). The predominant saturated FAs in different fractions were palmitic and stearic acid (16:0, 18:0). Membrane homogenates contained 62% of saturated FAs on average as compared with 48–51% of saturated FAs in MVs. The greatest difference in FA content in different fractions was observed in the monounsaturated FAs. Monounsaturated FAs, specifically the level of oleic acid (18:1n-9), was higher in MVs (27.25%) than in membrane homogenates derived from chondrocytes (6.48%) [30]. It is noteworthy that the total ratio of n-3 to n-6 polyunsaturated fatty acids (PUFAs) is markedly lower in rafts as well as in MVs, which is in accordance with a particular lipid composition of these domains, as commonly reported.

Membrane lipid raft microdomains organize signaling molecules into functional complexes for targeted transport of transmembrane and GPI-anchored proteins and hence their protein composition is highly fluctuating (Tab. 2) [34]. Caveolin-1 is one of the essential proteins serving as a scaffold in caveolar raft formation and playing a key role in caveolae-mediated endocytosis and transport. However, other proteins serving similar functions by providing platforms for the assembly of signaling molecules are found in caveolin-independent rafts. Reggies and flotillins are also an indispensable prerequisite for raft formation in non caveolar or so-called reggie microdomains [35,36].

Proteome analysis of lipid rafts prepared from various cells revealed the presence of following components: TCR-associated signaling molecules (TCR-R, Lck, calmodulin); cytoskeletal proteins or proteins involved in locomotion and membrane function (vimentin, tubulin, actin, tropomyosin), or specific protein components connecting actin with the extracellular matrix AnxA2 [20]; heat shock proteins (HSP60, HSP90); GTP-binding regulatory proteins (Gs(α), Gi(α)-2, Gq, Gβ2, Gβ4); intrinsic membrane proteins (stomatin-like protein); and transport/channel proteins (Kv3.1 potassium channel subunit, H<sup>+</sup> transporting ATPase) [37-39].



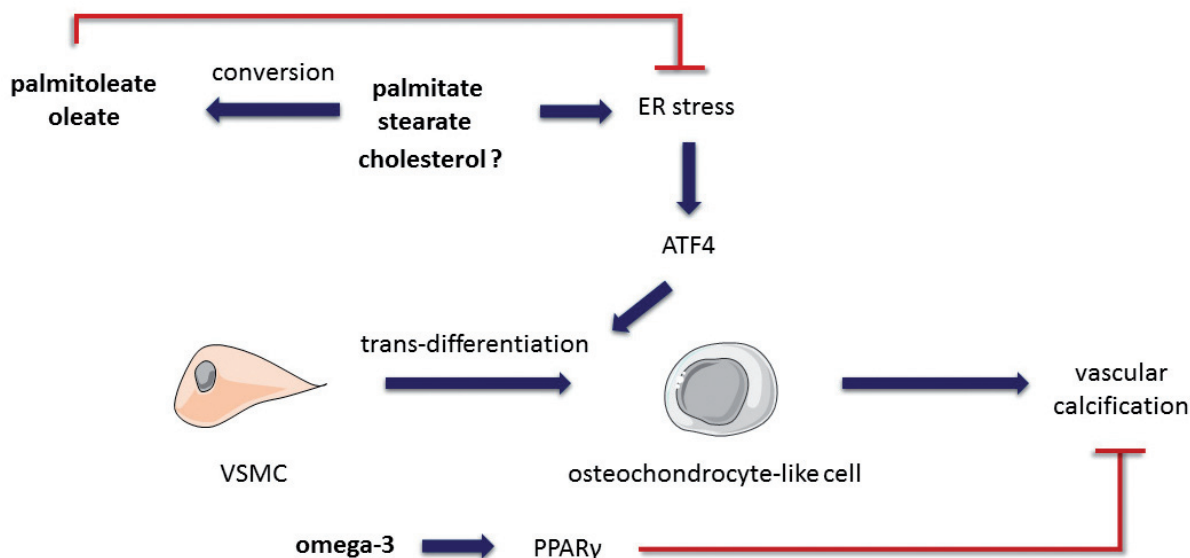


**Figure 1.** The effect of Chol and FAs on VSMCs [57-64]. In VSMCs, palmitate and stearate generate saturated phosphatidic acid in the ER, triggering ER stress, activation of ATF4 and trans-differentiation, leading to vascular calcification. Unsaturated FAs such as palmitoleate and oleate seem to protect against calcification by decreasing ER stress. Omega 3 FAs can also inhibit mineralization by activating PPAR $\gamma$ , an endogenous inhibitor of calcification in VSMCs. The mechanism through which Chol stimulates mineralization is not known. One of the hypothesis is that, similarly to saturated FAs, it may provoke ER stress leading to trans-differentiation of VSMCs into mineralization-competent cells.

Recently, a mammalian raft proteome database was established based on multiple proteomic studies in a variety of cells and tissues [40]. Results from numerous biological processes and pathway analysis provide evidence supporting the hypothesis that lipid rafts are related to different cellular functions such as membrane transport and trafficking [34,41], signal transduction [15,42], cell junctions [43,44], and cytoskeleton organization [42,45].

Protein profile of MVs can be divided into following functional categories: ECM proteins, enzymes, annexins, surface receptors, transporters, regulatory proteins and cytoskeleton components [46,47]. Thouverey and collaborators succeeded in identifying novel proteins that may regulate PP<sub>i</sub> and P<sub>i</sub> homeostasis (inorganic pyrophosphatase 1), Ca<sup>2+</sup> ion homeostasis (voltage dependent Ca<sup>2+</sup> channel and sorcin), intravesicular pH (vacuolar H<sup>+</sup>-ATPase and SLC4A7, a sodium bicarbonate cotransporter) or lipid composition of MV membrane (sphingomyelin phosphodiesterase 3) [48]. The presence of several enzymes (alkaline phosphatase, 5'-nucleotidase), protein transporters (Na<sup>+</sup>/K<sup>+</sup> ATPase for example), regulatory proteins (Ras GTPase-activating protein, protein kinase C), cytoskeleton elements (filamin B, tubulin) and annexins (AnxA1, AnxA2, AnxA4, AnxA5, AnxA6 and AnxA11) both in lipid raft and MVs revealed a link between these two membrane domains, therefore, it may indicate the involvement of rafts in sorting and release of MVs.

### THE EFFECT OF CHOLESTEROL AND FATTY ACIDS ON PATHOLOGICAL CALCIFICATION IN ATHEROSCLEROSIS

#### ATHEROSCLEROSIS AND VASCULAR CALCIFICATION

Pathological calcification is a hallmark of atherosclerosis. In humans, the earliest atherosclerotic lesions can

usually be found in aorta in the first decade of life, and consist of subendothelial accumulations of lipids. Then, cholesterol-engorged macrophages, called "foam cells", characterize the type II "fatty streak" lesions. In type II lesions, VSMCs begin to migrate from the media towards the intima to secrete a "fibrous cap" enclosing a lipid core. Vascular calcification in atherosclerotic plaques is usually noted in stage III specimens, with intermediate and solid calcifications becoming increasingly prominent within advanced plaques [49,50]. It has been estimated that over 70% of atherosclerotic plaques observed in the aging population are calcified [51].

Plaque calcification results at least in part from the trans-differentiation of VSMCs into cells similar to growth plate chondrocytes. Indeed, in the apolipoprotein E-deficient (*ApoE*<sup>-/-</sup>) mouse model of atherosclerosis, calcified cartilage forms in advanced plaques [52,53]. In these mice, VSMC-derived hypertrophic chondrocytes are likely responsible for calcification since VSMC-specific RUNX2 deficiency prevents plaque calcification [54]. Finally, VSMC-derived chondrocytes appear to release MVs virtually identical to those released by hypertrophic chondrocytes [55].

#### CHOLESTEROL AND SEVERAL FATTY ACIDS ARE STIMULATORS OF CALCIFICATION

FAs appear to play an important role in calcification mediated by VSMCs in atherosclerotic plaques (Fig. 1). Four main FAs: palmitic acid, stearic acid, oleic acid and arachidonic acid, were reported to represent two thirds of the fatty acid pool in atherosclerotic plaques of *ApoE*<sup>-/-</sup> mice on a high-cholesterol diet [56]. Trans-differentiated VSMCs predominantly accumulate saturated and mono-unsaturated FAs: palmitate and stearate, palmitoleate [C16:1 (n-7)] and oleate [C18:1 (n-9)], but not polyunsatu-

rated acids such as arachidonic acid [57]. Of these, palmitate and stearate appear able to stimulate trans-differentiation of VSMCs [57-59], whereas unsaturated FAs reduce calcium accumulation [56].

Interestingly, endogenous stearate production strongly stimulates mineralization in VSMC cultures, and inhibition of stearoylCoA desaturase exacerbates calcification [56], suggesting that both exogenous and endogenous saturated FAs may participate in vascular calcification. In VSMCs, saturated FAs generate saturated phosphatidic acid in the ER, triggering ER stress, activation of ATF4 and VSMC trans-differentiation leading to calcification [60]. The mechanisms through which unsaturated FAs protect against calcification are not fully known. The conversion of saturated to unsaturated FAs may reduce the ER stress [59]. Alternatively, omega 3 FAs appear to inhibit calcification by activating peroxisome proliferator-activated receptor  $\gamma$  (PPAR $\gamma$ ) [61], an endogenous inhibitor of calcification in VSMCs [62].

Cholesterol stimulates TNAP and mineralization in a dose-dependent manner in VSMCs [63,64]. Remarkably, stimulation of cholesterol efflux, inhibition of 3-hydroxy-3-methyl-glutaryl-coenzyme A (HMG-CoA) reductase and the lack of LDL receptor, alone or in combination, appear to decrease vascular cell differentiation and calcification [62,63]. The mechanism through which cholesterol stimulates mineralization is not known. It may provoke ER stress as saturated fatty acids do, but it may also modulate membrane dynamics leading to MV release [62].

## CONCLUDING REMARKS

Taking into account the lipid composition of rafts and MVs, both structures are enriched in cholesterol, phosphatidylcholine and saturated fatty acids. These similarities suggest that lipid rafts may be necessary for the release of MVs, being a critical step during both physiological and pathological mineralization. Thanks to protein databases of lipid rafts and MVs, it is possible to compare the protein profile of these structures and, in consequence, to draw conclusions and form hypothesis concerning the mechanisms in which they are involved. A possible association of proteins normally expressed in mineralizing MVs (e. g. TNAP, annexins) with lipid rafts allows to suspect that these membrane microdomains may be involved in mineralization. However, further investigation of the stimulating role of saturated fatty acids and cholesterol is important to better understand the pathological process of vascular calcification.

## LITERATURE

1. Murshed M, Harmey D, Millán JL, McKee MD, Karsenty G (2005) Unique coexpression in osteoblasts of broadly expressed genes accounts for the spatial restriction of ECM mineralization to bone. *Genes Dev* 19: 1093-1104
2. Narisawa S, Yadav MC, Millán JL (2013) In vivo overexpression of tissue-nonspecific alkaline phosphatase increases skeletal mineralization and affects the phosphorylation status of osteopontin. *J Bone Miner Res* 28: 1587-1598

3. Millán JL, Whyte MP (2016) Alkaline Phosphatase and Hypophosphatasia. *Calcif Tissue Int* 98: 398-416
4. Liu J, Nam HK, Campbell C, Gasque KC, Millán JL, Hatch NE (2014) Tissue-nonspecific alkaline phosphatase deficiency causes abnormal craniofacial bone development in the *Alpl*(-/-) mouse model of infantile hypophosphatasia. *Bone* 67: 81-94
5. Thouverey C, Bechkoff G, Pikula S, Buchet R (2009) Inorganic pyrophosphate as a regulator of hydroxyapatite or calcium pyrophosphate dihydrate mineral deposition by matrix vesicles. *Osteoarthritis Cartil* 17: 64-72
6. Buchet R, Pikula S, Magne D, Mebarek S (2013) Isolation and characteristics of matrix vesicles. *Methods Mol Biol* 1053: 115-124
7. Thouverey C, Strzelecka-Kiliszek A, Balcerzak M, Buchet R, Pikula S (2009) Matrix vesicles originate from apical membrane microvilli of mineralizing osteoblast-like Saos-2 cells. *J Cell Biochem* 106: 127-138
8. Roberts S, Narisawa S, Harmey D, Millán JL, Farquharson C (2007) Functional involvement of PHOSPHO1 in matrix vesicle-mediated skeletal mineralization. *J Bone Miner Res* 22: 617-627
9. Yadav MC, Simão AM, Narisawa S, Huesa C, McKee MD, Farquharson C, Millán JL (2011) Loss of skeletal mineralization by the simultaneous ablation of PHOSPHO1 and alkaline phosphatase function: a unified model of the mechanisms of initiation of skeletal calcification. *J Bone Miner Res* 26: 286-297
10. Cmoch A, Strzelecka-Kiliszek A, Palczewska M, Groves P, Pikula S (2011) Matrix vesicles isolated from mineralization-competent Saos-2 cells are selectively enriched with annexins and S100 proteins. *Biochem Biophys Res Commun* 412: 683-687
11. Kirsch T, Harrison G, Golub EE, Nah HD (2000) The roles of annexins and types II and X collagen in matrix vesicle-mediated mineralization of growth plate cartilage. *J Biol Chem* 275: 35577-35583
12. Genge BR, Wu LN, Wuthier RE (2008) Mineralization of annexin-5-containing lipid-calcium-phosphate complexes: modulation by varying lipid composition and incubation with cartilage collagens. *J Biol Chem* 283: 9737-9748
13. Cotmore JM, Nichils G Jr, Wuthier RE (1971) Phospholipid-calcium phosphate complex: enhanced calcium migration in the presence of phosphate. *Science* 172: 1339-1341
14. Genge BR, Wu LN, Wuthier RE (2007) Kinetic analysis of mineral formation during in vitro modeling of matrix vesicle mineralization: Effect of annexin A5, phosphatidylserine, and type II collagen. *Anal Biochem* 367: 159-166
15. Simons K, Toomre D (2000) Lipid rafts and signal transduction. *Nat Rev Mol Cell Biol* 1: 31-39
16. Lisanti MP, Scherer PE, Vidugiriene J, Tang Z, Hermanowski-Vosatka A, Tu YH, Cook RF, Sargiacomo M (1994) Characterization of caveolin-rich membrane domains isolated from an endothelial-rich source: implications for human disease. *J Cell Biol* 126: 111-126
17. Parton RG, Simons K (2007) The multiple faces of caveolae. *Nat Rev Mol Cell Biol* 8: 185-194
18. de Almeida RF, Fedorov A, Prieto M (2003) Sphingomyelin/ phosphatidylcholine/ cholesterol phase diagram: boundaries and composition of lipid rafts. *Biophys J* 85: 2406-2416
19. Brown DA, Rose JK (1992) Sorting of GPI-anchored proteins to glycolipid-enriched membrane subdomains during transport to the apical cell surface. *Cell* 68: 533-544
20. Briolay A, Jaafar R, Nemoz G, Bessueille L (2013) Myogenic differentiation and lipid-raft composition of L6 skeletal muscle cells are modulated by PUFAs. *Biochim Biophys Acta* 1828: 602-613
21. Hein LK, Duplock S, Hopwood JJ, Fuller M (2008) Lipid composition of microdomains is altered in a cell model of Gaucher disease. *J Lipid Res* 49: 1725-1734
22. van Gestel RA, Brouwers JF, Ultee A, Helms JB, Gadella BM (2006) Ultrastructure and lipid composition of detergent-resistant membranes derived from mammalian sperm and two types of epithelial cells. *Cell Tissue Res* 363: 129-145
23. Fabelo N, Martín V, Santpere G, Marín R, Torrent L, Ferrer I, Díaz M (2011) Severe alterations in lipid composition of frontal cortex lipid

- rafts from Parkinson's disease and incidental Parkinson's disease. *Mol Med* 17: 1107-1118
24. Gelsomino G, Corsetto PA, Campia I, Montorfano G, Kopecka J, Castella B, Gazzano E, Ghigo D, Rizzo AM, Riganti C (2013) Omega 3 fatty acids chemosensitize multidrug resistant colon cancer cells by down-regulating cholesterol synthesis and altering detergent resistant membranes composition. *Mol Cancer* 12: 137
  25. Fabelo N, Martín V, Marín R, Moreno D, Ferrer I, Díaz M (2014) Altered lipid composition in cortical lipid rafts occurs at early stages of sporadic Alzheimer's disease and facilitates APP/BACE1 interactions. *Neurobiol Aging* 35: 1801-1812
  26. Bodin S, Tronchère H, Payrastré B (2003) Lipid rafts are critical membrane domains in blood platelet activation processes. *Biochim Biophys Acta* 1610: 247-257
  27. Damek-Poprawa M, Golub E, Otis L, Harrison G, Phillips C, Boesze-Battaglia K (2006) Chondrocytes utilize a cholesterol-dependent lipid translocator to externalize phosphatidylserine. *Biochemistry* 45: 3325-3336
  28. Pike LJ, Han X, Chung KN, Gross RW (2002) Lipid rafts are enriched in arachidonic acid and plasmalogen phospholipids and their composition is independent of caveolin-1 expression: a quantitative electrospray ionization/mass spectrometric analysis. *Biochemistry* 41: 2075-2088
  29. Stulnig TM, Huber J, Leitinger N, Imre EM, Angelisova P, Nowotny P, Waldhaus W (2001) Polyunsaturated eicosapentaenoic acid displaces proteins from membrane rafts by altering raft lipid composition. *J Biol Chem* 276: 37335-37340
  30. Abdallah D, Hamade E, Merhi RA, Bassam B, Buchet R, Mebarek S (2014) Fatty acid composition in matrix vesicles and in microvilli from femurs of chicken embryos revealed selective recruitment of fatty acids. *Biochem Biophys Res Commun* 446: 1161-1164
  31. Peress NS, Anderson HC, Sajdera SW (1974) The lipids of matrix vesicles from bovine fetal epiphyseal cartilage. *Calcif Tissue Res* 14: 275-281
  32. Wuthier RE (1975) Lipid composition of isolated epiphyseal cartilage cells, membranes and matrix vesicles. *Biochim Biophys Acta* 409: 128-143
  33. Glaser JH, Conrad HE (1981) Formation of matrix vesicles by cultured chick embryo chondrocytes. *J Biol Chem* 256: 12607-12611
  34. Lingwood D, Simons K (2010) Lipid rafts as a membrane-organizing principle. *Science* 327: 46-50
  35. Browman DT, Hoegg MB, Robbins SM (2007) The SPFH domain-containing proteins: more than lipid raft markers. *Trends Cell Biol* 17: 394-402
  36. Stuermer CA (2010) The reggie/flotillin connection to growth. *Trends Cell Biol* 20: 6-13
  37. Tu X, Huang A, Bae D, Slaughter N, Whitelegge J, Crother T, Bickel PE, Nel A (2004) Proteome analysis of lipid rafts in Jurkat cells characterizes a raft subset that is involved in NF-kappaB activation. *J Proteome Res* 3: 445-454
  38. Gu MX, Fu Y, Sun XL, Ding YZ, Li CH, Pang W, Pan S, Zhu Y (2012) Proteomic analysis of endothelial lipid rafts reveals a novel role of statins in antioxidation. *J Proteome Res* 11: 2365-2373
  39. Suica VI, Uyy E, Boteanu RM, Ivan L, Antohe F (2015) Alteration of actin dependent signaling pathways associated with membrane microdomains in hyperlipidemia. *Proteome Sci* 13: 30
  40. Shah A, Chen D, Boda AR, Foster LJ, Davis MJ, Hill MM (2015) Raft-Prot: mammalian lipid raft proteome database. *Nucleic Acids Res* 43: 335-338
  41. Diaz-Rohrer B, Levental KR, Levental I (2014) Rafting through traffic: Membrane domains in cellular logistics. *Biochim Biophys Acta* 1838: 3003-3013
  42. Head BP, Patel HH, Insel PA (2014) Interaction of membrane/lipid rafts with the cytoskeleton: impact on signaling and function: membrane/lipid rafts, mediators of cytoskeletal arrangement and cell signaling. *Biochim Biophys Acta* 1838(2): 532-545
  43. Causeret M, Taulet N, Comunale F, Favard C, Gauthier-Rouvière C (2005) N-cadherin association with lipid rafts regulates its dynamic assembly at cell-cell junctions in C2C12 myoblasts. *Mol Biol Cell* 16: 2168-2180
  44. Lin D, Zhou J, Zelenka PS, Takemoto DJ (2003) Protein kinase Cgamma regulation of gap junction activity through caveolin-1-containing lipid rafts. *Invest Ophthalmol Vis Sci* 44: 5259-5268
  45. Chichili GR, Rodgers W (2009) Cytoskeleton-membrane interactions in membrane raft structure. *Cell Mol Life Sci* 66: 2319-2328
  46. Balcerzak M, Malinowska A, Thouverey C, Sekrecka A, Dadlez M, Buchet R, Pikula S (2008) Proteome analysis of matrix vesicles isolated from femurs of chicken embryo. *Proteomics* 8: 192-205
  47. Cui Y, Xu Q, Luan J, Hu S, Pan J, Han J, Ji Z (2015) MvsCarta: A protein database of matrix vesicles to aid understanding of biomineralization. *Biosci Trends* 9: 190-192
  48. Thouverey C, Malinowska A, Balcerzak M, Strzelecka-Kiliszek A, Buchet R, Dadlez M, Pikula S (2011) Proteomic characterization of biogenesis and functions of matrix vesicles released from mineralizing human osteoblast-like cells. *J Proteomics* 74: 1123-1134
  49. Jeziorska M, McCollum C, Woolley DE (1998) Calcification in atherosclerotic plaque of human carotid arteries: associations with mast cells and macrophages. *J Pathol* 185: 10-17
  50. Roijers RB, Dutta RK, Cleutjens JP, Mutsaers PH, de Goeij JJ, van der Vusse GJ (2008) Early calcifications in human coronary arteries as determined with a proton microprobe. *Anal Chem* 80: 55-61
  51. Mintz GS, Popma JJ, Pichard AD, Kent KM, Satler LF, Chuang YC, Ditrano CJ, Leon MB (1995) Patterns of calcification in coronary artery disease. A statistical analysis of intravascular ultrasound and coronary angiography in 1155 lesions. *Circulation* 91: 1959-1965
  52. Rattazzi M, Bennett BJ, Bea F, Kirk EA, Ricks JL, Speer M, Schwartz SM, Giachelli CM, Rosenfeld ME (2005) Calcification of advanced atherosclerotic lesions in the innominate arteries of ApoE-deficient mice: potential role of chondrocyte-like cells. *Arterioscler Thromb Vasc Biol* 25: 1420-1425
  53. Rosenfeld ME, Polinsky P, Virmani R, Kauser K, Rubanyi G, Schwartz SM (2000) Advanced atherosclerotic lesions in the innominate artery of the ApoE knockout mouse. *Arterioscler Thromb Vasc Biol* 20: 2587-2592
  54. Sun Y, Byon CH, Yuan K, Chen J, Mao X, Heath JM, Javed A, Zhang K, Anderson PG, Chen Y (2012) Smooth muscle cell-specific runx2 deficiency inhibits vascular calcification. *Circ Res* 111: 543-552
  55. Tanimura A, McGregor DH, Anderson HC (1986) Calcification in atherosclerosis. I. Human studies. *J Exp Pathol* 2: 261-273
  56. Freigang S, Ampenberger F, Weiss A, Kanneganti TD, Iwakura Y, Hersberger M, Kopf M (2013) Fatty acid-induced mitochondrial uncoupling elicits inflammasome-independent IL-1 $\alpha$  and sterile vascular inflammation in atherosclerosis. *Nat Immunol* 14: 1045-1053
  57. Brodeur MR, Bouvet C, Barrette M, Moreau P (2013) Palmitic acid increases medial calcification by inducing oxidative stress. *J Vasc Res* 50: 430-441
  58. Ting TC, Miyazaki-Anzai S, Masuda M, Levi M, Demer LL, Tintut Y, Miyazaki M (2011) Increased lipogenesis and stearate accelerate vascular calcification in calcifying vascular cells. *J Biol Chem* 286: 23938-23949
  59. Kageyama A, Matsui H, Ohta M, Sambuichi K, Kawano H, Notsu T, Imada K, Yokoyama T, Kurabayashi M (2013) Palmitic acid induces osteoblastic differentiation in vascular smooth muscle cells through ACSL3 and NF- $\kappa$ B, novel targets of eicosapentaenoic acid. *PLoS One* 8: e68197
  60. Masuda M, Miyazaki-Anzai S, Keenan AL, Okamura K, Kendrick J, Chonchol M, Offermanns S, Ntambi JM, Kuro-O M, Miyazaki M (2015) Saturated phosphatidic acids mediate saturated fatty acid-induced vascular calcification and lipotoxicity. *J Clin Invest* 125: 4544-4558
  61. Abedin M, Lim J, Tang TB, Park D, Demer LL, Tintut Y (2006) N-3 fatty acids inhibit vascular calcification via the p38-mitogen-activated protein kinase and peroxisome proliferator-activated receptor-gamma pathways. *Circ Res* 98: 727-729

62. Woldt E, Terrand J, Mlih M, Matz RL, Bruban V, Coudane F, Foppolo S, El Asmar Z, Chollet ME, Ninio E, Bednarczyk A, Thiersé D, Schaefer C, Van Dorsselaer A, Boudier C, Wahli W, Chambon P, Metzger D, Herz J, Boucher P (2012) The nuclear hormone receptor PPAR $\gamma$  counteracts vascular calcification by inhibiting Wnt5a signaling in vascular smooth muscle cells. *Nat Commun* 3: 1077

63. Geng Y, Hsu JJ, Lu J, Ting TC, Miyazaki M, Demer LL, Tintut Y (2011) Role of cellular cholesterol metabolism in vascular cell calcification. *J Biol Chem* 286: 33701-33706

64. Liu S, Guo W, Han X, Dai W, Diao Z, Liu W (2016) Role of UBIAD1 in Intracellular Cholesterol Metabolism and Vascular Cell Calcification. *PLoS One* 11: e0149639

## Błony a mineralizacja w normie i patologii

Monika Roszkowska<sup>1,2,✉</sup>, Agnieszka Strzelecka-Kiliszek<sup>1</sup>, David Magne<sup>2</sup>, Sławomir Pikula<sup>1</sup>, Laurence Bessueille<sup>2</sup>

<sup>1</sup>Pracownia Biochemii Lipidów, Zakład Biochemii, Instytut Biologii Doświadczalnej im. M. Nenckiego Polskiej Akademii Nauk, ul. Pasteura 3, 02-093 Warszawa, Polska

<sup>2</sup>ICBMS, UMR CNRS 5246, Université Claude Bernard Lyon 1, Bâtiment Raulin, 43 Bd du 11 novembre 1918; 69622 Villeurbanne, Francja

✉ e-mail: m.roszkowska@nencki.gov.pl

**Słowa kluczowe:** mineralizacja, zwapnienie ścian naczyń krwionośnych, pęcherzyki macierzy pozakomórkowej, tratwy lipidowe, cholesterol, kwasy tłuszczowe

### STRESZCZENIE

Zwapnienie ścian naczyń krwionośnych towarzyszy procesowi odkładania się blaszki miażdżycowej. Jest ono wynikiem transdiferencjacji komórek mięśni gładkich w kierunku komórek zdolnych do mineralizacji, o fenotypie zbliżonym do osteoblastów i chondrocytów. Aktywność tkankowo niespecyficjnej alkalicznej fosfatazy (TNAP), enzymu niezbędnego w zapoczątkowaniu procesu fizjologicznej mineralizacji, może być również indukowana w komórkach mięśni gładkich naczyń w odpowiedzi na stan zapalny. TNAP zyskuje swą zdolność do mineralizacji dzięki zakotwiczeniu w błonach komórek mineralizujących lub w błonach wydzielonych przez nie pęcherzyków macierzy pozakomórkowej (MV). Najnowsze doniesienia wskazują na kluczową rolę błon w zapoczątkowaniu procesu tworzenia się minerału. W niniejszym artykule przeglądowym zostały opisane funkcje białek i lipidów związanych z błonami komórkowymi w procesach fizjologicznej oraz patologicznej mineralizacji, ze szczególnym uwzględnieniem procesów towarzyszących miażdżycy.